PROCEEDINGS
of the
OKLAHOMA ACADEMY OF SCIENCE
Volume 103
2023

EDITOR: Mostafa Elshahed

Production Editor: Tammy Austin

Business Manager: Adam Ryburn

The Official Organ of

the

OKLAHOMA ACADEMY OF SCIENCE

Which was established in 1909 for the purpose of stimulating scientific research;
to promote fraternal relationships among those engaged in scientific work in Oklahoma;
to diffuse among the citizens of the State a knowledge of the various departments of science;
and to investigate and make known the material, educational, and other resources of the State.

Affiliated with the American Association for the Advancement of Science.

Publication Date: January 2024

POLICIES OF THE *PROCEEDINGS*

The *Proceedings of the Oklahoma Academy of Science* contains papers on topics of interest to scientists. The goal is to publish clear communications of scientific findings and of matters of general concern for scientists in Oklahoma, and to serve as a creative outlet for other scientific contributions by scientists. ©*2023 Oklahoma Academy of Science*

The *Proceedings of the Oklahoma Academy of Science* contains reports that describe the results of original scientific investigation (including social science). Papers are received with the understanding that they have not been published previously or submitted for publication elsewhere. The papers should be of significant scientific quality, intelligible to a broad scientific audience, and should represent research conducted in accordance with accepted procedures and scientific ethics (proper subject treatment and honesty).

The Editor of the *Proceedings* expects that the author(s) will honor the following principles of the scientific community, which are also policies of the *Proceedings*.

1. Each author shall have contributed substantially to major aspects of the planning, execution, and /or interpretation of the study and to the preparation of the manuscript. It is assumed that all listed authors concur in the submission, that final copy of the manuscript has been seen and approved by all authors, and that all authors share responsibility for the paper.

2. Submission of manuscripts based on unique material (e.g. cloned DNAs; antibodies; bacterial, animal, or plant cells; hybridomas; viruses; and computer programs) implies that these materials will be available for noncommercial purposes to all qualified investigators.

3. Authors of manuscripts reporting nucleic acid sequence(s) must be prepared to submit relevant data to GenBank. Authors of manuscripts reporting crystallographic studies must be prepared to submit the relevant structural data to the Protein Data Base and/or other appropriate repository. Information necessary for retrieval of the data from the repository will be specified in a reference in the paper.

4. Manuscripts that report research involving human subjects or the use of materials from human organs must be supported by a copy of the document authorizing the research and signed by the appropriate official(s) of the institution where the work was conducted. Research involving humans and animals must have been performed in accordance with the recommendations from the Declaration of Helsinki and the appropriate guidelines of the National Institutes of Health.

5. Submission of manuscripts that report research on/with recombinant DNA implies that the relevant physical and biological containment levels conformed to the guidelines of the National Institutes of Health; the Editor may request proof to substantiate this implication.

6. The *Proceedings* does not publish statements of priority or novelty, or mere descriptions of work in progress or planned. The dates of manuscript receipt, revision, and acceptance will be published.

7. A primary research report must contain sufficient details and reference to public sources of information to permit other scientists to repeat the work.

8. Any unusual hazard encountered or anticipated in using chemicals, equipment, or procedures in the investigation should be clearly identified in the manuscript.

PROCEEDINGS OF THE OKLAHOMA ACADEMY OF SCIENCE

Volume 103

CONTENTS

REPORTS

A. Applied Ecology & Conservation

The Use of Coffee Bean Oil to Repel *Amblyomma americanum* (Acari:Ixodidae)

Heather R. Ketchum*
The University of Oklahoma School of Biological Sciences, Norman OK 73019

Eric G. Bright
The University of Oklahoma School of Biological Sciences, Norman OK 73019

Holly D. Loeffler
The University of Oklahoma School of Biological Sciences, Norman OK 73019

Sierra Gillette-Stouffer
The University of Oklahoma School of Biological Sciences, Norman OK 73019

Richard Anthony Russell
The University of Oklahoma Department of Anthropology, Norman OK 73019

Abstract: There is growing interest in using natural alternatives to repel ticks, particularly essential oils as opposed to synthetic chemicals. Previous studies have found volatile monoterpenes in many essential oils to be repellent or acaricidal, leading us to test the repellency of coffee bean oil to ticks. *Amblyomma americanum* (Acari: Ixodidae) were the subjects tested in two separate studies. One determined the repellency by testing the number of ticks repelled from five different dilutions of coffee bean oil, with dichloromethane as the solvent and control. The other study investigated the farthest distance at which the oil could repel ticks. The study shows that concentrations as low as one percent were effective at repelling *A. americanum,* however, twenty percent repelled the greatest number of ticks. We conclude that the twenty percent solution was repellent up to sixty centimeters. Coffee bean oil does show the ability to repel *A. americanum*. This work shows that coffee bean oil is another example of essential oils that show ability to repel ticks.

Introduction

The incidence of tick-borne diseases is increasing at an alarming rate (Swei *et al*. 2020). In the United States, the number of tick-borne diseases in humans, companion animals, and wildlife surpasses all other vector-borne diseases (Little *et al*. 2014; Rosenberg *et al*. 2018). Furthermore, ticks transmit a greater diversity of pathogens than any other arthropod vector (Shaw *et al*. 2001; de la Fuente *et al*. 2008). The lone star tick, *Amblyomma americanum*, has a broad host range; readily feeding on companion animals, wildlife, and humans and transmits several pathogens that cause disease such as human monocytic ehrlichiosis, tick-borne relapsing fever, tularemia, red meat allergy known as alpha-gal, and southern tick-associated rash illness (Hopla 1953; Hopla 1955; Anziani *et al.* 1990; Ewing *et al.* 1995; Godsey *et al.* 2016). *A. americanum* is established in the eastern, southeastern, and mid-western United States with expanding distribution into the northeastern US and southern Canada (Sonenshine 2018). Established populations exist in canopied and brushy habitats located between prairies and forests and are thus, a major pest species in many national and state parks (Semtner *et al.* 1971; Koch and Burg 2006). This is an aggressive tick that will move

***Corresponding author: heather.r.ketchum-1@ou.edu**

quickly across several meters when attracted to host odors (Sonenshine 2018). The broad host range, expanding geographical distribution, preferred habitat, and vector competence makes *A. americanum* a serious health threat to both humans and animals. Preventing ticks from biting humans and domestic animals can stop these tick-borne diseases from spreading.

There are many recommendations from experts on how to protect people and their animals from tick bites. The United States Center for Disease Control (CDC) recommends the use of repellents, some of which can be used on the skin while others should only be used on clothing (Center for Disease Control 2019). Permethrin, a synthetic repellent, is applied to clothing and has been shown to be effective in repelling *A. americanum* (Schreck *et al.* 1982). For direct skin usage, DEET (N,N-diethyl-3-methyl benzamide) has been used since the 1950s and is an effective tick synthetic repellent (Carroll *et al.* 2008). In recent years, the use of synthetic chemicals to repel arthropods has raised concerns related to environmental and human health risk and more interest in the use of natural alternatives to prevent tick bites, particularly essential oils.

Essential oils are extracted from plants and contain volatile chemical compounds. The volatile terpenes, sesquiterpenes, sulfur, menthol, and phenylpropenes in these oils, specifically are thought to repel ticks (Nerio *et al.* 2010). For example, spiderwisp (*Gynandropsis gynandra*) (Malonza *et al.* 1992; Lwande *et al.* 1999), catnip (*Nepeta cataria*) (Birkett *et al.* 2011), bog myrtle (*Myrica gale*) (Jaenson *et al.* 2005), citronella (*Cymbopogon*) (Sukkanon *et al.* 2019), lemon eucalyptus (*Corymbia citriodora*) (Sukkanon *et al.* 2019) and carnation (*Dianthus caryophyllus*) (Tunón *et al.* 2006), contain monoterpenes and have shown to be effective repellents. Oil of Citronella, oil of lemon eucalyptus, and catnip oil have been approved for use on skin by the US Environmental Protection Agency (EPA). These have comparable efficacy to synthetic repellents, with low toxicity (Katz *et al.* 2008). Other essential oils such as garlic (*Allium sativum*), onion (*Allium cepa)*, citrus peel, tea tree (*Melaleuca alternifolia*), geranium, peppermint (*Mentha piperita*), spearmint (*Mentha viridis*), marjoram (*Marjorana hortensis*), sweet basil (*Ocimum basilicum*), and lavender (*Lavandula officinalis*) oils have shown promise in repelling ticks but have not been approved by the EPA as tick repellents (Don-Pedro 1996; Abdel-Shafy and Soliman 2004; Iori *et al.* 2005; Jaenson *et al.* 2006; Štefanidesová *et al.* 2017). Many of these successful plant-derived repellents derived from plant essential oils are highly volatile and have limited residual activity (Sukumar *et al.* 1991; Zhu *et al.* 2018).

Other plant-derived compounds that are not as highly volatile have been shown to repel ticks. High levels of fatty acids in coconut oil have been shown to repel three different species of ticks (Zhu *et al.* 2018; Sukkanon *et al.* 2019; Barrozo *et al.* 2021) and have a longer repellent activity than DEET. Hence there is interest in studying other plant-based essential oils comprised of different active ingredients that could provide greater efficacy and extended repellent activity.

Coffee bean (*Coffea arabica)* oil is an inexpensive, natural oil that is primarily (80-85%) composed of triglycerides with diterpenes making up 13 - 15 % of the oil (Ratnayake *et al.* 1992; Al Kanhal 1997; Speer and Kölling-Speer 2006). The fatty acid composition of coffee bean oil is dominated by linoleic acid and palmitic acid with some minor contribution of stearic acid, oleic acid, arachidic acid, and alpha-linolenic acid (Speer and Kölling-Speer 2006).

To determine if coffee bean oil could be used as an efficient tick repellent, we tested five different concentrations of coffee bean (*Coffea arabica*, Plant Therapy®) oil to determine the most effective concentration at repelling *A. americanum*. This assay also investigated the efficacy of the coffee bean oil extract at several distances. To the best of our knowledge, there are no published studies on the repellent properties of coffee bean oil on ticks, or on the maximum distance at which any essential oil is repellent to ticks.

Methods

Ticks

Five hundred adult *A. americanum* ticks of both sexes were purchased from Texas A&M Tick Research Laboratory (College Station, Texas). Adults were housed temporarily in the Department of Biology at the University of Oklahoma (Norman, Oklahoma) in glass incubators (38.1 cm x 43.2 cm x 30.5 cm) and maintained at 90 % relative humidity using a saturated potassium chloride solution.

Repellency Assay

Coffee bean, *Coffea arabica*, oil was purchased from Plant Therapy® (Twin Falls, Idaho) and diluted to 1, 2, 5, and 20 percent using dichloromethane (DCM) purchased from Sigma-Aldrich (St. Louis, Missouri). Four sheets of Whatman™110 mm filter paper were cut in half; one half was treated with a coffee bean oil dilution (1 ml) (treatments) while the other half was treated with DCM (1 ml) (control). Treatment and control solutions were pipetted onto the center of each filter paper and allowed to diffuse across the filter paper. Each treatment was placed in a separate petri dish alongside the control leaving a centimeter of space between the treatment and control. The space between the two halves was deemed the "neutral zone." To eliminate a DCM affect, the same set up was used, but one side remained untreated while the other side was treated with one milliliter of DCM.

A slightly modified area preference method was used to test repellency (Tapondjou *et al.* 2005; Olivero-Verbel *et al.* 2010; Caballero-Gallardo *et al.* 2012; Lü and Shi 2012). Five ticks were simultaneously placed in the petri dish at random orientations. Ticks were monitored for a total of 15 minutes. At 5-minute intervals, each tick was scored with either 0 for staying in the neutral zone, 1 for moving toward the control, or -1 for moving toward the treatment. At the completion of the 15 minutes, the ticks were removed, killed and stored in 70 % ethanol for long-term preservation. The procedure was repeated five times using fresh assays and ticks.

Distance Efficacy

The distance efficacy of coffee bean oil extract was determined by constructing a testing arena. The testing arena was created by drawing four concentric circles (radii = 15 cm, 30 cm, 45 cm, and 60 cm) on a poster board (117.6 cm x 142.4 cm) (Figure 1). Five mL of the 20 % coffee bean oil dilution was placed in a watch glass on the center of the arena. The 20 % dilution was chosen because it was the most repellent treatment in the repellency assay. For each trial, five ticks were randomly oriented and placed at one of the four distance intervals and each tick's position was recorded every five minutes for 15 minutes. At the end of each 5-minute interval, each tick was scored with a 0 for staying in place, 1 for moving away from the oil, or -1 for moving toward the oil. Trials were repeated five times at each distance interval (15, 30, 45, and 60 cm) with different ticks for every replication.

Statistical Analysis

Statistical analyses were carried out in SigmaPlot, version 14.0 (Systat Software, Inc., Palo Alto, CA, USA). Since the data was categorical, we used a chi-squared analysis to determine statistical significance for both the repellency assay and distance efficacy tests

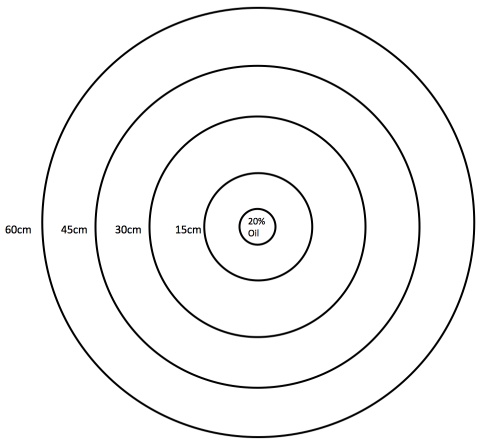

Figure 1. Distance assay arena. For each trial, 5 ml of 20 % concentration of oil were placed in a watch glass in the center of a 38.1x 43.2x 30.5 cm poster board. Five *A. americanum* ticks were placed at one distance interval (15, 30, 45, or 60 cm) for each test and positions were scored after 5, 10, and 15 minutes.

(Dowdy *et al.* 2011). For the repellency assay, we analyzed each time interval (t = 5, 10, and 15 minutes) independently and when significance was found, we ran pairwise comparison among all the different dilutions of each time period.

Results

Repellency Assay

More than half of ticks moved away from the coffee bean oil and after 15-minute exposure there was nearly a two-fold increase in the percentage of ticks that moved away from the coffee bean oil (Table 1). All four dilutions repelled a significantly greater number of ticks than the control treatment ($P < 0.001$; Table 2) hence DCM had no effect on tick repellency. While the first three dilutions (1 %, 2 %, and 5 %) repelled a similar number of ticks, the 20 % concentration repelled the greatest number of ticks (Table 1).

The repellency of coffee bean oil was not consistent over the entire testing interval (Table 2). At the five-minute interval, more ticks moved away from all the coffee bean oil dilutions than from the control. However, there was no difference in the number of ticks moving away from the different coffee bean oil dilutions. After ten minutes, there was no difference between the control and all coffee bean oil treatments. At the fifteen-minute time interval, all coffee bean oil dilutions repelled more ticks than the control treatment again. Among the coffee bean dilutions, the 20 % dilution repelled more ticks than the 2 % and 5 % dilutions while the 1% dilution repelled the same number of the other three dilutions.

Distance Efficacy

The purpose of the distance test was to determine the farthest distance at which the 20 % dilution was repellent to *A. americanum*. The 20 % dilution of coffee bean oil repelled ticks at all distances tested (Table 3); ticks were least repelled when the repellent was farthest away and more repelled when the repellent was close by. However, this was not a consistent trend as seen in the percent of ticks repelled when placed at 30 cm (44 %) compared to 45 cm (68 %) away from the oil. The final tick positions at the end of each time interval did not significantly differ with distance from the oil (t = 5, $\chi^2_6 = 5.91$, $P = 0.43$; t = 10, $\chi^2_6 = 8.77$, $P = 0.19$; t = 15, $\chi^2_6 = 5.91$ $P = 0.43$).

Table 1. The effect of coffee bean oil on *A. americanum* tick repellency as tested with dilutions of one, two, five, and twenty percent against the control (only DCM). Repellency was measured as the percent of ticks (out of 25 ticks at each concentration of oil) whose position was further away from the coffee bean oil than when the trial started at each of the time intervals.

Treatment (% dilution)	Ticks (%) that moved away from the coffee bean oil		
	5-minute	10-minute	15-minute
Control	20	44	52
1	56	72	76
2	60	64	68
5	64	64	64
20	64	64	96

Table 2. Statistical analysis values from chi-squared tests on the repellency of the different dilutions of coffee bean oil on *A. americanum* at the three different time intervals. Bolded data represent significant values. N.C. indicates the test was not conducted.

		5-min. interval		10-min. interval		15-min. interval	
Test	D.F.	χ^2 value	*P* value	χ^2 value	*P* value	χ^2 value	*P* value
Overall Dilution (%)	8	**16.81**	**0.032**	12.52	0.130	**36.24**	**< 0.001**
Control - 1	2	**7.05**	**0.029**	N.C.	N.C.	**15.43**	**< 0.001**
Control - 2	2	**10.00**	**0.007**	N.C.	N.C.	**10.93**	**0.004**
Control - 5	2	**10.12**	**0.006**	N.C.	N.C.	**11.71**	**0.003**
Control - 20	2	**9.96**	**0.007**	N.C.	N.C.	**16.27**	**< 0.001**
2 - 20	2	1.65	0.44	N.C.	N.C.	**6.86**	**0.032**
5 - 20	2	1.65	0.438	N.C.	N.C.	**8.17**	**0.017**
1 - 2	2	2.46	0.292	N.C.	N.C.	1.11	0.574
1 - 5	2	0.93	0.627	N.C.	N.C.	1.35	0.510
1 - 20	2	0.38	0.826	N.C.	N.C.	4.25	0.120
2 - 5	2	0.62	0.732	N.C.	N.C.	0.12	0.941

Discussion

For decades, CDC has recommended that the repellents permethrin and DEET be used to prevent tick bites. Concerns raised regarding the health and environmental safety of these synthetic chemicals have created an interest in using natural repelling products, such as essential oils to repel ticks. While many essential oils have been tested both on- and off-host and some approved by the US EPA, coffee bean oil has never been tested. The results of these preliminary off-host assays indicate that coffee bean oil, an essential oil, may repel adult *A. americanum*. Across the range of dilutions tested, the most effective was the 20 % dilution, which repelled ticks up to 60 cm away from the oil. Twenty-four of twenty-five ticks moved away from the 20% dilution, and more than half of the ticks still moved away from the oil when they were up to 60 cm away from it. The difference in the percent of ticks repelled from the 30 cm and 45 cm treatment was likely a random occurrence. There were no significant differences in the distance assay.

Using a variety of methodologies, other studies have shown essential oils to have repellency activity against varying life stages of *A. americanum* (Ellse and Wall 2014). Meng *et al.* (2016) in a vertical filter bioassay determined that of the eight essential oils tested (oregano, clove, thyme, sandalwood, cinnamon, cedarwood, and peppermint), oregano oil was the most effective and peppermint oil the least effective in repelling *A. americanum* nymphs. The LC_{50} values for all essential oils tested, ranged from 0.113 to 0.297 mg/cm^2, were significantly higher than that of DEET ($P < 0.05$). Luker *et al.* (2021) using a novel tick carousel assay determined that six hours post-treatment, oil of lemon eucalyptus repelled more adult *A. americanum* than the synthetic repellents tested (DEET, Picaridin, and IR3535). Elemol, a principal constituent of the essential oil of Osage orange, *Maclura pomifera* (Moraceae) in a vertical filter bioassay and a fingertip bioassay did not differ significantly in repelling *A. americanum* nymphs than the popular synthetic repellent DEET (Carroll *et al.* 2010).

Table 3. Distance efficacy of a twenty percent dilution of coffee bean oil on *A. americanum* movement measured the percent of ticks (out of 25) that moved away from the coffee bean oil. The tick positions did not significantly differ with distance from the oil across the different time intervals.

Distance (cm) from coffee bean oil	Ticks (%) that moved away from 20 % coffee bean oil		
	5-minute	10-minute	15-minute
15	92	96	92
30	44	76	84
45	68	84	84
60	80	76	76

Repellent activity of at least ten essential oils have been tested for their ability to repel varying life stages of *A. americanum* using a variety of in vitro and in vivo bioassay methodologies (Phillis III and Cromroy 1977; Carroll *et al.* 2010; Meng *et al.* 2016; Luker *et al.* 2021). Our preliminary work was the first to test coffee bean oil in a horizontal in vitro repellency and distance assay. The 20 % dilution resulted in greatest repellency while the distance of repellency was not significant. The distance study was unique, as no known studies have measured the farthest distance at which an oil is effective.

The results of this study suggest that coffee bean oil may be effective in repelling ticks and hence warrants further study. *A. americanum* is an aggressive tick, quickly moving toward its host. It is strongly attracted to carbon dioxide emitted from humans and animals and has simple eyes that may detect movements of host silhouettes against contrasting background (Phillis III and Cromroy 1977; Carroll *et al.* 2010). With the preliminary evidence that coffee bean oil may have repellent activity, its ability to repel should be tested against these host cues and hence, an in vivo vertical fingertip bioassay is warranted for both *A. americanum* nymphs and adults. Furthermore, in the current study the time interval for testing repellency was maximized at 15-minutes. In the fingertip bioassay this interval should be extended to closer reflect conditions in the field. The distance assay should be repeated however modified to a fingertip bioassay. We were unable to determine the maximum distance at which the oil was effective because none of the results from the distance assay were significant. Farther distances should be tested with the 20 % dilution to find the true limit of the oil's repellency. Lastly, to be considered an effective repellent, coffee bean oil should be tested against DEET and must show higher repellency activity than DEET for people to consider its use.

It is important to note that while natural products can be effective in repelling ticks, they may not be safer than synthetic chemicals. Natural products just like synthetic must be tested for their effectiveness and safety passing regulations set forth by the US EPA before they are used on humans or animals. Studies like this are only the first step in determining if an essential oil, coffee bean oil is worthy of future consideration for tick or other arthropod repellency.

Our preliminary findings suggest that coffee bean oil may be an effective tick repellent; however, further repellency assays are warranted. Future research should include a vertical in vivo fingertip bioassay with additional *A. americanum* life stages, longer repellency duration, distance of repellency, and a comparison to DEET. If future research confirms coffee bean oil to have high tick repellency, to be safe and effective, coffee bean oil could be tested by the US EPA.

Acknowledgements

We thank Dr. Marielle Hoefnagels, University of Oklahoma, Department of Microbiology and Plant Biology for editing and assistance with this manuscript. Dr. Pete D. Teel, Texas A&M University, Department of Entomology for providing the ticks used in this study.

References

Abdel-Shafy S, Soliman MMM. 2004. Toxicity of some essential oils on eggs, larvae, and females of *Boophilus annulatus* (Acarid: Ixodida: Amblyommidae) infesting cattle in Egypt. Acarologia, 44(1-2): 23–30. http://www1.montpellier.inra.fr/CBGP/acarologia/article.php?id=40

Al Kanhal MA. 1997. Lipid analysis of *Coffea arabica* Linn. beans and their possible hypercholesterolemic effects. Int. J. Food Sci. Nutr., 48(2): 135-139. doi:10.3109/09637489709006973

Anziani O, Ewing S, Barker R. 1990. Experimental transmission of a granulocytic form of the tribe Ehrlichieae by *Dermacentor variabilis* and *Amblyomma americanum* to dogs. Am. J. Vet. Res., 51(6): 929–931. PMID: 2368951

Barrozo MM, Zeringóta V, Borges LMF, Moraes N, Benz K, Farr A, Zhu JJ. 2021. Repellent and acaricidal activity of coconut oil fatty acids and their derivative compounds and catnip oil against *Amblyomma sculptum*. Vet. Parasitol., 300: 109591. doi:10.1016/j.vetpar.2021.10959

Birkett MA, Hassanali A, Hoglund S, Pettersson J, Pickett JA. 2011. Repellent activity of catmint, *Nepeta cataria*, and iridoid nepetalactone isomers against Afro-tropical mosquitoes, ixodid ticks and red poultry mites. Phytochemistry, 72(1): 109–114. doi:10.1016/j.phytochem.2010.09.016

Caballero-Gallardo K, Olivero-Verbel J, Stashenko EE. 2012. Repellency and toxicity of essential oils from *Cymbopogon martinii*, *Cymbopogon flexuosus* and *Lippia origanoides* cultivated in Colombia against *Tribolium castaneum*. J. Stored Prod. Res., 50: 62–65. doi:10.1016/j.jspr.2012.05.002

Carroll JF, Benante JP, Klun JA, White CE, Debboun M, Pound JM, Dheranetra W. 2008. Twelve-hour duration testing of cream formulations of three repellents against *Amblyomma americanum*. Med. Vet. Entomol., 22(2): 144–151. doi:10.1111/j.1365-2915.2008.00721.x

Carroll JF, Paluch G, Coats J, Kramer M. 2010. Elemol and amyris oil repel the ticks *Ixodes scapularis* and *Amblyomma americanum* (Acari: Ixodidae) in laboratory bioassays. Exp. Appl. Acarol., 51(4): 383–392. doi:10.1007/s10493-009-9329-0

Center for Disease Control. 2019. Prevent tick and mosquito bites [online]. Available from: https://www.cdc.gov/ncezid/dvbd/about/prevent-bites.html (Accessed August 9, 2021).

Don-Pedro KN. 1996. Investigation of single and joint fumigant insecticidal action of citrus peel oil components. Pestic. Sci., 46(1): 79–84. doi:10.1002/(SICI)1096-9063(199601)46:1<79::AID-PS319>3.0.CO;2-8

Dowdy S, Wearden S, Chilko D. 2011. Statistics for research. Hoboken (NJ): John Wiley & Sons. 627 p.

Ellse L, Wall R. 2014. The use of essential oils in veterinary ectoparasite control: a review. Med. Vet. Entomol., 28(3): 233–243. doi:10.1111/mve.12033

Ewing SA, Dawson JE, Kocan AA, Barker RW, Warner CK, Panciera RJ, Fox JC, Kocan KM, Blouin EF. 1995. Experimental transmission of *Ehrlichia chaffeensis* (Rickettsiales: Ehrlichieae) among white-tailed deer by *Amblyomma americanum* (Acari: Ixodidae). J. Med. Entomol., 32(3): 368–374. doi:10.1093/jmedent/32.3.368

de la Fuente J, Estrada-Pena A, Venzal JM, Kocan KM, Sonenshine DE. 2008. Overview: ticks as vectors of pathogens that cause disease in humans and animals. Front Biosci, 13(13): 6938–6946. doi:10.2741/3200

Godsey Jr. MS, Savage HM, Burkhalter KL, Bosco-Lauth AM, Delorey MJ. 2016. Transmission of Heartland virus (Bunyaviridae: Phlebovirus) by experimentally infected *Amblyomma americanum* (Acari: Ixodidae). J. Med. Entomol., 53(5): 1226–1233. doi:10.1093/jme/tjw080

Hopla CE. 1953. Experimental studies on tick transmission of tularemia organisms. Am. J. Hyg., 58(1): 101–118. doi:10.1093/oxfordjournals.aje.a119761

Hopla CE. 1955. The multiplication of tularemia organisms in the Lone Star tick. Am. J. Epidemiol., 61(3): 371–380. doi:10.1093/oxfordjournals.aje.a119761

Iori A, Grazioli D, Gentile E, Marano G, Salvatore G. 2005. Acaricidal properties of the essential oil of *Melaleuca alternifolia* Cheel (tea tree oil) against nymphs of *Ixodes ricinus*. Vet. Parasitol., 129(1): 173–176. doi:10.1016/j.vetpar.2004.11.035

Jaenson TGT, Pålsson K, Borg-Karlson A-K. 2005. Evaluation of extracts and oils of tick-repellent plants from Sweden. Med. Vet. Entomol., 19(4): 345–352. doi:10.1111/j.1365-2915.2005.00578.x

Jaenson TG, Garboui S, Pålsson K. 2006. Repellency of oils of lemon eucalyptus, geranium, and lavender and the mosquito repellent MyggA natural to *Ixodes ricinus* (Acari: Ixodidae) in the laboratory and field. J. Med. Entomol., 43(4): 731–736. doi:10.1603/0022-2585(2006)43[731:rooole]2.0.co;2

Katz TM, Miller JH, Hebert AA. 2008. Insect repellents: Historical perspectives and new developments. J. Am. Acad. Dermatol., 58(5): 865–871. doi:10.1016/j.jaad.2007.10.005

Koch KR, Burg JG. 2006. Relative abundance and survival of the tick *Amblyomma americanum* collected from sunlit and shaded habitats. Med. Vet. Entomol., 20(2): 173–176. doi:10.1111/j.1365-2915.2006.00617.x

Little SE, Beall MJ, Bowman DD, Chandrashekar R, Stamaris J. 2014. Canine infection with *Dirofilaria immitis*, *Borrelia burgdorferi*, *Anaplasma* spp., and *Ehrlichia* spp. in the United States, 2010–2012. Parasit. Vectors, 7(1): 257. doi:10.1186/1756-3305-7-257

Lü JH, Shi YL. 2012. The bioactivity of essential oil from *Ailanthus altissima* Swingle (Sapindales: Simaroubaceae) bark on *Lasioderma serricorne* (Fabricius) (Coleoptera: Anobiidae). Adv. Mater. Res., 365: 428–432. doi:10.4028/www.scientific.net/AMR.365.428

Luker HA, Rodriguez S, Kandel Y, Vulcan J, Hansen IA. 2021. A novel tick carousel assay for testing efficacy of repellents on *Amblyomma americanum* L. PeerJ, 9: e11138. doi:10.7717/peerj.11138

Lwande W, Ndakala AJ, Hassanali A, Moreka L, Nyandat E, Ndungu M, Amiani H, Gitu PM, Malonza MM, Punyua DK. 1999. *Gynandropsis gynandra* essential oil and its constituents as tick (*Rhipicephalus appendiculatus*) repellents. Phytochemistry, 50(3): 401–405. doi:10.1016/S0031-9422(98)00507-X

Malonza MM, Dipeolu OO, Amoo AO, Hassan SM. 1992. Laboratory and field observations on anti-tick properties of the plant *Gynandropsis gynandra* (L.) brig. Vet. Parasitol., 42(1): 123–136. doi:10.1016/0304-4017(92)90108-L

Meng H, Li AY, Junior LMC, Castro-Arellano I, Liu J. 2016. Evaluation of DEET and eight essential oils for repellency against nymphs of the lone star tick, *Amblyomma americanum* (Acari: Ixodidae). Exp. Appl. Acarol., 68(2): 241–249. doi:10.1007/s10493-015-9994-0

Nerio L.S, Olivero-Verbel J, Stashenko E. 2010. Repellent activity of essential oils: A review. Bioresour. Technol., 101(1): 372–378. doi:10.1016/j.biortech.2009.07.048

Olivero-Verbel J, Nerio LS, Stashenko EE. 2010. Bioactivity against *Tribolium castaneum* Herbst (Coleoptera: Tenebrionidae) of *Cymbopogon citratus* and *Eucalyptus citriodora* essential oils grown in Colombia. Pest Manag. Sci., 66(6): 664–668. doi:10.1002/ps.1927

Phillis III WA, Cromroy HL. 1977. The microanatomy of the eye of *Amblyomma americanum* (Acari: Ixodidae) and resultant implications of its structure. J. Med. Entomol., 13(6): 685–698. doi:10.1093/jmedent/13.6.685

Ratnayake WMN, Hollywood R, O'Grady E, Stavric B. 1993. Lipid content and composition of coffee brews prepared by different methods. Fd. Chem. Toxic. 31(4): 263-269. doi:10.1016/0278-6915(93)90076-B

Rosenberg R, Lindsey NP, Fischer M, Gregory CJ, Hinckley AF, Mead PS, Paz-Bailey G, Waterman SH, Drexler NA, Kersh GJ, Hooks H, Partridge SK, Visser SN, Beard CB, Petersen LR. 2018. Vital signs: Trends in reported vectorborne disease cases - United States and territories, 2004-2016. MMWR Morb. Mortal. Wkly. Rep., 67(17): 496–501. doi:10.15585/mmwr.mm6717e1

Schreck CE, Mount GA, Carlson DA. 1982. Wear and wash persistence of Permethrin used as a clothing treatment for personal protection against the lone star tick (Acari: Ixodidae). J. Med. Entomol., 19(2): 143–146. doi:10.1093/jmedent/19.2.143

Semtner PJ, Howell DE, Hair JA. 1971. The ecology and behavior of the lone star tick (Acarina: Ixodidae). I. The relationship between vegetative habitat type and tick abundance and distribution in Cherokee Co., Oklahoma. J. Med. Entomol., 8(3): 329–335. doi:10.1093/jmedent/8.3.329

Shaw SE, Day MJ, Birtles RJ, Breitschwerdt EB. 2001. Tick-borne infectious diseases of dogs. Trends Parasitol., 17(2): 74–80. doi:10.1016/S1471-4922(00)01856-0

Sonenshine DE. 2018. Range expansion of tick disease vectors in North America: Implications for spread of tick-borne disease. Int. J. Environ. Res. Public. Health, 15(3): 478. doi:10.3390/ijerph15030478

Speer K, Kölling-Speer I. 2006. The lipid fraction of the coffee bean. Braz. J. Plant Physiol., 18(1): 201-216. doi:10.1590/S1677-04202006000100014

Štefanidesová K, Škultéty L, Sparagano OAE, Špitalská, E. 2017. The repellent efficacy of eleven essential oils against adult *Dermacentor reticulatus* ticks. Ticks Tick Borne Dis., 8(5): 780-786. doi:10.1016/j.ttbdis.2017.06.003

Sukkanon C, Chareonviriyaphap T, Doggett SL. 2019. Topical and spatial repellent bioassay against the Australian paralysis tick, *Ixodes holocyclus* (Acari: Ixodidae). Austral Entomol 58(4): 866-874. doi:10.1111/aen.12420

Sukumar K, Perich MJ, Boobar LR. 1991. Botanical derivatives in mosquito control: a review. J. Am. Mosq. Control Assoc., 7(2): 210-237. PMID: 1680152

Swei A, Couper LI, Coffey LL, Kapan D, Bennett S. 2020. Patterns, drivers, and challenges of vector-borne disease emergence. Vector-Borne Zoonotic Dis., 20(3): 159–170. doi:10.1089/vbz.2018.2432

Tapondjou AL, Adler C, Fontem DA, Bouda H, Reichmuth C. 2005. Bioactivities of cymol and essential oils of *Cupressus sempervirens* and *Eucalyptus saligna* against *Sitophilus zeamais* Motschulsky and *Tribolium confusum* du Val. J. Stored Prod. Res., 41(1): 91–102. doi:10.1016/j.jspr.2004.01.004

Tunón H, Thorsell W, Mikiver A, Malander I. 2006. Arthropod repellency, especially tick (*Ixodes ricinus*), exerted by extract from *Artemisia abrotanum* and essential oil from flowers of *Dianthus caryophyllum*. Fitoterapia, 77(4): 257–261. doi:10.1016/j.fitote.2006.02.009

Zhu JJ, Cermak SC, Kenar JA, Brewer G, Haynes KF, Boxler D, Baker PD, Wang D. Wang C, Li AY, Xue R, Shen Y, Wang F, Agramonte NM, Bernier UR, de Oliveira Filho JG, Borges LMF, Friesen K, Taylor DB. 2018. Better than DEET repellent compounds derived from coconut oil. 8:14053. doi:10.1038/s41598-018-32373-7

Submitted December 27, 2022 Accepted November 16, 2023

Impact of Municipal Sewage Effluent on Nitrogen and Phosphorus Dynamics and Growth of Resident Filamentous Algae in a Second Order Stream in West-Central Oklahoma

Steven W. O'Neal*
Department of Biological and Biomedical Sciences, Southwestern Oklahoma State University, Weatherford, OK 73096

Caleb Murrow
Vortex Oilfield Solutions, Alva, OK 73717

Abstract: Elevated levels of stream nutrients due to municipal effluent have been identified as major stressors in streams around the world. We investigated the effects of municipal wastewater treatment plant effluent on nitrogen and phosphorus levels in Little Deep Creek, a 2nd order stream in Custer County, OK, USA. Nutrients were monitored in the effluent, an upstream site, and three downstream sites on three sample dates. Concentrations of nitrate-N, ammonia-N and total-P increased significantly downstream of the effluent release indicating a potential change to more eutrophic conditions. N:P stoichiometry indicated a shift from phosphorus limitation at the upstream site to nitrogen limitation at the downstream sites. Estimated nutrient retention length for total-P suggests a reduction in the stream's capacity to process phosphorus. Nitrate-N uptake length indicates little nitrogen retention by the stream, but suggests that ammonia-N is converted to nitrate-N. Growth of *Spirogyra* and *Cladophora* in effluent diluted with stream water showed that low effluent concentrations stimulated growth of both algae. At higher effluent concentrations estimated to exist downstream of the release, growth rate of *Cladophora* was inhibited relative to the rate of *Spirogyra* suggesting that effluent release into the stream could alter competitive abilities of these filamentous algae.

Introduction

Nitrogen and phosphorus have been identified as the most common stressors for streams in the United States (USEPA, 2006). In the US Southern Plains ecoregion 48% of streams reportedly have high total phosphorus levels and 36% have high nitrogen levels compared to reference streams (USEPA 2006). Sources of elevated nitrogen and phosphorus in streams may include both nonpoint and point sources (Waiser et al. 2010), but waste water treatment plant (WWTP) effluent has been found to account for 50-90% of nutrient inputs in watersheds around the world (Haggard et al. 2005). In the United States, 14,748 publicly owned WWTPs treat waste water generated by 238 million people (USEPA 2016). Treated effluents from these plants are discharged into streams and alter stream nutrient conditions. Nutrient levels may remain elevated for distances of 10 to 85 km downstream of WWTP discharges (reviewed by Carey and Migliaccio 2009).

Elevated levels of these nutrients lead to eutrophication of stream and river ecosystems (USEPA 2006) and contribute to dead zones that develop in the Gulf of Mexico and other coastal areas dominated by river inputs (Justić et al. 1995). Eutrophication has been shown to

***Corresponding author: swoneal53@gmail.com**

increase growth of algae, reduce water clarity, result in harmful diel fluctuations in dissolved oxygen and pH, and increased probability of fish kills (reviewed by Smith et al. 1999). The trophic structure of stream ecosystems has been shown to be altered by nutrient enrichment resulting in concentration and stoichiometric changes in nitrogen and phosphorus (Miltner and Rankin 1998; Evans-White et al. 2009; Dodds and Smith 2016). Excessive growth of the green alga, *Cladophora*, has often been associated with elevated nutrients and eutrophication (Dodds and Gudder 1992; Ensminger et al. 2000). However, the impacts of WWTP effluent and stream eutrophication on *Cladophora* and other filamentous algae have not been closely investigated (Dodds and Gudder 1992; Stevenson et al. 2006).

The purpose of this study was to investigate the effects of effluent from a WWTP of a small city in western Oklahoma on the nitrogen and phosphorus levels on the downstream water. The ability of this second order stream to ameliorate changes in nutrient levels was evaluated. In addition, the potential effects of effluent on growth of two filamentous algae (*Cladophora* and *Spirogyra*) resident in the receiving stream were investigated.

Materials and Methods

Sample Sites. Water sample collection sites (Fig. 1) were established on Little Deep Creek, a second order stream in Custer County OK, relative to the effluent release point of the Weatherford, OK waste water treatment plant. The stream is approximately 14 km in length and is located in the Cross Timbers Transition and the Rolling Red Hills Ecoregions of Oklahoma (Woods et al. 2005). Little Deep Creek carries water the year around and originates in springs in the Weatherford Gypsum Hills formation located west of the city (Fay et al. 1978). Water from Little Deep Creek empties into Deer Creek which in turn empties into the Canadian River. Water carried by Little Deep Creek ultimately ends up being released into the Gulf of Mexico as these streams are a part of the Mississippi River Basin.

Weatherford, OK is a small city with a population of just under 11,000 according to the 2010 U.S. census. Waste water carried by the city's sanitary sewers undergoes primary and secondary treatment in a modern WWTP

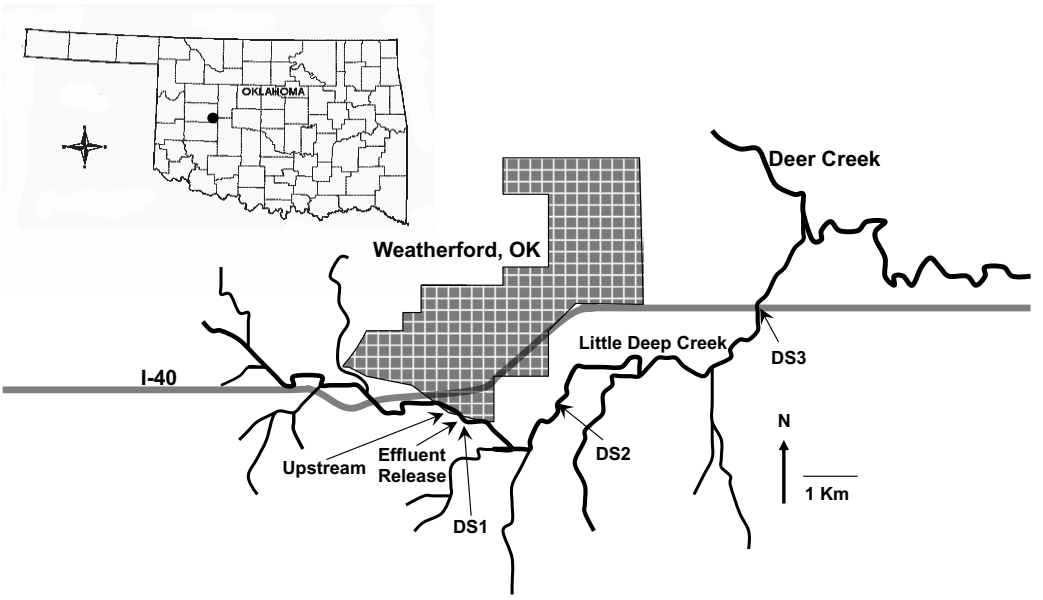

Figure 1. Map showing the location of Little Deep Creek and the sampling sites along the stream channel.

before being discharged into the receiving stream. The WWTP is rated to handle 7,571 m^3 of sewage per day but typically handles significantly less sewage. For example, during this study the average sewage volume processed in April 2012 was 4,000 m^3 per day (maximum = 5061 m^3 per day; minimum = 3021 m^3 per day). Information about the Weatherford WWTP was provided by Mr. Jack Olsen, who was the plants superintendent at the time of the study. Treated effluent is released into Little Deep Creek at latitude 35°31'4.53"N and longitude 98°41'55.23"W. Stream water prior to the addition of the effluent was collected approximately 70 meters upstream of the effluent release (Upstream site). Three downstream sites (Fig. 1) were established to monitor effects of the WWTP effluent addition. The first downstream site (DS-1) was located approximately 70 meters downstream of the effluent release. Sites DS-2 and DS-3 were located 3km and 8.25 km respectively downstream of the effluent release. Stream discharge at the upstream site was estimated on April 02 2012 by direct measurement of stream cross sectional area and average stream flow using a Marsh-McBirney Portable Water Flow Meter (Model 201D).

Stream Conditions and Effluent Nutrient Analysis. Duplicate readings of water temperature, dissolved oxygen, pH, and conductivity were made with a YSI Multi Probe System (Model 556) at the time of water sample collection and other times during the study period. We collected triplicate water samples at each of the Little Deep Creek stream sites and WWTP effluent on three dates (January 23, March 12, & April 02, 2012). Samples were collected in 125 mL sterile sample bags directly from the stream and from the effluent just before it entered the stream. Samples were returned to the laboratory where they were immediately filtered through Whatman 42 filter paper and refrigerated. The samples were analyzed within 4 days of collection for total-P, ammonia-N and nitrate-N using Hach test procedures and a Hach DR 2700 spectrophotometer (Hach Spectrophotometric Procedure Manual, DOC086.98.00801, 2009.

Nutrient uptake lengths for the three nutrients were calculated using the combined averages of the three sample dates at each location. The calculation used was that proposed by Marti et al. (1997), but modified by substituting electrical conductivity for chloride concentrations to determine dilution effects downstream of the effluent release. The formula used was:

$$\mathbf{N_x = N_i \cdot (Cond_x / Cond_i) \cdot e^{-bx}}$$

where N is the nutrient concentration and Cond is conductivity level at station DS-1 (i) and x is the distance where downstream levels are measure (DS-3). The nutrient uptake length is the inverse of the slope (- 1/b) and indicates the rate of removal of the effluent nutrients by stream processes. The substitution of conductivity is valid due to the fact that the upstream water is of high conductivity compared to the WWTP effluent and to surface runoff sources downstream. Furthermore, Vandenberg et al. (2005) found that monitoring of conductivity mirrored changes in chloride levels and could be used to monitor the mixing of effluent with stream water.

Algal Growth Experiments. We evaluated the potential effect of WWTP effluent on growth rates of two filamentous algae (*Cladophora glomerata*(?) and *Spirogyra grevelliana*[?]) that had previously been isolated from Little Deep Creek. The algae were grown for two weeks in batch cultures containing filter-sterilized (0.2µm microculture capsule filter, PALL Corp.) effluent diluted with filter-sterilized upstream stream water. Dilution treatments tested were 0%, 10%, 25%, 50%, and 100% effluent. Growth chamber (Percival Model E-30B) conditions were 25 C, 150 µmoles photons x m^{-2} x s^{-1}, and 16h:8h photoperiod. Clumps of algal biomass used to inoculate culture flasks were standardized by visually estimating biomass added to porcelain spot plates. Clumps were assigned to treatments using a table of random numbers and initial biomass inoculated was estimated as the average of 8 additional replicate clumps. Growth rate was measured as change in dry mass of algae in 4 replicates cultures per dilution.

Statistical Analysis. Data on stream

conditions, nutrient levels, and algal growth rates were analyzed with one-way and two way ANOVA along with Tukey's multiple comparison to identify differences between sample sites or sample dates using Graphpad Prism version 8.4.3 for MacOS, GraphPad Software, San Diego, California USA, www.graphpad.com. Values presented are means ± 1 standard deviation.

Results

Stream and Effluent Conditions. Temperature and dissolved oxygen were not significantly different between any of the sample sites and WWTP effluent (Fig. 2A & B). The pH at the DS-1 site was significantly lower ($p = 0.0146$) than at the DS-3 site but all other site comparisons yielded no significant differences in pH (Fig 2C). Conductivity measurements exhibited the most differences between the collection sites (Fig. 2D). The WWTP effluent was significantly lower in conductivity compared to the upstream water ($p = 0.001$). This difference is likely due to the different sources of the water. The upstream water originates from springs in the Weatherford Gypsum Hills formation located just to the west of Weatherford and is rich in calcium and sulfate ions. The water in the WWTP effluent originates from wells that draw from the Rush Springs Aquifer which lies below the gypsum layers of the geological formation (Fay et al. 1978). The upstream discharge of Little Deep Creek on April 02, 2012 was measured to be 6,647 $m^3 \cdot d^{-1}$. Using the April average effluent discharge of 4100 $m^3 \cdot d^{-1}$, the WWTP effluent comprised approximately 38% of the downstream flow. Predicted DS-1 site conductivity based on the above dilution factors and conductivity levels in the upstream water and the effluent was 1189 µS which is in good agreement with the measured value of 1139 µS. The dilution of the upstream water by the effluent and also by water from tributaries entering Little Deep Creek downstream of the effluent release (Fig. 1) was apparent in the decreasing conductivity at the DS-1, DS-2 ($p = 0.0003$), and DS-3 sites ($p < 0.0001$) compared to the upstream site.

Collection site nutrient levels. Nitrate-N concentrations at the upstream site were not significantly different on the three sampling dates (Fig. 3A) and averaged 1.42 ± 0.30 mg $\cdot L^{-1}$ (Fig. 3D). The WWTP effluent had significantly ($P < 0.0001$) higher levels of nitrate-N compared to the stream water and averaged 8.44 ± 3.27 mg $\cdot L^{-1}$. Effluent nitrate-N increased significantly ($P < 0.0001$) from the January 23 to April 02 sampling dates (Fig. 3A). The average nitrate-N at the DS-1 site (Fig. 3D) was statistically higher than the upstream concentration ($P < 0.0001$). The DS-1 April 02 sample had significantly higher nitrate-N levels ($P < 0.05$) than either of the January 23 and March 12 samples (Fig. 3A). Nitrate-N concentrations at all downstream sites (Fig. 3D) were significantly higher than the upstream concentration ($P < 0.0001$) and did not vary significantly by date ($P > 0.60$). The DS-3 nitrate-N level was not significantly different from the DS-2 level ($P = 0.92$) but was significantly lower ($P = 0.02$) than the level measured at DS-1 (Fig. 3D). Nutrient uptake length calculated for nitrate-N was unclear in that after accounting for dilution effects, the concentration of nitrate-N increased by about 4% between the DS-1 and DS-3 sites.

Ammonia-N concentrations at the upstream site showed significant differences between the three sample dates (Fig. 3B) with the March 12 date being significantly higher than the other dates ($P < 0.05$). Ammonia levels were below the detectable levels on the April 02 date. The WWTP effluent ammonia-N average concentration was significantly higher ($P < 0.0001$) than at the upstream site (Fig. 3E) and showed a high degree of variability between sample dates (Fig. 3B). The January 23 sample concentration was significantly higher ($P < 0.0001$) than concentrations for the March 12 and the April 02 sample dates (Fig. 3B). The DS-1 ammonia-N levels were significantly higher ($P < 0.0001$) than the levels measured at the upstream sample and significantly lower than the effluent levels ($P < 0.0001$) (Fig. 3E). The DS-2 and DS-3 ammonia-N levels were not statistically different than the upstream levels ($P = 0.23$, DS-2; $P = 0.51$, DS-3) but were significantly lower than levels at the DS-1 site ($P < 0.0001$). Nutrient uptake length for ammonia-N was

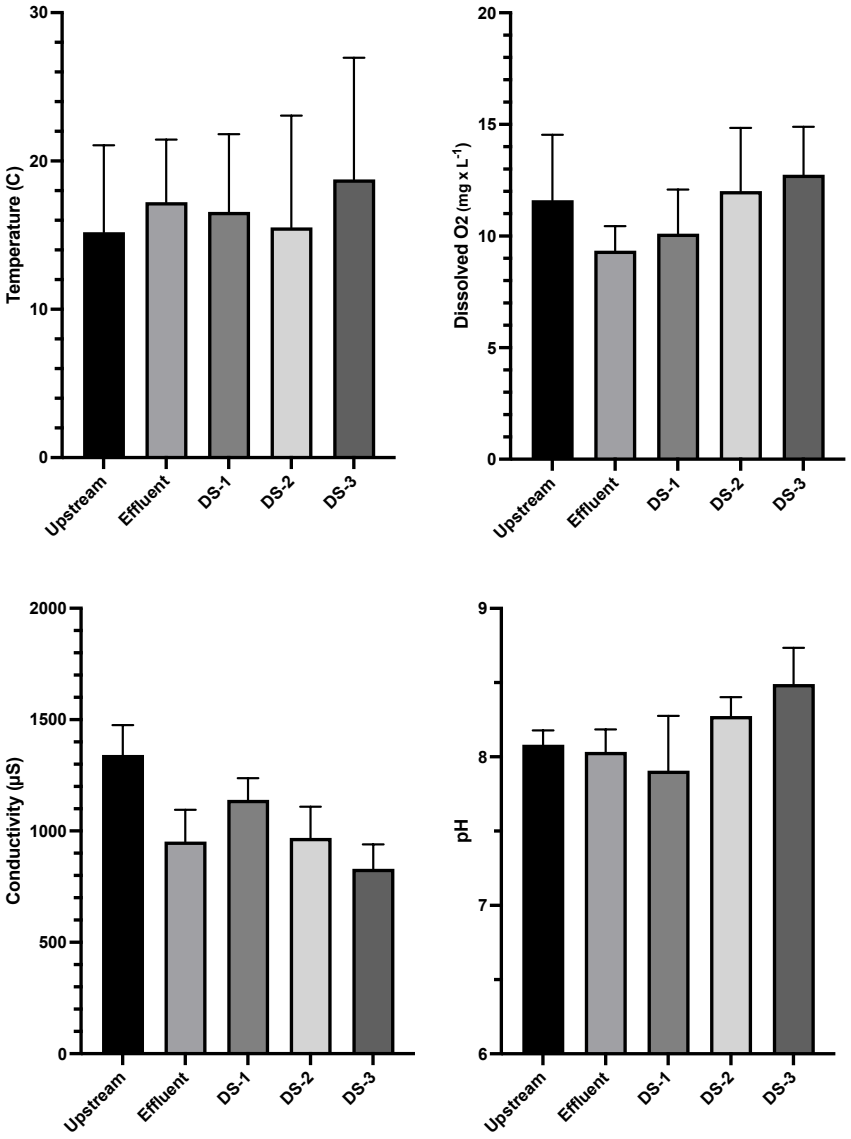

Figure 2. Physical/chemical conditions at the five sample sites. Bars represent means of measurements made on the three sample dates. Error bars represent one standard deviation.

calculated to be 11.2 km. Ammonia-N showed a 39% reduction in concentration between the DS-1 and DS-3 sites after accounting for estimated dilution effects.

Total phosphorus concentrations at the upstream site were not significantly different ($P > 0.90$) on the three sample dates sampled (Fig. 3C) and averaged 0.07 ± 0.017 mg · L^{-1} (Fig. 3F) . The WWTP effluent total phosphorus was significantly higher than the upstream water ($P < 0.0001$) (Fig. 3F) and averaged 2.04 ± 0.73 mg · L^{-1} (Fig. 3D). Total phosphorus in the effluent varied significantly between sample dates ($P < 0.0001$), and was lowest in the March 12 sample and highest in the April 02 sample (Fig. 3C). Total phosphorus concentrations measured at the three downstream sites were significantly higher than in the water at the upstream site ($P < 0.0001$), and differed significantly from the effluent ($P < 0.0001$) and each other ($P < 0.003$) (Fig. 3F). Nutrient uptake length for

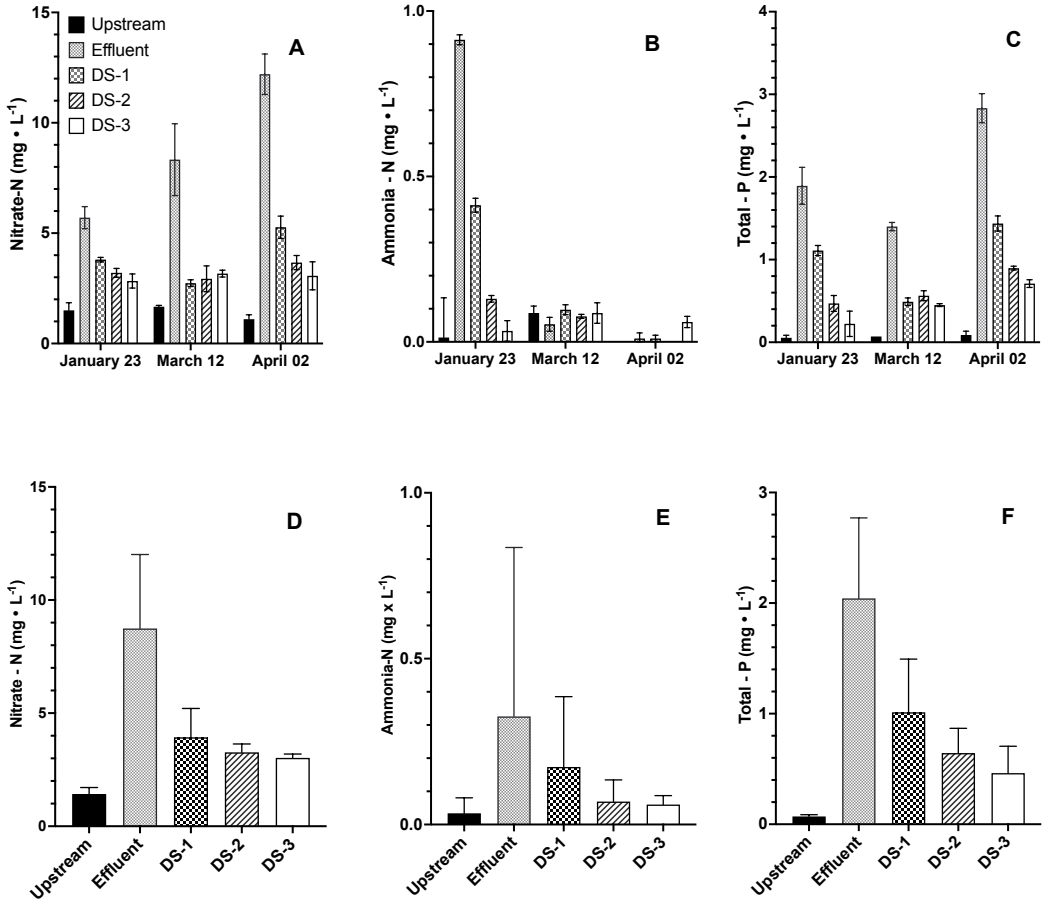

Figure 3. Nutrient concentrations measured at the stream sample sites on the three sample dates (Figs 3A-C). Comparison of nutrient concentrations at the five sample sites over the course of the study by combining measurements from the three sample dates (Figs 3D-F). Bars represent means based on triplicate samples and error bars represent one standard deviation.

total phosphorus was calculated to be 17.6 km. Total phosphorus showed a 27% reduction in concentration between the DS-1 and DS-3 sites after accounting for dilution effects.

The ratio of total nitrogen to total phosphorus (N/P) was calculated by adding the nitrate-N and ammonia-N and dividing by the total phosphorus for each sample and the results are presented in Figure 4. The upstream site water had a N/P ratio of 21.9 ± 8.18. The WWTP effluent had a significantly lower ratio of 4.59 ± 1.27 ($P = 0.003$). Ratios in the downstream samples (DS-1, DS-2, DS-3) were also significantly lower than the upstream ratio ($P < 0.01$) but not significantly different from the effluent or each other ($P > 0.72$).

Algal Growth Assay. Both of the filamentous algae isolated from Little Deep Creek showed nearly identical growth rates in the upstream water (*Spirogyra* = 0.121 ± 0.009 and *Cladophora* = 0.120 ± 0.008, $\mu \cdot d^{-1}$) (Fig. 5). Growth rate of *Spirogyra* increased 36% to 0.166 ± 0.003 $\mu \cdot d^{-1}$ when grown in a mixture of 10% WWTP effluent in upstream water ($P < 0001$). The elevated growth rate did not change when *Spirogyra* was grown in mixtures that had increased levels of effluent (25%, 50%, and 100%). *Cladophora* also exhibited a significant increase in growth rate in the 10% effluent treatment (0.152 ± 0.002 $\mu \cdot d^{-1}$, $P <$

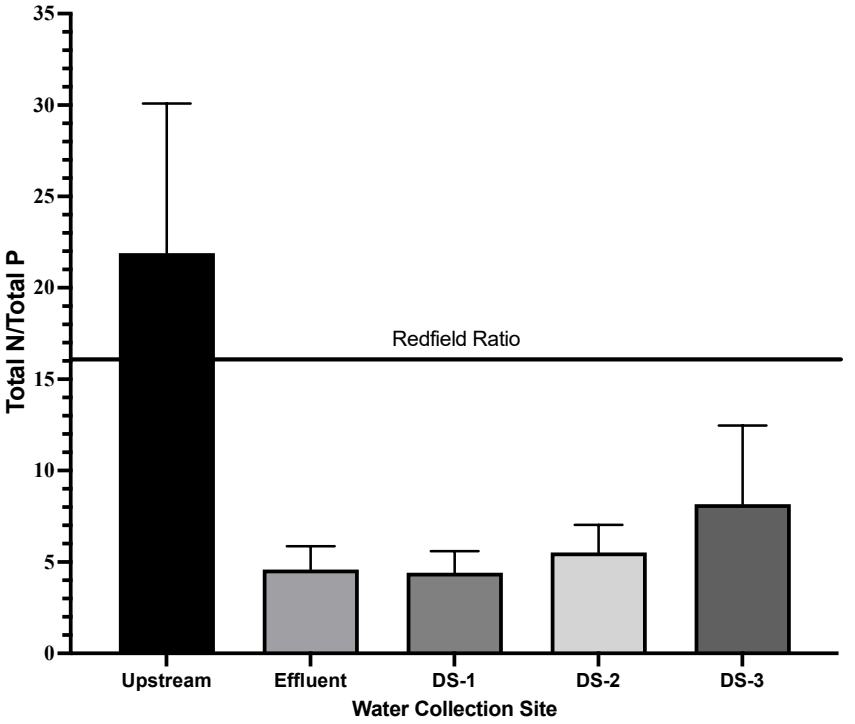

Figure 4. Comparison of N/P ratios at the five samples sites based on combined measurements on the three sample dates. Total nitrogen was obtained by summing nitrate-N and ammonia-N. Bars represent means and error bars represent one standard deviation.

0.0001) that was 27% greater than the growth rate in the upstream water. However, in contrast to the response seen in *Spirogyra*, *Cladophora* dropped back to a rate statistically identical to the growth rate in upstream water in both the 25% and 50% effluent treatment. *Cladophora* growth rate dropped to 60% of the rate measured in upstream water in the 100% effluent treatment (0.072 ± 0.008 $\mu \cdot d^{-1}$, $P < 0.0001$).

Discussion

The effluent discharge from the Weatherford WWTP significantly affected the nutrient conditions in Little Deep Creek with respect to both concentration and N:P stoichiometry. Concentrations of nitrate-N, ammonia-N, and total phosphorus were increased on average by 177%, 900%, and 1342% respectively at the DS-1 site compared to the Little Deep Creek upstream water. Similar increases in downstream nutrient levels due to WWTP effluent have been reported in other studies (Andersen et al. 2004; Ekka et al. 2006; Migliaccio et al. 2007; Popova et al. 2006; Waiser et al. 2011). The release of effluent greatly altered the trophic status of Little Deep Creek. Nutrient levels in the upstream water (total N = 1.42 mg $\cdot$ L^{-1}; total P = 0.07 mg $\cdot$ L^{-1}) place Little Deep Creek into the mesotrophic category (total N = 0.7 to 1.5 mg $\cdot$ L^{-1}; total P = 0.025 to 0.075 mg $\cdot$ L^{-1}) proposed by Dodd et al. (1998). In contrast, nutrient levels at the DS-3 site (total N = 3.08 mg $\cdot$ L^{-1}; total P = 0.46 mg $\cdot$ L^{-1}) located 8.25 Km downstream of the effluent release indicate the trophic status was well into the eutrophic range.

The elevated levels of nitrogen and phosphorus downstream of the effluent release are at levels that could potentially have effects on the stream macroinvertebrates and fish communities. For example, several studies have reported critical nutrient threshold values of total N = 1.0 mg $\cdot$ L^{-1}, total P = 0.06 mg $\cdot$ L^{-1} (Evans-White et al. 2009); total N = 0.61 mg $\cdot$ L^{-1}, total P = 0.06 mg $\cdot$ L^{-1} (Miltner and Rankin 1998); total N = 0.39 - 0.98 mg $\cdot$ L^{-1}, total P = 0.10 mg $\cdot$ L^{-1} (Chambers et al. 2012) above which

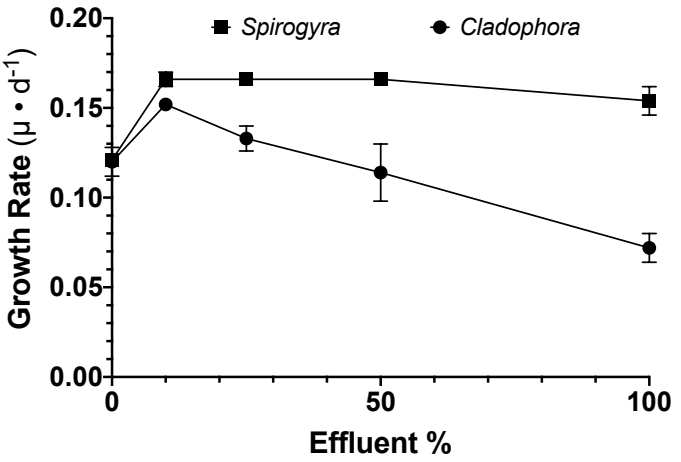

Figure 5. Growth rates of *Cladophora* sp. and *Spirogyra grevelliana* measured in dilutions of WWTP effluent. The 0% dilution is upstream water and other dilutions are made with effluent and upstream water. Symbols represent means and error bars represent one standard deviation. Four replicate cultures were measured for each data point.

macroinvertebrates and fish assemblages may be affected. In this study, total nitrogen and total phosphorus at all the downstream sites greatly exceeded these critical levels, making it likely that the downstream biological community in Little Deep Creek is impacted by the elevated nutrient concentrations. Furthermore, N:P ratios at the downstream sites indicate a shift from phosphorus limitation in the upstream water to a strong nitrogen limitation below the effluent release (Fig. 5) due to high levels of phosphorus relative to nitrogen in the WWTP effluent. Shifts in nitrogen and phosphorus stoichiometry have been linked to shifts in stream assemblages of algae (Stelzer and Lambert 2001; Felisberto et al. 2011) macroinvertebrates (Evans-White et al. 2009, Yun and An 2016) and fish (Yun and An 2016). Based on published research, the nutrient changes in Little Deep Creek caused by the effluent release from the Weatherford, OK WWTP are likely to impact the downstream biological communities.

Biological and physical-chemical processes in streams have been shown to alter and remove nutrients moving downstream (Chaubey et al. 2007) and that low order streams like, Little Deep Creek, play a significant role in this nutrient processing in stream systems (Peterson et al. 2001). One measure of the effectiveness of nutrient processing is the nutrient retention length in the stream. Previous studies have reported that in pristine streams nutrient uptake lengths are short indicating a high efficiency of nutrient retention. Nutrient uptake lengths were measured to be 0.37 km for PO_4-P and 0.549 to 1.839 km for NO_3-N in two headwater streams in Idaho (Davis and Minshall 1999). In two second order streams (one in North Carolina and one in Oregon), phosphorus (SRP) uptake lengths ranged from 0.032 to 1.00 km and NO_3-N ranged from 0.017 to 1.278 km (Munn and Meyer 1990). In a second order stream in Arkansas, the range of measure nutrient uptake lengths were 0.036 to 0.309 km for PO_4-P, 0.018 to 0.197 km for NH_4-N, but NO_3-N increased downstream indicating no retention of NO_3-N (Chaubey et al. 2007).

Streams that receive elevated nutrients from point sources have significantly longer uptake lengths than nonpolluted streams (Martí et al. 2004). Martí et al. (2004) hypothesized that streams receiving high levels of nutrients from waste water treatments plants would have lower nutrient retention efficiencies due to saturation of the stream communities with the nutrients and their results supported this hypothesis. Streams in their study that showed a decline in nutrient concentrations downstream from nutrient

inputs had measured uptake lengths of 0.140 to 29.00 km for dissolved inorganic nitrogen and 0.140 to 14.00 km for phosphate. In addition, 40 - 45% of the streams they studied showed no significant decline in nutrients measured suggesting nutrient saturation of these streams. Haggard et al. (2005) also found a significant impact of a WWTP on the nutrients of Columbia Hollow, a 3rd order stream in the Ozark Plateau in Arkansas. In this study, uptake lengths were estimated between 6.80 to 13.40 km for soluble reactive phosphorus and 0.40 to 1.40 km for ammonia-N. Downstream nitrate-N resulted in negative values in Columbia Hollow which the authors interpreted as indicating no significant uptake and retention of nitrate by the stream. Little Deep Creek in our study had estimated uptake lengths of 17.60 Km for Total P and 11.20 Km for ammonia-N. Nitrate-N did not decline downstream of the effluent release suggesting that the stream community was saturated by nitrate-N like many of the streams in the Martí et al. (2004) study and in the Haggard et al. (2005) study. These results suggest that high nitrogen and phosphorus inputs from the WWTP have impaired the ability of Little Deep Creek to efficiently process and remove these nutrients as hypothesized by Martí et al. (2204).

With respect to nitrogen levels in Little Deep Creek, differences seen between the three sample dates (January 23 to April 02) show a decline in ammonia-N that coincides with an increase in nitrate-N in the samples from the WWTP effluent and the downstream samples (Fig 3A & B), suggesting that nitrification increased over this time period as temperatures increased. Shammas (1986) reported that nitrification was sensitive to temperature changes and measured significant drops in ammonia oxidation rates in nitrifying sludge at temperatures below 15 C. This suggests that ammonia-N levels during the late spring and summer months would be at their lowest levels due to high levels of nitrification. Our results appear similar to those of Haggard et al. (2005) in that nitrogen dynamics in Little Deep Creek appear to be dominated by conversion of ammonia-N to nitrate but little evidence of nitrogen retention by the stream.

Municipal sewage effluent may affect algae in receiving streams by elevating concentrations of growth stimulating nutrients (Carey and Migliaccio 2009) but also by introducing toxic substances that may by inhibitory to growth (Smital et al. 2011). Exposure of *Cladophora* and *Spirogyra* isolated from Little Deep Creek to different dilutions of sewage effluent and upstream water produced both growth stimulation and inhibition that was dependent on the dilution level and the type of alga. Both algae exhibited significant increases in growth rate at the lowest effluent concentration (10%). *Spirogyra* growth rate remained at this elevated level as effluent concentration increased up to 100%. In contrast, the growth rate of *Cladophora* declined with increasing effluent concentration and was inhibited 40% below the rate in the control treatment (upstream water) in 100% effluent. This inhibition of *Cladophora* growth at high WWTP effluent levels suggest some minor toxicity is present in the effluent. These results suggest that the release of WWTP effluent into Little Deep Creek could alter competitive interactions between these two filamentous algae. Since these algae exhibited identical growth rates in the unaltered upstream water, they would normally be in a competitive balance with neither being able to outgrow the other, all else being equal. We estimate that the released WWTP would be diluted to approximately 38% by mixing with the upstream flow (see Results). Growth rate of *Spirogyra* would be 34% greater than that of *Cladophora* at this effluent dilution level, suggesting an enhanced competitive ability for *Spirogyra* downstream of the effluent release.

Our results indicate a significant elevation in concentrations of nitrogen and phosphorus in Little Deep Creek downstream the WWTP effluent release compared to upstream concentrations. These alterations in nitrogen and phosphorus concentrations and in the N/P ratio suggest a likely effect on the composition and functioning of the downstream biological communities, based on previously published studies. The high inputs of the nutrients in the effluent have impaired the ability of the stream to remove the nutrients as indicated

by large effective uptake lengths of total-P and ammonia-N. No uptake of nitrate-N was measured over the 8.25 km sampling length in the study which indicates that Little Deep Creek would act as a point source of nitrate-N for Deer Creek, the receiving stream. The algal growth experiment further supports the potential for the WWTP effluent to alter interactions between organisms in Little Deep Creek through differential effects on growth rates and toxicity. Our study shows that the impacts of small municipal WWTPs can have significant effects on the functioning of stream communities in low order streams.

Acknowledgements

Funding for this research and release time for S.W. O'Neal was provided by the Department of Biological Sciences and the Office of the Dean for Arts and Sciences at Southwestern Oklahoma State University. We would like to thank Mr. Jack Olsen, superintendent of the City of Weatherford sewage treatment facility, for permission to sample in the facility and providing information on facility operations at the time of this study.

References

Andersen CB, Lewis GP, Sargent KA. 2004. Influence of wastewater-treatment effluent on concentrations and fluxes of solutes in the Bush River, South Carolina, during extreme drought conditions. Environ Geosci 11:28-41.

Carey RO, Migliaccio KW. 2009. Contribution of wastewater treatment plant effluents to nutrient dynamics in aquatic systems: a review. Environ Manage 44:205-217.

Chambers PA, McGoldrick DJ, Brua RB, Vis C, Culp JM, Benoy,GA. 2012. Development of environmental thresholds for nitrogen and phosphorus in streams. J Environ Qual 41:7-20.

Chaubey I, Sahoo D, Haggard BE, Matlock MD, Costello, TA. 2007. Nutrient retention, nutrient limitation, and sediment-nutrient interactions in a pasture-dominated stream. Trans ASABE 50:35-44.

Davis JC, Minshall, GW. 1999. Nitrogen and phosphorus uptake in two Idaho (USA) headwater wilderness streams. Oecologia 119:247-255.

Dodds WK, Gudder DA. 1992. The ecology of *Cladophora*. J Phycol 28:415-427.

Dodds WK, Jones JR, Welch EB. 1998. Suggested classification of stream trophic state: distributions of temperate stream types by chlorophyll, total nitrogen, and phosphorus. Water Res 32:1455-1462.

Dodds WK, SmithVH. 2016. Nitrogen, phosphorus, and eutrophication in streams. Inland Waters 6:155-164.

Ekka SA, Haggard BE, Matlock MD, Chaubey I. 2006. Dissolved phosphorus concentrations and sediment interactions in effluent–dominated Ozark streams. Ecolog Engineering 26:375-391.

Ensminger I, Hagen C, Braune W. 2000. Strategies providing success in a variable habitat: I. Relationships of environmental factors and dominance of *Cladophora glomerata*. Plant, Cell & Environment 23:1119-28.

Evans-White MA, Dodds WK, Huggins DG, Baker DS. 2009. Thresholds in macroinvertebrate biodiversity and stoichiometry across water-quality gradients in Central Plains (USA) streams. *J North Amer Bentholog Soc 28*:855-868.

Fay RO. 1978. Geology and Mineral Resources (exclusive of Petroleum) of Custer County, *OK, Bulletin 114, 1978*. Oklahoma Geological Survey.

Felisberto SA, Leandrini JA, Rodrigues L. 2011. Effects of nutrients enrichment on algal communities: an experimental in mesocosms approach. Acta Limnologica Brasiliensia 23:128-137.

Haggard BE, Stanley EH, Storm, DE. 2005. Nutrient retention in a point-source-enriched stream. J North Amer Bentholog Soc 24:29-47.

Justić D, Rabalais NN, Turner RE, Dortch Q. 1995. Changes in nutrient structure of river-dominated coastal waters: stoichiometric nutrient balance and its consequences. Estuarine, Coastal and Shelf Science 40:339-356.

Martí E, Grimm NB, Fisher SG. 1997. Pre- and post-flood retention efficiency of nitrogen in a Sonoran Desert stream. J North Amer Bentholog Soc 16:805-819.

Marti E, Aumatell J, Godé L, Poch M, Sabater F. 2004. Nutrient retention efficiency in streams receiving inputs from wastewater treatment plants. J Environ Qual 33:285-293.

Migliaccio KW, Haggard BE, Chaubey I, Matlock MD. 2007. Linking watershed subbasin characteristics to water quality parameters in War Eagle Creek watershed. Trans ASABE 50:2007-2016.

Miltner RJ, Rankin AET. 1998. Primary nutrients and the biotic integrity of rivers and streams. Freshwater Biol 40:145-158.

Munn NL, Meyer JL. 1990. Habitat-specific solute retention in two small streams: an intersite comparison. Ecol 71:2069-2082.

Peterson BJ, Wollheim WM, Mulholland PJ, Webster JR, Meyer JL, Tank JL, Martí E, Bowden WB, Valett HM, Hershey AE, McDowell WH. 2001. Control of nitrogen export from watersheds by headwater streams. Sci 292:86-90.

Popova YA, Keyworth VG, Haggard BE, Storm DE, Lynch RA, Payton ME. 2006. Stream nutrient limitation and sediment interactions in the Eucha-Spavinaw Basin. J Soil Water Conserv 61:105-115.

Shammas NK. 1986. Interactions of temperature, pH, and biomass on the nitrification process. J Water Pollut Control Fed 58:52-59.

Smital T, Terzic S, Zaja R, Senta I, Pivcevic B, Popovic M, Mikac I, Tollefsen KE, Thomas KV, Ahel M. 2011. Assessment of toxicological profiles of the municipal wastewater effluents using chemical analyses and bioassays. Ecotoxicol Environ Safety 74:844-851.

Smith VH, Tilman GD, Nekola JC. 1999. Eutrophication: impacts of excess nutrient inputs on freshwater, marine, and terrestrial ecosystems. Environ Pollut 100:179-196.

Stelzer RS, Lamberti GA. 2001. Effects of N:P ratio and total nutrient concentration on stream periphyton community structure, biomass, and elemental composition. Limnol Oceanogr 46:356-367.

Stevenson RJ, Bennett BJ, Jordan DN, French RD. 2012. Phosphorus regulates stream injury by filamentous green algae, DO, and pH with thresholds in responses. Hydrobiologia 695:25-42.

USEPA. 2006. Wadeable Stream Assessment: a collaborative survey of the nation's streams. EPA 841-B-06-002, Washington, DC, USA.

USEPA. 2016. Clean Watersheds Needs Survey 2012. Report to Congress. EPA 830-R-15005, Washington, DC, USA.

Vandenberg JA, Ryan MC, Nuell DD, Chu A. 2005. Field evaluation of mixing length and attenuation of nutrients and fecal coliform in a wastewater effluent plume. Environ Monitoring Assess 107:45-57.

Waiser MJ, Tumber V, Holm J. 2011. Effluent-dominated streams. Part 1: Presence and effects of excess nitrogen and phosphorus in Wascana Creek, Saskatchewan, Canada. Environ Toxicol Chem 30:496-507.

Woods AJ, Omernik JM, Butler DR. 2005. Ecoregions of Oklahoma. US Geological Survey.

Yun YJ, An KG. 2016. Roles of N: P ratios on trophic structures and ecological stream health in lotic ecosystems. Water 8:22.

Submitted March 6, 2023 Accepted November 16, 2023

Development of Environmental DNA Assay for Screening of Blanchard's Cricket Frog (*Acris blanchardi*) Via Laboratory and Field Methods in Oklahoma, USA

Jessa L. Watters*
Sam Noble Museum, University of Oklahoma, Norman, OK 73072

Tamaki Yuri**
Sam Noble Museum, University of Oklahoma, Norman, OK 73072

Elyse S. Freitas
Sam Noble Museum, University of Oklahoma, Norman, OK 73072; School of Biological Sciences, University of Oklahoma, Norman, OK 73019

Lara Souza
Oklahoma Biological Survey, Norman, OK 73019; School of Biological Sciences, University of Oklahoma, Norman, OK 73019

Sierra N. Smith
Sam Noble Museum, University of Oklahoma, Norman, OK 73072; School of Biological Sciences, University of Oklahoma, Norman, OK 73019

Cameron D. Siler
Sam Noble Museum, University of Oklahoma, Norman, OK 73072; School of Biological Sciences, University of Oklahoma, Norman, OK 73019

Abstract: Amphibians represent one of the most threatened vertebrate groups, and although monitoring amphibian population dynamics is critical for conservation, most traditional survey efforts depend on time-consuming, often invasive monitoring activities and visual surveys. Screening environmental DNA (eDNA), a non-invasive monitoring technique, has the potential to identify species presence at a site, even in the absence of visual confirmation. In this study, we developed an aquatic eDNA detection protocol for a common and widespread frog species in Oklahoma (*Acris blanchardi*). We first conducted three laboratory tests to examine assay specificity and sensitivity. Once the primer-probe assay was confirmed to discriminate the target species from others consistently, we then sampled eDNA in four of Oklahoma's six ecological regions to assess how the variation of abiotic factors impact assay sensitivity. In field testing of over 500 samples, we were able to detect *A. blanchardi* eDNA at 60% of the waterbodies sampled, at nearly all field sites across all sampled ecoregions. The proportion of negative eDNA assay results in the waterbodies where the target species were visually observed underscore the importance of continuing traditional surveys alongside newer genetic screening techniques to improve species detection and occupancy modeling.

***Corresponding author: jwatters@ou.edu**

****Current address: Museum of Biological Diversity, Ohio State University, Columbus, OH 43212**

Introduction

Our planet is facing a biodiversity crisis, with extinctions increasing at unprecedented rates due to anthropogenic activities (Campbell Grant et al. 2020, Ford et al. 2020, Green et al. 2020). Among vertebrate taxa, amphibians are among the most impacted groups of species—it is currently estimated that 40% of the world's amphibians are threatened (Bolochio et al. 2020). Factors synergistically affecting amphibian populations include climate change, habitat loss, pollution, invasive species, and the proliferation of diseases such as the fungal pathogen *Batrachochytrium dendrobatidis* (Cohen et al. 2019; Campbell Grant et al. 2020; Ford et al. 2020). Therefore, it is critical to closely monitor changes in amphibian populations at a variety of geographic and temporal scales to observe population trends and develop effective conservation strategies (Canessa et al. 2019). However, nearly all amphibian conservation efforts depend on time-consuming visual surveys or invasive capturing activities, such as trapping, seining, dip netting, or hand-capture (Goldberg et al. 2015, 2016; McGrath et al. 2015; Thomsen and Willerslev 2015). These traditional methods require special equipment, training, and permits, making field work logistically challenging (Ficetola et al. 2019; Ruppert et al. 2019). Additionally, these methods often fail to locate rare or cryptic species, resulting in false negatives where species are undetected but actually present (McGrath et al. 2015; Ruppert et al. 2019). Therefore, many researchers have begun investigating and implementing innovative methods for species monitoring, including surveys by unmanned aerial vehicles (UAVs or drones), automated acoustic identification, and environmental DNA (eDNA) detection from air, water, or soil samples (e.g., Chabot and Bird 2015; Goldberg et al. 2015; Russo and Voigt 2016; Lynggaard et al. 2022). The use of eDNA to detect species in an environment is a particularly exciting development in conservation biology. Over the last decade, research efforts have focused on developing and refining eDNA assays, lab methods, and field methods to increase the efficacy of this tool for species monitoring (Goldberg et al. 2016; Harper et al. 2019; Ruppert et al. 2019; Thalinger et al. 2021).

We define eDNA as genetic material that organisms shed into their environment (e.g., within urine, feces, hair, skin, etc.). These eDNA can be collected from a study site and analyzed to determine the presence of target species in the environment without relying on traditional survey methods or disturbing the focal habitats (Wilcox et al. 2013; Diaz-Ferguson and Moyer 2014; Goldberg et al. 2015, 2016; Ficetola et al. 2019). The use of eDNA is a non-invasive approach for monitoring biodiversity that can be standardized and applied broadly across taxa and ecosystems (Goldberg et al. 2015; Ficetola et al. 2019; Ruppert et al. 2019) for a variety of purposes including determining community composition (Yu et al. 2012; Valentini et al. 2016; Lopes et al. 2017; Bálint et al. 2018), detecting cryptic or rare target species at sites where they are not detected by traditional survey methods (Hobbs et al. 2019; Wineland et al. 2019), detecting invasive species (Darling and Mahon 2011; Dejean et al. 2012; Goldberg et al. 2013; Thomas et al. 2019), and screening for infectious diseases within an ecosystem (Baker et al. 2020). Additionally, eDNA tools have the potential to be applied beyond species detection; for example, eDNA has been used to estimate species abundance or biomass of individuals of a target species at a site (Takahara et al. 2012), to determine whether a site has a viable population of a target species (Kamoroff and Goldberg 2018), and to examine within-species genetic variation (Adams et al. 2019a). Therefore, eDNA tools have enormous potential to be applied towards a wide range of biodiversity- and conservation-related research questions.

To use species-specific eDNA tools to detect and monitor a target species, a genetic assay must first be developed specifically for the species and tested to ensure specificity. The ultimate goal of an eDNA assay is to detect a target species across the species' geographic range without falsely detecting non-target species. Therefore, before an assay can be used for research or species monitoring, it must be rigorously tested against the target species, its congenerics

(regardless of sympatry), and additional non-related sympatric species (Thalinger et al. 2021). Evaluating eDNA assays provides a resultant value scale from Level 1 (incomplete) to Level 5 (operational), and is composed of three parts: 1) *in silico*, where software is used to analyze assay specificity using genetic databases; 2) *in vitro*, where the assay is tested and optimized under controlled laboratory conditions; and 3) *in situ*, where the assay is thoroughly tested in the field encompassing a variety of habitats and abiotic conditions (Thalinger et al. 2021). Here we report on protocols of the development of *in silico*, *in vitro*, and *in situ* assessments of an eDNA assay for Blanchard's Cricket Frog, *Acris blanchardi* (Family Hylidae), whose North American distribution covers the central great plains regions of the United States and Canada (McCallum et al. 2011), and in some areas, is experiencing decline (Lehtinen and Skinner 2006). We selected *A. blanchardi* for assay development because this species is common and widespread throughout a variety of aquatic habitats in most ecoregions across Oklahoma (Figure 1; Sievert and Sievert 2021), allowing us to assess the efficacy of the assay in the lab and in the field across multiple local geographic/ecological regions. Additionally, since *A. blanchardi* are found in high densities along shorelines regardless of water flow levels and do not have a strong preference for specific substrates, light levels, or temperatures (Smith et al. 2003; Sievert and Sievert 2021), their genetic material is expected to be found in the majority of sampling locations within their distributed range. Although we focus on *A. blanchardi* in the current study, our ultimate goal is to create a workflow for developing eDNA assays for a diverse group of amphibians across Oklahoma.

Methods

qPCR assay development and* in silico *testing of the primer-probe pair.—The *Acris*

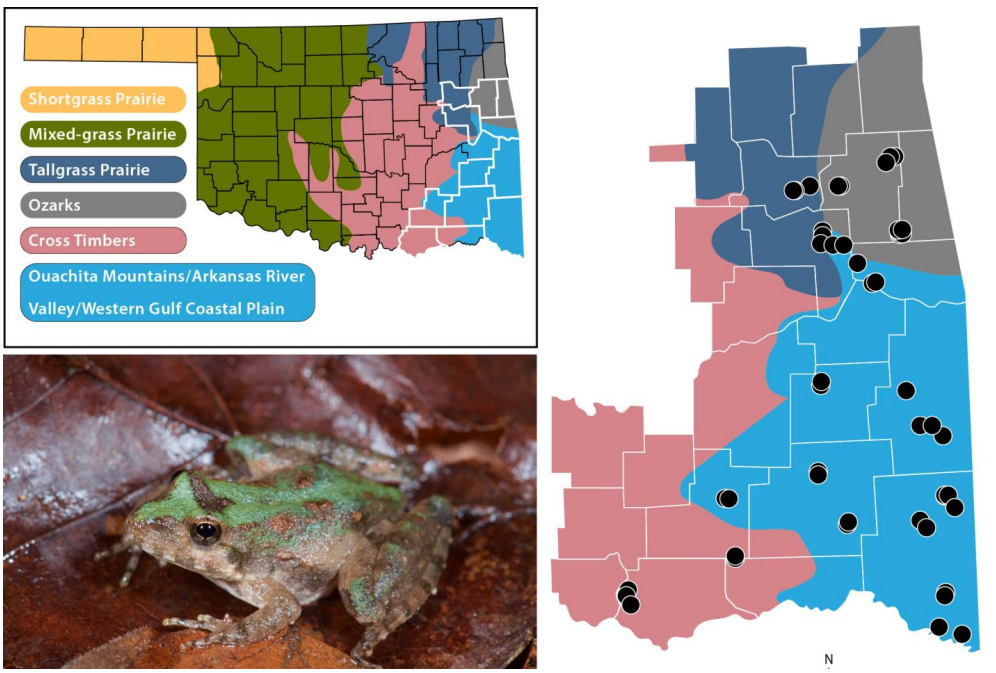

Figure 1. (Top Left) County map of Oklahoma showing the distribution of the six recognized ecoregions in Oklahoma, with counties included in the field sampling (*in situ*) portion of the study outlined in white for reference. (Bottom Left) Photograph in life of *Acris blanchardi* (Photo by K. Wang). (Right) Closeup view of aquatic waterbodies sampled in study (black circles) in eastern Oklahoma (counties outlined in white, ecoregions shown in color).

blanchardi-specific quantitative PCR (qPCR) assay was designed for the mitochondrial gene (mtDNA) cytochrome b (cytb). Mitochondrial genes are better for assay development than nuclear DNA because their faster rate of evolution when compared to nuclear DNA (Moriyama and Powell 1997) results in more species-specific single nucleotide polymorphisms (SNPs) that can distinguish one species from closely related congeneric species. We specifically chose cytb for assay development because of the availability of sequence data on GenBank (NCBI, Bethesda, MD) for multiple individuals of *A. blanchardi* and other North American anurans across a wide geographic range. Initial investigations into cytb suggested the presence of multiple *A. blanchardi*-specific single nucleotide polymorphisms (SNPs) that distinguished the species from other anurans. Other mtDNA genes, NADH dehydrogenase subunit 2 (ND2) and cytochrome c oxidase subunit I (COI), were also considered for assay development, but these genes did not have the needed *A. blanchardi*-specific SNPs.

We obtained cytb sequences of four *A. blanchardi* individuals from GenBank, from across the geographic range of the species (GenBank accession numbers: EF988109 [Illinois]; EF988144 [Mississippi]; EF988127 [Missouri]; EF9881260 [Oklahoma]) and four other anuran species that are often found in the same waterbodies as *A. blanchardi* in Oklahoma (*Anaxyrus americanus* EU938446 [Kansas]; *Pseudacris crucifer* EF988160 [Minnesota]; *Lithobates catesbeianus* AY083293 [Ohio]; *L. clamitans* AY083282 [Missouri]). We aligned the four *A. blanchardi* sequences using Geneious v9.0 (San Diego, CA) and created a consensus sequence (683 bp). The four sequences had a pairwise identity of 98.9% and were identical for 668/683 nucleotides for a site-wide identity of 97.8% (Figure 2). The consensus sequence was imported into the program Primer Express Software v3.01 (Applied Biosystems/Thermo Fisher Scientific, Waltham, MA).

We then aligned the *A. blanchardi* consensus sequence with the outgroup anuran sequences in Geneious and identified SNPs that distinguish *A. blanchardi* from the other species. For each SNP site, we used Primer Express to find acceptable sets of probe and primer sequences surrounding the SNP site, with default optimization settings (probe length = 13–25 base pairs, Tm = 68–70ºC, %GC = 30–80%). From those sets, we selected the one set with the lowest penalty score and shortest amplicon size for our assay. The resulting primers were AB_CytB_F2: 5'–CCTTTCTGCTGCCCCTTA–3' (18 bp) and AB_CytB_R1: 5'–GGTGGCGTTGTCTACTGAA–3', (19 bp) and the custom TaqMan MGB probe was 5'–CTGAGCTAGTCCAATG–3' (16 bp), with FAM reporter dye (Applied Biosystems/Thermo Fisher Scientific, Waltham, MA) (Figure 2).

To confirm that the selected primer-probe set worked across the geographic range of *A. blanchardi* beyond the four samples that were used to develop it, we aligned all 34 *A. blanchardi* cytb sequences available in GenBank as of 18 October 2021 (excluding those that were used in primer-probe design; Table S1) and compared the primer and probe to the alignment. To check if the identified primers were specific for *A. blanchardi*, we used Primer-BLAST (NCBI, Bethesda, MD; Ye et al. 2012) to compare them to additional anuran species in the GenBank database. The Primer-BLAST parameters were set as follows: Search mode

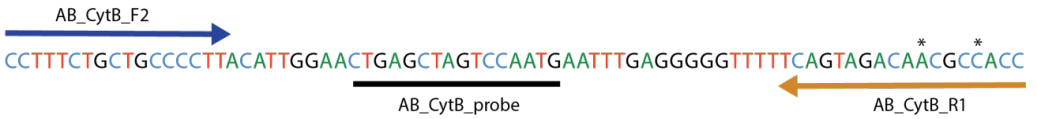

Figure 2. Quantitative PCR assay site covering 76 bp of mitochondrial cytochrome b (cytb) with the locations of forward and reverse primers, and probe. The sequence shown is the majority-rule consensus of the four *Acris blanchardi* sequences used for designing the assay. Two of four sequences include one transitional substitution in the reverse primer sequence (sites indicated by *).

= automatic; Database = nr; Primer specificity stringency = 2 total mismatches including at least 2 mismatches within the last 5 bps at the 3' ends and ignore targets that have 6 or more mismatches to the primer. The results of the Primer-BLAST search returned 57 sequences from two anuran families: Family Hylidae (*Hyla cinerea*, *Pseudacris clarkii*, *P. fouquetti*, *P. maculata*, *P. regilla*) and the Family Ranidae (*Lithobates palustris*, *L. sylvaticus*). Because Primer-BLAST only has the option to check two primers for specificity, all sequences returned in the Primer-BLAST search were downloaded into Geneious and manually compared to the probe sequence to determine the number of mismatches between those sequences and the probe sequence (Table S1). This analysis indicated that the primers were specific to *A. blanchardi* and would not cross-amplify other species.

In vitro *testing of the qPCR assay*.—To further evaluate the *A. blanchardi* eDNA assay, we ran three *in vitro* laboratory experiments using DNA extracted from tissues of the target and non-target anuran species or from dilute lab-created aquatic eDNA solutions to assess assay specificity and efficacy. All frogs used in *Experiment 2* and *Experiment 3*, described below, were euthanized via aqueous chloretone and prepared as voucher specimens for the SNM Herpetology Collection within a few hours of experiment completion, following Simmons (2015). All live anurans captured were collected under applicable Oklahoma Department of Wildlife Scientific Collecting Permits to CDS and JLW, with protocols approved by the University of Oklahoma Institutional Animal Care and Use Committee (IACUC #R14-026).

Experiment 1—testing assay using DNA extracts: The primer-probe set was first tested to ensure that it worked as expected under standard qPCR conditions and to determine validation estimates for the assay. To do this, we extracted DNA from five vouchered *A. blanchardi* tissue samples from Oklahoma (OMNH 46229 [Adair County (Co.)], 46414 [Delaware Co.], 46421–23 [Delaware Co.]; Fig. 1; Table 1) using the high salt DNA extraction method (Esselstyn et al. 2008) and created the following serial dilutions of each extraction starting from a standardized concentration of 20 ng/µl: 20.0, 2.0, 0.2, 0.02, 2×10^{-3}, 2×10^{-4}, 2×10^{-5}, 2×10^{-6} ng/µl. Each dilution was tested against the assay in triplicate using a Quant Studio 3 (Applied Biosystems/Thermo Fisher Scientific, Waltham, MA) qPCR machine following standardized protocols (Siler et al. 2020). Results of this test were used to obtain performance validation estimates for the assay, including values for the r^2, slope, efficiency, and the Limit of Detection (LoD; Klymus et al. 2020; https://github.com/cmerkes/qPCR_LOD_Calc).

Next, the qPCR assay designed for *A. blanchardi* was tested for specificity using DNA from nine anurans from Oklahoma—five individuals of *A. blanchardi* (Ellis Co., Marshall Co., McCurtain Co., Oklahoma Co., Sequoyah Co.; Table 1) and four outgroup co-distributed species (*Hyla chrysocelis/versicolor* [Latimer Co.], *Pseudacris clarkii* [Oklahoma Co.], *P. streckeri* [Le Flore Co.], *Lithobates catesbeianus* [McCurtain Co.]; Table 1). The DNA extracted from liver tissues for this test were obtained from specimens deposited at SNM using the high salt extraction method and were serially diluted to concentrations of 0.02 ng/µl and 0.002 ng/µl to simulate the low concentrations of eDNA that might be encountered in nature. We tested the qPCR assay on four of the five *A. blanchardi* extracts (excluding the individual from Sequoyah Co.) and on all four non-*Acris* species individually to confirm that the assay could detect *A. blanchardi* from multiple populations across Oklahoma without detecting the non-target species. We then tested the qPCR assay using combinations of extracts from the target and non-target species to determine whether the presence of DNA from multiple species would confound the assay and generate either false positive or negative results. To do this, we combined equal volumes of DNA of all four non-target species with and without DNA from the *A. blanchardi* individual from Sequoyah Co. (Table 1). These qPCR assay evaluation runs were conducted in duplicate on a single plate using a BioRad CFX96 Connect (Hercules, CA) following standard qPCR protocols, and

Table 1. *In vitro* testing for specificity of the *Acris blanchardi* qPCR assay, via three experimental approaches. Amplification by qPCR is represented as positive (+) or negative (–). Tissue sample acronyms are as follows: non-vouchered specimens collected by grants funded the Oklahoma Department of Wildlife Conservation (ODWC), vouchered species from Sam Noble Oklahoma Museum of Natural History (OMNH), and vouchered specimens from Louisiana State University (LSU).

Experiment 1—testing assay using DNA extracts		
Individual Species/Community Pools	Sample Numbers	Amplification
Acris blanchardi (Adair Co., OK)	OMNH 46229	+
Acris blanchardi (Delaware Co., OK)	OMNH 46414	+
Acris blanchardi (Delaware Co., OK)	OMNH 46421	+
Acris blanchardi (Delaware Co., OK)	OMNH 46422	+
Acris blanchardi (Delaware Co., OK)	OMNH 46423	+
Acris blanchardi (Ellis Co., OK)	OMNH 41666	+
Acris blanchardi (Marshall Co., OK)	OMNH 44270	+
Acris blanchardi (McCurtain Co., OK)	OMNH 44285	+
Acris blanchardi (Oklahoma Co., OK)	OMNH 44297	+
Hyla chrysocelis/versicolor (Latimer Co., OK)	OMNH 44340	–
Pseudacris clarkii (Oklahoma Co., OK)	OMNH 44432	–
Pseudacris streckeri (Le Flore Co., OK)	OMNH 44439	–
Lithobates catesbeianus (McCurtain Co., OK)	OMNH 44509	–
Mixture of *H. chrysocelis/versicolor*, *P. clarkii*, *P. streckeri*, *L. catesbeianus*, and *A. blanchardi* (Sequoyah Co., OK)	OMNH 44340, OMNH 44432, OMNH 44439, OMNH 44509, OMNH 44324	+
Mixture of *H. chrysocelis/versicolor*, *P. clarkii*, *P. streckeri*, and *L. catesbeianus* extracts	OMNH 44340, OMNH 44432, OMNH 44439, OMNH 44509	–
Acris crepitans (Tallapoosa Co., AL)	LSU H-18789	–
Acris crepitans (East Baton Rouge Parish, LA)	LSU H-20744	+
Acris gryllus (Macon Co., AL)	LSU H-18811	–
Acris gryllus (Livingston Parish, LA)	LSU H-20578	–
Experiment 2—testing assay using eDNA generated in the lab		
Individual Species/Community Pools	Sample Numbers	Amplification
Acris blanchardi (Nowata Co., OK); 250 mL	OMNH 46424	+
Acris blanchardi (Nowata Co., OK); 50 mL each, pooled to 250 mL total	OMNH 46361, OMNH 46362, OMNH 46366, OMNH 46370, ODWC 46371	+
Acris blanchardi, *Hyla chrysocelis/versicolor, Pseudacris maculata*, *Lithobates catesbeianus*, *Lithobates sphenocephalus* (all Nowata Co.); 50 mL each, pooled to 250 mL total	OMNH 46368, OMNH 46454, ODWC 46505, OMNH 46693, OMNH 46689	+
Hyla chrysocelis/versicolor, *Pseudacris maculata, Lithobates catesbeianus*, *Lithobates sphenocephalus* (all from Nowata Co., OK); 62.5 mL each, pooled to 250 mL total	OMNH 46447, OMNH 46508, OMNH 46531, OMNH 46698	–
250 mL ddH_2O water (no frogs)	---	–
Experiment 3—final efficacy testing of the assay using field and lab-generated eDNA samples		
Individual Species/Community Pools	Sample Numbers	Amplification
500 mL of pond water (N = 3) collected from Sutton Urban Wilderness (Cleveland Co., OK), within 1 ft. of live *Acris blanchardi*	---	+
Acris blanchardi (N = 1); 1 L	OMNH 47567	+
Acris blanchardi (N = 1); 2 L	OMNH 47567	+
Acris blanchardi (N = 1); 5 L	OMNH 47567	+
Acris blanchardi (N = 1); 10 L	OMNH 47567	+

the plate included a no-DNA control, also run in duplicate.

Finally, there are two additional species of *Acris* in North America; the ranges of these congenerics do not overlap with the range of *A. blanchardi* in Oklahoma although they do appear to overlap east of Oklahoma along the Mississippi River (Gamble et al. 2008). Therefore, we were interested in whether the assay could be used to distinguish *A. blanchardi* from its congenerics. We tested the assay for specificity against the species *A. crepitans* (from Tallapoosa Co., Alabama and East Baton Rouge Parish, Louisiana) and *A. gryllus* (from Macon Co., Alabama and Livingston Parish, Louisiana), obtained from tissue stored at Louisiana State University (LSU). Liver tissue for these four individuals were extracted using a DNeasy Blood and Tissue Kit (Qiagen, Hilden, Germany), and the extracted DNA was quantified and serially diluted to 1:10 and 1:100 for all four samples. A qPCR run was conducted in triplicate using standard protocols (Siler et al. 2020) on a Quant Studio 3 (Applied Biosystems/ Thermo Fisher Scientific, Waltham, MA).

Experiment 2—testing assay eDNA samples generated in the lab: The qPCR assay was tested using water samples obtained after submerging live frogs in water in a controlled laboratory setting, to determine if the assay could detect DNA that had been shed externally by a living organism into water. Frogs were collected three days before the test from Oologah Wildlife Management Reserve in Oklahoma (Nowata Co.) and were kept in captivity at the SNM. Each frog was placed individually in a separate sterilized glass jar with molecular grade distilled and deionized water (ddH_2O) and left for one hour. The following five samples of 250 mL water were created in the lab, and no individual frog was used more than once, for a total of one hour each: (1) one *A. blanchardi* (in 250 mL); (2) five *A. blanchardi* in separate jars (50 mL of ddH_2O each), then combined to form 250 mL in total; (3) one *A. blanchardi*, plus four co-distributed non-target species (*H. chrysocelis/ versicolor*, *P. maculata*, *L. catesbeianus*, *L. sphenocephalus*) in separate jars (50 mL of ddH_2O each), then combined to form 250 mL in total; (4) one each of the four non-target species in separate jars (62.5 mL of ddH_2O), then combined to form 250 mL in total; and (5) control sample of 250 mL ddH_2O and no frogs, as a negative control (Table 1). Each water sample was filtered on a separate 0.45µm pore PES filter (75 mm filter diameter) immediately after the experiment ended. The filter was stored overnight in 95% EtOH in a -20ºC freezer until the time of DNA extraction. Each experimental extraction was used in duplicate to test the qPCR assay on a QuantStudio 3 using standard qPCR protocols (Siler et al. 2020).

Experiment 3—final efficacy testing of the assay using field and lab-generated eDNA samples: An additional set of tests was conducted to evaluate the qPCR assay as well as the robustness of our filtration and extraction methods using more dilute water samples than those used in the experiment above to simulate sampling conditions in the field. Three separate 500 mL water samples were collected from the Sutton Urban Wilderness Area (Cleveland Co., Oklahoma; using the methods described below), from within one foot of a single live *A. blanchardi*. Additionally, one *A. blanchardi* individual each was collected by hand and placed sequentially into sterilized containers with 1 L, 2 L, 5 L, and 10 L of ddH_2O within four hours of capture, for a total of one hour each, to further mimic the small quantities of eDNA expected in a natural water body setting (Table 1). For all seven water samples (three from Sutton Urban Wilderness area, four from lab testing), 500 mL was filtered individually on separate 0.45µm pore PES filters (75 mm filter diameter), processed for DNA extraction and screened in triplicate on a QuantStudio 3, using standard qPCR protocols (Siler et al. 2020).

In situ *evaluation of the qPCR assay.*—We conducted preliminary *in situ* evaluation of the *A. blanchardi* qPCR assay using water samples collected across Oklahoma in spring–summer in years 2017–2018 to determine the efficacy of the assay when applied in the field. At all large-scale field sites sampled (Figure 1; Table S2), we had historical visual and/or auditory confirmation of

A. blanchardi presence and therefore expected our qPCR assay to return positive results.

Field eDNA collection and filtration.—Water samples were collected in aquatic habitats across four recognized ecoregions in eastern Oklahoma (Fig. 1; Table S2): Crosstimbers (July 2017), Ouachita Mountains/Arkansas Valley/West Gulf Coastal Plains (April–May 2017; March–May 2018), Ozarks (April–May 2018), and Tallgrass Prairie (May 2018). To minimize any seasonal factors that could impact eDNA detection (De Souza et al. 2016; Takahara et al. 2020), all field samples were collected in spring/early summer, which coincides with the active breeding season of *A. blanchardi* (McCallum et al. 2011). Our sampling scheme used the following hierarchy, represented from largest category to smallest: ecoregion (N = 4), counties (N = 11), field sites (N = 24), unique waterbodies within each field site (N = 79 total; 1–9 per field site) (Fig. 1; Table S2; Siler et al. 2020). The field sites included USDA national forests, USFWS national wildlife refuges (NWR), state parks (SP), state-run wildlife management areas (WMA), The Nature Conservancy preserves (TNCP), and public access points (PUA) affiliated with U.S. Army Corps of Engineers lakes (Table S2).

For each waterbody, 2–8 samples of 500–600 mL of water was collected 1–2 m from shore at a 5–10 cm water depth (N = 565 samples in total), using sterile 1,065 mL one-time use Whirl-pak sampling bags (Nasco, Madison, WI; Wineland et al. 2019; Siler et al. 2020). The number of samples collected per waterbody was determined based on the waterbody size and capacity to allow a minimum distance of 10 m between samples, with a maximum of eight samples regardless of waterbody size. Additionally, we created a negative control for each waterbody by filling a water sample bag with dH_2O, sealing it, and dipping the sealed bag into the water for approximately 30 seconds (N = 79 controls). Samples were stored cold, but not frozen, in a dark cooler to prevent potential DNA degradation by UV light or warm temperatures (Pilliod et al. 2013a; Strickler et al. 2015) and detection difficulties due to freezing samples prior to filtration (Takahara et al. 2014).

We filtered all samples within 24 hours of collection, maintaining strict sterility protocols, whether filtration occurred in the field or in the lab; no filtration occurred within the same space as *A. blanchardi* tissue extraction. Prior to sample filtration, all work surfaces were sterilized with ELIMINase (Decon Labs, King of Prussia, PA) or 10% bleach, and nitrile gloves were changed between each sample. Water was homogenized in the sample bag, then poured into a sterile, one-time use 500 mL polyethersulphone (PES) membrane filters, with a 75 mm filter diameter and a 0.45μm pore size (various vendors: Thermo Fisher Scientific, Waltham, MA; VWR, Radnor, PA; Foxx Life Sciences, Salem, NH). We vacuum-filtered both experimental samples and negative controls until the membranes became clogged or until 500 mL was filtered (whichever came first), cut out the filter membrane using a sterile from the sterile housing using a one-time use 11-blade scalpel, placed the membrane into a 10 mL cryovial with 95% ethanol, and stored the vial in a -20ºC freezer until the time of extraction (less than six months) (Siler et al. 2020).

Extraction and screening of eDNA samples.—All lab procedures for DNA extraction and qPCR screening were conducting at the SNM Genomics Core Facility using strict sterility protocols as described previously. For each batch of eDNA extractions, a second negative control sample was created by placing a PES membrane filter into sterile ddH_2O and extracted along with the experimental filters. We isolated total genomic eDNA using a modified protocol based on the DNeasy Blood and Tissue Kit/QIAshredder (Qiagen, Hilden, Germany; Buxton et al. 2017; Pilliod et al. 2013a; Siler et al. 2020), with additional steps for removal of PCR inhibitors using Zymo OneStep PCR Inhibitor Removal Kits (Zymo Research Products, Irvine, CA; McKee et al. 2015; Turner et al. 2015; Adams et al. 2019b; Baker et al. 2020; Siler et al. 2020). For these extractions, only one-half of each vouchered filter membrane was used, and the remaining one-half of the filter was returned to the freezer for archival purposes. The filter membrane was first diced into small pieces using forceps and scissors sterilized with

10% bleach. Because these membrane pieces did not fit in one 1.5mL microcentrifuge tubes, they were divided equally into two sterile 1.5mL microcentrifuge tubes and later combined during the QIAshredder process (Siler et al. 2020).

All eDNA extracts, including both field and laboratory created negative controls, were screened with the *A. blanchardi*-specific qPCR assay described above, following the protocols of Siler et al. (2020). All eDNA samples were tested in triplicates, which is a common protocol for samples collected from the field (Pilliod et al. 2013a,b; Barnes et al. 2014; Strickler et al. 2015; Adams et al. 2019b). A well was considered positive if it crossed the call threshold determined by the QuantStudio Design and Analysis software (v1.5.1) using the presence/absence experiment protocol. We considered *A. blanchardi* eDNA as present if two or more of the triplicate wells were called positive, or one of the triplicate wells crossed the threshold on two successive qPCR runs, following established protocols (e.g. Strickler et al. 2015; Siler et al. 2020). *Acris blanchardi* is ubiquitous across Oklahoma, and we expected each plate to have at least one positive, which acted as a positive control, and as such, these qPCR were run without additional positive controls.

Results and Discussion

Overall, our *A. blanchardi* eDNA successfully detected the presence of *A. blanchardi* in both lab (*in silico*, *in vitro*) and field (*in situ*) settings and did not detect non-target species under a variety of lab (*in silico*, *in vitro)* experiments. The *in silico* experiments, in which software was used to assess the efficacy of the primer-probe set using sequences of target and non-target species that were not used in the initial assay design, suggested that the assay was specific to multiple populations of *A. blanchardi* across its geographic range. Aligning the primers and probes to the available 34 *A. blanchardi* cytb sequences in GenBank indicated that across all sequences, the probe was a 97% match, the forward primer was a 100% match, and the reverse primer was a 94% match (Table S1). Furthermore, testing the primers against sympatric non-target anurans using BLAST indicated that there were 2–4 mismatches between all individuals tested and the forward primer and 0–3 mismatches between all individuals tested and the reverse primer. These mismatches included both transitions and transversions. Therefore, *in silico* testing validated the assay as being able to detect *A. blanchardi* across the known sequence diversity of the species while not detecting closely and distantly related non-target species that co-occur in the same habitats as *A. blanchardi.*

The second step of assay validation includes *in vitro* laboratory testing to determine if the assay works as expected under controlled conditions with known positive and negative samples. In this *in vitro* testing, the assay performed as expected in all three experiments (Table 1). In Experiment 1, we first tested the assay against extracted DNA from five Oklahoma *A. blanchardi* tissues to assess the performance of the assay under standard qPCR protocols and to measure the limit of detection (LOD). The LOD for our assay was 2×10^{-4} ng/µl. However, the assay detected *A. blanchardi* DNA down to a concentration of 2×10^{-5} ng/µl in 13/15 replicates and 2×10^{-6} ng/µl in 6/15 replicates. The r^2 was 0.995, the slope was -3.481, and the efficiency was 93.76%. We then examined the assay for specificity using extracted DNA from multiple Oklahoma populations of *A. blanchardi* and multiple closely and distantly related non-target anurans, some species of which were not used in the initial assay development or *in silico* testing. Results suggested that the assay was specific to *A. blanchardi* across a broad geographic range and would not provide false negatives when *A. blanchardi* DNA was present or false positives in the absence of *A. blanchardi* (Table 1). However, in Experiment 1, when testing the assay against *A. blanchardi* congenerics, a single sample of the closely related *A. crepitans* resulted in a positive result (LSU H-20744 from East Baton Rouge Parish, LA), but no *A. gryllus* tested positive (Table 1). *Acris blanchardi* and *A. crepitans* are sister species which were only recently segregated into two species and are also difficult to distinguish visually (Gamble et al. 2008). Therefore, this result could have (1) been caused by human error if the frog was

misidentified as *A. crepitans* upon capture and was actually *A. blanchardi* or (2) a result of the two species' cytb genes being similar due to recent divergence. Furthermore, although hybridization between *Acris* species has not been studied, hybridization is known to occur between other species in the family Hylidae, including, famously, historical and ongoing hybridization in the *H. versicolor/chrysocelis* species complex (e.g. Booker et al. 2020). This result indicates that any future researchers wishing to work on *A. blanchardi* versus *A. crepitans* specifically should further develop a more refined primer-probe assay, especially if they are working in areas where the two species may be sympatric (e.g. along the Ohio River; Gamble et al. 2008). This level of specificity was beyond the goals of our particular project. In Experiments 2 and 3 we further tested the assay against eDNA from a single population of *A. blanchardi* and several species of sympatric non-target anurans, one of which had not been used for assay development, *in silico* testing, or in previous *in vitro* testing to determine if the assay would work using standard filtration and filter extraction protocols. Once again, all experimental samples were positive in the presence of *A. blanchardi* DNA, with no false negatives or false positives (Table 1).

In contrast to the complete success of the *in silico* and *in vitro* experiments, *in situ* field validation of the *A. blanchardi* eDNA assay had varying results. The *in situ* screening of the *A. blanchardi* qPCR assay suggested that it was able to detect species-specific DNA in a wide variety of field conditions and locations across Oklahoma, but not all waterbodies returned positive results despite historical (within the last year), visual and/or auditory confirmation of *A. blanchardi* at the waterbody specifically and/or at the broader site more generally. Out of a total of 565 samples (excluding the field-based negative controls), *A. blanchardi* DNA was detected in 120 samples (21.24%; Table 2). These positive samples came from all four eastern Oklahoma ecoregions surveyed, in 21 of 24 field sites (87.5%), and in 48 of 79 waterbodies (60.8%; Table 2; Table S2). We found no *A. blanchardi* false positives in either the lab or field negative. All qPCR plates contained at least one positive well, with a single exception, which was likely a sample size artifact since only four eDNA extracts were screened on that plate (0.6% of all samples). Therefore, reagent or equipment failure or human error during the qPCR setup were unlikely to be the cause of negative results. Although we did not detect *A. blanchardi* in the field as often as we had originally expected given the success of our previous laboratory testing, our knowledge of our sampling sites, and well-documented information about the species in Oklahoma (Sievert and Sievert 2021), we did detect *A. blanchardi* in every ecoregion and at nearly every field site sampled. Overall, our results suggest that the assay is successful in the field, but continued refinement of field protocols is needed to ensure that false negatives, in which *A. blanchardi* is confirmed present at a site but not detected, are not obtained via eDNA screening.

Our results suggest that false negatives were a common result of our *in situ* testing. For the 31 waterbodies at which field crews made concrete notes about *A. blanchardi* presence at the time of eDNA sample collection and/or a specimen from the waterbody was vouchered on the same date as eDNA sample collection, qPCR screening failed to detect the species in 16 waterbodies within this subset (52% false negatives within this subset of sites with known presence; Table S2). These false negatives may be attributed to several unforeseen challenges related to water turbidity and stagnation at our sampling sites. High levels of turbidity observed at our sites may have reduced *A. blanchardi* eDNA detection rates, through direct effects (filter clogging) or indirect effects (introduction of PCR inhibitors). Oklahoma waters are known to be highly turbid (Penfound 1953), which we also observed, with the exception of a handful of sampled streams. Approximately one-third of our field samples clogged before reaching the desired filter volume of 500 mL, presumably resulting in less overall captured eDNA. We considered changing to a larger pore size (i.e. 0.8 µm), but filters with a 0.45 µm pore size, such as those used in our research, were the most commonly used at the time we began sampling

Table 2. Summary qPCR results of eDNA field surveys screening using the *Acris blanchardi* qPCR assay. The total number of waterbodies and samples by county are shown (excluding field-based negative controls), followed by the number and percentage (%) of positive (+) samples detected by Oklahoma ecoregion.

Ecoregion	No. waterbodies (No. samples)	No. + waterbodies (No. + samples)	% + waterbodies (% + samples)
Crosstimbers	7 (42)	4 (10)	57.14% (23.81%)
Ouachita Mountains/Arkansas River Valley/Western Gulf Coastal Plain	54 (383)	34 (87)	62.96% (22.72%)
Ozarks	14 (126)	8 (20)	57.14% (17.86%)
Tallgrass Prairie	4 (32)	2 (3)	50.00% (10.71%)
TOTAL	**79 (565)**	**48 (120)**	**60.76% (21.24%)**

in 2017 (e.g. Goldberg et al. 2013; Pilliod et al. 2013a,b). More recent studies have shown that either there is no statistical difference in eDNA collection between the two pore sizes (Li et al. 2018) or that the 0.45 µm pore size is still optimal (Capo et al. 2019). It is generally accepted that large pore sizes, above those mentioned, often result in a lack of DNA particulate collection (Turner et al. 2014). In addition to filter clogging, the high turbidity we observed could be linked to an increase in PCR inhibitors that can decrease the ability to detect eDNA in qPCR screening and interfere with various extraction steps, potentially leading to an increase in false negatives (Buxton et al. 2017; Williams et al. 2017; Li et al. 2018). These PCR inhibitors tend to build up in stagnant water systems (Harper et al. 2019), such as in those in which we primarily sampled. Inhibitor reduction through dilutions of the eDNA extracts with ddH_2O or buffers was not feasible as it would result in an over-dilution of samples, to the point of undetectability of target species DNA (Williams et al. 2017; Harper et al. 2019). Instead of employing dilution, we incorporated OneStep PCR Inhibitor Removal Kits (Siler et al. 2020), to remove potential PCR inhibitors from turbidity and/or other elements in the water, as these kits have successfully been used for removing PCR inhibitors (McKee et al. 2015; Turner et al. 2015; Adams et al. 2019b; Baker et al. 2020). In fact, McKee et al. (2015) confirmed that samples treated with OneStep PCR Inhibitor Removal Kits performed better in qPCR than samples that were diluted 5- or 10-fold, resulting in more precise DNA concentration estimates, particularly in samples obtained from sediment-laden wetlands.

Therefore, although *in silico* and *in vitro* testing of our *A. blanchardi* eDNA assay validated the efficacy of our assay for detecting and monitoring populations of *A. blanchardi* across a wide geographic range, our *in situ* testing suggests that further refinement of the field and laboratory extraction and/or screening protocols are necessary before the assay can be implemented successfully (Burian et al. 2021). These refinements might include increasing the number of samples that are collected from a site and increasing the number of replicates on a qPCR run. Recent research has explored optimal sample and replicate number for eDNA field protocols and has shown that to optimize eDNA detectability, field sample sizes and qPCR replicate number should be adjusted according to species-specific factors, including whether the focal taxa are rare vs. common (Akre et al. 2019; Erickson et al. 2019; Ficetola et al. 2019), and the type of habitat (Goldberg et al. 2018). Specifically, Akre et al. (2019) propose a minimum of four water samples per waterbody, whereas Goldberg et al. (2018) and Erickson et al. (2019) state that up to 15 water samples may be required for detection of a common species and over 45 samples may be required for detection of a rare species. Additionally, according to Ficetola et al. (2019), a minimum of four qPCR replicates is required to ensure eDNA detection and eight is recommended, whereas Erickson et al. (2019) suggest up to 16 qPCR replicates per sample if the species is rare. Based on this recent research, both the number of water samples collected in our field sampling regime and the number of qPCR replicates used for each site were lower than what is necessary to ensure detection of *A. blanchardi*. Nevertheless, despite our suboptimal field and laboratory protocol, we were able to detect *A. blanchardi* in more

than 60% of all waterbodies tested, comprising more than 87% of all our field sites. These results indicate that our *A. blanchardi* eDNA assay is viable and with the refinement of field and lab protocols, can be applied to monitoring and conservation efforts Oklahoma. Given the results of our *in silico* and *in vitro* testing, the assay also will likely be successful across the full geographic range of *A blanchardi* but *in situ* testing needs to be done in locations beyond Oklahoma to confirm this.

Finally, additional research has argued for different criteria employed across studies to determine whether a positive well in a qPCR run reflects the presence of a species at a site. As stated above, we considered an eDNA sample positive for the target species if two or more of the triplicate wells crossed this experimental threshold in a single qPCR run, or if one of the triplicate wells crossed the threshold on two successive qPCR runs, but compared to other published studies, our value could be considered either too conservative (Raemy and Ursenbacher 2018) or too liberal (Kamoroff and Goldberg 2018; Wineland et al. 2019). Furthermore, some studies have suggested follow-up Sanger sequencing for any positive qPCR sample to confirm target DNA was accurately detected (e.g. De Souza et al. 2016); however Goldberg et al. (2016) suggest that this is only necessary when an assay consists of primers only and not a primer-probe set, as in our assay. Ruppert et al. (2019) argue that although field and laboratory methods vary greatly in the realm of eDNA research, the most important component is primer-probe specificity to the target species; given the specificity of our assay we are confident that our *in situ* testing reflects true positives, true negatives, and false negatives, and not false positives.

Therefore, based on the eDNA assessment scale developed by Thalinger et al. (2021) we suggest that our *A. blanchardi* eDNA assay meets Level 4 out of five levels of validation for routine species monitoring for *A. blanchardi* in Oklahoma, and Level 2 for routine species monitoring across the geographic range of *A. blanchardi* more broadly. Our *in silico* and *in vitro* testing of the assay indicated that the assay is specific to *A. blanchardi* and works effectively in controlled laboratory conditions. Under field conditions, our assay was shown to be successful but not completely effective. Additional *in situ* testing and optimization, including determining and minimizing the rate of false negatives, needs to be done before the sampling protocols and eDNA detection assay are fully validated and field ready.

Acknowledgements

The authors wish to thank the following people for laboratory assistance: K. Anaya, J. Brown, S. Eliades, E. Ellsworth, E. Higgins, M. Capps, J. Norris, S. Smith, M. Squires. We would additionally like to thank the following people for field work assistance: A. Allen, A. Carriere, K. Castillioni, A. Cooper, D. Curtis, S. Eliades, E. Ellsworth, K. Gill, N. Huron, D. Kopp, J. Kouri, S. Maguire, J. Norris, T. Ortery, S. Smith, and J. Tucker. Finally, we also thank T. Hartog and R. Drake for conducting data quality control. Funding provided by Oklahoma Department of Wildlife OK-WILD, grant/ award number: F16AF01213 (T-91-R-1), the University of Oklahoma School of Biological Sciences, and the Sam Noble Museum.

References

Adams CIM., Knapp M, Gemmell NJ, Jeunen G-J, Bunce M, Lamare MD, Taylor HT. 2019a. Beyond biodiversity: can environmental DNA (eDNA) cut it as a population genetics tool? Genes 10:192. https://doi.org/10.3390/genes10030192

Adams CIM, Hoeskstra LA, Muell MR, Janzen FJ. 2019b. A brief review of non-avian reptile environmental DNA (eDNA), with a case study of painted turtle (*Chrysemys picta*) eDNA under field conditions. Diversity 11:50. https://doi.org/10.3390/d11040050

Akre TS, Parker LD, Ruther E, Maldonado JE, Lemmon L, McInerney NR. 2019. Concurrent visual encounter sampling validates eDNA selectivity and sensitivity for the endangered Wood Turtle (*Glyptemys insculpta*). PLOS ONE 14:e0215586. https://doi.org/10.1371/journal.pone.0215586

Baker SJ, Niemiller ML, Stites AJ, Ash KT, Davis MA, Dreslik MJ, Phillips CA. 2020. Evaluation of environmental DNA to detect *Sistrurus catenatus* and *Ophiomyces ophiodiicola* in crayfish burrows. Conserv Gene Resour 12:13–15. https://doi.org/10.1007/s12686-018-1053-9

Bálint M, Nowak C, Márton O, Pauls SU, Wittwe C, Aramayo JL, Schultze A, Cambert T, Cocchiararo B, Jansen M. 2017. Accuracy, limitations and cost efficiency of eDNA-based community survey in tropical frogs. Mol Ecol Resour 18:1415–1426. https://doi.org/10.1111/1755-0998.12934

Barnes MA, Turner CR, Jerde CL, Renshaw MA, Chadderton WL, Lodge DM. 2014. Environmental conditions influence eDNA persistence in aquatic systems. Environ Sci Technol 48:1819–1827. https://doi.org/10.1021/es404734p

Bolochio BE, Lescano JN, Cordier JM, Loyola R, Nori J. 2020. A functional perspective for global amphibian conservation. Biol Conserv 245:108572. https://doi.org/10.1016/j.biocon.2020.108572

Booker WW, Gerhardt HC, Lemmon AR, Ptacek MB, Hassinger ATB, Schul J, Lemmon EM. 2022. The complex history of genome duplication and hybridization in North American gray treefrogs. Mol Biol Evol 39:msab316. https://doi.org/10.1093/molbev/msab316

Burian A, Mauvisseau Q, Bulling M, Domisch S, Qian S, Sweet M. 2021. Improving the reliability of eDNA data interpretation. Mol Ecol Resour 21:1422–1433. https://doi-org.ezproxy.lib.ou.edu/10.1111/1755-0998.13367

Buxton AS, Groombridge JJ, Griffiths RA. 2017. Is the detection of aquatic environmental DNA influenced by substrate type? PLOS ONE 12:e0183371. https://doi.org/10.1371/journal.pone.0183371

Campbell Grant, EHD, Miller AW, Muths E. 2020. A synthesis of evidence of drivers of amphibian declines. Herpetol 76:101–107. https://doi.org/10.1655/0018-0831-76.2.101

Cannessa S, Spitzen-van der Sluijs A, Martel A, Pasmans F. 2019. Mitigation of amphibian disease requires a stronger connection between research and management. Biol Conserv 236:236–242. https://doi.org/10.1016/j.biocon.2019.05.030

Capo E, Spong G, Königsson H, Byström P. 2019. Effects of filtration methods and water volume on the quantification of Brown Trout (*Salmo trutta*) and Arctic Char (*Salvelinus alpinus*) eDNA concentrations via droplet digital PCR. Environ DNA 2:152–160. https://doi.org/10.1002/edn3.52

Chabot D, Bird DM. 2015. Wildlife research and management methods in the 21st century: where do unmanned aircraft fit in? J Unmanned Veh Syst 3:137–155. https://doi.org/10.1139/juvs-2015-0021

Cohen JM, Civitello DJ, Venesky MD, McMahon TA, Rohr JR. 2019. An interaction between climate change and infectious disease drove widespread amphibian declines. Global Change Biol 25:927–937. https://doi.org/10.1111/gcb.14489

Darling, JA, Mahon AR. 2011. From molecules to management: adopting DNA-based methods for monitoring biological invasions in aquatic environments. Environ Res 111:978–988. https://doi.org/10.1016/j.envres.2011.02.001

De Souza LS, Godwin JC, Renshaw MA, Larson E. 2016. Environmental DNA (eDNA) detection probability is influenced by seasonal activity of organisms. PLOS ONE 11:e0165273. https://doi.org/10.1371/journal.pone.0165273

Dejean T, Valentini A, Miquel C, Taberlet P, Bellemain E, Miaud C. 2012. Improved detection of an alien invasive species through environmental DNA barcoding: the example of the American Bullfrog *Lithobates catesbeianus*. J Appl Ecol 49:953–959. https://doi.org/10.1111/j.1365-2664.2012.02171.x

Diaz-Ferguson EE, Moyer GR. 2014. History, applications, methodological issues and perspectives for the use of environmental DNA (eDNA) in marine and freshwater environments. Rev Biol Trop 62:1273–1284. https://doi.org/10.15517/rbt.v62i4.13231

Erickson RA, Merkes CM, Mize EL. 2019. Sampling designs for landscape-level eDNA monitoring programs. Integr Environ Assess 15:460–771. https://doi.org/10.1002/ieam.4155

Esselstyn JA, Garcia HJD, Saulog MG, Heaney LR. 2008. A new species of *Desmalopex* (Pteropodidae) from the Philippines, with a phylogenetic analysis of the Pteropodini. J Mammal 89:815–825. https://doi.org/10.1644/07-MAMM-A-285.1

Ficetola F, Manenti R, Taberlet P. 2019. Environmental DNA and metabarcoding for the study of amphibians and reptiles: species distribution, the microbiome, and much more. Amphibia-Reptilia 40:129–148. https://doi.org/10.1163/15685381-20191194

Ford J, Hunt DAGA, Haines GE, Lewis M, Lewis Y, and Green DM. 2020. Adrift on a sea of troubles: can amphibians survive in a human-dominated world? Herpetologica 76:251–256. https://doi.org/10.1655/0018-0831-76.2.251

Gamble T, Berendzen PB, Shaffer HB, Starkey DE, and Simons AM. 2008. Species limits and phylogeny of North American cricket frogs (*Acris*: Hylidae). Mol Phylogenet Evol 48:112–125. https://doi.org/10.1016/j.ympev.2008.03.015

Goldberg CS, Sepulveda A, Ray A, Baumgardt J, and Waits LP. 2013. Environmental DNA as a new method for early detection of New Zealand Mudsnails (*Potamopyrgus antipodarum*). Freshw Sci 32:792–800. https://doi.org/10.1899/13-046.1

Goldberg CS, Strickler KM, Pilliod DS. 2015. Moving environmental DNA methods from concept to practice for monitoring aquatic macroorganisms. Biol Conserv 183:1–3. https://doi.org/10.1016/j.biocon.2014.11.040

Goldberg CS, Turner CR, Deiner K, Klymus KE, Thomsen PF, Murphy MA, Spear SF, McKee A, Oyler-McCance SJ. Cornman RS, Laramie MB, Mahon AR, Lance RF, Pilliod DS, Strickler KM, Waits LP, Fremier AK, Takahara T, Herder JE, Taberlet P. 2016. Critical considerations for the application of environmental DNA methods to detect aquatic species. Methods Ecol Evol 7:1299–1307. https://doi.org/10.1111/2041-210X.12595

Goldberg CS, Strickler KM, Fremier AK. 2018. Degradation and dispersion limit environmental DNA detection of rare amphibians in wetlands: increasing efficacy of sampling designs. Sci Total Environ 633:695–703. https://doi.org/10.1016/j.scitotenv.2018.02.295

Green DM, Lannoo MK, Lesbarrères D, Muths E. 2020. Amphibian population declines: 30 years of progress confronting a complex problem. Herpetologica 76:97–100. https://doi.org/10.1655/0018-0831-76.2.97

Harper LR, Buxton AS, Rees HC, Bruce K, Brys R, Halfmaerten F, Read DS, Watson HV, Sayer CD, Jones EP, Priestley V, Mächler E, Múrria C, Garcés-Pastor S, Medupin C, Burgess K, Benson G, Boonham N, Griffiths RA, Handley LL, Hänfling B. 2019. Prospects and challenges of environmental DNA (eDNA) monitoring in freshwater ponds. Hydrobiologia 826:25–41. https://doi.org/10.1007/s10750-018-3750-5

Hobbs J, Round JM, Allison MJ, Helbing CC. 2019. Expansion of the known distribution of the Coastal Tailed Frog, *Ascaphus truei*, in British Columbia, Canada, using robust eDNA detection methods. PLOS ONE 14:e0213849. https://doi.org/10.1371/journal.pone.0213849

Kamoroff C, Goldberg CS. 2018. An issue of life or death: using eDNA to detect viable individuals in wilderness restoration. Freshw Sci 37:685–696. https://doi.org/10.1086/699203

Klymus KE, Merkes CM, Allison MJ, Goldberg CS, Helbing CC, Hunter ME, Jackson CA, Lance RF, Mangan AM, Monroe EM, Piaggio AJ, Stokdyk JP, Wilson CC, Richter CA. 2020. Reporting the limits of detection and quantification for environmental DNA assays. Environ DNA 2:271–282. https://doi.org/10.1002/edn3.29

Lehtinen RM, Skinner AA. 2006. The enigmatic decline of Blanchard's Cricket Frog (*Acris crepitans blanchardi*): a test of the habitat acidification hypothesis. Copeia 2006:159–167. https://doi.org/10.1643/0045-8511(2006)6[159:TEDOBC]2.0.CO;2

Li J, Handley LL, Read DS, Hänfling B. 2018. The effect of filtration method on the efficiency of environmental DNA capture and quantification via metabarcoding. Mol Ecol Resour 18:1102–1114. https://doi.org/10.1111/1755-0998.12899

Lopes CM, Sasso T, Valentini A, Dejean T, Martins M, Zamudio KR, Haddad FBC. 2017. EDNA metabarcoding: a promising method for anuran surveys in highly diverse tropical forests. Mol Ecol Resour 17:904–914. https://doi.org/10.1111/1755-0998.12643

Lynggaard C, Bertelsen MF, Jensen CV, Johnson MS, Frøslev TG, Olsen MT, Bohmann K. 2022. Airborne environmental DNA for terrestrial vertebrate community monitoring. Curr Biol 32:701–707. https://doi.org/10.1016/j.cub.2021.12.014

McCallum, ML, Brooks C, Mason R, Trauth SE. 2011. Growth, reproduction, and life span in Blanchard's Cricket Frog (*Acris blanchardi*) with notes on the growth of the Northern Cricket Frog (*Acris crepitans*). Herpetol 4:25–35.

McGrath T, Guillera-Arroita G, Lahoz-Monfort JJ, Osborne W, Hunter D, Sarre SD. 2015. Accounting for detectability when surveying for rare or declining reptiles: turning rocks to find the Grassland Earless Dragon in Australia. Biol Conserv 182:53–62. https://doi.org/10.1016/j.biocon.2014.11.040

McKee AM, Spear SF, Pierson TW. 2015. The effect of dilution and the use of a post-extraction nucleic acid purification column on the accuracy, precision, and inhibition of environmental DNA samples. Biol Conserv 183:70–76. https://doi.org/10.1016/j.biocon.2014.11.031

Moriyama EN, Powell JR. 1997. Synonymous substitution rates in *Drosophila*: mitochondrial versus nuclear genes. J Mol Evol 45:378–391. https://doi.org/10.1007/pl00006243

Penfound WT (1953). Plant communities of Oklahoma lakes. Ecology 34:561–583. https://doi.org/10.2307/1929728

Pilliod DS, Goldberg CS, Arkle RS, Waits LP. 2013a. Factors affecting detection of eDNA from a stream-dwelling amphibian. Mol Ecol Resour 14:109–116. https://doi.org/10.1111/1755-0998.12159

Pilliod DS, Goldberg CS, Arkle RS, Waits LP. 2013b. Estimating occupancy and abundance of stream amphibians using environmental DNA from filtered water samples. Can J Fish and Aquat Sci 70:1123–1130. https://doi.org/10.1139/cjfas-2013-0047

Raemy M, Ursenbacher S. 2018. Detection of the European Pond Turtle (*Emys orbicularis*) by environmental DNA: is eDNA adequate for reptiles? Amphibia-Reptilia 39:135–143. https://doi.org/10.1163/15685381-17000025

Ruppert KM, Kline RJ, Rahman MS. 2019. Past, present, and future perspectives of environmental DNA (eDNA) metabarcoding: a systematic review in methods, monitoring, and applications of global eDNA. GECCO 17:e00547. https://doi.org/10.1016/j.gecco.2019.e00547

Russo D, Voigt CC. 2016. The use of automated identification of bat echolocation calls in acoustic monitoring: a cautionary note for sound analysis. Ecol Indic 66:598–602. https://doi.org/10.1016/j.ecolind.2016.02.036

Sievert G, Sievert L. 2021. Field Guide to Oklahoma's Amphibians and Reptiles. 4th ed. Oklahoma City (OK): Oklahoma Department of Wildlife Conservation. 231 p.

Siler CD, Freitas ES, Yuri T, Souza L, Watters JL. 2020. Development and validation of four environmental DNA assays for species of conservation concern in the South-Central United States. Conserv Genet Resour 13:35–40. https://doi.org/10.1007/s12686-020-01167-3

Simmons J. 2015. Herpetological collecting and collections management (3rd ed.). SSAR Herpetol. Circ. 42:1–191.

Smith GR, Rodd A, Rettig JE, Nelson F. 2003. Microhabitat selection by Northern Cricket Frogs (*Acris crepitans*) along a west-central Missouri creek: field and experimental observations. J Herpetol 37:383–385. https://doi.org/10.1670/0022-1511(2003)037[0383:MSBNCF]2.0.CO;2

Strickler KM, Fremier AK, Goldberg CS. 2015. Quantifying effects of UV-B, temperature, and pH on eDNA degradation in aquatic microcosms. Biol Conserv 183:85–82. https://doi.org/10.1016/j.biocon.2014.11.038

Takahara T, Minamoto T, Yamanaka H, Doi H, Kawabata Z. 2012. Estimation of fish biomass using environmental DNA. PLOS ONE 7:e35868. https://doi.org/10.1371/journal.pone.0035868

Takahara T, Minomoto T, Doi H. 2014. Effects of sample processing on the detection rate of environmental DNA from the Common Carp (*Cyprinus carpio*). Biol Conserv 183:64–69. https://doi.org/10.1016/j.biocon.2014.11.014

Takahara T, Iwai N, Yasumiba K, and Igawa T. 2020. Comparison of the detection of 3 endangered frog species by eDNA and acoustic surveys across 3 seasons. Freshw Sci 39:18–27. https://doi.org/10.1086/707365

Thalinger B, Deiner K, Harper LR, Rees HC, Blackman RC, Sint D, Traugott M, Goldberg CS, Bruce K. 2021. A validation scale to determine the readiness of environmental DNA assays for routine species monitoring. Environ DNA 3:823–836. https://doi.org/10.1002/edn3.189

Thomas, AC, Tank S, Nguyen PL, Ponce J, Sinnesael M, and Goldberg CS. 2019. A system for rapid eDNA detection of aquatic invasive species. Environ DNA 1:1–10. https://doi.org/10.1002/edn3.25

Thomsen, PF, Willerslev E. 2015. Environmental DNA—an emerging tool in conservation for detectability: monitoring past and present biodiversity. Biol Conserv 183:4–18. https://doi.org/10.1016/j.biocon.2014.11.019

Turner CR, Barnes MA, Xu CCY, Jones SE, Jerde CL, and Lodge DM. 2014. Particle size distribution and optimal capture of aqueous macrobial eDNA. Meth Ecol Evol 5:676–684. https://doi.org/10.1111/2041-210X.12206

Turner CR, Uy KL, Everhart RC. 2015. Fish environmental DNA is more concentrated in aquatic sediments than surface water. Biol Conserv 183:93–102. https://doi.org/10.1016/j.biocon.2014.11.017

Valentini A, Taberlet P, Miaud C, Civade R, Herder J, Thomsen PF, Bellemain E, Besnard A, Coissac E, Boyer F, Gaboriaud C, Jean P, Polet N, Roset N, Copp GH, Goniez P, Pont D, Argillier C, Baudoin J-M, Peroux T, Crivelli AJ, Olivier A, Acqueberge M, Le Brun M, Møller PR, Willerslev E, Dejean T. 2016. Next-generation monitoring of aquatic biodiversity using environmental DNA barcoding. Mol Ecol 25:929–942. https://doi.org/10.1111/mec.12428

Wilcox TM, McKelvey KS, Young MK, Jane SF, Lowe WH, Whiteley AR, Schwartz MK. 2013. Robust detection of rare species using environmental DNA: the importance of primer specificity. PLOS ONE 8:e59520. https://doi.org/10.1371/journal.pone.0059520

Williams KE, Huyvaert KP, Piaggio AJ. 2017. Clearing muddied waters: capture of environmental DNA from turbid waters. PLOS ONE 12:e0179282. https://doi.org/10.1371/journal.pone.0179282

Wineland SM, Arrick RF, Welch SM, Pauley TK, Mosher JJ, Apodaca JJ, Olszack M, Holmes JN, Waldron JL. 2019. Environmental DNA improves Eastern Hellbender (*Cryptobranchus alleganiensis alleganiensis*) detection over conventional sampling methods. Environ DNA 1:86–96. https://doi.org/10.1002/edn3.9

Ye J, Coulouris G, Zaretskaya I, Cutcutache I, Rozen S, Madden T. 2012. Primer-BLAST: A tool to design target-specific primers for polymerase chain reaction. BMC Bioinf 13:134. https://doi.org/10.1186/1471-2105-13-134

Yu DW, Ji Y, Emerson BC, Wang X, Ye C, Yang C, Ding Z. 2012. Biodiversity soup: metabarcoding of arthropods for rapid biodiversity assessment and biomonitoring. Meth Ecol Evol 3:613–623. https://doi.org/10.1111/j.2041-210X.2012.00198.x

Submitted August 1, 2023 Accepted November 16, 2023

Supplementary Materials

Table S1. GenBank (NCBI, Bethesda, MD) samples used for primer-probe development and *in silico* testing of the qPCR assay. For each individual, the quantity of mismatches are provided, for both forward (F) and reverse (R) primers, as well as the number of probe mismatches.

Primer-probe Development					
Species	GenBank No.	Locality (State)	No. F Primer Mismatches	No. R Primer Mismatches	No. Probe Mismatches
Acris blanchardi	EF988109	Illinois	0	0	0
Acris blanchardi	EF988127	Missouri	0	1	0
Acris blanchardi	EF988141	Oklahoma	0	0	0
Acris blanchardi	EF988144	Mississippi	0	1	0
Anaxyrus americanus	EU938446	Kansas	4	2	2
Lithobates catesbeianus	AY083293	Ohio	6	0	0
Lithobates clamitans	AY083282	Missouri	5	1	1
Pseudacris crucifer	EF988160	Minnesota	4	3	1
Primer-probe Specificity Confirmation					
Species	GenBank No.	Locality (State)	No. F Primer Mismatches	No. R Primer Mismatches	No. Probe Mismatches
Acris blanchardi	EF988097	Iowa	0	0	0
Acris blanchardi	EF988098	Iowa	0	0	0
Acris blanchardi	EF988099	Iowa	0	0	0
Acris blanchardi	EF988100	Iowa	0	0	0
Acris blanchardi	EF988101	Arkansas	0	1	0
Acris blanchardi	EF988102	Arkansas	0	1	0
Acris blanchardi	EF988103	Arkansas	0	1	0
Acris blanchardi	EF988104	Arkansas	0	0	0
Acris blanchardi	EF988105	Arkansas	0	1	0
Acris blanchardi	EF988106	Arkansas	0	0	0
Acris blanchardi	EF988107	Arkansas	0	1	0
Acris blanchardi	EF988108	Illinois	0	0	0
Acris blanchardi	EF988114	Kansas	0	0	0
Acris blanchardi	EF988115	Wisconsin	0	0	1
Acris blanchardi	EF988116	Wisconsin	0	0	0
Acris blanchardi	EF988117	Louisiana	0	0	0
Acris blanchardi	EF988119	Louisiana	0	0	0
Acris blanchardi	EF988120	Texas	0	0	0
Acris blanchardi	EF988121	Texas	0	0	0
Acris blanchardi	EF988122	Texas	0	0	0
Acris blanchardi	EF988133	Kentucky	0	0	0
Acris blanchardi	EF988137	Ohio	0	0	0
Acris blanchardi	EF988138	Minnesota	0	0	0
Acris blanchardi	EF988139	Minnesota	0	0	0
Acris blanchardi	EF988140	Oklahoma	0	0	0
Acris blanchardi	EF988142	Mississippi	0	0	0
Acris blanchardi	EF988143	Mississippi	0	0	0
Acris blanchardi	EF988145	Mississippi	0	0	0
Acris blanchardi	EU835890	---	0	1	0
Acris blanchardi	EU835891	---	0	1	0
Acris blanchardi	EU835892	---	0	1	0
Acris blanchardi	EU835893	---	0	2	0
Acris blanchardi	EU835888	---	0	0	0
Acris blanchardi	EU835889	---	0	1	0
BLAST Confirmation of Primers against Non-target Anurans					
Species	GenBank No.	Locality (State)	No. F Primer Mismatches	No. R Primer Mismatches	No. Probe Mismatches
Hyla cinerea	FJ226874	Georgia	3	3	4
Hyla cinerea	KJ536188	Florida	3	3	4
Lithobates palustris	KX269353	New York	4	3	4
Lithobates sylvaticus	EU203528	---	4	2	3
Lithobates sylvaticus	EU203529	---	4	2	3
Lithobates sylvaticus	EU203530	---	4	1	3
Lithobates sylvaticus	EU203531	---	4	1	3
Lithobates sylvaticus	EU203532	---	3	1	3
Lithobates sylvaticus	EU203533	---	4	1	3

Table S1. Continued.

Lithobates sylvaticus	EU203534	---	5	1	3
Lithobates sylvaticus	EU203535	---	4	1	3
Lithobates sylvaticus	EU203536	---	4	1	3
Lithobates sylvaticus	EU203537	---	4	1	3
Lithobates sylvaticus	EU203538	---	4	1	3
Pseudacris clarkii	KJ536214	Texas	3	1	2
Pseudacris clarkii	KJ536216	Kansas	3	1	2
Pseudacris fouquettei	KJ536226	Louisiana	3	2	2
Pseudacris fouquettei	KJ536227	Arkansas	2	2	2
Pseudacris maculata	EF988161	Minnesota	3	2	2
Pseudacris maculata	KJ536215	Illinois	3	1	2
Pseudacris maculata	KJ536217	Kansas	3	1	2
Pseudacris regilla	AY363181	---	3	0	5
Pseudacris regilla	AY363182	---	3	0	5
Pseudacris regilla	AY363183	---	3	0	6
Pseudacris regilla	AY363184	---	3	0	5
Pseudacris regilla	AY363185	---	3	0	5
Pseudacris regilla	AY363186	---	3	0	5
Pseudacris regilla	AY363187	---	3	0	5
Pseudacris regilla	AY363188	---	3	0	5
Pseudacris regilla	AY363190	---	3	0	5
Pseudacris regilla	AY363191	---	3	0	5
Pseudacris regilla	AY363192	---	3	0	5
Pseudacris regilla	AY363193	---	3	0	5
Pseudacris regilla	AY363194	---	3	0	5
Pseudacris regilla	AY363195	---	3	0	5
Pseudacris regilla	AY363196	---	3	0	5
Pseudacris regilla	AY363197	---	3	0	5
Pseudacris regilla	AY363198	---	3	0	5
Pseudacris regilla	AY363199	---	3	0	5
Pseudacris regilla	AY363200	---	3	0	5
Pseudacris regilla	AY363201	---	3	0	5
Pseudacris regilla	AY363206	---	3	0	4
Pseudacris regilla	AY363207	---	3	0	5
Pseudacris regilla	AY363208	---	3	0	5
Pseudacris regilla	AY363209	---	3	0	5
Pseudacris regilla	AY363210	---	3	0	5
Pseudacris regilla	AY363211	---	3	0	5
Pseudacris regilla	AY363212	---	3	0	5
Pseudacris regilla	AY363213	---	3	0	5
Pseudacris regilla	AY363214	---	3	0	5
Pseudacris regilla	AY363215	---	3	0	5
Pseudacris regilla	AY363216	---	3	0	5
Pseudacris regilla	AY363217	---	3	0	5
Pseudacris regilla	AY363219	---	3	0	5
Pseudacris regilla	DQ195206	California	3	1	3
Pseudacris regilla	KJ536195	Oregon	3	0	5
Pseudacris regilla	KJ536196	Oregon	3	0	5

Table S2. Detailed summary qPCR results of eDNA field surveys screening using the *Acris blanchardi* qPCR assay, by waterbody. Each field site is listed with a number afterward to indicate each individual waterbody located within the site (i.e. Boehler Seeps TNCP 1, 2, 3 are three waterbodies sampled at Boehler Seeps preserve, owned by The Nature Conservancy). Total number of eDNA samples collected (excluding field-based negative controls) is followed by number of samples exhibiting *A. blanchardi* positive (+) detection. The proportion of samples testing positive at each waterbody is also provided (% *Acris* eDNA). Lines designated with an asterisk (*) represent waterbodies in which live *A. blanchardi* were also observed at the time of eDNA sampling. Abbreviations are as follows: NWR = National Wildlife Refuge (US Fish & Wildlife Service); PUA = Public Use Area (US Army Corps of Engineers); SP = Oklahoma State Park; TNCP = The Nature Conservancy Preserve; WMA = Wildlife Management Area (Oklahoma Department of Wildlife Conservation).

Ecoregion	Waterbody name	No. samples (No. + samples)	% *Acris* eDNA
Crosstimbers	Boehler Seeps TNCP 1	8 (4) *	50.0%
	Boehler Seeps TNCP 2	8 (2) *	25.0%
	Boehler Seeps TNCP 3	8 (2)	25.0%
	Johnson Creek PUA 1	4 (0) *	0.0%
	Johnson Creek PUA 2	4 (0) *	0.0%
	Lakeside PUA 1	4 (0) *	0.0%
	Lakeside PUA 2	6 (2) *	33.3%
	TOTAL	**42 (10)**	**23.8%**
Ouachita Mountains/ Arkansas River Valley/Western Gulf Coastal Plain	Grassy Slough WMA 1	8 (2) *	25.0%
	Grassy Slough WMA 2	8 (0) *	0.0%
	Honobia WMA 1	8 (1)	12.5%
	Honobia WMA 2	8 (4)	50.0%
	Little River NWR 1	8 (8)	100.0%
	Little River NWR 2	8 (2)	25.0%
	McClellan-Kerr WMA, Billy Creek/Chouteau Portion 1	4 (1) *	25.0%
	McClellan-Kerr WMA, Billy Creek/Chouteau Portion 2	8 (1) *	12.5%
	McClellan-Kerr WMA, Billy Creek/Chouteau Portion 3	8 (0)	0.0%
	McClellan Kerr WMA, Robert S. Kerr Portion 1	8 (0) *	0.0%
	McClellan Kerr WMA, Robert S. Kerr Portion 2	8 (0)	0.0%
	McClellan Kerr WMA, Robert S. Kerr Portion 3	8 (0)	0.0%
	McClellan-Kerr WMA, Webbers Falls Portion 1	8 (0) *	0.0%
	McClellan-Kerr WMA, Webbers Falls Portion 2	8 (1)	12.5%
	McClellan-Kerr WMA, Webbers Falls Portion 3	8 (1)	12.5%
	McClellan-Kerr WMA, Webbers Falls Portion 4	8 (0)	0.0%
	McClellan-Kerr WMA, Webbers Falls Portion 5	8 (0) *	0.0%
	McCurtain County WMA 1	6 (2)	33.3%
	McCurtain County WMA 2	6 (2)	33.3%
	McGee Creek WMA 1	8 (1)	12.5%
	McGee Creek WMA 2	8 (3)	37.5%
	McGee Creek WMA 3	6 (1)	16.7%
	McGee Creek WMA 4	8 (8)	100.0%
	Ouachita National Forest, Le Flore Unit 1	8 (5) *	62.5%
	Ouachita National Forest, Le Flore Unit 2	8 (0)	0.0%
	Ouachita National Forest, Le Flore Unit 3	8 (1) *	12.5%
	Ouachita National Forest, Le Flore Unit 4	8 (7)	87.5%
	Ouachita National Forest, McCurtain Unit 1	8 (1)	12.5%
	Ouachita National Forest, McCurtain Unit 2	6 (1)	16.7%
	Pushmataha WMA 1	4 (1)	25.0%
	Pushmataha WMA 2	2 (1)	50.0%
	Pushmataha WMA 3	4 (0)	0.0%
	Pushmataha WMA 4	4 (3)	75.0%
	Pushmataha WMA 5	2 (1)	50.0
	Pushmataha WMA 6	6 (0)	0.0%
	Red Slough WMA 1	8 (3) *	37.5%
	Robbers Cave WMA 1	8 (4)	50.0%
	Robbers Cave WMA 2	8 (1)	12.5%
	Robbers Cave WMA 3	7 (0) *	0.0%
	Sequoyah NWR 1	8 (0) *	0.0%

Table S2. Continued

	Sequoyah NWR 2	8 (4) *	50.0%
	Sequoyah NWR 3	8 (0) *	0.0%
	Sequoyah NWR 4	8 (0) *	0.0%
	Sequoyah NWR 5	8 (0)	0.0%
	Sequoyah NWR 6	8 (0)	0.0%
	Sequoyah NWR 7	8 (1) *	12.5%
	Sequoyah NWR 8	8 (1) *	12.5%
	Sequoyah NWR 9	6 (4)	66.7%
	Sequoyah NWR 10	8 (0) *	0.0%
	Three Rivers WMA 1	2 (0)	0.0%
	Three Rivers WMA 2	8 (2) *	25.0%
	Three Rivers WMA 3	6 (0)	0.0%
	Wister WMA 1	8 (7)	87.5
	Wister WMA 2	8 (1)	12.5
	TOTAL	**383 (87)**	**22.7%**
Ozarks	Cookson WMA 1	8 (0)	0.0%
	Cookson WMA 2	8 (0)	0.0%
	Cookson WMA 3	8 (1)	12.5%
	Cookson WMA 4	8 (0)	0.0%
	Cookson WMA 5	8 (1) *	12.5%
	Cookson WMA 6	8 (1)	12.5%
	Cookson WMA 7	8 (0) *	0.0%
	Cookson WMA 8	8 (1)	12.5%
	Green Leaf SP 1	8 (1)	12.5%
	Green Leaf SP 2	8 (0) *	0.0%
	Hopewell Park PUA 1	8 (0)	0.0%
	Nickel Family TNCP 1	8 (1)	12.5%
	Nickel Family TNCP 2	8 (7)	87.5%
	Nickel Family TNCP 3	8 (7)	87.5%
	TOTAL	**126 (20)**	**17.9%**
Tallgrass Prairie	Fort Gibson WMA 1	4 (1)	25.0%
	Fort Gibson WMA 2	8 (0)	0.0%
	Fort Gibson WMA 3	8 (0) *	0.0%
	Fort Gibson WMA 4	8 (2) *	25.0%
	TOTAL	**32 (3)**	**10.7%**
TOTAL		**565 (120)**	**21.2%**

Examination of Wild Birds and Feral Hogs from Oklahoma, USA, for Infection with *Trichinella*

Ryan W. Koch*
Oklahoma State University, Department of Integrative Biology, Stillwater, OK 74078

João Brandão
Oklahoma State University, Department of Veterinary Clinical Sciences, College of Veterinary Medicine, Stillwater, OK 74078

Corey S. Riding
Oklahoma State University, Department of Natural Resource Ecology and Management, Stillwater, OK 74078

Scott R. Loss
Oklahoma State University, Department of Natural Resource Ecology and Management, Stillwater, OK 74078

Alexis Steckley
Oklahoma State University Department of Veterinary Pathobiology, Center for Veterinary Health Sciences, Stillwater, OK 74078

Mason V. Reichard
Oklahoma State University Department of Veterinary Pathobiology, Center for Veterinary Health Sciences, Stillwater, OK 74078

Abstract: *Trichinella* species infect many groups of vertebrates throughout the world. Data for *Trichinella* in wildlife in Oklahoma, USA, is limited, and key reservoir hosts have yet to be identified. We performed artificial digestions on feral hogs (*Sus scrofa*; n=42) and wild birds (19 species; n=36) from Oklahoma to detect the presence of *Trichinella* larvae. Artificial digestions involved heating and mixing host tissue in pepsin and hydrochloric acid and mimic the excystment of larvae in the host bowels once tissue is consumed. Additionally, a subset of feral hogs (n=31) was examined for antibodies to *Trichinella* spp. Among all wildlife species examined, no *Trichinella* spp. larvae were detected in the tissues via digestions. However, ELISA testing detected antibodies to *Trichinella* spp. in 2 of 31 (6.5%) feral hogs. These relatively low seroprevalence levels in feral hogs are consistent with other reports of *Trichinella* in Oklahoma wildlife and suggest feral hogs may not be key reservoir hosts in the sylvatic cycle. Differences in results from the two detection methods we used indicate the importance of utilizing an integrative approach when examining animals for *Trichinella* infections. Further surveillance in bird populations is necessary to adequately determine whether birds are serving as reservoirs for *Trichinella* species.

Introduction

The genus *Trichinella* includes species of nematodes infecting various groups of vertebrates throughout the world. To date, 13 species and/or genotypes of *Trichinella* have been described from carnivores, omnivores, and scavengers

***Corresponding author: ryan.koch@okstate.edu**

(Pozio and Zarlenga 2013; Sharma et al. 2020). Reports of *Trichinella* predominantly occur in wild mammals, comprising over 100 species of mammals from 11 orders. Additionally, all attempts to experimentally infect mammals with *Trichinella* have been successful, hinting at this parasite group's ability to infect and survive in new hosts, including domestic animals (Pozio and Murrell 2006). Therefore, the lack of reports in certain mammal species is likely a result of geographical limitations to host-parasite contact. Novel host infections and range expansions appear to be a result of human activity, specifically where poor feeding and farming practices (exposure to infected meat) exist (Pozio and Murrell 2006; Crisóstomo-Jorquera and Landaeta-Aqueveque 2022).

Species of *Trichinella* are known to have a complex, two host life cycle. Briefly, when tissue from an infected host that contains *Trichinella* larvae is ingested by another host, larvae are released and develop into adults in the small intestine. From here, male and female worms mate, release larvae that migrate to muscle, and become encapsulated or non-encapsulated inside muscle cells, until they are ingested by the next host (Pozio and Murrell 2006; Rawla and Sharma 2022). Unlike the majority of nematode species, transmission is strictly via trophic transfer, including predation, cannibalism, or scavenging. Two types of *Trichinella* life cycles exist: one in wildlife (sylvatic cycle), predominantly carnivores, and one in domestic animals (domestic cycle), predominantly scavengers. The difference between these types of life cycles is merely dependent on the context of the host species (i.e., wildlife vs domestic animals) and whether they become infected and transmit the parasite to subsequent hosts. Sylvatic cycles utilize many more host species than in domestic cycles and are the primary origin of human infections in the United States (Pozio and Murrell 2006; Casillas and Jones 2017). Humans, although dead-end hosts, can become infected with *Trichinella* if raw or undercooked meat containing larvae are ingested. In general, *Trichinella* appears to be a very opportunistic genus of nematodes, with a low degree of host specificity.

Strict government regulation as well as improved education has greatly reduced the transmission of *Trichinella* to humans, yet it remains an important zoonotic parasite due to its constant widespread existence (Pozio and Murrell 2006; Pozio and Zarlenga 2013; Crisóstomo-Jorquera and Landaeta-Aqueveque 2022). Despite the low number of human cases of trichinellosis (i.e., the disease resulting from *Trichinella* infection) in the United States, cases have remained relatively constant in recent years (Centers for Disease Control and Prevention 2019). Wild animals such as black bears and feral hogs have been implicated as the most common sources of infection (Casillas and Jones 2017). Birds have also rarely been reported to be infected with *Trichinella pseudospiralis* larvae, and these infections tend to have a patchy distribution in the United States (Pozio and Murrell 2006; Pozio and Zarlenga 2013). The role of birds as hosts in sylvatic cycles remains unclear but may be important due to their high mobility, allowing birds to facilitate the spread of *Trichinella* into new hosts and geographical areas. The rarity of *Trichinella* infection reports in birds may be due at least in part to limited sampling effort, emphasizing the need for increased surveillance efforts. Although studies have tested wildlife for *Trichinella* in Oklahoma (e.g., coyotes, *Canis latrans*, Reichard et al. 2011; bobcats, *Lynx rufus*, Reichard et al. 2021; feral hogs, *Sus scrofa*, Hill et al. 2014), this U.S. state remains under-sampled in general. Additionally, no studies have examined birds from Oklahoma for *Trichinella*. Therefore, the objective of this study was to survey feral hogs and various bird species from Oklahoma for *Trichinella*.

Methods

Bird carcasses used in this study were collected in two different ways. A subset of bird carcasses were collected in Stillwater, Oklahoma (Payne County), USA, as part of permitted research on bird-window collisions (Riding et al. 2020) and under appropriate federal and state permits (see acknowledgements for permit numbers). These birds included residents and migrants and were collected between April and

October of 2015-2017. They capture a variety of species, most of which were passerines (e.g., American robin, northern cardinal, and scissor-tailed flycatcher), but also include non-passerines (e.g., mourning dove and yellow-billed cuckoo). Additional birds were obtained as donations from the Oklahoma State University (OSU) Zoological Medicine service from Kay, Lincoln, Noble, and Payne Counties, Oklahoma throughout the year between 2015–2018 (Table 1); this sample included a similar mix of passerine and non-passerine species, but was notable in also including raptors (e.g., Mississippi kite, turkey vulture, and barred owl). The animals donated by the OSU Zoological Medicine service were injured animals presented for wildlife rehabilitation that were euthanized due to their injuries, unrelated to this study. Pectoralis muscle from birds was removed with forceps and a scalpel by dissection. Tongues and jowl tissues were obtained from feral hogs (*Sus scrofa*) through the United States Department of Agriculture (USDA) Animal and Plant Health Inspection Service (APHIS) Wildlife Services during routine hunting and disease surveillance from Jefferson, Love, Osage, Pawnee, Pittsburg, and Tillman Counties, Oklahoma between March and April, 2015 (Johnson et al. 2017). All bird and hog tissues were transported on ice to the Oklahoma Animal Disease Diagnostic Laboratory and frozen at -18°C until evaluation.

For detecting *Trichinella* spp. infections, tissues from birds and hogs were thawed and immediately used for artificial digestions (Reichard et al. 2017). Briefly, tissues were weighed (to the nearest 0.1 g) and homogenized using a Polytron (Kinematica GmbH, Kriens-Luzern, Switzerland). Samples were then mixed with 10 ml of artificial digestive fluid (1% pepsin, 1:10,000 IU, and 1% hydrochloric acid) per gram of tissue and mixed on stir plates at 37°C for 30 min. After 30 min, samples were cooled on ice and allowed to settle for 20 min, in which the top transparent supernatant layers were then carefully removed and resuspended in tap water. This washing process was repeated 3–5 times depending on the amount of cellular debris, and larvae were searched for under a stereomicroscope at 20–40x magnification. All averages include ± 1 standard deviation and range, and prevalence include 95% confidence intervals.

Sera from a subset of hogs were tested for antibodies to *Trichinella* spp. using a

Table 1. Potential hosts from Oklahoma examined for *Trichinella* spp. via artificial digestion and ELISA methods. County names in bold indicate counties where antibodies to *Trichinella* spp. were detected in feral hogs.

Host class	Host order	Host species	Oklahoma county collected (sample size)	Hosts infected /hosts examined: via digestions	Hosts infected /hosts examined: via ELISA
Mammalia	Artiodactyla	Feral hog (*Sus scrofa*)	Jefferson (6), **Love** (4), **Osage** (13), Pawnee (9), Pittsburg (4), Tillman (6)	0/42	2/31
Aves	Accipitriformes	Mississippi kite (*Ictinia mississippiensis*)	Noble (1)	0/1	–
Aves	Accipitriformes	Red-tailed hawk (*Buteo jamaicensis*)	Kay (1)	0/1	–
Aves	Cathartiformes	Turkey vulture (*Cathartes aura*)	Lincoln (1), Payne (2)	0/3	–
Aves	Columbiformes	Mourning dove (*Zenaida macroura*)	Payne (1), Unknown (1)	0/2	–
Aves	Cuculiformes	Yellow-billed cuckoo (*Coccyzus americanus*)	Payne (2)	0/2	–
Aves	Falconiformes	American kestrel (*Falco sparverius*)	Lincoln (1), Payne (1)	0/2	–
Aves	Passeriformes	Eastern meadowlark (*Sturnella magna*)	Payne (1)	0/1	–
Aves	Passeriformes	American robin (*Turdus migratorius*)	Payne (8)	0/8	–
Aves	Passeriformes	Common grackle (*Quiscalus quiscula*)	Payne (1)	0/1	–
Aves	Passeriformes	Northern cardinal (*Cardinalis cardinalis*)	Payne (4)	0/4	–
Aves	Passeriformes	Scissor-tailed flycatcher (*Tyrannus forficatus*)	Payne (2)	0/2	–
Aves	Passeriformes	Eastern kingbird (*Tyrannus tyrannus*)	Payne (1)	0/1	–
Aves	Passeriformes	European starling (*Sturnus vulgaris*)	Payne (1)	0/1	–
Aves	Passeriformes	House sparrow (*Passer domesticus*)	Payne (1)	0/1	–
Aves	Passeriformes	Northern mockingbird (*Mimus polyglottos*)	Payne (2)	0/2	–
Aves	Passeriformes	Orchard oriole (*Icterus spurius*)	Payne (1)	0/1	–
Aves	Passeriformes	House finch (*Haemorhous mexicanus*)	Payne (1)	0/1	–
Aves	Piciformes	Northern flicker (*Colaptes auratus*)	Payne (1)	0/1	–
Aves	Strigiformes	Barred owl (*Strix varia*)	Payne (1)	0/1	–
Total				**0/78**	**2/31**

commercial ELISA kit (SafePath Laboratories, Carlsbad, CA, USA). Each sample was tested using the manufacturer's recommended testing procedure. Positive and negative control sera from hogs were included with the kit and used for each ELISA plate. Samples that had absorbance values ≥0.3 after subtraction of the negative control absorbance value were considered positive (SafePath Laboratories; Hill et al. 2014). Samples reading less than 0.3 after subtraction of the negative control were considered negative.

Results

A total of 78 wild animals were examined for *Trichinella* spp. infection. These included 42 tissue samples from feral hogs (17 females, 8 males, 17 sex unknown) and 36 bird carcasses (2 females, 4 males, 30 sex unknown) from 8 orders and 19 species (Table 1). An average of 5.5 g ± 4.6 (0.2–18.5) of bird tissue and 4.6 g ± 0.8 (2.5–5.5) of hog tissue were included in artificial digestions. No *Trichinella* larvae were detected in any bird or hog samples examined via artificial digestion. A subset of 31 feral hogs had sera that was available and was tested for antibodies to *Trichinella* spp. Of these 31 samples, 2 feral hogs (6.5%; 0.76–21.8%), one each from Love and Osage Counties, Oklahoma, had detectable antibodies to *Trichinella*.

Discussion

Previous reports of *Trichinella* in Oklahoma wildlife indicate an overall low prevalence. For example, prevalence of *Trichinella murrelli* in coyotes was 6.8% (Reichard et al. 2011); overall prevalence of *T. murrelli* and *T. pseudospiralis* in bobcats was 5.9% (Reichard et al. 2021); and seroprevalence of *Trichinella* spp. in feral hogs was 1.4% (Hill et al. 2014). The mapped distribution of all known Oklahoma counties with *Trichinella* in wildlife shows a patchy distribution, suggesting that other counties may contain infected hosts (Fig. 1). Our finding of a seroprevalence of 6.5% in feral hogs is similar to the findings of Hill et al. (2014), in which only 6 (1.4%) of the 425 feral hogs tested were positive for antibodies to *Trichinella*. Taken together, this suggests feral hogs may not be serving as important hosts in the sylvatic cycle in Oklahoma. However, the threat of feral hogs introducing pathogens, such as *Trichinella*, into domestic pig populations and vice versa may increase with the range expansion of invasive feral hogs (Hill et al. 2014; VerCauteren et al. 2019; USDA 2023). Feral hogs likely become infected via cannibalism, such as tail biting, a typical behavior in feral hogs (Hill et al. 2014). Common hunting practices such as leaving field-dressed pig carcasses behind may also facilitate the transmission of *Trichinella* to scavenging feral hogs (Hill et al. 2014). Thus, managing feral hog populations has the potential to help reduce *Trichinella* infections in animals and humans.

In Oklahoma, Reichard et al. (2011; 2021) conducted the most extensive surveys for *Trichinella* in carnivores, including bobcats and coyotes, and suggested rodents may be a potential source of *Trichinella* infection in bobcats. Coyotes have a variable diet but consume predominantly small mammals in Oklahoma (Best et al. 1981). Therefore, small mammals may be important in the sylvatic transmission cycle. However, some small mammals such as rodents may not live long enough to transmit the parasites to larger carnivores, and they may not be able to ingest enough infected tissue to permit transmission (Pozio and Murrell 2006). Regardless, many species of small mammals have been shown to harbor *Trichinella* larvae (Pozio 2005) and may be important reservoirs, especially in scavengers. Studies in Oklahoma have yet to examine small mammals for *Trichinella*, making them a useful candidate host group for future studies.

Trichinella reports in birds are overall few, and this has been suggested to be a result of the fewer examinations of birds compared to mammals (Pozio and Murrell 2006). To date, *T. pseudospiralis* is the only species reported in birds, which may be due to the non-encapsulated nature of the species, and can survive at higher temperatures of 40.5–42.5 °C in birds compared to all other *Trichinella* species (Pozio 2005). Reports of *Trichinella* spp. exist from at least 13

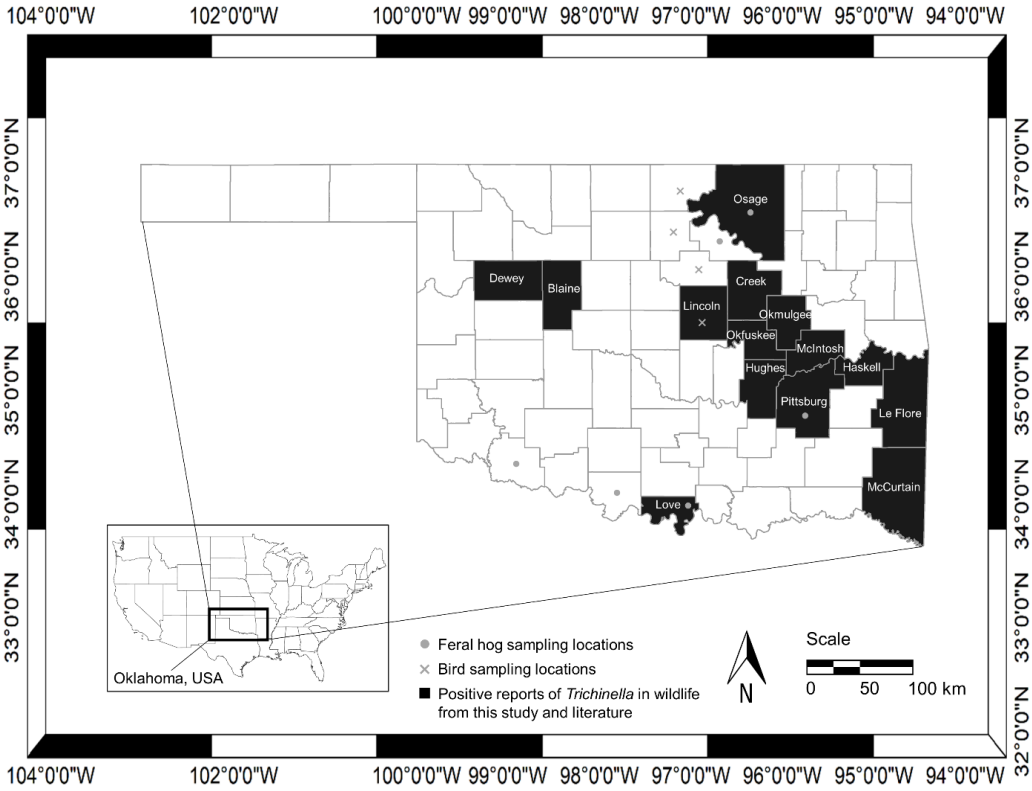

Figure 1. Map of Oklahoma showing all known* *Trichinella* reports in wildlife. Counties in which *Trichinella* larvae or antibodies to *Trichinella* spp. have been detected are shaded black. Counties sampled for feral hogs from this study are indicated as a grey circle. Counties sampled for birds from this study are indicated as a grey x (Reichard et al. 2011; Reichard et al. 2021).*County-level data on antibodies to *Trichinella* spp. in Oklahoma feral hogs reported by Hill et al. 2014 were not available for inclusion in this map.

species and five orders of birds: six species of Accipitriformes (osprey, kites, hawks, eagles), four species of Strigiformes (owls), one species of Charadriiformes (shorebirds), one species of Falconiformes (falcons, caracaras), and one species of Passeriformes (perching birds); however, *T. pseudospiralis* has only been confirmed in seven bird species (Pozio 2005). Reports in birds represent a cosmopolitan distribution, including occurrences in Australia, Asia, Europe, and North America, and prevalence of *T. pseudospiralis* in birds appears to be relatively low. For example, Rausch et al. (1956) reported a prevalence of 10% (1/10) in pomarine jaegers (*Stercorarius pomarinus*) from Alaska; Zimmermann and Hubard (1969) reported a prevalence of 0.4% (1/237) in great horned owls (*Bubo virginianus*) from Iowa; and Shaikenov (1980) reported a prevalence of 0.7% (2/296) in rooks (*Corvus frugilegus*) from Kazakhstan.

The lack of detections of *Trichinella* larvae in the birds in this study may similarly be due to low sample size, but may also be due to the majority of birds examined occupying a lower trophic position in the food web. A smaller proportion of birds (22%) were raptors, including the Mississippi kite, red-tailed hawk, turkey vulture, American kestrel, and barred owl (Table 1). These groups have a higher probability of ingesting *Trichinella* in carcasses, which may explain why most reports of natural infection are for meat-eating birds. Although not true

predators, additional birds sampled in this study may occasionally ingest meat via opportunistic scavenging or predation, such as house sparrows (MacGregor-Fors et al. 2020), adding to the importance of testing non-carnivorous birds for *Trichinella*. Interestingly, *T. pseudospiralis* has been shown experimentally to infect a wide range of bird species from at least five additional orders of birds, suggesting it has a very wide host spectrum in birds (Pozio 2005). Finally, it should be noted that birds were collected from various months throughout the year, yet the seasonality of *Trichinella* in birds remains poorly studied.

The detection of *Trichinella* antibodies in feral hog sera, despite not finding larvae in artificial digestions, suggests there are limitations of tissue digestion. A similar trend was also observed in Hill et al. (2014), in which antibodies for *Trichinella* spp. were detected in 2.9% (29/984) of feral hogs, but *Trichinella spiralis* larvae were only found in 1.81% (6/330) of tongues. The artificial digestion technique has also failed to detect *Trichinella* larvae in sheep while real-time PCR showed five positive samples (Wang et al. 2023), implying digestions have an overall low sensitivity. Several reasons may explain these differences. The current study examined a small portion of hog tissue (average 4.6 g), yet the recommended tissue sample to detect 1 larvae per gram (LPG) of *Trichinella* is 5 g (Gajadhar et al. 2019). If the actual intensity in feral hogs is less than 1 LPG, larvae may have been missed. This may also be true for bird tissues, although the average tissue amount examined was 5.5 g. Additionally, only tongues and jowl tissue were examined from feral hogs, which may have biased our detection results. Other striated muscles, such as diaphragm and foreleg tissues, have been recently suggested as predilection muscles for detecting *Trichinella* in feral hogs, and evaluation of additional tissue types may have revealed larvae that were not present in the tissues sampled in this study (Gajadhar et al. 2019). Another factor affecting the accuracy of digestions may be the freezing and thawing of tissues. Because the majority of *Trichinella* species have a low freeze resistance and some have a very thin collagen capsule (i.e., non-encapsulated clade), the artificial digestion process can potentially degrade individuals of these species and reduce sensitivity of their detection. Overall, the digestion technique has been considered the gold standard for *Trichinella* detection (Crisóstomo-Jorquera and Landaeta-Aqueveque 2022). However, there are limitations to this method, such as being insensitive and failing to detect low numbers of larvae in muscle samples (Wang et al. 2023). Utilizing additional techniques (e.g., antibody detection) may be important to consider in future studies.

This is the second study to detect *Trichinella* spp. in feral hogs in Oklahoma and the first to examine various bird species in Oklahoma for *Trichinella* spp. Identifying additional reservoir hosts for *Trichinella* species remains an important goal. This study examined potential host species in Oklahoma, a state known for few *Trichinella* reports. Further surveillance of Oklahoma wildlife for *Trichinella* is required to properly assess the unknown routes of transmission and potential reservoir hosts. Additionally, it is not known whether humans are increasing their risk of *Trichinella* infection with anthropogenic changes (e.g., increased interactions between humans and areas with infected wildlife). We recommend that studies incorporate multiple collecting methods such as blood and tissue sampling to help answer these questions.

Acknowledgements

We thank personnel at the OSU Zoological Medicine Service for help with processing bird carcasses. This study was funded by internal funds available to MVR, Oklahoma State University. Bird carcasses were collected under a federal Scientific Collecting Permit (U.S. Fish and Wildlife Service permit #MB05120C-0), and Oklahoma Department of Wildlife Conservation Scientific Collector permits (multiple permit numbers) with protocols approved by the OSU Institutional Animal Care and Use Committee (protocol #AG-14-8), or obtained as donations from the OSU Zoological Medicine Service. Feral hogs were obtained through the USDA APHIS Wildlife Service during routine hunting

and disease surveillance.

References

Best TL, Hoditschek B, Thomas HH. 1981. Foods of coyotes (*Canis latrans*) in Oklahoma. Southwest Nat 26:67–69.

Casillas SM, Jones JL. 2017. Surveillance for trichinellosis—United States, 2015 annual summary. U. S. Department of Health and Humans Services, CDC, Atlanta, Georgia.

Centers for Disease Control and Prevention. 2019. Parasites – Trichinellosis. https://www.cdc.gov/parasites/trichinellosis/epi.html. Accessed October 2023.

Crisóstomo-Jorquera V, Landaeta-Aqueveque C. 2022. The genus *Trichinella* and its presence in wildlife worldwide: A review. Transbound Emerg Dis 69:1269–1279.

Gajadhar AA, Noeckler K, Boireau P, Rossi P, Scandrett B, Gamble HR. 2019. International Commission on Trichinellosis: Recommendations for quality assurance in digestion testing programs for *Trichinella*. Food Waterborne Parasitol 16:00059.

Hill DE, Dubey JP, Baroch JA, Swafford SR, Fournet VF, Hawkins-Cooper D, Pyburn DG, Schmit BS, Gamble HR, Pedersen K, Ferreira LR. 2014. Surveillance of feral swine for *Trichinella* spp. and *Toxoplasma gondii* in the USA and host-related factors associated with infection. Vet Parasitol 205:653–665.

Johnson EM, Nagamori Y, Duncan-Decocq RA, Whitley PN, Ramachandran A, Reichard MV. 2017. Prevalence of *Alaria* infection in companion animals in north central Oklahoma from 2006 through 2015 and detection in wildlife. J Am Vet Med Assoc 250:881–886.

MacGregor-Fors I, García-Arroyo M, Marín-Gómez OH, Quesada J. 2020. On the meat scavenging behavior of House Sparrows (*Passer domesticus*). Wilson J Ornithol 132:188–191.

Pozio E. 2005. The broad spectrum of *Trichinella* hosts: from cold-to warm-blooded animals. Vet Parasitol 132:3–11.

Pozio E, Murrell KD. 2006. Systematics and epidemiology of *Trichinella*. Adv Parasitol 63:367–439.

Pozio E, Zarlenga DS. 2013. New pieces of the *Trichinella* puzzle. Int J Parasit 43:983–997.

Rausch R, Babero BB, Rausch RV, Schiller EL. 1956. Studies on the helminth fauna of Alaska. XXVII. The occurrence of larvae of *Trichinella spiralis* in Alaskan mammals. J Parasitol 42:259–271.

Rawla P, Sharma S. 2022. *Trichinella spiralis* infection. In StatPearls. StatPearls Publishing.

Reichard MV, Tiernan KE, Paras KL, Interisano M, Reiskind MH, Panciera RJ, Pozio E. 2011. Detection of *Trichinella murrelli* in coyotes (*Canis latrans*) from Oklahoma and North Texas. Vet Parasitol. 182:368–371.

Reichard MV, Logan K, Criffield M, Thomas JE, Paritte JM, Messerly DM, Interisano M, Marucci G, Pozio E. 2017. The occurrence of *Trichinella* species in the cougar *Puma concolor couguar* from the state of Colorado and other regions of North and South America. J Helminthol 91:320–325.

Reichard MV, Sanders TL, Prentiss NL, Cotey SR, Koch RW, Fairbanks WS, Interisano M, La Rosa G, Pozio E. 2021. Detection of *Trichinella murrelli* and *Trichinella pseudospiralis* in bobcats (*Lynx rufus*) from Oklahoma. Vet Parasitol: Reg Stud Rep 25:100609.

Riding CS, O'connell TJ, Loss SR. 2020. Building façade-level correlates of bird–window collisions in a small urban area. Condor 122:duz065.

Shaikenov B. 1980. Spontaneous infection of birds with *Trichinella pseudospiralis* Garkavi, 1972. Folia Parasitol 27:227–230.

Sharma R, Thompson PC, Hoberg EP, Scandrett WB, Konecsni K, Harms NJ, Kukka PM, Jung TS, Elkin B, Mulders R, Larter NC. 2020. Hiding in plain sight: discovery and phylogeography of a cryptic species of *Trichinella* (Nematoda: Trichinellidae) in wolverine (*Gulo gulo*). Int J Parasitol 50:277–287.

USDA (2023) History of feral swine in the Americas. Animal and Plant Health Inspection Service.

VerCauteren KC, Beasley JC, Ditchkoff SS, Mayer JJ, Roloff GJ, Strickland BK. 2019. Invasive wild pigs in North America: ecology, impacts, and management. CRC Press, Boca Raton, FL.

Wang Y, Sang X, El-Ashram S, Ding Y, Yu K, Feng Y, Yang N. 2023. Establishment of a method for detecting *Trichinella spiralis* in ovine muscle tissues using real-time fluorescence quantitative PCR. Exp Parasitol 246:108457.

Zimmermann WJ, Hubard ED. 1969. Trichiniasis in wildlife of Iowa. Am J Epidemiol 90:84–92.

Submitted August 4, 2023 Accepted October 30, 2023

Coccidian Parasites of Eastern Cottontail, *Sylvilagus floridanus* (Lagomorpha: Leporidae) from Oklahoma, with a Summary of Coccidians (Apicomplexa: Eimeriidae) from Mammals of the State

Chris T. McAllister*
Division of Natural Sciences, Northeast Texas Community College, Mt. Pleasant, TX 75455

John A. Hnida
Department of Microbiology and Immunology, Midwestern University, Glendale, AZ 85308

Henry W. Robison
602 Big Creek Drive, Sherwood, AR 72120

Abstract: A single eastern cottontail, *Sylvilagus floridanus*, collected opportunistically in January 2023 from McCurtain County, Oklahoma, was examined for coccidian parasites. Two coccidians were passed in feces of this host, including *Eimeria neoirresidua* and *Eimeria poudrei*. Ellipsoidal to ovoidal oocysts of *E. neoirresidua* averaged (L × W) 28.6 × 17.5 µm; a polar granule and an oocyst residuum were absent but a micropyle was present. Ellipsoidal sporocysts of *E. neoirresidua* averaged 14.4 by 7.1 µm and a sporocyst residuum was present. Ovoidal to ellipsoidal oocysts of *E. poudrei* averaged 24.9 × 17.1 µm; a polar granule was absent but a micropyle and an oocyst residuum were present. Ellipsoidal to ovoidal sporocysts of *E. poudrei* averaged 13.2 × 6.5 µm and a sporocyst residuum was present. Here, we provide the first report of these two coccidians from *S. floridanus* in Oklahoma, including a summary of the coccidians documented from mammals of the state.

Introduction

Coccidians are apicomplexan parasites that are accountable for an intestinal disease that affects several different vertebrates, including rabbits (Lagomorpha). As such, they are hosts of one of the most common North American protozoan infections.

The eastern cottontail, *Sylvilagus floridanus* (J.A. Allen) has been the subject of several coccidian studies, including harboring 16 species (Duszynski and Couch 2013). However, we are not aware of previous reports of coccidians from *S. floridanus* in Oklahoma. Here, we document two species of *Eimeria* from a single *S. floridanus* collected from southeastern Oklahoma. In addition, we provide a summary of the coccidians documented from mammals of the state.

Methods

On 30 January 2023, a single adult *S. floridanus* was found freshly dead on the road (DOR) in Broken Bow, McCurtain County.

***Corresponding author: cmcallister@ntcc.edu**

It was taken to the lab and examined for coccidians. A mid-ventral incision was made to expose the lower gastrointestinal tract and a fresh fecal sample as well as rectal contents was placed in an individual vial containing 2.5% (w/v) aqueous potassium dichromate ($K_2Cr_2O_7$). The sample was further examined for coccidia via flotation in a 15-ml conical centrifuge tube (with centrifugation) containing Sheather's sugar solution (Ricca Chemical Company, Arlington, Texas; specific gravity: 1.25) using an Olympus BX43 light microscope (Olympus Corporation, Center Valley, Pennsylvania). Partially sporulated oocysts were placed in a Petri dish containing a small layer of $K_2Cr_2O_7$ for 48–72 hr to allow complete sporulation. All morphological measurements are reported in micrometers (µm) with the means followed by the ranges in parentheses. Oocysts were ca. 90 days old from the time they were found in host feces to the time when they were measured and photographed using Nomarski interference-contrast optics at ×1,000 magnification. Oocyst and sporocyst descriptions follow the standard guidelines of Wilber et al. (1998) including oocyst length (L) and width (W), their ranges and ratios (L/W), micropyle (M), oocyst residuum (OR), polar granule(s) (PG), sporocyst length (L) and width (W), their ranges and ratio (L/W), sporocyst (SP), Stieda body (SB), sub-Stieda body (SSB), para-Stieda body (PSB), sporocyst residuum (SR), sporozoites (SZ) anterior (ARB) and posterior (PRB) refractile bodies, and nucleus (N).

A photovoucher of *S. floridanus* was accessioned into the Eastern Oklahoma State Collection, Idabel, Oklahoma. Photovouchers of sporulated oocysts were accessioned into the Harold W. Manter Laboratory of Parasitology (HWML), Lincoln, Nebraska.

Results and Discussion

Two coccidians were recovered from the fecal sample as follows: *Eimeria neoirresidua* and *Eimeria poudrei*. Data are provided on each in an annotated format below.

Eimeria neoirresidua Duszynski and Marquardt, 1969

(Figs. 1A–B)

Description of sporulated oocyst: Oocyst shape (n = 15): ellipsoidal to ovoidal; bilayered wall, ~1.3 (1.0–1.5) outer layer smooth (n = 10) or lightly pitted (n = 5), colorless to ~/2/3 total thickness; darker inner layer. L × W (n = 15): 28.6 × 17.5 (26–31 × 16–19); L/W ratio: 1.6 (1.5–1.8); M present, 4.0 (3.0–5.0); OR: and PG both absent.

Description of sporocyst and sporozoites: Sporocyst shape: ellipsoidal; L × W (n = 15): 14.4 × 7.1 (16–18 × 6–8); L/W ratio: 2.0 (1.9–2.3); nipple-like SB present, SSB, PSB: both absent; SR: present; SR characteristics: spheroidal to irregular mass of large granules. Sporozoite shape: elongate with large PRB and small central N.

Taxonomic Summary

Host: Eastern cottontail, *Sylvilagus floridanus* (J. A. Allen, 1890); photovoucher host deposited in the EOSC collection.

New geographic distribution: USA: Oklahoma: McCurtain County, off Hatchery Road, Broken Bow (34.008114°N, -94.756989°W).

Type host and locality: Desert cottontail, *Sylvilagus audubonii* (Baird); USA: Colorado, Larimer County, near Ft. Collins (Duszynski and Marquardt 1969).

Other localities: USA: Pennsylvania (Wiggins et al. 1980); Italy: Province of Alessandria (Bertolino et al. 2010).

Prevalence: 1/1.

Sporulation: Oocysts were passed partially sporulated and completed sporulation in 24–48 hr in $K_2Cr_2O_7$.

Site of infection: Unknown; oocysts passed in feces.

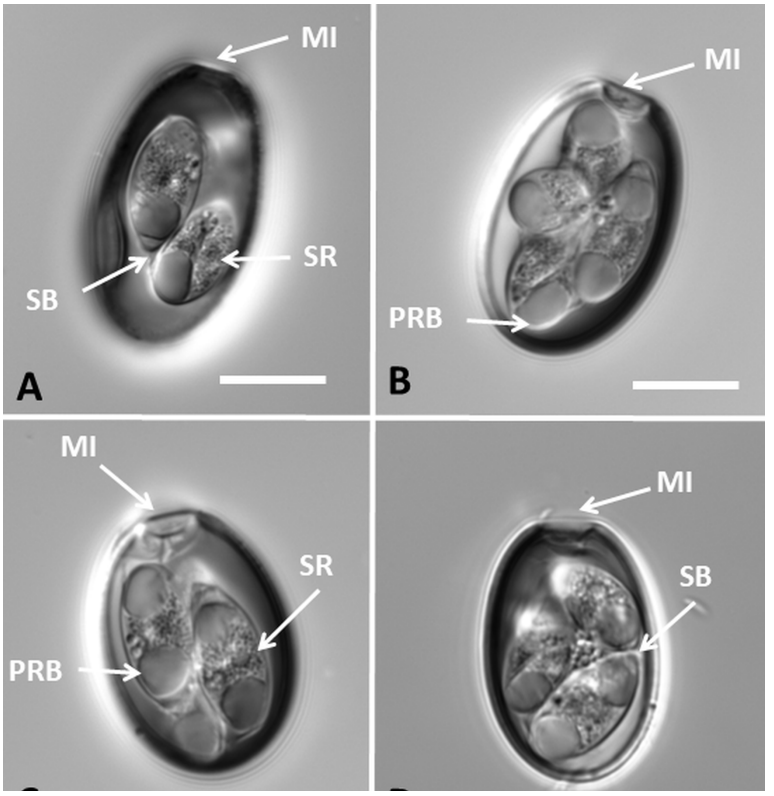

Figure 1. Sporulated oocysts of two coccidians from *Sylvilagus floridanus*. (A–B) *Eimeria neoirresidua*. (C–D) *Eimeria poudrei*. Scale bars = 10 µm. Abbreviations: MI (micropyle); PRB (posterior refractile body); SB (Stieda body); SR (sporocyst residuum).

Materials deposited: Photovoucher of sporulated oocysts are deposited as HWML 217042.

Remarks

Oocysts from the present sample were not significantly different from those described originally by Duszynski and Marquardt (1969) from *S. audubonii* from Colorado and those described by Wiggins et al. (1980) from *S. floridanus* from Pennsylvania. Our oocysts were, on average, slightly greater in length (28.6 *vs.* 25.7 µm) than those reported by Duszynski and Marquardt (1969) and slightly greater in length and width (28.6 × 17.5 *vs.* 25.2 × 16.8 µm) than those reported by Wiggins et al. (1980). Average L×W sizes of our sporocysts were nearly identical (14.4 × 7.1 *vs.* 14.5 × 6.4 µm) to those reported by Duszynski and Marquardt (1969) and slightly larger (14.4 × 7.1 *vs.* 12.6 × 6.4 µm) than those reported by Wiggins et al. (1980). All other morphological and mensural characteristics of the oocysts from the present sample were similar to those previously reported for *E. neoirresidua*.

Eimeria poudrei Duszynski and Marquardt, 1969

(Figs. 1C–D)

Description of sporulated oocyst: Oocyst shape (n = 15): ovoidal to ellipsoidal; bilayered wall, ~1.3 (1.3–1.5) outer layer smooth, colorless to ~/2/3 total thickness; darker inner layer. L × W (n = 15): 24.9 × 17.1 (20–30 × 16–19); L/W ratio: 1.5 (1.3–1.7); M present, 3.9 (3.0–4.5); OR present, irregular to spheroidal mass of medium to large granules; PG absent.

Description of sporocyst and sporozoites: Sporocyst shape: ellipsoidal to ovoidal; L × W (n = 15): 13.2 × 6.5 (10–16 × 6–8); L/W ratio: 2.1 (1.7–2.2); nipple-like SB present, SSB, PSB: both absent; SR: present; SR characteristics:

Irregular mass of medium to large granules. Sporozoite shape: elongate with large PRB and small central N.

Taxonomic Summary

Host: Eastern cottontail, *Sylvilagus floridanus* (L., 1758); photovoucher host deposited in the EOSC collection.

New geographic distribution: USA: Oklahoma: McCurtain County, off Hatchery Road, Broken Bow (34.008114°N, -94.756989°W).

Type host and locality: Desert cottontail, *Sylvilagus audubonii* (Baird); USA: Colorado, Larimer County, near Ft. Collins.

Other localities: Italy: Province of Alessandria (Bertolino et al. 2010).

Prevalence: 1/1.

Sporulation: Oocysts were passed partially sporulated and completed sporulation in 24–48 hr in $K_2Cr_2O_7$.

Site of infection: Unknown; oocysts passed in feces.

Materials deposited: Photovoucher of sporulated oocysts are deposited as HWML 217043.

Remarks

Oocysts from the present sample were not significantly different from those described originally by Duszynski and Marquardt (1969) from *S. audubonii* from Colorado. Average L×W sizes of our oocysts (24.9 × 17.1 *vs.* 26.0 × 18.1 µm) and sporocysts (13.2 × 6.5 *vs.* 14.4 × 6.4 µm) were nearly identical to those reported by Duszynski and Marquardt (1969) as well as all other mensural and morphological characteristics fitting *E. poudrei*.

Interestingly, Bertolino et al. 2010 reported that *S. floridanus* from Italy harbored both *E. poudrei* (40% prevalence), and *E. neoirresidua* (49% prevalence). They found a total of eight eimerians in 113 *S. floridanus*, of which all but one had North American origins, and were presumably introduced into Italy together with imported cottontails.

Including the mammalian host species included herein, 11 species of coccidians have been reported in six species of Oklahoma mammals, including those in two chiropterans, and a single each of eulipotyphlan and lagomorph, as well as two rodents (Table 1). As Oklahoma supports 108 native species of mammals (Caire et al. 2019) and only 6% have been reported with coccidia to date, much more survey work remains in determining the coccidian fauna of this class of vertebrates, including salvaging DOR specimens as in the present case.

Acknowledgements

The Oklahoma Department of Wildlife Conservation issued Scientific Collecting Permit No. 1551646 to CTM. Drs. Scott L. Gardner and Gabor Racz (HWML) are acknowledged for expert curatorial assistance.

References

Bertolino S, Hofmannová L, Girardello M, Modry D. 2010. Richness, origin and structure of an *Eimeria* community in a population of eastern cottontail (*Sylvilagus floridanus*) introduced into Italy. Parasitology 137:1179–1186.

Caire W, Loucks LS, Haynie ML, Coyner BS, Braun JK. 2019. Updated and revised checklist of the mammals of Oklahoma, 2019. Proc Oklahoma Acad Sci 99:1–6.

Duszynski DW, Couch L. 2013. The biology and identification of the coccidia (Apicomplexa) of rabbits of the world. London (UK): Elsevier Science. 352 p.

Duszynski DW, Marquardt WC. 1969. *Eimeria* (Protozoa: Eimeridae) of the cottontail rabbit, *Sylvilagus audubonii*, in northeastern Colorado with descriptions of three new species. J Protozool 16:128–137.

Table 1. Coccidians reported from Oklahoma mammals.*

Coccidian	Host	Prevalence†	County Locality	Reference
Eimeria catronensis	*Myotis septentrionalis*	1/4 (25)	Le Flore	McAllister et al. (2012)
Eimeria lukfataensis	*Sciurus carolinensis*	1/3 (33)	McCurtain	McAllister et al. (2019)
Eimeria macyi	*Perimyotis subflavus*	1/2 (50)	Delaware	McAllister et al. (2016)
Eimeria neoirresidua	*Sylvilagus floridanus*	1/1 (100)	McCurtain	This study
Eimeria poudrei	*S. floridanus*	1/1 (100)	McCurtain	This study
Eimeria roperi	*Sigmodon hispidis*	4/30 (13)	Payne	Faulkner and Lochmiller (1997)
Eimeria sigmodontis	*S. hispidis*	15/30 (50)	Payne	Faulkner and Lochmiller (1997)
Eimeria tkachi	*Blarina carolinensis*	2/3 (67)	McCurtain	McAllister and Seville (2017)
Eimeria tumlisoni	*M. septentrionalis*	1/4 (25)	Le Flore	McAllister et al. (2012)
Eimeria tuskegenesis	*S. hispidis*	3/30 (10)	Payne	Faulkner and Lochmiller (1997)
Eimeria webbae	*S. hispidis*	2/30 (7)	Payne	Faulkner and Lochmiller (1997)

*Not including large game (deer, elk, bears, pronghorn antelopes) and farm animals (goats, sheep, cattle, pigs).

†Prevalence = number infected/number examined (%).

Faulkner BC, Lochmiller RL. 1977. New locality records of coccidian parasites (Apicomplexa: Eimeridae) of the hispid cotton rat (*Sigmodon hispidus*) from Oklahoma. Proc Oklahoma Acad Sci 77:131–132.

McAllister CT, Connior MB, Bursey CR, Durden LA, Seville RS, Robison HW, Trauth SE. 2016. Parasites (Coccidia, Trematoda, Acari) of tri-colored bats, *Perimyotis subflavus* (Chiroptera: Vespertilionidae): New geographical records for Oklahoma. Proc Oklahoma Acad Sci 96:63–69.

McAllister CT, Seville RS. 2017. A new eimerian (Apicomplexa: Eimeriidae) from southern short-tailed shrews, *Blarina carolinensis* (Bachman) (Soricimorpha: Soricidae: Soricinae) from southeastern Oklahoma, USA. Syst Parasitol 94:711–716.

McAllister CT, Seville RS, Roehrs ZP. 2012. A new species of *Eimeria* (Apicomplexa: Eimeriidae) from the northern myotis, *Myotis septentrionalis* (Chiroptera: Vespertilionidae), in Oklahoma. J Parasitol 98:1003–1005.

McAllister CT, Motriuk-Smith D, Seville RS. 2019. A new species of *Eimeria* (Apicomplexa: Eimeriidae) from eastern gray squirrel, *Sciurus carolinensis* (Rodentia: Sciuridae: Sciurinae: Sciurini) from Oklahoma, USA. Syst Parasitol 96:417–421.

Wiggins JP, Cosgrove M, Rothenbacher H. 1980. Gastrointestinal parasites of the eastern cottontail (*Sylvilagus floridanus*) in central Pennsylvania. J Wildl Dis 16:541–544.

Wilber PG, Duszynski DW, Upton SJ, Seville RS, Corliss JO. 1998. A revision of the taxonomy and nomenclature of the *Eimeria* spp. (Apicomplexa: Eimeriidae) from rodents in the Tribe Marmotini (Sciuridae). Syst Parasitol 39:113–135.

Submitted August 22, 2023 Accepted October 30, 2022

First Report of *Batrachochytrium dendrobatidis* (Chytridiomycota: Rhizophydiales) from American Bullfrog, *Rana catesbeiana* (Anura: Ranidae) from Western Arkansas

Chris T. McAllister
Division of Natural Sciences, Northeast Texas Community College, Mt. Pleasant, TX 75455

Isaac F. Standish
La Crosse Fish Health Center–Midwest Fisheries Center, U. S. Fish and Wildlife Service, Onalaska, WI 54650

Eric M. Leis
La Crosse Fish Health Center–Midwest Fisheries Center, U. S. Fish and Wildlife Service, Onalaska, WI 54650

Irvin Arroyo-Torres
Department of Biology, University of New Mexico, Albuquerque, NM 87131

Henry W. Robison
602 Big Creek Drive, Sherwood, AR 72120

Abstract: A single American bullfrog, *Rana catesbeiana*, collected in May 2023 from Polk County, Arkansas, harbored the skin fungus, *Batrachochytrium dendrobatidis* (*Bd*). However, the host showed no obvious pathological signs of infection. Three larval salamanders and six additional anurans collected from the same general locality were negative for *Bd* as well as other amphibian pathogens, including Ranavirus (specifically FV3) and *Batrachochytrium salamandrivorans* (*Bs*). This is the first time *R. catesbeiana* from Arkansas has been reported with *Bd* as well as being the fourth species of amphibian from the state harboring the fungus.

Introduction

Chytrid fungus causes the disease chytridiomycosis, originally produced by *Batrachochytrium dendrobatidis* (*Bd*). It was initially discovered in 1989 and is an amphibian chytrid that causes a skin infection, with an affinity to occur in anurans (frogs and toads) worldwide (Lips et al. 1999). Unfortunately, the disease has caused a serious decline in, and in some instances, extinction of more than 200 species of amphibians worldwide and poses the greatest threat to biodiversity of any known disease (Stuart 2004; Skerratt et al. 2007; Pounds et al. 2016; Collins 2020).

Arkansas supports a great diversity of 56 species and subspecies of amphibians (Trauth et al. 2004). However, to date, only three (5%) species from the state have been reported to be infected with the fungus. Federally endangered Ozark hellbenders, *Cryptobranchus alleganiensis bishopi* Grobman collected from the Eleven Point River in Randolph County

***Corresponding author: cmcallister@ntcc.edu**

were reported to harbor *Bd* (Briggler et al. 2008; Hardman et al. 2020). In another study, *Bd* was found in Blanchard's cricket frogs, *Acris blanchardi* Harper from the Wapanocca National Wildlife Refuge in Crittenden County (Hanlon et al. 2014). Interestingly, no specimens exhibited clinical signs of a *Bd* infection (e.g., lethargy, sloughing of skin), perhaps indicating that *Bd* in this population may persist without yielding to *Bd*-induced mortality. In a third study, frogs collected from the Bald Knob National Wildlife Refuge (White County) and Felsenthal National Wildlife Refuge (Union County), including postmetamorphic *A. blanchardi* from the former and tadpoles of Coastal Plains leopard frog, *Rana sphenocephala utricularia* (Cope) from the latter site, harbored *Bd* (Rothermel et al. 2008). Obviously, much more work needs to be done in the state to survey additional populations of amphibians for *Bd* and other amphibian pathogens. Here we attempt to help fill that void with examination of four species of amphibians from Arkansas for amphibian pathogens, specifically *Bd*.

Methods

Host collection and processing

On 31 July and 1 June 2023, the following 10 amphibians from Polk County were collected by hand and examined for *Bd* as well as for other amphibian pathogens, including Ranavirus (specifically FV3) and *Batrachochytrium salamandrivorans* (*Bs*): three juvenile Ouachita dusky salamanders, *Desmognathus brimleyorum* Stejneger from Grace Fountain Spring at Big Fork (34°29′07.1232″N, -93°58′05.16″W), and adults of four green frogs, *Rana clamitans* (Latreille), two American green treefrogs, *Dryophytes* (=*Hyla cinerea*) *cinereus* (Schneider), and a single juvenile American bullfrog, *Rana catesbeiana* (Shaw) from the Ouachita Mountains Biological Station (OMBS) pond (34°27'43.4484''N, -93°59'54.3264''W). We followed the protocols of Livo (2004) and Standish et al. (2018) by swabbing the ventral and dorsal skin of each amphibian (including the hind-toe webbing of anurans) 15 to 20× with 15.24 cm sterile cotton-tipped applicators (Medline, Northland, Illinois) and preserving the swabs in individual sterile vials containing 95% DNA grade ethanol. Several preventative steps were taken to avoid cross-contamination by keeping individuals separate from the time of collection, using a new pair of gloves to handle each specimen, and swabbing individuals before taking their snout-vent length (SVL) measurements. Following processing, all amphibians were photographed and released unharmed at their site of collection. We follow the use of the genus *Rana* versus *Lithobates* for North American ranid frogs following Yuan et al. (2016).

Molecular techniques

To examine swab DNA, ethanol was decanted, and swabs were air-dried. Sample DNA was extracted using 150 µL of the PrepMan™ Ultra Sample Preparation Reagent (Thermo Fisher Scientific, Waltham, Massachusetts) following the manufacturer's instructions. Extracted DNA was analyzed using a multiplex quantitative PCR (qPCR) targeting *B. dendrobatidis* (*Bd*), *B. salamandrivorans* (*Bsal*) and frog virus 3-like Ranavirus as described by Standish et al. (2018). A synthetic gBlock® containing all three amplicons was used as a positive control and standard curve of 10× dilutions ranging from 10^7 to one copy per reaction was used to quantify copies per µL (Standish et al. 2018). Sample concentration (copies per ng total DNA) was calculated using a Qubit™ 3.0 Fluorometer (Thermo Fisher Scientific) and the Qubit™ DNA High Sensitivity Kit (Thermo Fisher Scientific) following the manufacturer's instructions.

Results

Ranavirus and *B. salamandrivorans* were not detected. One of 10 (10%) of the amphibians sampled harbored *Bd*. The host was a juvenile *R. catesbeianus* collected from the OMBS pond. The specimen appeared otherwise healthy and exhibited no overt symptoms of the infection. All other amphibians sampled were negative for the presence of pathogens.

No significant inhibition was observed in and qPCR reactions and amplification was only observed in one sample of this host. Samples

were initially screened (not quantified) then archived at -80º as we did not recognize the significance of this positive result. After two weeks samples, extracts were quantified and copy number determined. An average Cq value of 30.99 was observed across triplicate reactions which contained an average of 2382 copies of the *Bd* target amplicon or 9102 *Bd* copies per ng of total DNA.

Discussion

Interestingly, American bullfrogs have been reported to be seemingly resistant (asymptomatic) to the disease and may act as vectors or reservoir hosts (Daszak et al. 2004; Hanselmann et al. 2004). Although the factors are not fully understood, one characteristic that appears to protect *R. catesbeiana* from *Bd* involve the production of immunoprotective peptides (Eskew et al. 2018). This resistance has been thought to allow *R. catesbeiana* to spread *Bd* to various parts of North America and even other continents (Jenkinson et al. 2016; Yap et al. 2018). In addition, Garner et al. (2006) detected *Bd* infections in introduced *R. catesbeiana* from six countries, including Brazil, Canada (British Columbia), France, Italy, United Kingdom, and Uruguay; they also found *Bd* in introduced American bullfrogs from Arizona, USA. Standish et al. (2018) identified *Bd* and FV3 from 33.3% and 16.7%, respectively, of adult *R. catesbeiana* sampled in Wisconsin with none of the bullfrog tadpoles sampled testing positive for either pathogen. Rothermel et al. (2008) reported five of 229 (2%) individuals of *R. catesbeiana* from Georgia, North Carolina, and Virginia harbored *Bd* but specimens from Florida, Louisiana, Mississippi, and South Carolina were not infected; no *R. catesbeiana* from Arkansas were sampled. However, in adjacent Oklahoma, several studies have reported *Bd* in *R. catesbeiana* from the state either rarely or in high prevalence (Watters et al. 2016, 2018, 2019, 2021; Marhanka et al. 2017; Nichols et al. 2022).

We suggest additional amphibians from the state be surveyed for *Bd* as well as other amphibian pathogens. Undoubtedly, more individuals will be discovered to harbor this fungus, including the possibility, more importantly, of finding it in Arkansas endemic and protected species.

Acknowledgements

The Arkansas Game and Fish Commission issued Scientific Collecting Permit No. 032820232 to CTM. Dr. Laurence M. Hardy and Larry R. Raymond (OMBS) are acknowledged for providing gratis housing and laboratory space to CTM and IA-T. Usage of trade names does not imply endorsement by the U.S. Government. The findings and conclusions in this article are those of the authors and do not necessarily represent the views of the U.S. Fish and Wildlife Service.

References

Briggler JT, Larson KA, Irwin KJ. 2008. Presence of the amphibian chytrid fungus (*Batrachochytrium dendrobatidis*) on hellbenders (*Cryptobranchus alleganiensis*) in the Ozark highlands. Herpetol Rev 39:443–444.

Collins JP. 2010. Amphibian decline and extinction: what we know and what we need to learn. Dis Aquat Organ 92:93–99.

Daszak P, Streiby A, Cunningham AA, Longcore JE, Brown CC, Porter D. 2004. Experimental evidence that the bullfrog (*Rana catesbeiana*) is a potential carrier of chytridiomycosis, an emerging fungal disease of amphibians. Herpetol J 14:201–207.

Eskew EA, Shock BC, LaDouceur EEB, Keel K, Miller MR, Foley JE, Todd BD. 2018. Gene expression differs insusceptible and resistant amphibians exposed to *Batrachochytrium dendrobatidis*. Royal Soc Open Sci 5:170910. http://dx.doi.org/10.1098/rsos.170910

Garner TWJ, Perkins M, Govindarajulu P, Seglie D, Walker SJ, Cunningham AA, Fisher MC. 2006. The emerging amphibian pathogen *Batrachochytrium dendrobatidis* globally infects introduced populations of the North American bullfrog, *Rana catesbeiana*. Biol Lett 2:455–459.

Hanlon S., Smith S, Gerby JL, Berg E, Peterson W, Parris MJ, Moore JE. 2014. Occurrence of *Batrachochytrium dendrobatidis* in Wapanocca National Wildlife Refuge, Arkansas, USA. Herpetol Rev 45:31–32.

Hanselmann R, Rodriguez A, Lampo M, Fajardo-Ramos L, Aguirre AA, Kilpatrick AM, Rodriguez JP, Daszak P. 2004. Presence of an emerging pathogen of amphibians in introduced bullfrogs (*Rana catesbeiana*) in Venezuela. Biol Cons 120:115–119.

Hardman RH, Irwin KJ, Sutton WB, Miller DL. 2020. Evaluation of severity and factors contributing to foot lesions in endangered Ozark hellbenders, *Cryptobranchus alleghaniensis bishopi*. Front Vet Sci 7:34. doi: 10.3389/fvets.2020.00034

Jenkinson TS, Betancourt RCM, Lambertini C, Valencia-Aguilar A, Rodriguez D, Nunes-de-Almeida CHL, Ruggeri J, Belasen AM, da Silva Leite D, Zamudio KR, Longcore JE, Toledo LF, James TY. 2016. Amphibian-killing chytrid in Brazil comprises both locally endemic and globally expanding populations. Mol Ecol 25:2978–2996.

Lips KR, Brem F, Brenes R, Reeve JD, Alford RA, Voyles J, Carey C, Livo L, Longcore JE, Pessier AP, Nichols DK. 1999. *Batrachochytrium dendrobatidis* gen. et sp. nov., a chytrid pathogenic to amphibians. Mycologia 91:219–227.

Livo LJ. 2004. [online]. Methods for obtaining *Batrachochytrium dendrobatidis* (*Bd*) samples for PCR testing. Colorado Division of Wildlife, Denver, Colorado. Available from: http://wildlife.state. co.us/NR/rdonlyres/710BBC95-2DCF-4CF9-8443-D4561DBC3B69/0/PCRsampling2004.pdf. (Accessed 30 July 2023)

Marhanka EC, Watters JL, Huron NA, McMillin SL, Winfrey CC, Curtis DJ, Davis DR, Farkas JK, Kerby JL, Siler CD. 2017. Detection of high prevalence of *Batrachochytrium dendrobatidis* in amphibians from southern Oklahoma, USA. Herpetol Rev 48:70–74.

Nichols MH, Smith SN, Watters JL, Siler CD. 2022. Implementation of a citizen science program to assess chytridiomycosis (*Batrachochytrium dendrobatidis*) prevalence in amphibians across Oklahoma, USA. Proc Okla Acad Sci 102:1–18.

Pounds JA, Bustamante MR, Coloma LA, Consuegra JA, et al. 2006. Widespread amphibian extinctions from epidemic disease driven by global warming. Nature 439:161–167.

Rothermel BB, Walls SC, Mitchell JC, Dodd CK Jr, Irwin LJ, Green DE, Vazquez V, Petranka JW, Stevenson DJ. 2008. Widespread occurrence of the amphibian chytrid fungus *Batrachochytrium dendrobatidis* in the southeastern USA. Dis Aquat Organ 82:3–18.

Skerratt LF, Berger L, Speare R, Cashins S, McDonald KR, Phillott A, Hines H, Kenyon N. 2007. Spread of chytridiomycosis has caused the rapid global decline and extinction of frogs. EcoHealth 4:125–134.

Standish I, Leis E, Schmitz N, Credico J, Erickson S, Bailey J, Kerby J, Phillips K, Lewis T. 2018. Optimizing, validating, and field testing a multiplex qPCR for the detection of amphibian pathogens. Diseases of Aquatic Organisms 129:1–13.

Stuart SN. 2004. Status and trends of amphibian declines and extinctions worldwide. Science 306:1783–1786.

Trauth SE, Robison HW, Plummer MV. 2004. The amphibians and reptiles of Arkansas. Fayetteville (AR): University of Arkansas Press. 421 p.

Watters JL, Davis DR, Yuri T, Siler CD. 2018. Concurrent infection of *Batrachochytrium dendrobatidis* and ranavirus among native amphibians from northeastern Oklahoma, USA. J Aquat Anim Health 30:291–301.

Watters JL, Flanagan RL, Davis DR, Farkas JK, Kerby JL, Labonte MJ, Penrod ML, Siler CD. 2016. Screening natural history collections for historical presence of *Batrachochytrium dendrobatidis* from anurans in Oklahoma, USA. Herpetol Rev 42:214–220.

Watters JL, Hall SE, Siler CD. 2021. Human impacts on the prevalence of the amphibian infectious diseases, *Batrachochytrium dendrobatidis* and ranavirus, in Oklahoma, USA. Proc Okla Acad Sci 101:1–13.

Watters JL, McMillin SL, Marhanka EC, Davis DR, Farkas JK, Kerby JL, Siler CD. 2019. Seasonality in *Batrachochytrium dendrobatidis* detection in amphibians in central Oklahoma, USA. J Zoo Wildl Med 50:492–497.

Yap TA, Koo MS, Ambrose RF, Vredenburg VT. 2018. Introduced bullfrog facilitates pathogen invasion in the western United States. PLoS One 13 (4):e0188384. doi: 10.1371/journal.pone.0188384.

Yuan, Z-Y, Zhou W-W, Chen X, Poyarkov NA Jr, Chen H-M, Jang-Liaw N-H, Chou W-H, Matzke NJ, Iizuka K, Min M-S, Kuzmin SL, Zhang Y-P, Cannatella DC, Hillis DM, Che J. 2016. Spatiotemporal diversification of the true frogs (genus *Rana*): A historical framework for a widely studied group of model organisms. Syst Biol 65:824–842.

Submitted August 28, 2023 Accepted October 30, 2023

New Geographic Distribution Record for Quillback, *Carpiodes cyprinus* (Cypriniformes: Catostomidae) in the Verdigris River (Arkansas River Drainage) of Northern Oklahoma

Chris T. McAllister
Division of Natural Sciences, Northeast Texas Community College, Mt. Pleasant, TX 75455

Eric M. Leis
La Crosse Fish Health Center–Midwest Fisheries Center, U. S. Fish and Wildlife Service, Onalaska, WI 54650

Donald G. Cloutman
P. O. Box 197, Burdett, KS 67523

Henry W. Robison
602 Big Creek Drive, Sherwood, AR 72120

Abstract: A single adult quillback, *Carpiodes cyprinus* was collected on 22 May 2022 by boat electrofisher from the Verdigris River, Wagoner County, Oklahoma (Arkansas River Drainage). Interestingly, few records exist for *C. carpiodes* in Oklahoma. The current discovery represents a new geographic distributional record for *C. cyprinus* in the state.

Introduction

The overall range of the quillback, *Carpiodes cyprinus* (Lesueur) includes the Great Lakes-St. Lawrence River, Hudson Bay, and Mississippi River basins from Québec and Alberta, Canada, south to the Gulf Slope drainages of Louisiana, Mississippi, and Alabama, and west to Wyoming (Platania and Jenkins 1980; Page and Burr 2011). In Oklahoma, this sucker is relatively uncommon but has been collected from the Salt Fork of the Arkansas River and possibly some eastern reservoirs (Miller and Robison 2004). The quillback prefers large permanent pools, backwaters, and main channels of clear to turbid watersheds, with firm gravel bottoms (Pflieger 1997). It feeds by indiscriminately consuming bottom materials (ooze) but also ingests insect larvae, bivalve molluscs, and small crustaceans, as well as algae and plant material (Becker 1983; Ross 2001). Here, we document a new geographic distribution for *C. cyprinus* in northern Oklahoma.

***Corresponding author: cmcallister@ntcc.edu**

Methods

On 25 May 2022, a single adult *C. cyprinus* (265 mm total length [TL]) was collected with a boat electrofisher from the Verdigris River (Fig. 1), Wagoner County, at the Tullahassee Loop Recreation Area (35°53′31.56″N, -95°26′55.76″W) (Arkansas River drainage). It was immediately placed on ice, photographed, and examined for myxozoan parasites (see McAllister et al. 2024). We follow the common and scientific names for *Carpiodes* spp. in Page

Figure 1. Habitus of *Carpiodes cyprinus* from off the Tullahassee Loop Recreation Area on the Verdigris River, Oklahoma.

et al. (2023).

Results and Discussion

The carpsucker was confirmed as *C. cyprinus* based on the morphological characteristics outlined in Pflieger (1997, see his couplet 6a), including the lack of a nipple-like projection or median knob at the center of the lower lip (Fig. 2A) compared to the presence of that structure (Fig. 2B) in river carpsucker, *Carpiodes carpio* (Rafinesque) collected from same locality and date. The quillback further differs from two other *Carpiodes* spp. in Oklahoma as follows: (1) it possesses larger scales in the lateral line as well as the upper jaw not extending backward beyond the front of eye *vs.* those in *C. carpio* (Rafinesque) and highfin carpsucker, *Carpiodes velifer* (Rafinesque), (3) from *C. carpio* by having elongate dorsal rays which are as long as the dorsal base, (4) and by its head being more slender and the snout more blunter than both (Miller and Robison 2004).

Just to the north in extreme southcentral Kansas, *C. carpiodes* has been collected from the Little Arkansas River (Eberle 2014). Additional collecting using boat electrofishers as well as hoop nets in some of the other major Oklahoma rivers and their tributaries may reveal a larger distribution for *C. cyprinus*.

Acknowledgements

The Oklahoma Department of Wildlife Conservation (ODWC) issued Scientific Collecting Permit no. 1551646 to CTM. We especially want to thank Brad Johnston (Fisheries Biologist, Northeast Region, ODWC, Miami, Oklahoma) and his helpful crew for collecting the carpsucker. Usage of trade names does not imply endorsement by the U.S. Government. The findings and conclusions in this article are those of the authors and do not necessarily represent the views of the U.S. Fish and Wildlife Service.

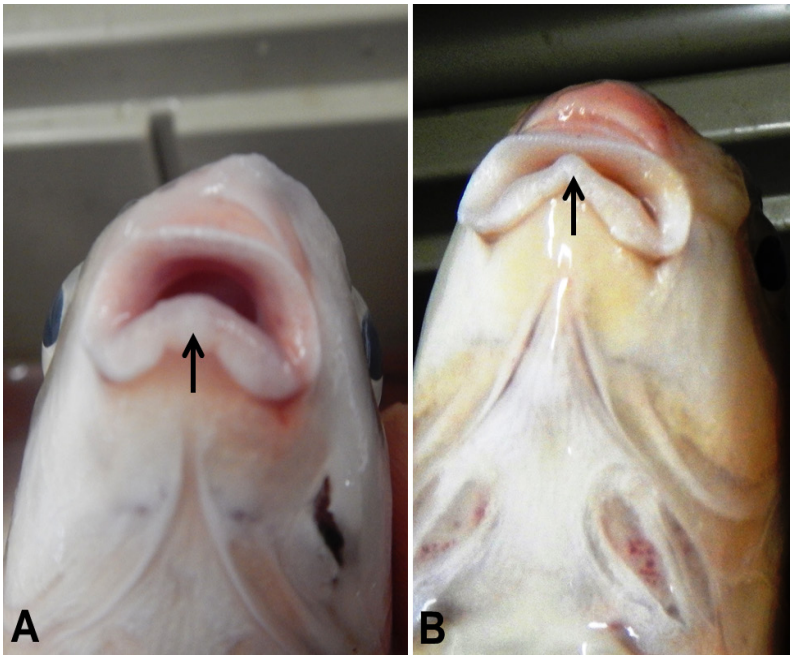

Figure 2. Comparison of lower lips of two *Carpiodes* spp. collected from the Verdigris River. (A) *Carpiodes cyprinus*; note absence of nipple-like projection on middle of lower lip (arrow). (B) *Carpiodes carpio*; note presence of nipple-like structure on middle of lower lip (arrow).

References

Becker GC. 1983. Fishes of Wisconsin. Madison (WI): University of Wisconsin Press. 1052 p.

Eberle ME. 2014. Quillback, *Carpiodes cyprinus* (Lesueur 1817). In: Kansas Fishes Committee, editors. Kansas Fishes. Lawrence (KS): University Press of Kansas. p 253-255.

McAllister CT, Cloutman DG, Leis EM, Camus AC, Woiak Z, Robison HW. 2024. A new species of *Thelohanellus* (Cnidaria: Myxosporea: Myxobolidae) from gill of quillback, *Carpiodes cyprinus* (Cypriniformes: Catostomidae), from the Arkansas River drainage of Oklahoma. J Parasitol 110:(In press).

Miller RJ, Robison HW. 2004. Fishes of Oklahoma. Norman (OK): University of Oklahoma Press. 450 p.

Page LM, Bemis KE, Dowling TE, Espinosa-Pérez H, Findley LT, Gilbert CR, Hartel KE, Lea RN, Mandrak NE, Neighbors MA, Schmitter-Soto JJ, Walker HJ Jr. 2023. Common and scientific names of fishes from the United States, Canada, and Mexico, 8th edition. Bethesda (MD): American Fisheries Society, Special Publication 37. 439 p.

Page LM, Burr BM. 2011. Peterson field guide to freshwater fishes of North America north of Mexico, 2nd ed. New York (NY): Houghton Mifflin Harcourt. 663 p.

Pflieger WL. 1997. The fishes of Missouri. 2nd ed. Jefferson City (MO): Missouri Department of Conservation. 372 p.

Platania SP, Jenkins RE. 1980. *Carpiodes cyprinus* (Lesueur). In: Atlas of North American Freshwater Fishes. Lee DS, Gilbert CR, Hocutt CH, Jenkins RE, McAllister DE, Stauffer JR Jr, editors. Raleigh (NC): North Carolina State Museum of Natural History. p 368.

Submitted September 19 Accepted October 22, 2023

Second Report of *Isospora boulengeri* from Satanic Leaf-Tailed Geckos, *Uroplatus phantasticus* (Sauria: Gekkonidae), with a New Host Record for *Choleoeimeria* (Apicomplexa: Eimeriidae) and a Summary of the Choleoeimerians from the Gekkonidae

Chris T. McAllister*
Division of Natural Sciences, Northeast Texas Community College, Mt. Pleasant, TX 75455

John A. Hnida
Department of Microbiology and Immunology, Midwestern University, Glendale, AZ 85308

Henry W. Robison
602 Big Creek Drive, Sherwood, AR 72120

Abstract: Five adult captive specimens of satanic leaf-tailed geckos, *Uroplatus phantasticus*, housed at the Dallas Zoo, Dallas County, Texas, were examined for coccidian parasites. One was found to harbor *Isospora boulengeri* in its feces while another was infected with an unknown species of *Choleoeimeria*. Spheroidal to subspheroidal oocysts of *I. boulengeri* averaged (L × W) 16.9 × 16.1 µm; one (typically) or two polar granule(s) were present but an oocyst residuum and micropyle were absent. Ovoidal sporocysts of *I. boulengeri* averaged 9.6 × 6.9 µm and possessed a sporocyst residuum and Stieda and sub-Stieda bodies. Cylindroidal to elongate oocysts of a *Choleoeimeria* sp. averaged 28.0 × 14.8 µm. Here, we provide the second report of *I. boulengeri* from *U. phantasticus* as well as the first report of a *Choleoeimeria* sp. from this host. In addition, we provide a summation of the choleoeimerians from the family Gekkonidae.

Introduction

Geckos are excellent hosts of coccidian parasites (El-Toukhy et al. 2013; McAllister et al. 2016, 2020) and the satanic leaf-tailed gecko, *Uroplatus phantasticus* Boulenger is no exception. McAllister et al. (2016) described *Isospora boulengeri* and *Eimeria schneideri* from *U. phantasticus* originally collected in Madagascar and housed at the Dallas Zoo, Dallas County, Texas. Here, we report *I. boulengeri* for the second time from *U. phantasticus* housed at the Dallas Zoo as well as documenting, for the first time, a *Choleoeimeria* from this host. We also provide a summary of the choleoeimerians from geckos of the world.

Methods

Between July 2018 and June 2019, feces from five adult *U. phantasticus* housed at the Dallas Zoo were collected and placed in individual vials containing 2.5% (w/v) aqueous potassium

***Corresponding author: cmcallister@ntcc.edu**

dichromate ($K_2Cr_2O_7$). They were not shipped to the senior author until July 2023 for initial coccidial examination. Those samples found positive were sent to JAH for further examination via flotation in a 15-ml conical centrifuge tube (with centrifugation) containing Sheather's sugar solution (Ricca Chemical Company, Arlington, Texas; specific gravity: 1.25) using an Olympus BX43 light microscope (Olympus Corporation, Center Valley, Pennsylvania). All morphological measurements are reported in micrometers (µm) with the means followed by the ranges in parentheses. Oocysts were ~1,825 days old once they were deposited, measured, and photographed using Nomarski interference-contrast optics at ×1,000 magnification. Oocyst and sporocyst descriptions follow the standard guidelines of Wilber et al. (1998) including oocyst length (L) and width (W), their ranges and ratios (L/W), micropyle (M), oocyst residuum (OR), polar granule(s) (PG), sporocyst length (L) and width (W), their ranges and ratio (L/W), sporocyst (SP), Stieda body (SB), sub-Stieda body (SSB), para-Stieda body (PSB), sporocyst residuum (SR), sporozoites (SZ) anterior (ARB) and posterior (PRB) refractile bodies, and nucleus (N).

A photovoucher of a *U. phantasticus* was accessioned into the Eastern Oklahoma State Collection, Idabel, Oklahoma. Photovouchers of sporulated oocysts of the coccidians were accessioned into the Harold W. Manter Laboratory of Parasitology (HWML), Lincoln, Nebraska.

Results and Discussion

Two coccidians were recovered from the fecal samples and identified as: *Isospora boulengeri* and *Choleoeimeria* sp. Data are provided on each in an annotated format below.

Isospora boulengeri McAllister, Seville, and Hartdegen, 2016

(Figs. 1–3)

Description of sporulated oocyst: Oocyst shape (n = 15): spheroidal to subspheroidal; bilayered wall, ~1.2 (1.0–1.5) tan outer layer smooth to lightly pitted, ~/2/3 total thickness; darker inner layer. L × W (n = 15): 16.9 × 16.1 (15–20 × 14–19); L/W ratio: 1.1 (1.0–1.1); M and OR absent; 1 (typically) or 2 PG(s) present.

Description of sporocyst and sporozoites: Sporocyst shape (n = 15): ovoidal; L × W (n = 15): 9.6 × 6.9 (9–11 × 6–8); L/W ratio: 1.4 (1.3–1.7); knob-like SB and rounded SSB present, PSB: absent; SR: present; SR characteristics: compact rounded or irregular mass of various-sized granules. Sporozoite (not measured) shape: sausage-shaped, small subspheroidal ARB, large subspheroidal PRB, N posterior to midpoint.

Taxonomic Summary

Host: Satanic leaf-tailed gecko, *Uroplatus phantasticus* (Boulenger, 1888); photovoucher host deposited in the EOSC collection.

Geographic distribution: USA: Texas, Dallas, Dallas Zoo Herpetarium (32°44'26.28"N, -96°49'00.12"W).

Type host and locality: U. phantasticus, Madagascar (exact locale unknown) (McAllister et al. 2016).

Other localities: Dallas Zoo (McAllister et al. 2016).

Prevalence: 1/5 (20%).

Sporulation: Oocysts were completely sporulated when samples were received in July 2023.

Site of infection: Unknown; oocysts passed in feces.

Materials deposited: Photovoucher of sporulated oocysts are deposited as HWML 217049.

Remarks

All morphological and mensural characteristics of the present oocysts and sporocysts were quite similar to those from *I. boulengeri* previously reported for *U. phantasticus* (McAllister et al. 2016). This

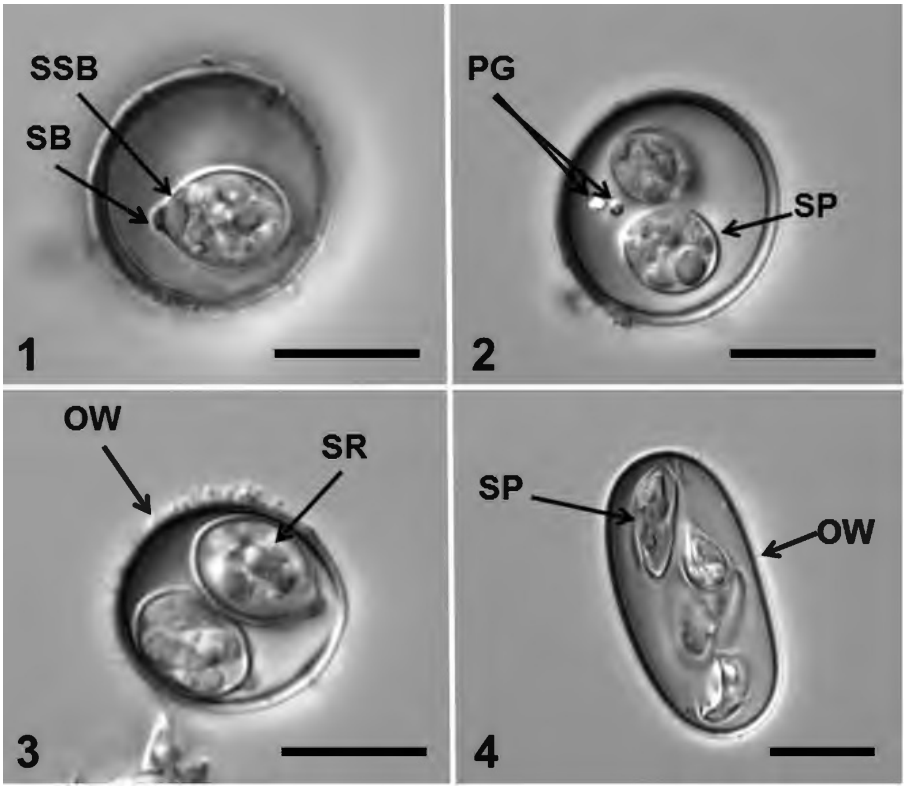

Figures 1–4. Sporulated oocysts of coccidians from *Uroplatus phantasticus*. (1–3) *Isospora boulengeri*. (4) *Choleoeimeria* sp. Scale bars = 10 µm. Abbreviations: OW (oocyst wall); PG (polar granule); SB (Stieda body); SSB (sub-Stieda body); SP (sporocyst); SR (sporocyst residuum).

is the second report of *I. boulengeri* from *U. phantasticus* since the original report more than seven years ago.

***Choleoeimeria* sp.**
(Fig. 4)

Taxonomic Summary

Host: Satanic leaf-tailed gecko, *Uroplatus phantasticus* (Boulenger, 1888); photovoucher host deposited in the EOSC collection.

Description of sporulated oocyst, sporocysts and sporozoites: Regrettably, all cylindroidal oocysts possessed collapsed sporocysts likely due to aging (~5 yr); five oocysts measured (L × W) 28.0 × 14.8 (27–29 × 14–15), with a L/W ratio of 1.9.

Geographic distribution: USA: Texas, Dallas, Dallas Zoo Herpetarium (32°44’26.28”N, -96°49’00.12”W).

Prevalence: 1/5 (20%).

Site of infection: Unknown; oocysts passed in feces. However, choleoeimerians develop in the gallbladder and biliary epithelium.

Materials deposited: Photovoucher of sporulated oocysts are deposited as HWML 217050.

Remarks

There are 17 choleoeimerians (Table 1) that have been previously reported from the gallbladder of gekkonid lizards of the world. Of these, only two taxa possess oocysts that are (1) similar in size, (2) elongate-ellipsoidal or cylindroidal in shape, and (3) with L/W ratios

Table 1. Comparison of the sporulated oocysts of elongate-ellipsoidal/cylindroidal *Choleoeimeria* (syn. *Eimeria*) spp. from the gallbladder of gekkonids.

Choleoeimeria spp.	Type host or host and type locality or locality	Oocyst shape, size, features*†	Sporocyst shape, size, features*†	References
Choleoeimeria sp.	*Uroplatus phantasticus* Dallas Zoo, USA	Cylindroidal 28.0 × 14.8; L/W 1.9 27–29 × 14–15	Unknown‡	This study
Choleoeimeria sp. (III)	*Hemidactylus frenatus* Taiwan	Elongate-ellipsoidal 26.0–27.6 × 14.4–15.6; L/W 1.8 Not given	Not given	Yamamoto (1933)
C. bunopusi	*Bunopus tuberculatus* Saudi Arabia	Ellipsoidal 31.0 × 21.0; L/W 1.5 30–33 × 20–22 PG: –	Ellipsoidal 12.0 × 7.0; L/W 1.4 11–13 × 6–8 SR: +	Al-Quraishy et al. (2013)
C. delalandii	*Tarentola delalandii* Canary Islands	Cylindroidal 45.1 × 21.7; L/W 2.1 42–48 × 20–26 PG: –	Subspheroidal-ovoidal 13.8 × 10.3; L/W 1.3 12–15 × 10–11 SR: +	Matushka and Bannert (1986)
C. duszynskii	*Stenodactylus doriae* Saudi Arabia	Ellipsoidal 24.0 × 17.0; L/W 1.4 23–25 × 16–18 PG: –	Ellipsoidal 9.0 × 5.0; L/W 1.7 8–10 × 4–6 SR: +	Abdel-Baki (2014)
C. flaviviridis	*Hemidactylus flaviviridis* India	Ellipsoidal 25–34 × 11–14; L/W 2.4 Not given PG: –	Ovoidal 8.0 × 6.0; L/W 1.3 Not given SR: +	Setna and Bana (1935)
C. gehyrae n. comb.	*Gehyra variegata* Australia	Elongate-ellipsoidal 32.8 × 20.5; L/W 1.6 30–35 × 20–22 PG: –	Elongate-ellipsoidal 13.6 × 7.7; L/W 1.8 13–14 × 7–8 SR: +	Cannon (1967)
C. hailensis n. comb.	*Ptyodactylus hasselquistii* Saudi Arabia	Cylindroidal 36.7 × 17.2; L/W 2.1 36–38 × 16–20 PG: +	Subsheroidal to ovoidal 10.1 × 8.1; L/W 1.2 8–12 × 8–9 SR: +	Abdel-Aziz (2001)
C. heteronotis	*Heteronotia binoei* Australia	Oblong 32.8 × 16.9; L/W 1.9 33–34 × 16–18 PG: –	Ellipsoidal 9.9 × 7.6; L/W 1.3 8–10 × 6–8 SR: +	Paperna (2007)
C. japonicus n. comb.	*Gekko japonicus* Japan	Cylindroidal 31.0 × 15.0; L/W 2.1 28–35 × 14–19 PG: –	Ellipsoidal 12.0 × 7.0; L/W 1.8 11–14 × 7–10 SR: +	Bovee (1971)
C. koidzumii n. comb.	*G. japonicus* Japan	Elongate-ellipsoidal 30.0 × 14.0; L/W 2.1 Not given PG: –	Ovoidal 13.0 × 9.0; L/W 1.4 Not given SR: +	Matubayasi (1941)
C. pachydactyli	*Pachydactylus capensis* South Africa	Cylindroidal 28.3 × 13.9; L/W 2.1 25–31 × 11–17 PG: –	Ellipsoidal 11.4 × 6.9; L/W 1.7 10–13 × 6.5–7.2 SR: +	Paperna and Landsberg (1989)

similar to this unidentified taxon. They include: an unnamed choleoeimerian from *Hemidactylus frenatus* Duméril and Bibron from Taiwan (Yamamoto 1933) and *Choleoeimeria scabrum*

Table 1 Continued.

C. phelsumae n. comb.	*Phelsuma grandis* Madagascar	Cylindroidal 31.8 × 15.0; L/W 2.1 30– 33 × 14–17 PG: –	Ellipsoidal 9.8 × 7.0; L/W 1.4 8–12 × 7–9 SR: +	Daszak and Ball (1991)
C. rochalimai	*Hemidactylus mabouia* Brazil	Ellipsoidal 30.6 × 16.8; L/W 1.8 Not given PG: –	Spheroidal-subspheroidal 9.0 × 8.0; L/W 1.1 Not given SR: +	Carini and Pinto (1926)
C. scabrum	*Cyrtopodion scabrum* Egypt	Ellipsoidal 26.0 × 13.0; L/W 1.8 25–27 × 12–14 PG: –	Ellipsoidal 8.0 × 5.0; L/W 1.5 7–9 × 4–6 SR: +	Abdel-Haleem (2015)
C. turcicus	*Hemidactylus turcicus* USA: Texas	Cylindroidal 38.2 × 17.9; L/W 2.1 35–41 × 17–20 PG: +	Ovoidal 11.0 × 8.8; L/W 1.3 10–12 × 8–9 SR: +	Upton et al. (1988)
C. vittati n. comb.	*Gekko vittatus* Solomon Islands	Elongate-ellipsoidal 34.3 × 16.9; L/W 2.0 33–37 × 17–18 PG: –	Ovoidal 11.0 × 6.5; L/W 1.7 10–13 × 5–8 SR: +	Ball and Daszak (1995)
C. xiangmati	*Hemidactylus frenatus* Thailand	Oblong 29.7 × 15.1; L/W 2.0 29–33 × 13–16 PG: –	Subspheroidal to ellipsoidal 9.3 × 5.7; L/W 1.7 8–10 × 5–8 SR: +	Paperna (2007)

*Measurements in µm.

†Descriptions of oocysts and sporocysts follow guidelines of Wilber et al. (1998) as follows: oocyst length (L) and width (W), their ranges and ratios (L/W), polar granule(s) (PG), sporocyst (SP) length (L) and width (W), their ratio (L/W), and sporocyst residuum (SR). A micropyle (M), oocyst residuum (OR), Stieda body (SB), sub-Stieda (SSB), and para-Stieda (PSB) do not occur in oocysts of *Choleoeimeria* spp,

‡Sporocysts were collapsed due to aging.

Abdel-Haleem, 2015 from rough-tailed geckos, *Cyrtopodion scabrum* (Heyden) from Egypt. Unfortunately, the only information reported on Yamamoto's (1933) sample was some measurements on oocysts; no other morphological data is available. Comparison of our oocysts to *C. scabrum* is similar in size and shape but Abdel-Haleem (2015) did not report a polar granule for *C. scabrum*. Unfortunately, without fresh samples containing viable oocysts and sporocysts, it is impossible to distinguish our form and provide a complete description.

Paperna and Landsberg (1989) erected the genus *Choleoeimeria* to accommodate eimeriid-like coccidians infecting the lumen of the gallbladder and biliary epithelium of reptiles and their view has been supported (Megía-Palma et al. 2015; and others). This genus is further characterized by elongate-ellipsoidal oocysts that usually have an L/W ratio ≥1.4 and sporocysts without a SB/SSB complex, but with two plates with meridional sutures in their walls (Kruth et al. 2020). Therefore, as our oocysts conform to this description, we document the first report of a *Choleoeimeria* sp. from *U. phantasticus*.

Acknowledgements

Drs. Scott L. Gardner and Gabor Racz (HWML) are acknowledged for expert curatorial assistance. We thank members of the Dallas Zoo, particularly Veterinary Technician Javier Mendez for forwarding the samples as well as Drs. Burgdorf-Moisuk, Connolly, Raines, and Ratliff for collecting them.

References

Abdel-Aziz A. 2001. On some new species of coccidian (Apicomplexa: Eimeriidae) and some parasitic amoebae from reptiles in Egypt and Saudi Arabia. Egyptian J Med Sci 22:95–114.

Abdel-Baki A-AS. 2014. Description of *Choleoeimeria duszynskii* n. sp. (Apicomplexa: Eimeriidae) from the gallbladder of the Middle Eastern short-fingered gecko *Stenodactylus doriae* (Blanford) (Sauria: Gekkonidae) in Saudi Arabia. Syst Parasitol 87:399–404.

Abdel-Haleem HM. 2015. A new species of *Choleoeimeria* (Apicomplexa: Eimeriidae) parasitic in the rough-tailed gecko *Cyrtopodion scabrum* (Sauria: Gekkonidae) in Egypt. Parasitol Res 114:1153–1157.

Al-Quraishy S, Abdel-Baki A-AS, Al Otaibi MSA. 2013. *Choleoeimeria bunopusi* sp. n. (Apicomplexa:Eimeriidae) infecting the gall bladder of the tuberculated gecko *Bunopus tuberculatus* (Reptilia: Gekkonidae) from Saudi Arabia. Acta Protozool 52:267–272.

Ball SJ, Daszak P. 1995. Description of the oocysts of three new species of *Eimeria* (Apicomplexa:Eimeriidae) from geckoes (Sauria: Gekkonidae). Syst Parasitol 32:101–106.

Bovee EC. 1971. New species of *Eimeria* from lizards of Japan. Trans Amer Micros Soc 90:336–343.

Cannon LRG. 1967. New coccidians from Australian lizards. II. *Eimeria*. Parasitol 57:237–250.

Carini A, Pinto C. 1926. Estudos sobre coccideas. Arq de Biol, São Paulo 11:83–86.

Daszak P, Ball SJ. 1991. Five new species of *Eimeria* (Apicomplexa: Eimeriidae) from lizards. Syst Parasitol 20:141–147.

El-Toukhy AA, Abdel-Aziz A, Abo-Senna FM, Abou El-Nour MF. 2013. Three coccidian parasites from Moorish gecko, *Tarentola mauritanica* (Gekkonidae) 2-*Eimeria alexandriensis* n. sp. (Apicomplexa: Eimeriidae). Int J Adv Res 1:526–534.

Kruth PS, Michel C, Amery-Gale J, Barta JR. 2020. Full mitochondrial genome and nuclear *18S rDNA* sequences refine the taxonomic placement of *Choleoeimeria taggarti* n. comb. from the prostate of *Antechinus flavipes* (yellow-footed antechinus). J Parasitol 106:71–81.

Matubayasi H. 1941. On a new species of coccidia parasitic in the *gecko*, *Gekko japonicus*. Zool Mag Tokyo 53:312–314.

Matuschka F-R, Bannert B. 1986. *Eimeria tarentolae* n. sp. from the Moorish gecko, *Tarentola mauritanica*. J Protozool 33:309–311.

McAllister CT, Hnida JA, Fisher SR, Del-Pinto LA, Quah ESH. 2020. A new acroeimerian (Apicomplexa: Eimeriidae) in spotted house gecko, *Gekko monarchus* (Schlegel) (Sauria: Gekkonidae) from Peninsular, Malaysia. Syst Parasitol 97:529–534.

McAllister CT, Seville RS, Hartdegen R. 2016. Two new species of coccidia (Apicomplexa: Eimeriidae) from leaf-tailed geckos, *Uroplatus* spp. (Sauria: Gekkonidae) from Madagascar, including a new host of *Eimeria brygooi* Upton & Barnard, 1987. Syst Parasitol 93:815–823.

Megía-Palma R, Martínez J, Acevedo I, Martín J, García-Roa R, Ortega J, Peso-Fernández M, Albaladejo G, Cooper RD, Paranjpe DA, et al. 2015. Phylogeny of the reptilian *Eimeria*: Are *Choleoeimeria* and *Acroeimeria* valid names. Zool Scripta 44:684–692.

Paperna I. 2007. Ultrastructural review of *Choleoeimeria* spp., a coccidium infecting the gall-bladder epithelium of reptiles. Parassitologia 49:247–256.

Paperna I, Landsberg JH. 1989. Description and taxonomic discussion of eimerian coccidia from African and Levantine geckoes. South African J Zool 24:345–355.

Setna SB, Bana RH. 1935. *Eimeria flaviviridis* n. sp. from the gall-bladder of *Hemidactylus flaviviridis*. J Royal Micros Soc 55:256–260.

Upton SJ, McAllister CT, Freed PS. 1988. *Eimeria turcicus* n. sp. (Apicomplexa: Eimeriidae) from the Mediterranean Gecko, *Hemidactylus turcicus* (Sauria: Gekkonidae). J Protozool 35:24–25.

Wilber PG, Duszynski DW, Upton SJ, Seville RS, Corliss JO. 1998. A revision of the taxonomy and nomenclature of the *Eimeria* spp. (Apicomplexa: Eimeriidae) from rodents in the Tribe Marmotini (Sciuridae). Syst Parasitol 39:113–135.

Yamamoto K. 1933. Studien über die Kokzidean. Fuk Acta Med 26:40–43.

Submitted September 22, 2023 Accepted October 30, 2023

Parasites of the Silver Chub, *Macrhybopsis storeriana* (Cypriniformes: Leuciscidae) from the Red River, Choctaw County, Oklahoma

Chris T. McAllister

Division of Natural Sciences, Northeast Texas Community College, Mt. Pleasant, TX 75455

Anindo Choudhury
Division of Natural Sciences, St. Norbert College, 100 Grant Street, DePere, WI 54115

Donald G. Cloutman
P. O. Box 197, Burdett, KS 67523

Nikolas H. McAllister
North Lamar High School, 295 Stone Avenue, Paris, TX 75460

Henry W. Robison
602 Big Creek Drive, Sherwood, AR 72120

Abstract: Three adult silver chubs, *Macrhybopsis storeriana* were collected by seine in August 2023 from the Red River, Choctaw County, Oklahoma, and examined for parasites. Found were a monogenean, *Dactylogyrus texomensis*, an encysted strigeid (neascus) trematode, a proteocephalidean metacestode, and the Asian fish tapeworm, *Schyzocotyle acheilognathi*. All are reported as new hosts for these parasites, and *S. acheilognathi* is documented from an Oklahoma fish for the third time.

Introduction

The silver chub, *Macrhybopsis storeriana* (Kirtland, 1845) ranges from southern Manitoba, Canada, and the Lake Erie drainage and Lake Ontario, Canada, south through the Ohio River drainage and Mississippi River Basin from Wyoming south through Louisiana, Mississippi, and Alabama; an isolated population occurs in Brazos River drainage, Texas (Gilbert 1978; Page and Burr 2011). In Oklahoma, *M. storeriana* occurs in about the eastern three-quarters of the state primarily in the Arkansas and Red River drainages and their tributaries (Miller and Robison 2004). It prefers larger, sandy-bottomed silty rivers and streams with deep water and moderate to swift current but also occurs in gravel-bottomed pools and backwaters of small and large rivers (Miller and Robison 2004; Page and Burr 2011). This species feeds mostly at or near the bottom on various insects, crustaceans, and molluscs (Becker 1983).

Information is available on the natural history and ecology of the silver chub (Kinney 1954; Gilbert 1978), including information on its parasites (under the old name, *Hybopsis storeriana*). Three monogeneans have been reported from *M. storeriana*, including

***Corresponding author: cmcallister@ntcc.edu**

Dactylogyrus alabamensis Rogers and Mizelle, 1966 from Alabama and Georgia, *Dactylogyrus magnus* Rogers, 1967 from Alabama, and *Dactylogyrus texomensis* Seamster, 1960 from Oklahoma (Seamster 1960; Rogers and Mizelle 1966; Rogers 1967). Other parasites of the silver chub include: two trematodes, a 'neascus' sp. and *Plagioporus cooperi* (Hunter and Bangham, 1932) Price, 1934 from Lake Erie, Ohio, a cestode, *Ligula intestinalis* (L., 1758), and an acanthocephalan, *Leptorhynchoides thecatus* (Linton, 1891) Kostylew, 1924 (Bangham and Hunter 1939; Hoffman 1999). Here we report new records for some parasites of *M. storeriana* from the Red River of Oklahoma, including the third report of the Asian fish tapeworm (AFT), *Schyzocotyle acheilognathi* (Yamaguti, 1934) Brabec, Waeschenbach, Scholz, Littlewood, and Kuchta, 2015, from an Oklahoma fish.

Methods

Host collection

On 13 August 2023, three adult *M. storeriana* (mean ± SD total length [TL] = 64.0 ± 7.9, range 57–75 mm TL) were collected by seine by CTM and NHM from the Red River (Fig. 1) just north of Arthur City, Texas, off US 271 in Choctaw County, Oklahoma (33°52′36.77″N, -95°30′07.05″W). Additional attempts to collect more specimens from the same site were made by us on 17 September 2023 and 8 October 2023 but, unfortunately, none were collected.

Host processing

Specimens were placed in an aerated container of habitat water, taken to the lab for processing, and killed by cervical dislocation. Their gills, gallbladders, urinary bladders, fins, integument, other major organs, and musculature were placed in Petri dishes containing 0.9% saline and macroscopically examined for myxozoan plasmodia with a stereomicroscope at 20-30× magnification. The gills were also examined for monogeneans, which were mounted on slides in Grey and Wess medium stained with Gomori's trichrome (Kritsky et al. 1978), and observed and photographed with an AccuScope 3000LED series phase contrast microscope (Accu-Scope Inc., Commack, New York). Digital images of syntypes of *Dactylogyrus texomensis* Seamster, 1960 (USNPC 30026 = USNM 1339486), previously examined and photographed by DGC with an Olympus OLY-200 camera mounted on an Olympus BX41 phase contrast microscope (Olympus Optical Co., Ltd., Tokyo, Japan), were compared with material found. Terminology for sclerites is that of Cloutman et al. (2020). The gastrointestinal tract was likewise examined for helminth parasites and split lengthwise from the esophagus to anus. A metacestode cyst as well as an encysted trematode were found in the coelomic cavity, placed on a cover-slipped microscopic slide with saline, and photographed as photovouchers. A tapeworm was taken from the small intestine, rinsed in saline, and its terminal proglottid was removed and placed in 95% DNA grade ethanol for future molecular analysis. The remaining specimen was fixed in hot 4% formalin, stained in Semichon's acetocarmine, cleared in methyl salicylate, and mounted in Canada Balsam.

A voucher for the monogenean and tapeworm was deposited in the Harold W. Manter Laboratory of Parasitology (HWML), Lincoln,

Figure 1. Habitus of silver chub in Red River, Choctaw Co., Oklahoma.

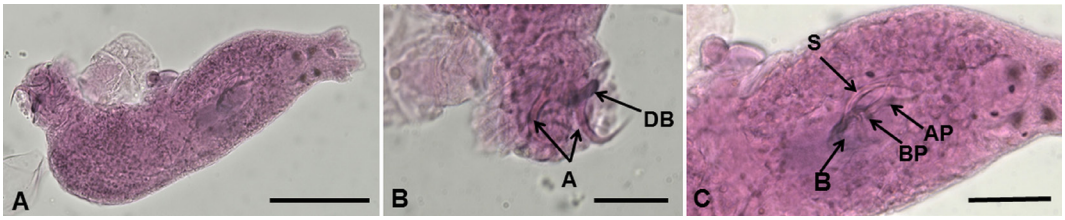

Figure 2. Digital images of voucher specimen of *Dactylogyrus texomensis* from the Red River, Choctaw Co., Oklahoma. (A) Whole mount. Scale bar = 50 µm. (B) Haptor. Abbreviations: A = dorsal anchors, DB = dorsal bar. Scale bar = 20 µm. (C) Male copulatory organ (MCO). Abbreviations: AP = accessory piece, B = base of MCO, BP = basal process of MCO (bent downward), S = shaft of MCO. Scale bar = 20 µm.

Nebraska. Photovouchers of the strigeid trematode and metacestode were also deposited in the HWML, and voucher hosts were deposited in the Eastern Oklahoma State College (EOSC) Vertebrate Collection, Idabel, Oklahoma.

Results and Discussion

All three individual silver chubs harbored parasites. Two silver chubs harbored one each of the monogenean, *Dactylogyrus texomensis* Seamster, 1960 (HWML 217058; Figs. 2–3); one (57 mm TL) possessed an unknown digenean strigeid (neascus) cyst in its coelomic cavity (HWML 217084; Fig. 4A); one (75 mm TL) had an unknown encysted metacestode in its coelomic cavity (HWML 217085; Fig. 4B); and another (60 mm TL) had a mature (gravid) AFT in its small intestine (HWML 217847; Fig. 5).

This is the second report of *D. texomensis* (Figs. 2A–C*)*, confirmed by comparison with syntype specimens (Figs. 3A–F), both recorded from the silver chub from the Red River drainage. All specimens were very similar, with notable differences in the angle of the basal process (Fig. 2C and Figs. 3C, E, F) due to effects of preservation, mounting, and angle of view. Seamster (1960) reported studying 10 specimens and depositing a holotype (but he did not specify a particular specimen) and unspecified number of paratypes for *D. texomensis* as USNM 30026. The two available slides examined by DGC (USNPC 30026 = present USNM 1339486)

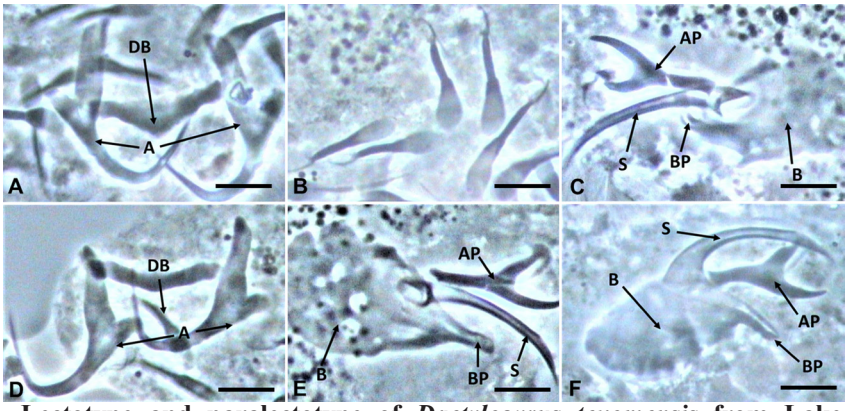

Figure 3. Lectotype and paralectotype of *Dactylogyrus texomensis* from Lake Texoma, Oklahoma. (A) Haptor of lectotype. Abbreviations: A = dorsal anchors, DB = dorsal bar. (B) Hooks of lectotype. (C) MCO of lectotype. Abbreviations: AP = accessory piece, B = base of MCO, BP = basal process of MCO (bent upward), S = shaft of MCO. (D) Haptor of a paralectotype. A = dorsal anchors, DB = dorsal bar. (E) MCO of a paralectotype. Abbreviations: AP = accessory piece, B = base of MCO, BP = basal process of MCO (straight), S = shaft of MCO. (F) MCO of a paralectotype. Abbreviations: AP = accessory piece, B = base of MCO, BP = basal process of MCO (bent downward), S = shaft of MCO. Scale bars = 10 µm.

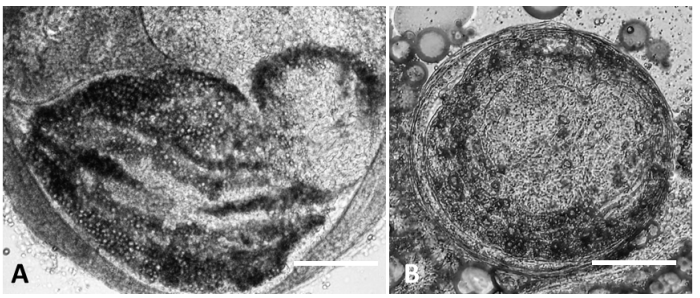

Figure 4. Immature helminths from silver chub. (A) Unknown encysted strigeid neascus (Trematoda: Digenea). (B) Unknown encysted metacestode (Cestoda). Scale bars = 25 µm.

are labelled as cotypes (a term to be avoided and should be referred to as syntypes according to Recommendation 73E of the International Code of Zoological Nomenclature [ICZN 1999]). One slide with Seamster's accession number 692-12 contains three specimens. The other slide with Seamster's accession number 692-13 contains one specimen and is labelled cotypes. This plural "cotypes" designation on a slide with one specimen indicates that both slides are part of a cotype (=syntype) series, rather than a holotype and paratype series. In addition, two different male copulatory organs (MCOs) and dorsal bars and one set of dorsal anchors and a hook were drawn in Seamster's (1960) description of *D. texomensis*, neither of which conform unequivocally to any particular of the four specimens on the two slides, but appear to represent the same species as the four specimens on the two slides. Thus, there is no clearly indicated holotype specimen in Seamester's (1960) description. In accordance with Recommendation 73F and Article 73.2 of the code (ICZN 1999), we propose designation of the specimen on slide 692-13 of USNM 1339486 (= USNPC 30026) as the lectotype of *D. texomensis*, and the three specimens on slide 692-12 as paralectotypes.

Two other monogeneans have been reported from *M. storeriana*, *D. alabamensis* from Alabama and Georgia, and *D. magnus* from Alabama. *Dactylogyrus texomensis* has not been found with these other two species east of the Mississippi River, and the other two have not been found west of the Mississippi River (Seamster 1960; Rogers and Mizelle 1966; Rogers 1967; present study).

The AFT is a very successful invasive parasite known from various freshwater fishes. To date, it has been reported from more than 300 fish species with the greatest number of records from North American cyprinid (or leuciscid) hosts (Kuchta et al. 2018). The tapeworm has been previously reported from fishes from Canada, México, and Puerto Rico as well at least 20 US states, including Arkansas, Arizona, California, Colorado, Florida, Kansas, Hawaii, Indiana, Kentucky, Louisiana, Michigan, Nebraska, New Hampshire, New Mexico, New York, Nevada, North Carolina, Texas, Utah, and Wisconsin, but no records were posted from Oklahoma (Kuchta et al. 2018, see their fig. 4). However, McAllister et al. (2015) reported *S. acheilognathi* from 1 of 16 (6%) Western mosquitofish, *Gambusia affinis* (Baird and Girard), and McAllister et al. (2016) found a larval AFT in 1 of 13 (8%) Western creek chubsucker, *Erimyzon claviformis* Mitchell, both collected from Yanubbee Creek, McCurtain County, Oklahoma. To our knowledge this is the first report of AFT from the silver chub or any species of *Macrhybopsis* (see host lists in Hoffman 1999; Cole and Choudhury 2015; Kuchta et al. 2018). The tapeworm is easily identified by its heart shaped scolex (when viewed laterally) with deep bothria (Fig. 5A), and also possesses characteristic acraspedote proglottids (Figs. 5B, C). The stained and cleared wholemount also shows the typical distribution of vitelline follicles and testes (Figs. 5B, C). It is evident from the gravid worm we collected here that the silver chub is a very suitable host, capable of sustaining the tapeworm population in the Red River. It is possible that AFT was introduced into the Red River drainage by invasive grass carp, *Ctenopharyngodon idella* (Valenciennes

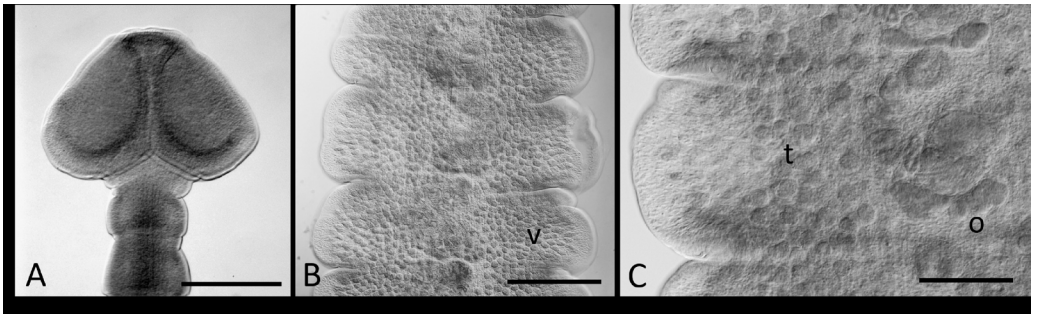

Figure 5. Asian fish tapeworm, *Schyzocotyle acheilognathi* from silver chub. (A) Scolex of tapeworm in lateral view. Scale bar = 400 µm. (B) An early gravid segment (proglottid) showing the typical superficial distribution of vitelline follicles (v). Scale bar = 500 µm. (C) An early mature but non-gravid segment (proglottid) showing the testes (t) and ovary (o). Scale bar = 200 µm

in Cuvier and Valenciennes) now established in that drainage (Hargrave and Gido 2004; Shelton and Snow 2017). The grass carp is considered to be a principal host of this tapeworm and is responsible for its original introduction into the U.S. in the 1970s (Hoffman 1999; Choudhury and Cole 2012). It would not be surprising to also find other leuciscid fish species in the Red River infected with this tapeworm. However, McAllister et al. (2015) reported that they did not find any AFT in 256 fishes from various Arkansas watersheds, including 10 species of leuciscids (n = 72). Therefore, prevalence can be quite low for the AFT.

In the life cycle of *S. acheilognathi*, procercoids are found in copepods, with smaller fishes occasionally acting as "carriers", and the adult occurs in the intestine of teleost fishes, with a predilection for cyprinid and leuciscid fishes (see Hoffman 1999; Choudhury and Cole 2012; Kuchta et al. 2018). Although this tapeworm is a known pathogen having a potential negative impact on many fishes, particularly cyprinids (Scott and Grizzle 1979; Salgado-Maldonado and Pineda-Lopez 2003; Scholz et al. 2012), the effect on these Oklahoma fishes is unknown.

Acknowledgements

The Oklahoma Department of Wildlife Conservation issued Scientific Collecting Permit No. 1551646 to CTM. We thank Drs. Scott L. Gardner and Gabor Racz (HWML) for expert curatorial assistance, Patricia A. Pilitt (USNPC) for loan of type specimens of *D. texomensis*, and Roman Kuchta (Institute of Parasitology, Biology Centre of the Czech Academy of Sciences, Ceské Budějovice, Czech Republic) for information on the AFT. AC thanks the Division of Natural Sciences, St. Norbert College for material support.

References

Bangham RV, Hunter GW III. 1936. Studies on fish parasites of Lake Erie. III. *Microcotyle spinicirrus* MacCallum (1918) char. emend. and *M. eriensis* sp. nov. Trans Amer Micros Soc 55:334–339.

Becker GC. 1983. Fishes of Wisconsin. Madison (WI): University of Wisconsin Press. 1052 p.

Choudhury A, Cole RA. 2012. The Asian fish tapeworm *Bothriocephalus acheilognathi*. In: A handbook of global freshwater invasive species, Chapter 32. Francis RA, editor. London (UK): Earthscan. p 389–404.

Cloutman DG, Adrian AB, McAllister CT, Stallsmith BW, Fayton TJ, Robison HW. 2020. Revision of monogeneans parasitizing *Lythrurus* (Cypriniformes: Leuciscidae) in eastern U.S.A., with description of *Dactylogyrus lythruri* sp. n. and new records of *Dactylogyrus crucis* Rogers, 1967 (Monogenoidea: Dactylogyridae). Folia Parasitol 67:011. https:/www.doi: 10.14411/fp.2020.011.

Cole RA, Choudhury A. 2015. Commonwealth Bureau of Agriculture International (CABI) Invasive Species Compendium Datasheet: *Bothriocephalus acheilognathi*. CABI Compendium [online]. Available from: http://www.cabi.org/isc/datasheet/91669. (Accessed July 31, 2023).

Gilbert CR. 1978. *Macrhybopsis storeriana*. In: Atlas of North American freshwater fishes. Lee DS, Gilbert CR, Hocutt CH, Jenkins RE, McAllister DE, Stauffer JR Jr. (editors). Raleigh (NC): North Carolina State Museum of Natural History. p 194.

Hargrave CW, Gido KB. 2004. Evidence of reproduction by exotic grass carp in the Red and Washita Rivers, Oklahoma. Southwest Nat 49:89–93.

Hoffman GL. 1999. Parasites of North American freshwater fishes. 2nd ed. Ithaca (NY): Comstock Publishing Associates. 539 p.

ICZN. 1999. International Code of Zoological Nomenclature. Fourth Edition. London (UK): The International Trust for Zoological Nomenclature. 306 p.

Kinney EC. 1954. A life history of the silver chub, *Hybopsis storeriana* (Kirtland), in western Lake Erie with notes on associated species. Diss Abstr 20(6):1978–1980.

Kritsky, DC, Leiby PD, Kayton RJ. 1978. A rapid stain technique for the haptoral bars of *Gyrodactylus* species (Monogenea). J Parasitol 64:172–174.

Kuchta R, Choudhury A, Scholz T. 2018. Asian fish tapeworm: the most successful invasive parasite in freshwaters. Trends Parasitol 34:511–523.

McAllister CT, Bursey CR, Fayton TJ, Connior MB, Robison HW. 2015. First report of the Asian fish tapeworm, *Bothriocephalus acheilognathi* (Cestoidea: Bothriocephalidea: Bothriocephalidae) from Oklahoma with new host records in non-hatchery fishes in Arkansas. Proc Okla Acad Sci 95:35–41.

McAllister CT, Bursey CR, Robison HW, Connior MB, Trauth SE. 2016. New records of helminth parasites (Trematoda, Cestoda, Nematoda) from fishes in the Arkansas and Red River drainages, Oklahoma. Proc Okla Acad Sci 96:83–92.

Miller RJ, Robison HW. 2004. Fishes of Oklahoma. Norman (OK): University of Oklahoma Press. 450 p.

Page LM, Burr BM. 2011. Peterson field guide to freshwater fishes of North America north of Mexico, 2nd ed. New York (NY): Houghton Mifflin Harcourt. 663 p.

Rogers WA 1967. Studies on Dactylogyrinae (Monogenea), with description of 24 new species of Dactylogryrinae, 5 new species of *Peleucidhaptor*, and the proposal of *Aplodiscus* gen. n. J Parasitol 53:500–524.

Rogers WA, Mizelle JD. 1966. New species of Dactylogryinae from Alabama fishes. J Parasitol 52:707–712.

Salgado-Maldonado G, Pineda-Lopez RF. 2003. The Asian fish tapeworm *Bothriocephalus acheilognathi*: a potential threat to native freshwater fish species in Mexico. Biol Inv 5:261–268.

Scholz T, Kuchta R, Williams C. 2012. *Bothriocephalus achelognathi*. In: Woo PTK, Buchmann K, editors. Fish parasites. Pathobiology and protection, Chapter 17. Wallingford (UK): CAB International. p 282–297.

Scott AL, Grizzle JM. 1979. Pathology of cyprinid fishes caused by *Bothriocephalus gowkongensis* Yea, 1955 (Cestoda: Pseudophyllidea). J Fish Dis 2:69–73.

Seamster A. 1960. A new species of *Dactylogyrus* from the silver chub. Sobr. Libro. Homen. Dr. Eduardo Caballero Caballero. Caballero Jub vol. p 269–270.

Shelton WL, Snow RA. 2017. Recruitment of two non-native river-spawning fishes in Lake Texoma, Oklahoma and Texas. Proc Okla Acad Sci 97:61–66.

Submitted September 30, 2023 Accepted October 22, 2023

Evaluation of Hole-Punching Operculums as a Marking Technique in Centrarchids

Shelby E. Jeter
Oklahoma Department of Wildlife Conservation, Oklahoma Fishery Research Laboratory, Norman, OK 73072

Alexis N. Whiles
Oklahoma Department of Wildlife Conservation, Oklahoma Fishery Research Laboratory, Norman, OK 73072

Douglas L. Zentner
Oklahoma Department of Wildlife Conservation, Oklahoma Fishery Research Laboratory, Norman, OK 73072

Richard A. Snow
Oklahoma Department of Wildlife Conservation, Oklahoma Fishery Research Laboratory, Norman, OK 73072

Abstract: Mark-recapture studies provide important information about fisheries. There are many ways to mark or tag fish, but some populations of fish, like Largemouth Bass (Micropterus salmoides) and sunfish (*Lepomis* spp.), will require a large number of fish to be tagged. The cost of tags could be prohibitive to these studies. Lower-cost methods help to reduce this barrier. This study was split into a lab and field trial to investigate the applicability of operculum hole-punching as a viable, low-cost option for Centrarchid mark-recapture studies. In the lab, 63 Largemouth Bass and 105 sunfish were collected and marked with a self-piercing tag on their left operculum. Of those, 33 bass and 53 sunfish were marked with a 6.4mm paper hole-punch tool on their right operculum then fish were held in pools to test growth rates, mortality, and longevity. Results showed no significant difference between hole-punch and control fish for growth or mortality. Next, 60 Largemouth Bass and 328 sunfish were collected from a 6-acre pond. Fish were marked with a hole-punch and a fin clip. Hole-punch and fin clip locations varied based on the date collected. In both studies, hole-punch closure rate was observed in 25% increments. Overall, hole-punches closed faster in the lab study, suggesting environment can affect growth rates. Also, Largemouth Bass marks closed faster than sunfish showing a species-specific difference. Approximate operculum hole-punches closure rates take 26 days to close in Largemouth Bass and 164 days in sunfish. Our results suggest operculum hole-punching is a viable low-cost method for marking fish.

Introduction

Mark-recapture studies provide information about fisheries population dynamics and vital rates. These studies allow for the estimation of metrics such as mortality, population abundance, recruitment, and stocking success (Conover and Sheehan 1999). To estimate these parameters via mark-recapture, fish are marked or tagged externally (e.g., fin clipping, strap tags, floy tags) or internally (e.g., passive integrated transponder [PIT] tags, oxytetracycline [chemical marking of hard structures; Parker et al. 1990]). Tag cost can range anywhere from

***Corresponding author: shelby.jeter@odwc.ok.gov**

~$2.11 (PIT Tags) to ~$0.29 (straps tags) per tag (Nathanael Hull, Oklahoma Department of Wildlife Conservation, unpublished data). In certain populations (e.g., high abundance) a large number of fish will likely need to be tagged, potentially making the cost of tags prohibitive (Schneider 1998). In these instances, lower-cost methods (e.g., marking via fin clipping or punching) are commonly used; however, this generally does not allow for the recognition of individuals (Wagner et al. 2009, McFarlane et al. 1990). Date specific (e.g., left pelvic clip day one, right pelvic day two) or batch marks (e.g., all fish get right pelvic clip) are commonly applied in these instances.

Though generally not an issue for batch marking, date specific marking often limits the number of possible mark-recapture samples. For example, Everhart et al (1975) found only 10 possible date specific marks when two paired fins were used. One common alternative to fin clipping is punching holes in fins. Fin hole punches have been used since 1896 (Mcfarlane et al. 1990). Punching holes leaves a smaller mark and likely induces less stress on the fish. However, the mark is smaller making it harder to identify and allowing it to regenerate faster (Murphy and Willis 1996). Hole-punching operculums is another method that has received more attention in recent years. Operculum hole punches have been applied to Lake Trout *Salvelinus namaycush* (Allison 1963), Masu Salmon *Oncorhynchus masou* (Miyakoshi and Kudo 1999), Common Carp *Cyprinus carpio* (Snow et al. 2020), and Rainbow Trout *O. mykiss* (Rosburg et al. 2022). The retention of operculum marks has yet to be studied on Centrarchids.

Centrarchids are high-value sportfish (e.g., Largemouth Bass *Micropterus salmoides*) or commonly targeted (e.g., Bluegill *Lepomis macrochirus*) throughout their range (Quinn and Paukert 2009). Different tagging and marking methods have been studied using Centrarchids. Largemouth Bass and Bluegill have been PIT tagged (Siepker et al. 2012, Kaemingk et al. 2011), marked with injectable fluorescent tags, implant elastomers (Catalano et al. 2001), and t-bar anchor tagged (Tranquilli and Childers 1982, Parsons and Reed 1998), to name a few. Having additional low-cost marking strategies for these species would benefit fisheries managers, especially given they can occur in high abundances (Jennings 1997). Therefore, the goal of our study was to investigate the applicability of operculum hole-punching as a viable option for Centrarchid mark-recapture studies. Our specific objectives were to (1) estimate the longevity of operculum hole-punches for Centrarchids and (2) determine if hole-punch longevity varied between species group (specifically Largemouth Bass *Micropterus salmonids* and *Lepomis* spp.) or lab and field settings.

Methods

Lab Trial

Twenty-one Bluegill were collected from Sparks Lake, Oklahoma on March 31, 2021. Eighty-four Bluegill, Redear Sunfish *Lepomis microlophus*, Green Sunfish *L. cyanellus*, and hybrid sunfish *Lepomis* spp. were collected from Dahlgren Lake on April 1-2, 2021. Additionally, sixty-three Largemouth Bass were collected from Konawa Lake, OK on April 6, 2021. Fish were collected using boat-mounted electrofishing regulated via a Smith-Root 7.5 generator-powered pulsator (settings: 120 DC, 120 & 60 pulses per second, 20-40 % of power). Only fish ≥ 127 mm total length (TL) were retained for use in the lab study. Fishes were held in the live well while on the boat, offloaded into a hauling tank at the ramp, and then transported to the Oklahoma Fishery Research Laboratory in Norman, OK.

At the lab, fish were measured to the nearest 1-mm TL and a style 1005-3 self-piercing tag (National Band & Tag Company) was placed on their left operculum so fish could be uniquely identified. A 6.4 mm (diameter) handheld paper single-hole punch tool was used to mark fishes in the center of the operculum. Fifty-three *Lepomis* spp. received a hole punch in their right operculum and 52 were used as controls. Thirty-three Largemouth Bass were hole-punched on their right operculum and 30 were used as unmarked controls. After marking, fish were

placed in holding pools (4.6 m diameter, 1.2 m deep; Intex Recreation). Holding pools were aerated and received fresh well water. Bass and sunfish were placed into separate pools, with the exception of three Largemouth Bass < 230 mm TL that were placed with the *Lepomis* spp. Dissolved oxygen and water temperature were monitored regularly via a handheld YSI Pro 1020 (Xylem Inc.). Fish were fed once daily with either a size 3 floating pellet (Purina) or Trophy Fish Feed Multispecies formula (Sportsman's Choice). Minnows were placed into both pools for additional forage. In addition to minnows, Largemouth Bass received *Lepomis* spp. < 120 mm TL for forage.

Pools were sampled intermittently to check the progression of the hole closure (Figure 1). Largemouth Bass were sampled four times over six weeks and *Lepomis* spp. were sampled five times over seven weeks. During sampling, fishes were enclosed in a seine to reduce capture area. Fishes were then netted out using a short-handled dip net and placed into 757-L holding tanks. Fishes were examined to see if they had a hole-punch, how much of it had filled in (%), and their self-piercing tag was recorded. If their self-piercing tag had fallen out TL was recorded to try and match individuals based on size. For *Lepomis* spp., species was also noted. Any mortalities were collected from pools and assigned to either hole-punched or control fish groups. At the end of the study, TLs were recorded for all fishes to estimate growth rates.

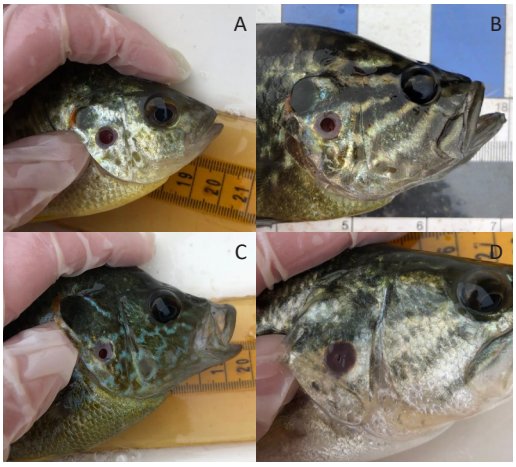

Figure 1. Photographs showing hole-punch closure percentages in the operculum of sunfish and Largemouth Bass from the lab study. (A – 75% closure, B-50% closure, C-25% closure, D-5% closure).

Field Trial

Largemouth Bass and sunfish were sampled via boat-mounted electrofishing regulated by a Smith-Root 5.0 generator-powered pulsator (settings: High Range, DC, 120 pulses per second, 20-60 % of power) at Northeast Lions Park Pond, a 6-acre pond in Norman, OK. Six samples were taken between 9/21/22 and 4/6/23. Fish ≥ 127 mm TL were measured (mm), weighed (g), and hole-punched in the same manner described prior for the lab trial. Fishes were marked with unique pelvic fin clip and hole-punch combinations during each sampling event so marking day could be estimated (Table 1). All recaptures were weighed and measured, and we noted the side tagged and fin clipped. We observed the progression of the hole punch closing in 25% increments, with 100% being completely open to 0% being fully closed.

Data Analysis

To determine if hole punching resulted in reduced growth, we estimated growth rates for each fish that survived until the end of the lab trial by subtracting their final TL from their initial TL. We then compared growth rates using a two-sample Kolmogorov–Smirnov (K–S) test ($\alpha = 0.05$, Kolmogorov 1933, Smirnov 1939). To determine the amount of similarity between growth rates for control and marked fish we estimated distributional overlap ($\hat{\eta}$; Pastore and Calcagnì 2019) via the "boot.overlap()" function from the "overlapping" package (Pastore 2020). We used because it is a distribution-free metric that allows for estimates of relative similarity between distributions. We derived means and 95% confidence intervals (CIs) for by bootstrapping the comparison 1,000 times. We interpreted based on its relationship with Cohen's d (Cohen 1988); meaning $\hat{\eta} = 0.20$ indicates a small distributional overlap, $\hat{\eta} = 0.50$ indicates moderate distributional overlap, and $\hat{\eta} = 0.80$ indicates large distributional overlap (Pastore 2020).

Table 1. Dates when hole-punching samples were taken from Northeast Lions Park Pond, OK. Included are the side of operculum that was punched and the side of the pelvic fin that was clipped during each sampling event. During the last two sampling events, only recaptures were collected.

Date	Side Operculum Punched	Side Fin Clipped
9/21/2022	Left	Left
9/23/2022	Left	Right
10/7/2022	Right	Left
10/27/2022	Right	Right
11/17/2022	Recaptures Only	Recaptures Only
4/6/2023	Recaptures Only	Recaptures Only

To determine if hole-punching resulted in significantly ($\alpha = 0.05$) higher mortality a χ^2-test was used to compare survival and mortality between hole -punched and control fish. Strength of association was estimated for the χ^2-test using Cramér's V statistic (Acock and Stavig 1979). Cramér's V was interpreted based on its association with Cohen's ω statistic when a table has two rows (Choen 1988). Meaning $V < 0.30$ indicates low association, $V < 0.50$ indicates medium association, and $V \geq 0.50$ indicates strong association between groups. We derived 95% CIs for Cramér's V using 1,000 bootstrap replicates.

Total lengths of marked Largemouth Bass and sunfish from lab and field trial were compared using a K–S test ($\alpha = 0.05$). Estimates of (mean and 95% CI) were also obtained for both species TL comparisons. The procedure for obtaining estimates was the same as described prior for lab growth rate comparisons.

To determine if mark-retention was similar between lab and field trials a binomial distributed generalized linear model with a probit link was fit via the "glm()" function within R Statistical Computing Platform version 4.3.0 (R Core Team 2023). The global model included predictive parameters day (number of days since marking), system type (i.e., lab vs field), and species (i.e., *Lepomis* spp. vs Largemouth Bass). Also included in the global model were two- and three-way interactions between predictors. Prior to analysis Pearson's product-moment correlations were compared for all predictive variables to ensure no strong correlations (i.e., $r > |0.70|$, Akoglu 2018) existed.

A backwards selection process was used to determine which variables and interactions were most important in describing mark retention (James et al. 2013). Insignificant parameters ($p > 0.05$) were removed starting with the highest order interaction (i.e., three-way interaction), then second-order interactions, followed by main effects if necessary. Fit of the final model was assessed via residual, scale location, and leverage plots. The final model (i.e., model with only significant predictors or interactions) was compared to all prior models using a likelihood ratio test ($\alpha = 0.05$) via the "lrtest()" function from the "lmtest" package (Hothorn et al. 2022). This allowed us to confirm that the backwards selection process (i.e., removal of insignificant predictors) did not result in a model with poorer relative fit to the data (Achim and Torsten 2002). Predictions from the final model were used to estimate the longevity of hole punch marks for Centrarchids.

Results

Lab sample size consisted of 33 Largemouth Bass and 53 sunfish, which were recaptured 127 and 225 times, respectively (Table 2). During lab trials 8 control and 8 hole-punched sunfish died, and no bass mortality was observed. In the field trial, 60 Largemouth Bass and 328 sunfish were hole-punched during fall and spring months. Of those, 16 Largemouth Bass and 37 sunfish were recaptured in the fall, and 11 bass and 12

Table 2. Total number of marked fish and number of recaptures for *Lepomis* species and Largemouth Bass (*Micropterus salmoides*) from the lab and Northeast Lions Park Pond (Field).

System	Species	Marked	Recaptures
Lab	*Mciropterus salmoides*	33	127
Lab	*Lepomis* spp.	53	225
Field	*Mciropterus salmoides*	60	27
Field	*Lepomis* spp.	328	49

sunfish were recaptured in the spring. The hole-punches from field trial fish were fully filled in but observable in spring samples.

Hole punching did not appear to increase mortality or decrease growth of bass or sunfish based on lab trials. The chi-squared test showed no significant difference in mortality between hole-punched and control fish ($\chi^2 = 0.47$, $p = 0.49$). Cramér's V suggested low association between hole punching and mortality (mean [95% CI] = 0.08 [0.01-0.22]). Confirming hole punching did not increase fish mortality. Additionally, hole punches did not affect fish growth rates. The K-S test suggested growth was not significantly different between hole-punched and control fish ($D = 0.20$, $p = 0.29$). Estimates of $\hat{\eta}$ suggested moderate-to-high similarity between both groups (mean [95% CI] = 0.67 [0.49-0.82]). Confirming hole punching did not decrease fish growth.

We compared TLs of fish studied between lab and field trials. The total length of bass in the lab study ranged from 180-540mm and from the field component ranged 127-585mm. KS test for Largemouth Bass suggested there was a significant difference between TLs for fish marked in the lab and field trials ($D = 0.32$, $p < 0.05$). Estimates of $\hat{\eta}$ suggested moderate-to-low similarity between both groups (mean [95% CI] = 0.52 [0.35-0.71]). Suggesting that there was at least a moderate statistical difference between TLs for Largemouth Bass in the lab and field setting. This was likely due to smaller Largemouth Bass being marked during the field trial. The total length of sunfish in the lab study ranged from 127-221mm and from 127-215mm in the field study. The K–S test for sunfish suggested there was no significant difference between TLs for fish marked in the lab and field trials ($D = 0.18$, $p > 0.05$). Estimates of $\hat{\eta}$ suggested moderate-to-high similarity between both groups (mean [95% CI] = 0.71 [0.60-0.81]). This suggests that sunfish from both the lab and field trial were similar in size.

All predictor variables appeared to be important in explaining mark closure phenomena. Person's product-moment correlations suggested none of our predictors were strongly correlated (r range = -0.07 – 0.57). The final model from our backward selection process included additive effects between day, system type, and species predictors along with interaction between day and species predictors and day and system predictors (Table 3). Diagnostic plots suggested adequate model fit for the final model. The likelihood-ratio test comparing the final model to prior models from the backward selection process suggested removal of non-significant interactions did not significantly decrease model fit to the data (χ^2 range = 0.25 to 1.90, all $p > 0.05$). Two-way interactions were plotted using the "ggplot2" package to determine the effect of day and species and day and system on mark retention (Wickham 2016). Interpretation of the first interaction suggested that mark retention had an inverse relationship with days since marking lasted longer in bass compared to sunfish (Figure 2). Interpretation of the second interaction indicates that for both bass and sunfish marks were retained longer in

Table 3. Mean and standard error (SE) estimates for each parameter from the final binomial model with a probit link function obtained via backward selection. Parameters include the intercept, lab or field (System), days since marking (Day), and *Lepomis* species or Largemouth Bass (Species). Included are z-values and resulting p-values for each parameter.

Parameter	Mean	SE	z-value	p-value
Intercept	5.10	0.88	5.81	<0.05
System	-4.15	0.61	-6.84	<0.05
Day	-0.26	0.05	-5.88	<0.05
Species	-1.22	0.89	-1.37	0.17
Day × Species	0.09	0.05	2.04	<0.05
Day × System	0.17	0.03	6.39	<0.05

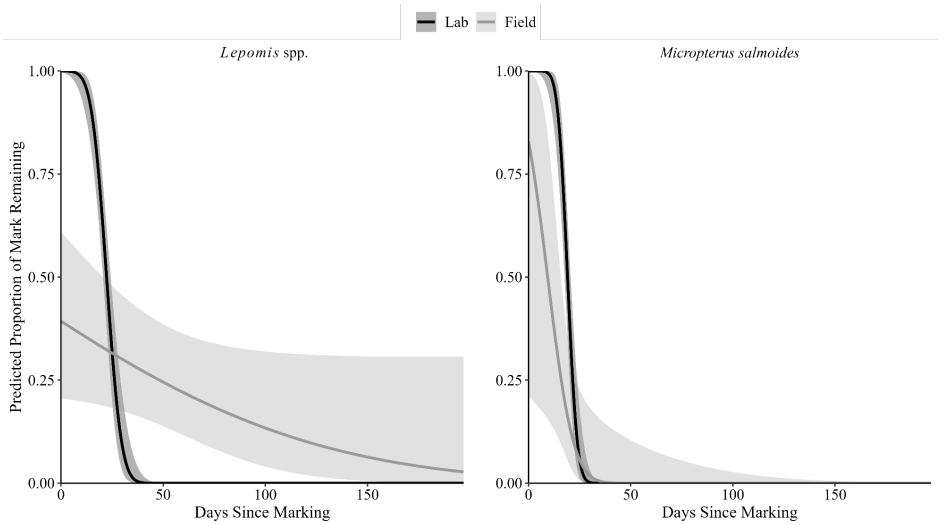

Figure 2 . Predicted proportion of mark remaining from the final probit regression model plotted across days since marking for Lepomis species and Largemouth Bass (*Mciropterus salmoides*) from lab and Northeast Lions Park Pond (Field) trials.

the field environment than lab trials (Figure 2). This suggests that mark retention estimates will vary based on species specific and environmental phenomena.

Hole punch closure rate estimates varied. Estimates at 75% and 50% open for bass suggest that marks close more rapidly in the lab setting (Figure 3). The estimates for 25% and 5% open suggested similar proportions of mark remaining in both lab and pond settings for bass. In sunfish, the 75% and 50% marks closed sooner in the pond setting than lab trials (Figure 3). Estimates for 25% and 5% open suggest that marks closed sooner in lab trials than in the pond environment. This suggests that hole punch retention measured in the field generally lasted longer than seen in lab trials, though the magnitude of this difference varied by species.

Discussion

Prior investigations into operculum hole-punch mark retentions have suggested marks remain open for < 60 (Common Carp; Snow et al. 2020) to 99 days (Rainbow Trout; Rosburg et al. 2022). Our results suggested operculum-hole punches could be reasonably expected (based on 5% open estimate) to last 26 days (95% CI = 23-29 days) for Largemouth bass and 164 days (95% CI = 93 – 174 days) for *Lepomis* spp., based on field estimates. Snow et al. (2020) showed operculum-hole punch retention was greater for Common Carp > 330 mm TL relative to those that were smaller. These results appear contradictory to our findings as *Lepomis* spp. were generally smaller than Largemouth Bass used in our study yet retained marks for a longer period. However, this is likely the result of differences in hole-punch retention between species or different definitions of hole-punch retention. Given variation in hole-punch retention present between species the literature (e.g., Allison 1963; Snow et al. 2020; Rosburg et al. 2022) it is likely that there is a difference between *Lepomis* spp. and Largemouth Bass was not due to size, but instead due to species specific differences. Furthermore, Snow et al. (2020) counted filled but still visible hole-punches as retentions as opposed to our classification of the hole punch still being open. Miyakoshi and Kudo (1999) noted that hole-punch regeneration did not affect their ability to discern marked fish, though no data were provided. No statistical analyses were performed regarding regenerated but visible punches due to our inability to discern hole-punch misclassifications. Despite this, we did note that marks could still be visually observed and that a void in the opercle bone was easily distinguished when backlighted (see Allison

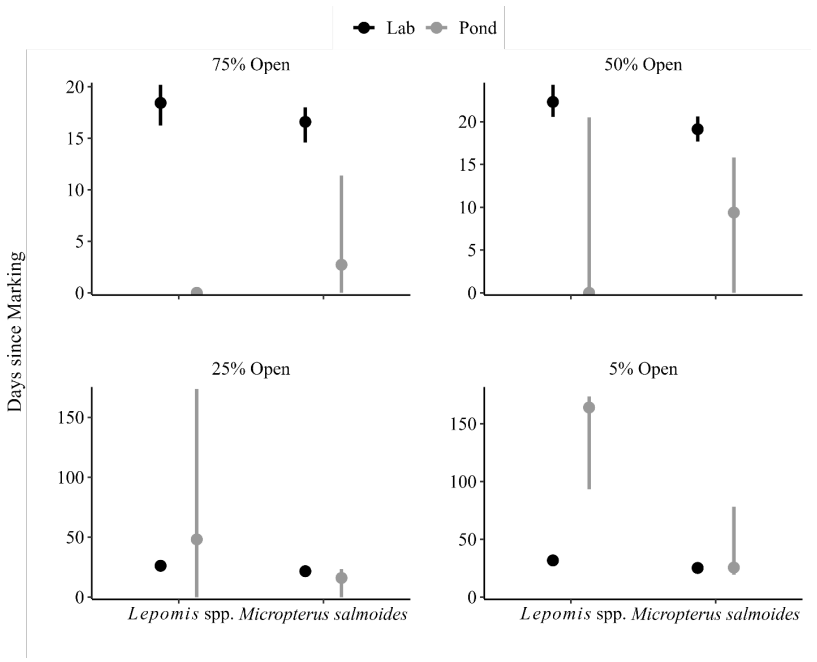

Figure 3. Closure plots showing the estimated number of days since marking at which 75, 50, 25, 5 % of the hole punch is predicted to be remaining for Lepomis species and Largemouth Bass (*Micropterus salmoides*) in lab and Northeast Lions Park Pond (Field) settings based on the final probit regression. Circles represent the mean number of days since marking and lines represent 95% confidence intervals for those day estimates.

1963). Further investigation into the ability of individuals to discern a closed hole-punch mark is needed.

Marks from hole punching operculum appeared to have different retention rates based on environment (i.e., lab vs field) and species (i.e., Largemouth Bass vs *Lepomis* spp.). In the lab, the average mark closure time for hole punches was approximately 30 days for both species. Hole-punch marks appeared to close slower in the field, though this was more extreme for *Lepomis* spp. than for Largemouth Bass. This agrees with prior studies on tags that suggested lab settings may underestimate the retention rates (Dieterman and Hoxmeier 2009). Given that a large number of variables influence tag- and mark-retention (e.g., location, fish size; Acolas et al. 2007; Pine et al. 2012; Snow et al. 2020) further field-based research into operculum hole-punch mark retention should be conducted. Potential areas for future research include Centrarchids of different sizes (e.g., < 127 mm TL), different high-abundance species (e.g., White Bass *Morone chrysops*), or different environments (i.e., different systems).

It is important to note that we are not suggesting lab-based studies are wholly unuseful for investigation into tagging or marking phenomena. Despite recent questions into their applicability (e.g., Dieterman and Hoxmeier 2009; this paper), lab-based studies are not without their merits. For example, effects of marks or tags on growth and survival are easily estimated from lab studies (e.g., Dewey and Zigler 1996; Malone et al. 1999; this study). Lab-based studies may also be preferable when investigating retention of novel tags such as pop-up satellite archival tags (Naisbett-Jones et al. 2023) or novel tag placements (e.g., operculum modified Carlin dangler tags, Montague and Shoup 2022). To the best of our knowledge, the only alternative to those worried about the validity of lab-based retention estimates are field based enclosures (e.g., net pens). Field based enclosures have been used prior to estimate tag retention (Scholten et al. 2002), along

with tagging effects on growth and survival of fishes (FitzGerald et al. 2004; Dembkowski et al. 2018). However, it is unclear if field-based enclosures mimic the retention phenomenon of they systems they are placed within. Further study into the applicability of field-enclosure estimates and comparison to field estimates from non-enclosed fish is likely needed.

Our results suggest that hole-punching operculum in Largemouth Bass and *Lepomis* spp. is a viable technique for mark-recapture studies. Current estimates of retention, based on hole-punch openness, suggest this technique is best suited for closed-system techniques such as Schnabel and Lincoln-Peterson models (Pine et al. 2012). Operculum hole-punching when paired with fin clips allows for date-specific marks and can used estimates of more complex closed mark-recapture models (e.g., Otis et al. 1978; Huggins 1991). If future studies are able to discern the period of time that closed hole-punch marks are identifiable in Largemouth Bass and *Lepomis* spp. (e.g., Snow et al. 2020), it is possible that open-population mark-recapture models (e.g., Jolly-Seber; Pine et al. 2012) may be estimated with this technique. Our results suggest operculum hole-punching is a viable low-cost methods for marking fish. Investigations such as these help to reduce financial barriers for mark-recapture studies.

Acknowledgements

We thank Michael Richardson, Jory Bartnicki, Corrie McClees, Graham Montague, Steve O'Donnell, and Dustin Mullinix for assisting in field sampling and laboratory sampling. We also thank Dr. Mostafa Elshahed and anonymous reviewers for providing edits that improved this manuscript. Financial support for this publication was provided by the Sport Fish Restoration Program grant [F22AF00257] to the Oklahoma Department of Wildlife Conservation.

References

Achim Z, Torsten H. 2002. Diagnostic checking in regression relationships. R News 2(3), 7-10. URL https://CRAN.R-project.org/doc/Rnews/

Acock AC, Stavig RG. 1979. A measure of association for nonparametric statistics. Social Forces 57:1381–1386.

Acolas ML, Roussell JM, Lebel JM, Baglinière JL. 2007. Laboratory experiment on survival, growth and tag retention following PIT injection into the body cavity of juvenile brown trout (*Salmo trutta*). Fisheries Research 86:280–284.

Akoglu H. 2018. User's guide to correlation coefficients. Turkish Journal of Emergency Medicine 18:91–93

Allison LN. 1963. Marking fish with a paper punch. Michigan: Institute for Fisheries Research, Division of Fisheries, Michigan Department of Conservation. Report Number 1656.

Catalano MJ, Chipps SR, Bouchard MA, Wahl DH. 2001. Evaluation of injectable fluorescent tags for marking centrarchid fishes: retention rate and effects on vulnerability to predation. North American Journal of Fisheries Management 21:911-917.

Cohen J. 1988 Statistical power analysis for the behavioral sciences. 2nd edition. Mahwah, New Jersey: Lawrence Erlbaum Associates.

Conover GA, Sheehan RJ. 1999. Survival, growth, and mark persistence in juvenile black crappies marked with fin clips, freeze brands, and oxytetracycline. North American Journal of Fisheries Management 19:824-827.

Dembkowski DJ, Isermann DA, Sass GG. 2018. Short-term mortality and retention associated with tagging age-0 walleye using passive integrated transponders without anesthesia. Journal of Fish and Wildlife Management 9:393-401.

Dewey MR, Zigler SJ. 1996. An evaluation of fluorescent elastomer for marking bluegills in experimental studies. The Progressive Fish-Culturist, 58:219-220.

Dieterman DJ, Hoxmeier RJH. 2009. Instream evaluation of passive integrated transponder retention in brook trout and brown trout: effects of season, anatomical placement, and fish length. North American Journal of Fisheries Management 29:109-115.

Everhart W, Eipper A, Youngs W. 1975. Principles of fishery science. Cornell University Press, Ithaca, New York, USA.

FitzGerald JL, Sheehan TF, Kocik JF. 2004. Visibility of visual implant elastomer tags in atlantic salmon reared for two years in marine net-pens. North American Journal of Fisheries Management 24:222-7.

Hothorn T, Zeileis A, Farebrother RW, Cummins C, Millo G, Mitchell D. 2022. Package 'lmtest' version 0.9-40: Testing linear regression models. Available:https://cran.r-project.org/web/packages/lmtest/lmtest.pdf

Huggins RM. 1991. Some practical aspects of a conditional likelihood approach to capture experiments. Biometrics 47:725–732.

James G, Witten D, Hastie T, Tibshirani R. 2013. An introduction to statistical learning with applications in R. Springer Science + Business Media. Berlin, Germany.

Jennings MJ. 1997. Centrarchid Reproductive Behavior: Centrarchid reproductive behavior: implications for management. North American Journal of Fisheries Management 17:493-495.

Kaemingk MA, Weber MJ, McKenna PR, Brown ML. 2011. Effect of passive integrated transponder tag implantation site on tag retention, growth, and survival of two sizes of juvenile bluegills and yellow perch. North American Journal of Fisheries Management 31: 726-732.

Kolmogorov AN. 1933. Sulla determinazione empirica di una legge di distribuzione. Giornale dell'Instituto Italiano degli Attuari 4:83–91.

Malone JC, Forrester GE, Steele MA. 1999. Effects of subcutaneous microtags on the growth. Survival, and vulnerability to predation of small reef fishes. Journal of Experimental Marine Biology and Ecology 237:243-253.

McFarlane GA, Wydoski RS, Prince ED. 1990. Historical review of the development of external tags and marks. American Fisheries Society Symposium 7:9-29.

Miyakoshi Y, Kudo S. 1999. Mark-recapture estimation of escapement of Masu Salmon *Oncorhynchus masou* with a comparison to a fence count. North American Journal of Fisheries Management 19:1108-1111.

Montague GF, Shoup DE. 2022. Accuracy, Precision, and optimal sampling duration of low-frequency electrofishing for sampling reservoir Flathead Catfish populations. North American Journal of Fisheries Management 42:1269-1284.

Murphy BR, Willis DW, editors. 1996. Fisheries techniques, 2nd edition. American Fisheries Society, Bethesda, Maryland.

Naisbett-Jones LC, Branham C, Birath S, Paliotti S, McMains AR, Joel Fodrie F, Morley JW, Buckel JA, Lohmann KJ. 2023. A method for long-term retention of pop-up satellite archival tags (PSATs) on small migratory fishes. Journal of Fish Biology 102:1029-1039.

Otis DL, Burnham KP, White GC, Anderson DR. 1978. Statistical inference for capture data from closed populations. Wildlife Monographs 62:3-135

Parker NC, Giorgi AC, Heidinger RC, Jester Jr. DB, E.D. Prince, G.A. Winans, editors. 1990. Fish-marking techniques. American Fisheries Society, Symposium 7, Bethesda, Maryland.

Parsons BG, Reed JR. 1998. Angler exploitation of bluegill and black crappie in four west-central Minnesota lakes. Minnesota Department of Natural Resources Investigational Report 468.

Pastore M. 2020. Estimation of overlapping in empirical distributions. R package version 1.6. Available: https://CRAN.R-project.org/package=overlapping

Pastore M, Calcagnì A. 2019. Measuring distribution similarities between samples: a distribution-free overlapping index. Frontiers in Psychology 10:1089.Available:https://www.frontiersin.org/articles/10.3389/fpsyg.2019.01089/full

Pine WE, Hightower JE, Coggins LG, Lauretta MV, Pollock KH. 2012. Design and analysis of Tagging Studies. Pages 521-572 in Zale AV, Parrish DL, Sutton TM, editors. Fisheries Techniques, 3rd edition. American Fisheries Society, Bethesda, Maryland.

Quinn S, Paukert C. 2009. Centrarchid fisheries. In: Cooke SJ, Philipp DP, editors. Centrarchid fishes: diversity, biology, and conservation. West Sussex (UK). p 312-339.

R Core Team. 2023. _r: A language and environment for statistical computing_. R foundation for statistical computing, Vienna, Austria. ,https://www.R-project.org/>.

Rosburg AJ, Davis JL, & Barnes ME. 2022. Retention of fin clips and fin and operculum punch marks in rainbow trout. Aquaculture and Fisheries 7: 660-663.

Schneider, James C. 1998. Lake fish population estimates by mark-and-recapture methods. Chapter 8 in Schneider, James C. (ed.) 2000. Manual of fisheries survey methods II: with periodic updates. Michigan Department of Natural Resources, Fisheries Special Report 25, Ann Arbor

Scholten GD, Isermann DA, Willis DW. 2002. Retention and survival rates associated with the use of t-bar anchor tags in marking yellow perch. Proceedings of the South Dakota Academy of Science 81:35-38.

Siepker MJ, Knuth DS, Ball EL, Koppelman JB. 2012. Evaluating a novel passive integrated transponder tag in largemouth bass. North American Journal of Fisheries Management 32:528-532.

Smirnov NV. 1939. Estimate of derivation between empirical distribution function in two independent samples. Bulletin of Moscow University 2:3–16.

Snow RA, Shoup DA, Porta MJ. 2020. Mark retention and fish survival associated with a low-cost marking technique for common carp *Cyprinus carpio* (Linnaeus, 1758). Journal of Applied Ichthyology 36:693-698.

Tranquilli JA, Childers WF. 1982. Growth and survival of largemouth bass tagged with floy anchor tags. North American Journal of Fisheries Management 2:184-187.

Wagner CP, Einfalt LM, Scimone AB, Wahl DH. 2009. Effects of fin-clipping on the foraging behavior and growth of age-0 muskellunge. North American Journal of Fisheries Management 29: 1644-1652

Wickham H. 2016. Ggplot2:elegant graphics for data analysis. Springer-Verlag, New York

Submitted October 14, 2023 Accepted November 16, 2023

A Comparison of Eight Channel Catfish Populations across the Central Region of Oklahoma

Austin D. Griffin
Oklahoma Department of Wildlife Conservation, Oklahoma Fishery Research Laboratory, Norman, OK 73072

Jory B. Bartnicki
Oklahoma Department of Wildlife Conservation, Oklahoma Fishery Research Laboratory, Norman, OK 73072

Douglas L. Zentner
Oklahoma Department of Wildlife Conservation, Oklahoma Fishery Research Laboratory, Norman, OK 73072

Richard A. Snow
Oklahoma Department of Wildlife Conservation, Oklahoma Fishery Research Laboratory, Norman, OK 73072

Abstract: Channel catfish (*Ictalurus punctatus*) are a popular sportfish in Oklahoma, ranking as the 3rd overall most preferred species from 1985 - 2019. Due to this popularity, species-specific surveys are conducted, and stockings accrue to ensure population dynamics are within acceptable levels and abundances can meet angler demands. Therefore, the goals of this study were to: 1) compare catch rates and size distribution of fish caught using 25-mm mesh vs 12.5-mm mesh hoop nets to determine if populations are properly indexed and if bias occurs when only using 25-mm mesh nets and 2) explore population characteristics of Channel Catfish across eight small impoundments in central Oklahoma. Channel catfish were collected across 8 small impoundments during the months of July and August from 2020 - 2022 using baited hoop nets (tandem set of three nets consisting of two 25-mm bar mesh and one 12.5-mm bar mesh in random order or three 25-mm bar mesh nets per set run concurrently with sets of three 12.5-mm bar mesh nets). A combined total of 1985 Channel Catfish ranging from 25-657 mm TL were collected during this study with length distribution varying between systems. Weights ranged from 10-3,470 g with a mean W_r of 88. Fish ranged from 0-22 years of age and 95% of individuals reached maturity at 419 mm TL. Richards growth models indicated growth was relatively slow and mortality rates ranged from 13 to 52% depending on impoundment. Of the Channel Catfish sampled, 26% of them were captured with 12.5 mm mesh nets. Kolmogorov-Smirnov test results showed distributions from 25- and 12.5-mm mesh nets to differ significantly.

Introduction

Channel Catfish (*Ictalurus punctatus*) are a popular and commercially important sportfish native to the central drainages of the United States (Griffin et al. 2022; Bouska et al. 2011). Historically Channel Catfish were sought after as table fare; however, tournament and recreational trophy angling has become popular among

***Corresponding author: richard.snow@odwc.ok.gov**

some fishing enthusiasts (Shrader et al. 2003). In Oklahoma, Channel Catfish rank third in popularity since 1985, behind largemouth bass (*Micropterus salmoides*) and crappie (*Pomoxis* spp.) as the most desirable sportfish (York 2019). Due to this popularity, the Oklahoma Department of Wildlife Conservation (ODWC) has implemented stocking programs to create or supplement Channel Catfish populations within the 242,811 ha of public waters they are entrusted to manage.

Standardized sampling for Channel Catfish in small Oklahoma reservoirs is conducted using baited tandem hoop nets with 25-mm bar mesh (OFAA 2022). Data collected from these samples are used to monitor population trends, set regulations, and dictate stocking needs. Important assumptions of standardized sampling data are that relative catch from these samples is representative of the abundance and size structure of the fishery (Hubert and Fabrizio 2007). These assumptions are commonly assumed and rarely tested for passive gears relative to active sampling gears (Hubert et al. 2012). Prior study has suggested 25-mm bar mesh tandem hoop nets produce the most accurate relative catch and size structure information (see Bodine et al. 2013). However, 25-mm bar mesh tandem hoop nets may not accurately represent catch or size structure of small Channel Catfish, with bias suggested to occur < 150 (Michaletz 2001) or < 250 mm in total length (TL; Michaletz and Sullivan 2002; Buckmeier and Schlechte 2009) dependent on the system. One prior study, from Meeker Lake, Oklahoma determined that 25-mm mesh tandem hoop nets fail to detect abundant small Channel Catfish in the system and suggested small mesh sizes be incorporated into standardized surveys (Montague et al. 2022).

Failure to accurately represent small Channel Catfish in standardized sampling data may lead to mismanagement of high-density, slow-growing, and stunted populations. Currently, ODWC manages Channel Catfish in aggregate with Blue Catfish (*Ictalurus furcatus*) using a statewide regulation due to anglers having difficulty distinguishing between the species (Page et al. 2012). Given the statewide regulation, management of Channel Catfish populations is primarily done via stocking to supplement natural recruitment, especially in small reservoirs. This management technique is generally implemented to safeguard the population from recruitment overfishing. Recruitment overfishing generally occurs when high exploitation rates reduce the abundance of mature individuals such that recruitment is impaired (Myers et al. 2007). However, stocking generally has little effect on growth overfishing. Growth overfishing occurs when fishing mortality is high enough to limit the growth potential of a population or when harvest occurs at too young of an age (Slipke et al. 2002). Both recruitment and growth overfishing may occur simultaneously in a population (Slipke et al. 2002, Chestnut-Faull et al. 2021). To detect potential recruitment and growth overfishing managers require sampling techniques that can properly index size structure and relative abundance of fish populations (see Slipke et al. 2002). This is especially true in Oklahoma given current limitations for modifying the exploitation of Channel Catfish populations through size-based regulation.

Failure to properly index Channel Catfish populations in Oklahoma may result in overstocking. Overstocking in channel catfish population generally results in density-dependent responses. Density-dependent responses are thought to occur when the number of fish in the population exceeds or approaches carry capacity due to resource limitations (e.g., productivity, prey resources; Shoup et al. 2007, Michaletz 2009). Overstocking Channel Catfish has been documented to result in density-dependent responses such as increases in relative abundance and mortality, and decreases in condition, growth rate, and size structure (Michaletz 2009).

Given the limitations of Channel Catfish management strategies in Oklahoma and the potential for negative effects that may occur due to overstocking these populations, sampling strategies that properly index their population metrics and vital rates are critical. Especially

since Montague et al. (2022) suggested small Channel Catfish may not be properly indexed using standard 25-mm mesh tandem hoop nets. Past standardized surveys for Channel Catfish may have failed to properly index their populations, especially if stunting (i.e., reduction in size) is occurring. This is especially concerning for small impoundments in the central region of Oklahoma as this is where Meeker Lake is situated. Therefore, the objectives of our study were to: 1) compare catch rates and size distribution of Channel Catfish caught using 25-mm mesh vs 12.5-mm mesh hoop nets and 2) describe size structure, condition, maturity schedule, and growth rate for Channel Catfish across and among small impoundments in the central region of Oklahoma.

Methods

Study Area

Channel Catfish were sampled from eight small (< 200 ha) lakes located in the Cross Timbers and Central Great Plains ecoregions of central Oklahoma (Woods et al. 2005). Descending from North to South these include Langston Lake (169.9 ha), Guthrie Lake (82.9 ha), Liberty Lake (79.7 ha), Lake El Reno (68.8 ha), Purcell Lake (63.5 ha), Lindsay Lake (8.9

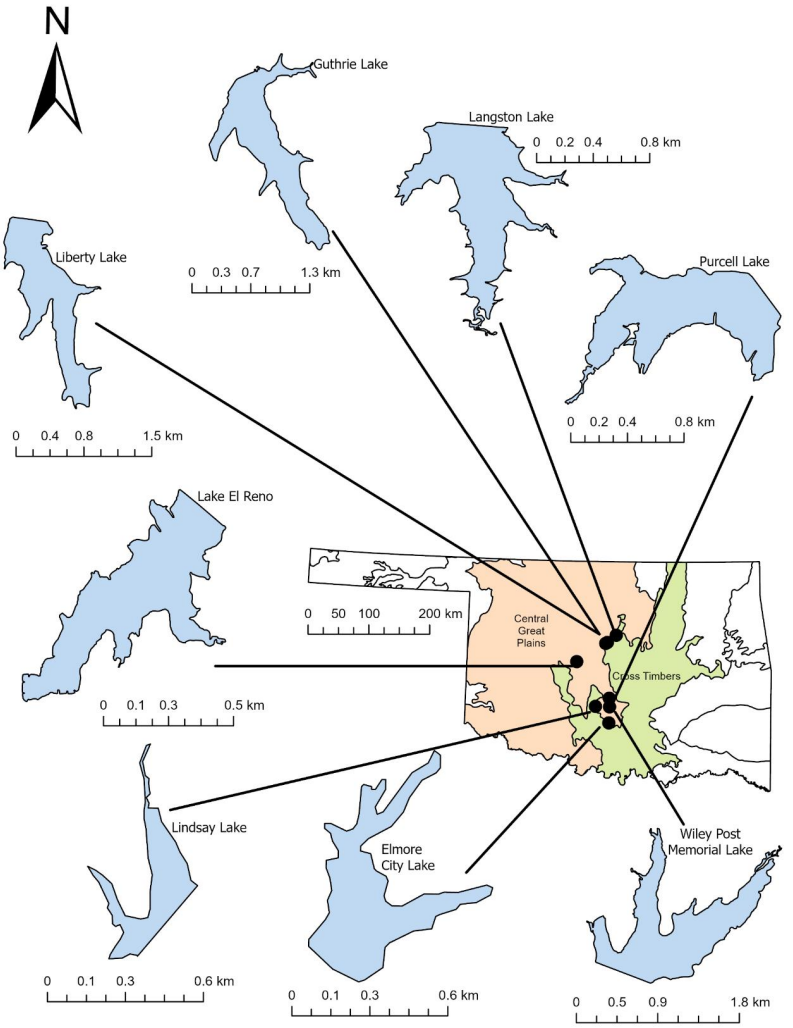

Figure 1. Location and outline of study lakes distributed across the Cross Timbers and Central Great Plains ecoregions.

ha), Wiley Post Memorial Lake (also known as Maysville Lake, 122.2 ha), and Elmore City Lake (23.1 ha; Figure 1). Each lake is associated with its namesake municipality and primary uses include municipal water supply, flood control, and recreation. Lake impoundment dates range from 1919 (Guthrie Lake) to 1971 (Wiley Post Memorial Lake; OWRB 2023) Each lake is affected by siltation to some degree within the river reservoir interface, contains limited aquatic vegetation, some standing timber/ brush piles, and a mixture of sandstone, coarse gravel, clay, and sand substrates with riprap rock primarily along the dam and fishing jetties. All lakes support recreational fisheries for Channel Catfish, White Crappie (*Pomoxis annularis*), and Largemouth Bass (*Micropterus salmoides*). Although not highly sought after, Common Carp (*Cyprinus carpio*) and Flathead Catfish (*Pylodictis olivaris*) are present at all lakes, and a stunted Blue Catfish (*Ictalurus furcatus*) population exists at Wiley Post Memorial Lake. Primary forage species include Gizzard Shad (*Dorosoma cededianum*), *Lepomis spp*., and in most cases Inland Silversides (*Menidia berylina*). Trophic class ranges from mesotrophic to hypereutrophic, pH is generally slightly alkaline (7.17-9.22), and turbidity varies from a mean secchi depth of 25 cm at El Reno Lake to 104 cm at Langston Lake (OWRB 2023).

Sampling

Channel Catfish were collected during the months of July and August in 2020 (Langston, Wiley Post Memorial), 2021 (Liberty, Guthrie, Purcell, El Reno, Elmore City), and 2022 (Lindsay) using baited hoop nets. In all lakes except Langston and Wiley Post Memorial, hoop nets were placed in tandem sets of three nets consisting of two 25-mm bar mesh, and one 12.5-mm bar mesh, 3.4-m long net tied 0.9 m apart in random order. In Langston and Wiley Post Memorial Lakes, three tandem sets of only 25-mm bar mesh hoop nets and three tandem sets of only 12.5-mm bar mesh hoop nets were used. The 12.5-mm mesh nets were used in conjunction with the 25-mm mesh nets to determine if they capture smaller sized fish in potentially stunted populations (Michaletz and Sullivan 2002, Montague et al. 2022). Nets were set in accordance with ODWC standardized sampling protocols and the methods of Montague et al. (2022). Dissolved oxygen (DO) and temperature (°C) were recorded adjacent to the bottom at each set to ensure that DO was ≥ 4 mg/L to avoid unnecessary mortality (YSI, model Pro 2030, Yellow Springs Instruments, Yellow Springs, OH).

Total length (TL; mm) and weight (g) were recorded for each captured Channel Catfish, apart from Langston and Wiley Post Memorial Lakes where only TL was recorded. Up to 20 fish per 25-mm TL group were sacrificed for age estimation. Sacrificed fish were euthanized using a 1:1 ice water slurry (Blessing et al. 2010) and brought back to the Oklahoma Fisheries Research Lab (OFRL), Norman, Oklahoma. At the OFRL, sex and maturity were determined via visual examination of the gonads (Davis and Posey 1958; Perry and Carver 1972). Lapilli otoliths were removed for age estimation (Buckmeier et al. 2002).

Otoliths were prepared according to the methods described in Buckmeier et al. (2002), save the browning process (Waters et al. 2020b). Otoliths were cut and polished in the transverse plane until all annuli were visible. Otoliths were then illuminated using a fiber optic filament attached to a light source and viewed under a dissecting microscope capable of 130x magnification (Buckmeier et al. 2002, Waters et al. 2020b). Two independent readers initially estimated ages for each otolith. Disagreements between readers' initial age estimates were resolved with a final consensus read (Hoff et al. 1997).

Analysis

Hoop net mesh size comparison

A Kolmogorov–Smirnov test (K-S test, Kolmogorov 1933, Smirnov 1939) was used to determine if 12.5-mm mesh hoop nets captured significantly different sizes of Channel Catfish relative to 25-mm mesh hoop nets across study lakes ($\alpha = 0.05$). Distributional overlap ($\hat{\eta}$, Pastore and Calcagnì 2019) was also estimated for this pooled comparison to determine the amount of

similarity between the length distributions from 12.5- and 25-mm mesh hoop nets. Means and 95% confidence intervals (CI) of $\hat{\eta}$ were derived by bootstrapping the comparison 10,000 times. Estimates of $\hat{\eta}$ were interpreted based on their relationship to Cohen's d (Cohen 1988) with $\hat{\eta}$ = 0.20, 0.50, and 0.80 indicating the thresholds for small, moderate, and large overlap, respectively. Length-frequency histograms constructed using 10-mm length bins were created for 12.5- and 25-mm mesh hoop nets then overlaid and interpretated qualitatively to determine if there appeared to be a size threshold where 12.5-mm hoop nets captured more individuals. Mean catch per unit effort (CPUE; mean number of fish captured with a defined unit of sampling effort, in this case sampling effort is equal to one set of nets soaked for 72 hours) was estimated separately for 12.5- and 25-mm mesh hoop nets to determine if qualitative differences in Channel Catfish CPUE exist between mesh types. Mean CPUE for 12.5- and 25-mm mesh hoop nets was also compared for different size classes of Channel Catfish. Size classes used for this comparison were sub-stock (< 280 mm TL), stock (≥ 280 mm TL), quality (≥ 410 mm TL) and preferred (≥ 610 mm TL, Gabelhouse 1984). These size classes were selected as they are commonly used in fisheries management. Mean CPUE for 12.5- and 25-mm mesh hoop nets was estimated using combined data from Guthrie, Liberty, El Reno, Purcell Lake, Lindsay, and Elmore City Lakes. Mean CPUE for 12.5- and 25-mm mesh hoop nets was also estimated using combined data from Langston and Wiley Post Memorial Lakes. Mean CPUE was estimated separately for these systems due to differences between how 12.5- and 25-mm mesh tandem hoop nets were deployed (see Sampling).

Channel Catfish population metrics

To assess Channel Catfish size structure, weight-length relationships, and condition of fish sampled, data from 12.5- and 25-mm mesh hoop nets was pooled. Size structure for Channel Catfish from all lakes was described using length-frequency histograms and proportional size distribution (PSD, Gabelhouse 1984). Length category groupings used for PSD analysis were PSD S-Q (280.0-409.9 mm TL), PSD Q-P (410.0-609.9 mm TL) and PSD P-M (610- 709.9 mm TL, see Neumann et al. 2012). Simple linear regression was used to predict the weight-length relationships for Channel Catfish based on $\log_{10}$ transformed weights and TLs (Neumann et al. 2012). Relative weight (*Wr*) was used to assess body condition via the standard weight equation present in Neumann et al. (2012). Only Channel Catfish ≥ 70-mm TL were included in *Wr* calculations (Brown et al. 1995). All statistics were estimated for each individual study lake and across all lakes combined.

To assess Channel Catfish maturity, growth rates, and mortality sacrificed fish sampled via 12.5- and 25-mm mesh hoop nets were also pooled. Logistic regression was used to estimate TL at maturity for Channel Catfish using a binary system (0 = immature, 1 = mature). To determine if there were sex-specific differences in TL at maturity for Channel Catfish, logistic regression models were fit with and without a sex specific parameter and compared via a likelihood ratio test to determine if including sex significantly improved model fit (α = 0.05). Growth trajectories were described using Richards growth model (Richards 1959, Ricker 1975) as there were issues trying to fit the standard von Bertalanffy growth equation to populations. Weighted catch curves were used to estimate instantaneous mortality (*Z*; Maceina 1997). Catch curves for analysis were fit using the first fully recruited age class to the maximum age class in each sample (see Miranda and Bettoli 2007); with the first fully recruited age class varying between lakes (range 1-5 years old). Total annual mortality (*A*) was estimated based on its relationship with *Z* (i.e., $1 - e^{-Z}$, Ricker 1975). Growth and mortality calculations were performed using the Oklahoma Fisheries Analysis Application (OFAA 2022) and the Fisheries Stock Analysis R Package (Ogle 2023). All statistics were estimated for each individual study lake and across all lakes combined.

Results

In total, 1,470 and 515 Channel Catfish were captured in the 25-mm and 12.5-mm mesh nets respectively. K-S test results confirm that the two distributions differ significantly from one another (D = 0.59, $P < 0.01$, mean overlap = 0.47; Figure 2). Estimates of $\hat{\eta}$ suggest small-to-moderate overlap is present within these distributions. Length frequency distribution based on net size shows that fish ≤ 230 mm TL are underrepresented or altogether missing from the 25-mm mesh net sample (Figure 2). Catch per unit effort (CPUE) for 12.5-mm mesh nets (2.05) was 63.4 % of 25-mm mesh net catch rates (3.24) for Guthrie, Liberty, El Reno, Purcell, Lindsay, and Elmore City Lakes combined (Table 1). Conversely, in Langston and Wiley Post Memorial Lakes, CPUE from 12.5-mm mesh nets (4.94) was 172.5 % of the 25-mm mesh net catch rates (2.84), likely affected by the stunted population at Langston (Table 2, Figure 3). Overall catch rates for the 12.5 mm mesh were higher than that of the 25-mm mesh for substock Channel Catfish, but lower for stock-size and larger fish across all systems (Tables 1 and 2).

A total of 1985 Channel Catfish ranging from 25-657 mm TL (mean = 330 mm) were collected from all study lakes combined (Figure 3). Length frequency distributions were variable dependent on system, ranging from normal at Liberty, to multimodal distributions at Langston, El Reno, and Elmore City (Figure 3). Overall, the population was dominated by stock size fish with a PSD S-Q of 61, a PSD Q-P of 39, and a PSD P-M of 1 (Figure 3); though, this analysis excluded substock individuals. PSD S-Q and PSD Q-P range from 33-94 and 6-67 across study systems, with only Wiley Post Memorial Lake having fish with TLs falling into the PSD P-M category. Length-weight relationships exhibited exceptional fit (r^2 range = 0.94-0.98) and individual lake and pooled estimates suggested allometric growth (mean β range = 3.02 – 3.33; Figure 4). Weights ranged from 10-3,470 g (mean = 414 g) with W_r ranging from 82-94 (mean = 88).

Likelihood ratio tests suggested sex did not influence the TL-maturity relationship when the

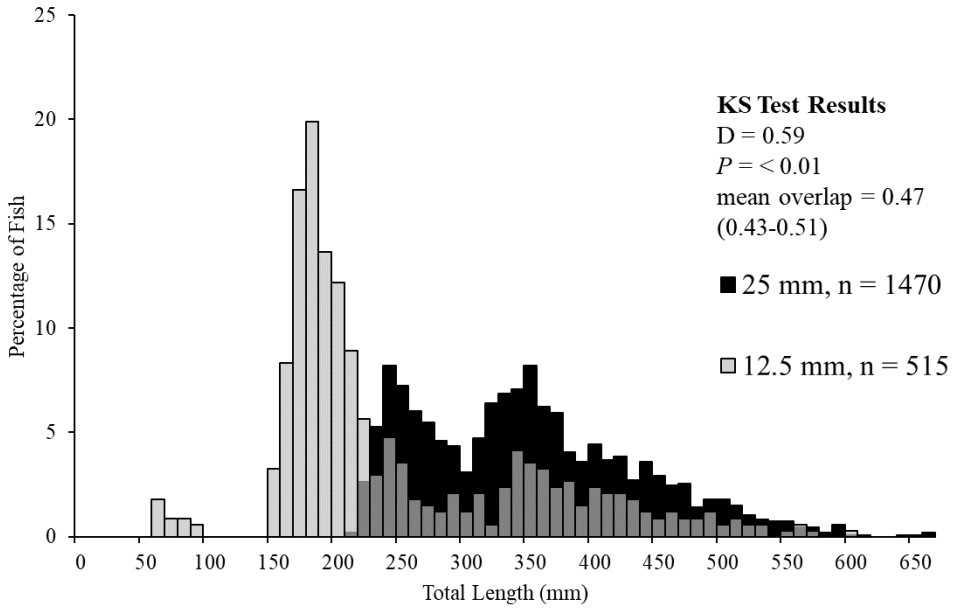

Figure 2. Length-frequency histograms for channel catfish captured from all study lakes using either 25- or 12.5-mm hoop nets. Included are K-S test results and the mean (95% confidence interval) for an overlap test.

Table 1. Catch per unit effort (CPUE; mean number of fish captured per set of nets) of Channel Catfish from 12.5 and 25-mm bar mesh hoop nets on Guthrie, Liberty, El Reno, Purcell Lake, Lindsay, and Elmore City Lakes. Included are CPUE estimates for sub-stock (< 280 mm TL), stock (≥ 280 mm TL), quality (≥ 410 mm TL) and preferred (≥ 610 mm TL) Channel Catfish from each bar mesh type.

Bar mesh	CPUE				
	Total	substock	stock	quality	preferred
12.5 mm	2.05	1.2	0.58	0.28	0.00
25 mm	3.24	0.57	1.73	0.94	0.01

model was fit for individual lakes or when all lakes were pooled (χ^2 range = 0.12-3.19, p range = 0.07 – 0.73). Ninety-five percent maturity was reached by 419 mm TL for all lakes combined and ranged from 348-425 mm TL dependent on the system (Figure 5). Channel Catfish ranged from 0 to 22 years of age (mean = 5 years) for all lakes. The majority of fish (76%) fell between ages 1-7. Pooled regional estimates from Richards growth models suggested growth was slow (k = 0.21), though this varied based on mean individual lake estimates (k range = 0.08 – 0.42; Figure 6). Theoretical mean maximum length also varied between systems (L_∞ range = 487 – 897) with a regional mean estimate of 531 mm (Figure 6). Regionally, the majority of Channel Catfish reached 75 % of L_∞ by age-7 (Figure 6). Mortality rates in lakes were highly variable (Z range = 0.13 – 0.52, A range = 14 – 41; Figure 7) with a pooled regional estimate of 0.31 for instantaneous mortality and 27 for annualized mortality. Age-catch frequencies suggest variable recruitment in populations based on the variability of catch for age classes occurring after the first fully recruited age reflected in fit statistics (r^2 range = 0.06 – 0.59; Figure 7)

Discussion

Our results confirm the suggestion by Montague et al. (2022) that 25-mm bar mesh hoop nets likely underrepresent the biomass of small Channel Catfish in central Oklahoma small impoundments. This is not surprising given the findings of other papers that suggest that 25-mm bar mesh hoop nets may be biased for smaller Channel Catfish (Michaletz 2001; Michaletz and Sullivan 2002; Buckmeier and Schlechte 2009). However, to the best of our knowledge, this size bias has received little attention in the literature. This is likely due to prior studies suggesting that 25-mm bar mesh hoop nets properly index Channel Catfish populations (see Bodine et al. 2013). To be clear, we do not believe the findings of prior studies to be incorrect as the size-based limitations of the gear are clearly stated. We hypothesize that the general acceptance of constant catchability (q) passive gears (Hubert et al. 2012) has resulted in an overreliance on the accuracy of CPUE data obtained from hoop nets. It is likely that q of hoop nets with different mesh sizes needs to be treated similarly to that of gillnets (e.g., Shoup and Ryswyk 2016). A better understanding of the changes in q for different sized bar mesh of hoop nets will allow

Table 2. Catch per unit effort (CPUE; mean number of fish captured per set of nets) of Channel Catfish from 12.5 and 25-mm bar mesh hoop nets on Langston and Wiley Post Memorial Lakes. Included are CPUE estimates for sub-stock (< 280 mm TL), stock (≥ 280 mm TL), quality (≥ 410 mm TL) and preferred (≥ 610 mm TL) Channel Catfish from each bar mesh type.

Bar mesh	CPUE				
	total	substock	stock	quality	preferred
12.5 mm	4.94	4.69	0.19	0.06	0.00
25 mm	2.84	1.6	1.11	0.11	0.01

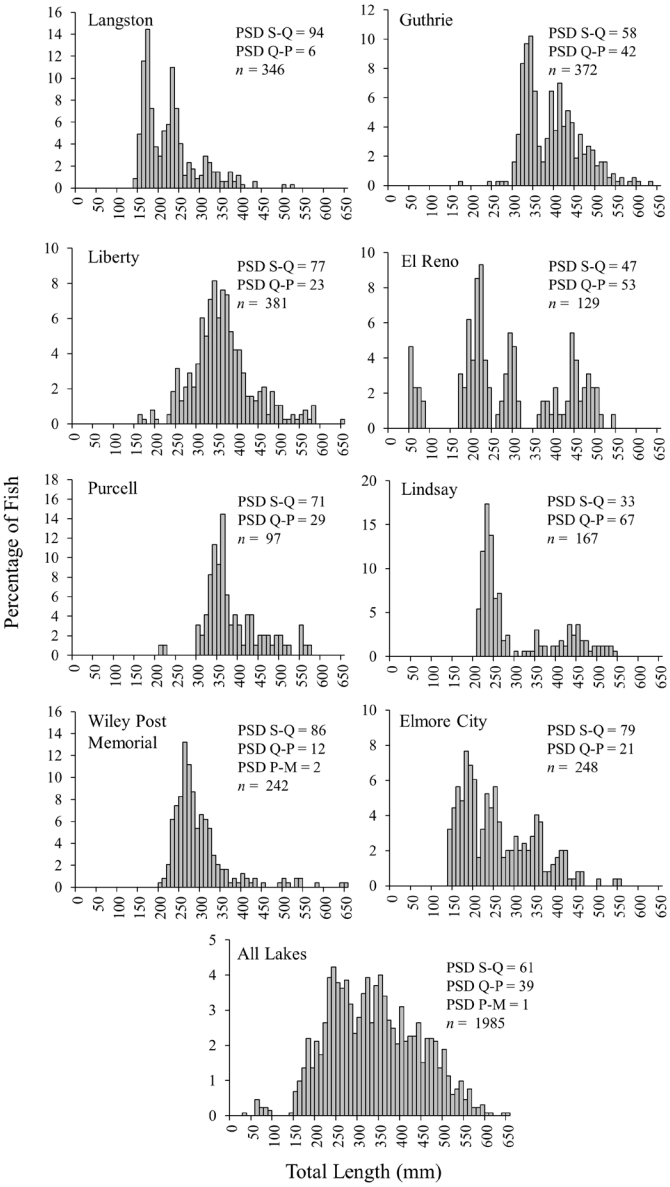

Figure 3. Length frequency histograms and proportional size distributions (PSD) of Channel Catfish collect from each study lake and all lakes combined from baited tandem hoop-nets.

for more accurate assessment of Channel Catfish populations in Oklahoma reservoirs.

The Richards growth model used in this study is less commonly applied than the more common relative growth functions (e.g., von Bertalanffy, Gompertz, *sensu* Quist et al. 2012). Richards growth model is advantageous due to its flexibility, containing von Bertalanffy, Gompertz, and logistic models in special cases (Richards 1959; Chiang 2004; Cerdenares-Ladrón De Guevara 2011). This flexibility allowed us to model slow early growth in some of our central Oklahoma Channel Catfish populations, perhaps most evident in Wiley Post Memorial Lake. Interestingly, Wiley Post Memorial Lake exhibited higher mean mortality estimates relative to the pooled estimate obtained for the region. Higher mortality rates have been noted prior for stunted channel catfish

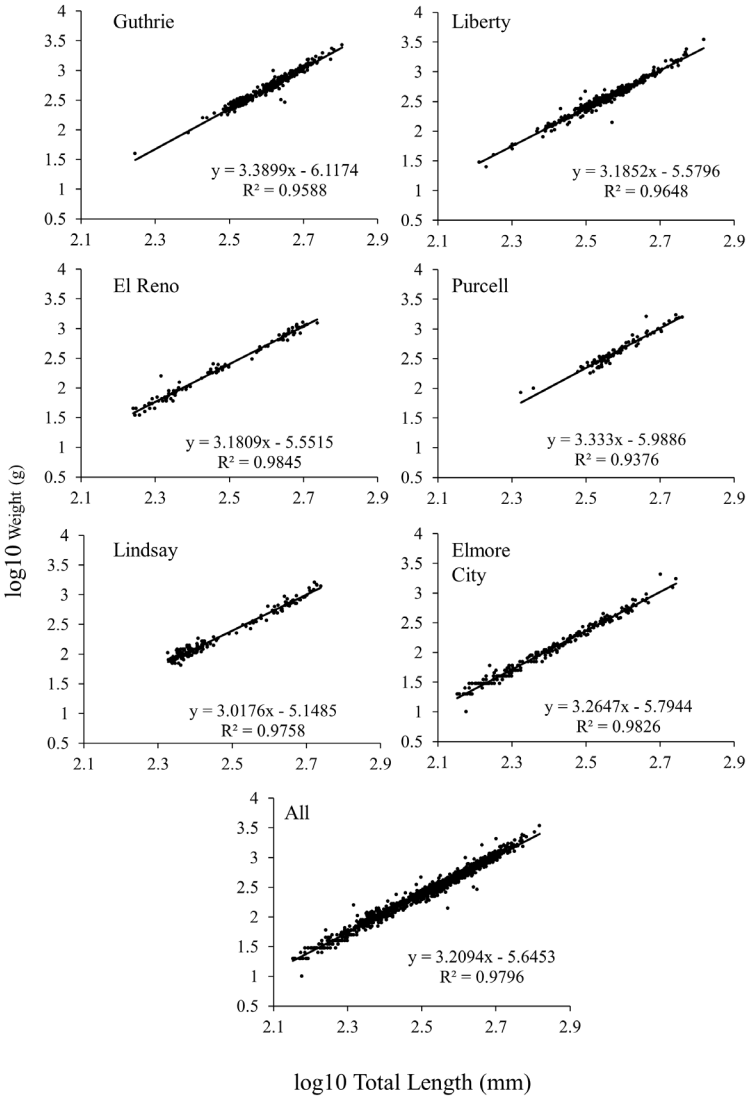

Figure 4. Length-weight relationships with associated r^2 and equations of Channel Catfish collected from each study lake (except Wiley Post and Langston due to lack of weight data) and all lakes combined.

populations (Michaletz 2009). This suggests overstocking may have occurred, likely due to the inability of 25-mm bar mesh hoop nets to properly index small Channel Catfish in this system. It's likely that a better understanding of harvest rates in these systems is needed to determine the best management strategy moving forward. Future research should focus on relating changes in growth with harvest rates in small impoundments.

Regionally, Channel Catfish populations in Oklahoma appear to be relatively long lived and slow growing. However, both growth rate and maximum observed age appeared to vary by system. Interestingly, large growth potential appears to be possible in these populations, as the maximum size and weight estimates from central region lakes is comparable to the 95th percental of statewide Channel Catfish populations (OFAA 2022). Regionally, PSD and *Wr* estimates appear to be average relative

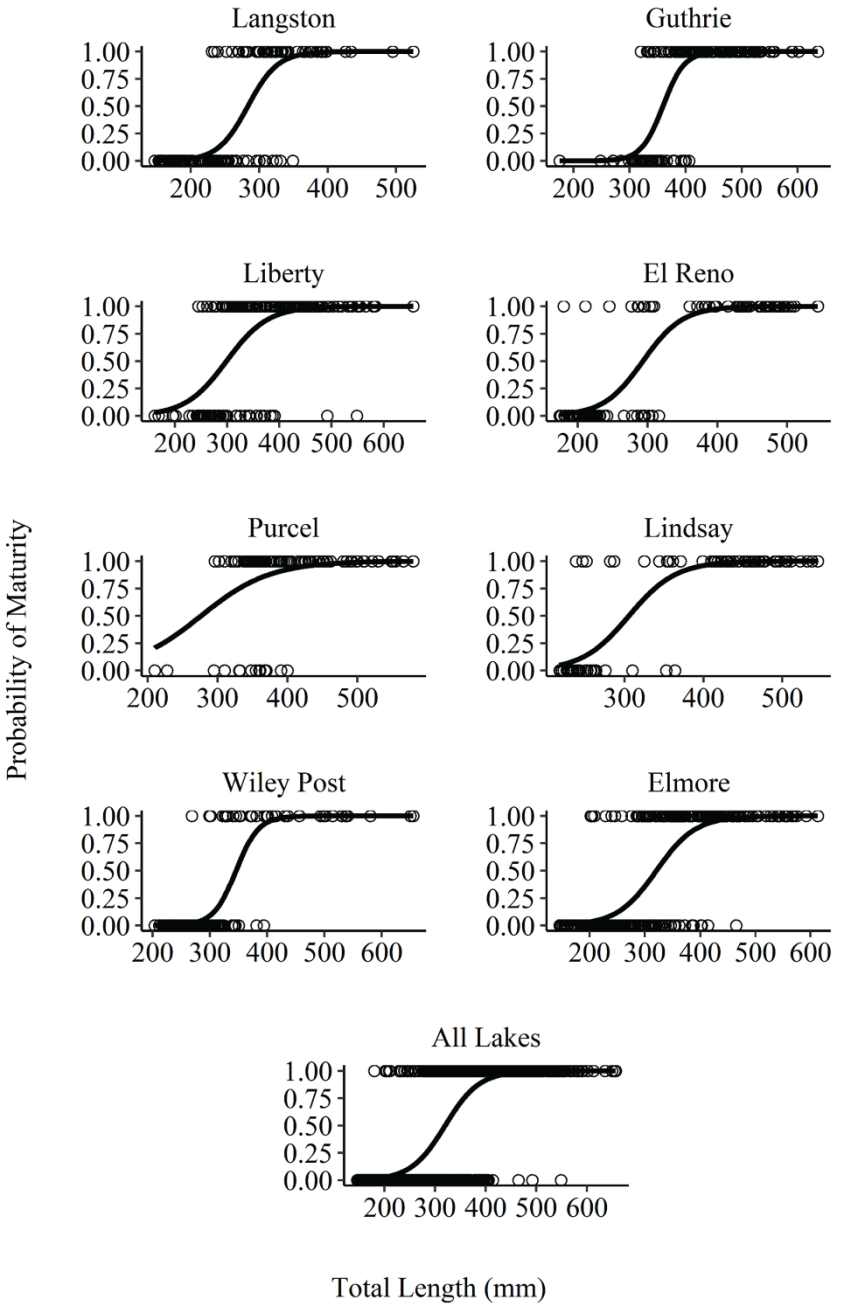

Figure 5. Channel catfish maturity curves for each study lake and all lakes combined. Included are raw data indicating the maturity information (0 = immature, 1 = mature) for each individual (circles).

to other Oklahoma reservoirs (OFAA 2022). However, these metrics were also variable across study systems. This is not surprising as Channel Catfish population dynamics and vital rates are known to vary based on abiotic and biotic variables (Shoup et al. 2007; Michaletz 2009). Furthermore, water level and resulting access to the riparian zones in lotic and semi-lotic systems

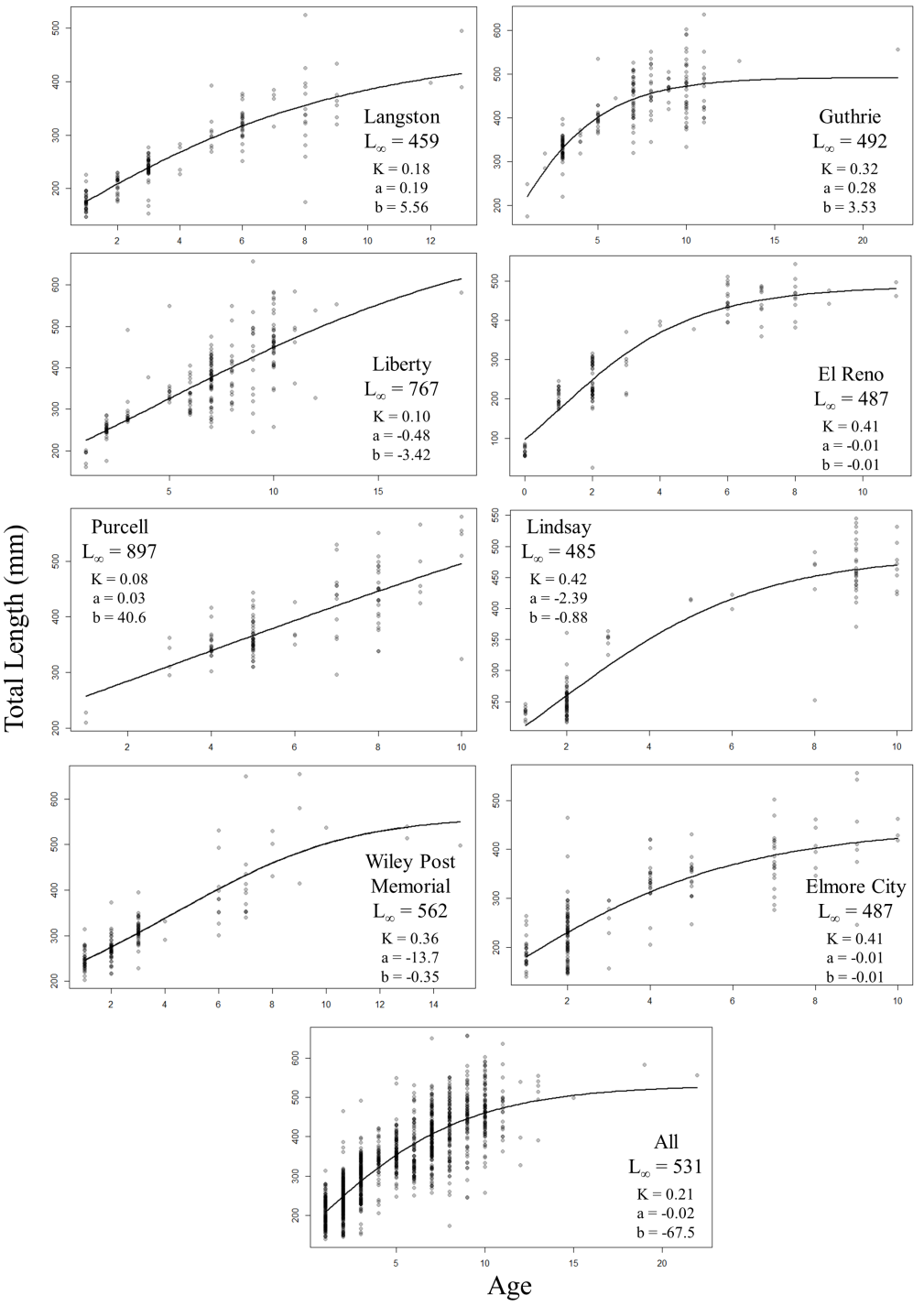

Figure 6. Channel catfish growth curves for each study lake and all lakes combined from baited tandem hoop nets. Circles indicate observed age estimates for each individual. Included are parameter estimates from the Richard's growth model (L_∞ = predicted maximum total length, K = growth constant, a =horizontal position of the inflection point, and b = vertical position of the inflection point).

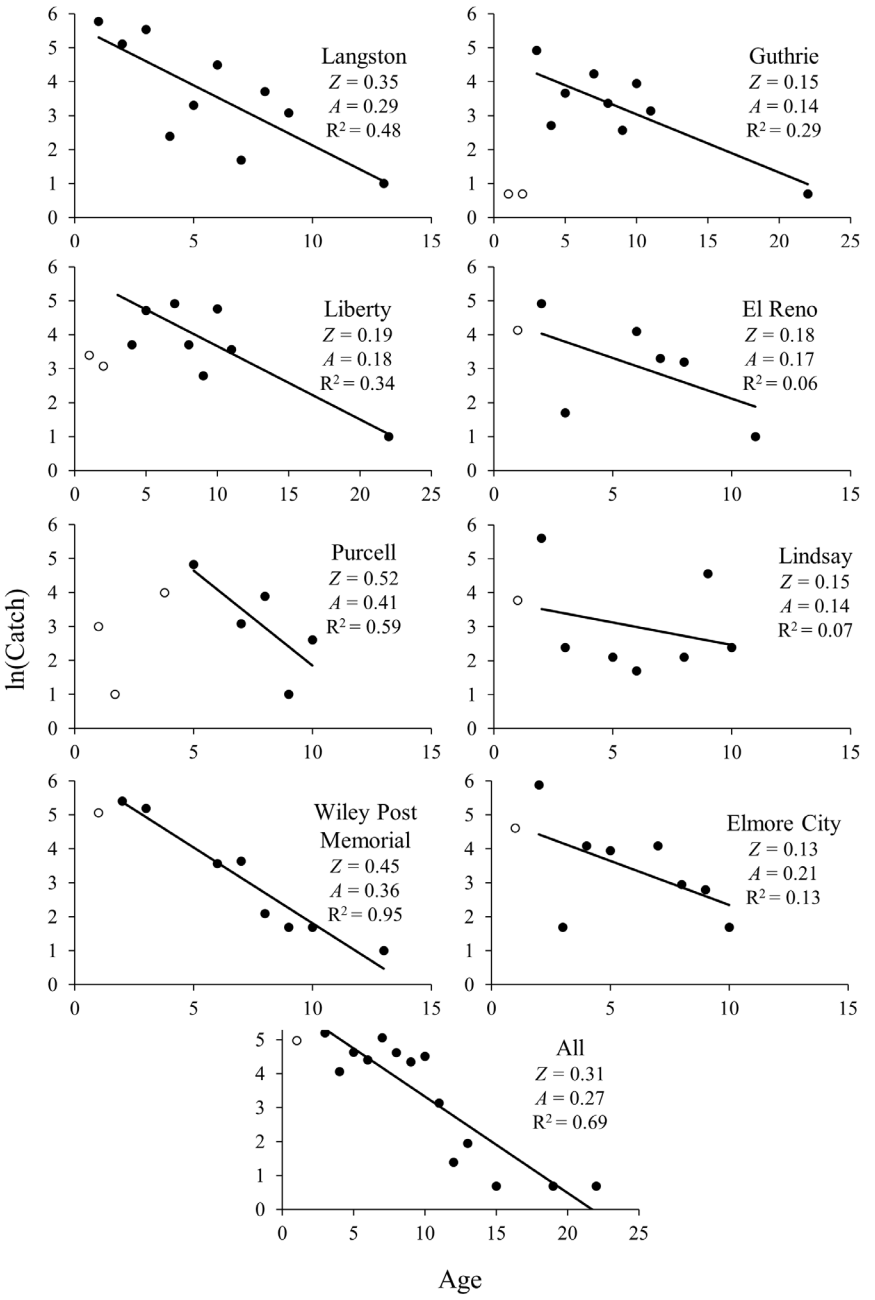

Figure 7. Weighted catch curves for Channel catfish for each study lake and all lakes combined. Age classes that were unrecruited (not used for estimation, white circles) and fully recruited (used for estimation, black circles) are provided. Estimates of instantaneous mortality (Z), total annual mortality (*A*), and fit (R^2) are provided.

are known to influence catfish condition (Schall and Lucchesi 2021). Further study of abiotic and biotic relationships with Channel Catfish dynamics and vital rates is likely needed in these systems to understand applicability of stocking and other management actions.

Manipulation of Channel Catfish populations

in small impoundments through stocking is common and often necessary (Michaletz 2009). However, stocking rates are hard to determine when sampling bias is present as overstocking has the potential to result in stunted Channel Catfish populations (Michaletz 2009; Montague et al. 2022). Our results agree with prior studies that suggest lake specific effects and Channel Catfish population structure need to be appropriately accounted for prior to stocking to maximize the influence of stocking on Channel Catfish populations. This is especially true when Blue Catfish and Channel Catfish occur in high densities within the same small impoundment (Waters et al. 2020a, Montague et al. 2022), as these species exhibit high interspecific overlap in diet (Graham 1999, Hubert 1999, Bentley 2023). This interspecific competition may also be true for populations of Channel Catfish that occur with Common Carp, as small Channel Catfish and Common Carp overlap in diet prior to Channel Catfish becoming piscivorous (Hubert 1999; García-Berthou 2001, Kloskowski 2011). Further study of the effects of this potential interspecific competition is likely needed for Channel Catfish populations across Oklahoma.

Channel Catfish populations present a unique challenge to fisheries management in Oklahoma. Our results suggest that Channel Catfish populations within the central region of Oklahoma exhibit variable dynamics and vital rates. Several potential explanations exist to describe this variability (e.g., interspecific competition, abiotic variability; Waters et al. 2020a; Michaletz 2009; Schall and Lucchesi 2021). Further study will be needed to determine the influence of biotic and abiotic factors on these populations. The accuracy of future studies will rely on sampling methods that appropriately index these populations. For that reason, we recommend that sampling on these reservoirs incorporate 12.5-mm bar mesh hoop nets so smaller Channel Catfish are represented in the samples. Further study of the effects of different sizes of bar mesh on hoop net *q* are also warranted. Such studies will allow for management guidelines that avoid overstocking of Channel Catfish in small impoundments and allow fisheries managers to maintain robust Channel Catfish populations.

Acknowledgements

We thank Shelby Jeter, Corrie McClees, Graham Montague, Michael Porta, Michael Richardson, and Alexis Whiles for assisting in field sampling and laboratory sampling. We also thank Dr. Mostafa Elshahed and anonymous reviewers for providing edits that improved this manuscript. Financial support for this publication was provided by the Sport Fish Restoration Program grant [F22AF00257] to the Oklahoma Department of Wildlife Conservation.

References

Bentley, J. 2023. Seasonal variation in the feeding ecology of Channel Catfish *Ictalurus punctatus* and Blue Catfish *Ictalurus furcatus* in Ohio Reservoirs. [Research Thesis]. Columbus (OH), Ohio State University. Available from OSU library.

Blessing J., J. C. Marshall, and S. Balcombe. 2010. Humane killing of fish for scientific research: a comparison of two methods. Journal of Fish Biology 76:2571-2577.

Bodine, K. A, D. E. Shoup, J. Olive, Z. L. Ford, R. Krogman, and T. J. Stubbs. 2013. Catfish sampling techniques: Where we are now and where we should go. Fisheries 38:529-546.

Bouska, W. W., C. Longhenry, P. Bailey, D. Fryda, and H. Headley. 2011. Channel Catfish populations, management, and angler use in the main-stem Missouri River reservoirs. pp 167-176 in P. H. Michaletz and V. H. Travnichek, editors. Conservation, Ecology, and Management of Catfish: The Second International Symposium. American Fisheries Society, Symposium 77, Bethesda, Maryland.

Brown, M. L., J. Francisco Jr., D. M. Gatlin III, and B. R. Murphy. 1995. A revised standard weight (*Ws*) equation for Channel Catfish. Journal of Freshwater Ecology 10:295-302.

Buckmeier, D. L., E. R. Irwin, R. K. Betsill, and J. A. Prentice. 2002. Validity of otoliths and pectoral spines for estimating ages of Channel Catfish. North American Journal of Fisheries Management 22:934-942.

Buckmeier, D. L., and J. W. Schlechte. 2009. Capture efficiency and size selectivity of Channel Catfish and Blue Catfish sampling gears. North American Journal of Fisheries Management 29:404–416.

Cerdenares-Ladrón De Guevara, G., E. Morales-Bojórquez, and R. Rodríguez-Sánchez. 2011. Age and growth of the sailfish *Istiophorus platypterus* (Istiophoridae) in the Gulf of Tehuantepec, Mexico. Marine Biology Research 7:488–499.

Chestnut-Faull, K. L., Q. E. Phelps, D. M. Smith, D. I. Wellman. 2021. Using Population Dynamics to Model Harvest Regulation Impacts to Channel Catfish in the Monongahela River, West Virginia. North American Journal of Fisheries Management. 41:259-267.

Chiang, W. C., C. L. Sun, S. Z. Yehand, and W. C. Su. 2004. Age and growth of Sailfish (*Istiophorus platypterus*) in waters off eastern Taiwan. Fishery Bulletin 102:251-263.

Cohen J. 1988 Statistical power analysis for the behavioral sciences. 2nd edition. Mahwah, New Jersey: Lawrence Erlbaum Associates.

Davis, J. T., and L. E. Posey. 1958. Length at maturity of channel catfish in Louisiana. Proceedings of the Annual Conference Southeastern Association of Game and Fish Commissioners 12:72-75.

Gabelhouse, D. W. Jr. 1984. A lengthcategorization system to assess fish stocks. North American Journal of Fisheries Management 4:273-285

García-Berthou, E. 2001. Size- and depth-dependent variation in habitat and diet of the Common Carp (*Cyprinus carpio*). Aquatic Sciences 63:466-76.

Graham, K. 1999. A review of the biology and management of Blue Catfish. pp. 37-49 in E. R. Irwin, W. A. Hubert, C. F. Rabeni, H. L. Schramm Jr., and T. Coon, editors. Catfish 2000: Proceedings of the International Ictalurid Symposium. American Fisheries Society, Bethesda, Maryland.

Griffin, A. D., J. B. Bartnicki, D. L. Zentner, and R. A. Snow. 2022. An Investigation into the Effects of Elevated Water Hardness on Channel Catfish Egg Viability. Proc. Okla. Acad. Sci. 102: pp 29 – 38

Hoff, G. R., D. J. Logen, and M. F. Douglas. 1997. Otolith morphology and increment validation in young Lost River and Shortnose Suckers. Transactions of the American Fisheries Society 126:488-494.

Hubert, W. A. 1999. Biology and management of Channel Catfish. pp. 37-49 in E. R. Irwin, W. A. Hubert, C. F. Rabeni, H. L. Schramm Jr., and T. Coon, editors. Catfish 2000: Proceedings of the International Ictalurid Symposium. American Fisheries Society, Bethesda, Maryland.

Hubert, W. A., and M. C. Fabrizio. 2007. Relative abundance and catch per unit effort. pp. 279-326 in C. S. Guy, and M. L. Brown, editors. Analysis and Interpretation of Freshwater Fisheries Data. American Fisheries Society, Bethesda, Maryland.

Hubert, W. A., K. L. Pope, and J. M. Dettmers. 2012. Passive capture techniques. pp. 223-265 in A. V. Zale, D. L. Parrish, and T. M. Sutton, editors. Fisheries Techniques: 3rd edition. American Fisheries Society, Bethesda, Maryland.

Kloskowski, J. 2011. Differential effects of age-structured Common Carp (*Cyprinus carpio*) stocks on pond invertebrate communities: implications for recreational and wildlife use of farm ponds. Aquaculture International 19:1151-1164.

Kolmogorov, A. N. 1933. Sulla determinazione empirica di una legge di distribuzione. Giornale dell'Instituto Italiano degli Attuari 4:83–91.

Maceina, M. J. 1997. Simple application of using residuals from catch-curve regressions to assess year-class strength in fish. Fisheries Research 32:115-121.

Michaletz, P. H. 2001. Evaluation of Channel Catfish sampling methods in small impoundments. Missouri Department of Conservation, Federal Aid in Sport Fish Restoration, Project F-1-50, Study I-36, Job 1, Final Report, Jefferson City

Michaletz, P. H. 2009. Variable responses of Channel Catfish populations to stocking rate: Density-dependent and lake productivity effects. North American Journal of Fisheries Management 29:177-188.

Michaletz, P. H., and K. P. Sullivan. 2002. Sampling Channel Catfish with tandem hoop nets in small impoundments. North American Journal of Fisheries Management 22:870-878.

Miranda, L. E., and P. W. Bettoli. 2007. Mortality pp. 229-277 in C. S. Guy, and M. L. Brown, editors. Analysis and Interpretation of Freshwater Fisheries Data. American Fisheries Society, Bethesda, Maryland.

Montague, G. F., R. A. Snow, and A. Whiles. 2022. Population Characteristics of Channel Catfish in Meeker Reservoir, Oklahoma, a Small Impoundment. Proc. Okla. Acad. Sci. 102: pp 19 – 28.

Myers, R. A., J. K. Baum, T. D. Shepherd, S. P. Powers, and C. H. Peterson. 2007. Cascading effects of the loss of apex predatory sharks from a coastal ocean. *Science* **315**: 1846–1850.

Neumann, R. M., C. S. Guy, and D. W. Willis. (2012). Length, weight, and associated indices. Pp. 637-676 in A. V. Zale, D. L. Parrish, and T. M. Sutton, editors. Fisheries Techniques: 3rd edition. American Fisheries Society, Bethesda, Maryland.

Ogle, D. H., J. C. Doll, P. Wheeler, and A. Dinno. 2023. FSA: Simple Fisheries Stock Assessment Methods. R package version 0.9.5 https://fishr-core-team.github.io/FSA/.

Oklahoma Fisheries Analysis Application (OFAA). 2022. Version 2.0. Oklahoma Department of Wildlife Conservation.

Oklahoma Water Resources Board (OWRB). 2023. Beneficial Use Monitoring Program. https://www.oklahoma.gov/owrb/science-and-research/beneficial-use-monitoring-program.html.

Page, K. S., R. D. Zweifel, G. Carter, N. Radabaugh, M. Wilkerson, M. Wolfe, M. Greenlee, K. Kipp. 2012. Do Anglers Know What They Catch? Identification Accuracy and Its Effect on Angler Survey-Derived Catch Estimates. North American Journal of Fisheries Management. 32:1080-1089.

Pastore, M. and A. Calcagni. 2019. Measuring distribution similarities between samples: a distribution-free overlapping index. Frontiers in Psychology 10. https://www.frontiersin.org/articles/10.3389/fpsyg.2019.01089/full.

Perry Jr., W. G., and D. C. Carver. 1972. Length at maturity and total length-collarbone length conversions for Channel Catfish, *Ictalurus punctatus*, and Blue Catfish, *Ictalurus furcatus*, collected from the marshes of southwest Louisiana. Proceedings of the Annual Conference Southeastern Association of Game and Fish Commissioners 26:541-553.

Quist, M. C., M. A. Pegg, and D. R. DeVries. 2012. Age and Growth. pp. 677- 731 in A. V. Zale, D. L. Parrish, and T. M. Sutton, editors. Fisheries Techniques: 3rd edition. American Fisheries Society, Bethesda, Maryland.

Richards, F. J. 1959. A flexible growth function for empirical use. Journal of Experimental Botany 10:290-301.

Ricker, W. E. 1975. Computation and interpretation of biological statistics in fish populations. Fisheries Research Board of Canada, Bulletin 191.

Schall, B. J., and D. O. Lucchesi. 2020. Population dynamics and simulated effects of length-based trophy regulations for Flathead and Channel Catfish in the Lower James River, South Dakota. North American Journal of Fisheries Management 41:S277-S292.

Shoup, D. E., S. P. Callahan, D. H. Wahl, and C. L. Pierce. 2007. Size specific growth of Bluegill, Largemouth Bass, and Channel Catfish in relation to prey availability and limnological variables. Journal of Fish Biology 70:21-34.

Shoup, D. E., and R. G. Ryswyk. 2016. Length selectivity and size-bias correction for the North American standard gill net. North American Journal of Fisheries Management 36:485-496.

Shrader, T. M., B. Moody, and M. Buckman. 2003. Population dynamics of Channel Catfish in Brownlee Reservoir and the Snake River, Oregon. North American Journal of Fisheries Management 23:822-834.

Slipke, J. W., A. D. Martin, J. Pitlo Jr., and M. J. Maceina. 2002. Use of the spawning potential ratio for the upper Mississippi River Channel Catfish fishery. North American Journal of Fisheries Management22:1295–1300.

Smirnov NV. 1939. Estimate of derivation between empirical distribution function in two independent samples. Bulletin of Moscow University 2:3–16

Waters, M. J., R. A. Snow, and M. J. Porta. 2020a. Population dynamics of a stunted Blue Catfish population in a small Oklahoma impoundment. Proceedings of the Oklahoma Academy of Science 100:38-50.

Waters, M. J., R. A. Snow, and M. J. Porta. 2020b. Comparison of browned and standard otolith preparation methods for estimating age of catfish in Oklahoma. Journal of the Southeastern Association of Fish and Wildlife Agencies 7:64-71.

Woods, A. J., J. M. Omernick, D. R. Butler, J. G. Ford, J. E. Henley, B. W. Hoagland, D. S. Arndt, and B. C. Moran. 2005. Ecoregions of Oklahoma (color poster with map, descriptive text, summary tables, and photographs): Reston, Virginia, U.S. Geological Survey (map scale 1:1,250,000).

York, C. A. 2019. Oklahoma Department of Wildlife Conservation 2019 Oklahoma angler survey. Oklahoma Department of Wildlife Conservation, Oklahoma City, Oklahoma. Pages 14-15.

Submitted October 14, 2023 Accepted December 5, 2023

Illicit Fentanyl: A Perfect Storm in Science

Donna J. Nelson*
Department of Chemistry, University of Oklahoma, Norman, OK 73019

Abstract: Characteristics, uses, and impacts of illicit fentanyl upon society have combined to create a perfect storm in science. In recent years, fentanyl has been responsible for almost 210,000 poisonings in the US, with hundreds of people dying each day, and the number is rapidly growing. More research to understand better and to increase illicit fentanyl mitigation, such as naloxone and vaccination, is needed. Confidence in literature data and results is necessary in order to inspire scientists to enter a field, but fentanyl has displayed anomalies in its chemical behavior and has experienced anomalies in its data compilation and analysis, which has made it confusing and daunting.

Introduction

An increasing number of news reports of U.S. illicit fentanyl poisonings reveals our growing opioid crisis. Almost 210,000 people died from illicit fentanyl in the years 2015 – 2021.[1] In six states, illicit fentanyl fatalities recently increased by almost a factor of 5 in only 2 years.[1] Fentanyl is the leading cause of death for U. S. adults aged 18–45.[1,2] Synthetic opioid (fentanyl) fatalities among children are rising faster than in any other age group, and these tripled in just two years.[1] More research to understand better and to increase illicit fentanyl mitigation, such as naloxone and vaccination,[3] is needed. Much effort has been expended to reduce illicit fentanyl deaths and incidences of addiction, but fentanyl has displayed anomalous behavior[4] and has been impacted by anomalous data compilation and analysis,[4-8] which have combined to impede progress. Thus, illicit fentanyl has become a "perfect storm" in science.

Results and Discussion

Anomalies have contributed to confusion, research delays, and thereby an increasing number of deaths. Using CDC reports [2], we determined death rates for years 1999 through 2022 due to fentanyl, as shown in Figure 1 below. The displayed surge in death rates starting in 2013 reveals how the fentanyl data caught the US scientists, politicians, and public off guard. The death numbers increase from less than 3000 in 2013 up to about 73,000 in 2022.

Furthermore, we disaggregated the CDC fentanyl deaths for years 2015 through 2021 by race and gender, as shown in Figure 2 below. These data reveal that black males constitute the demographic group which is most impacted by fentanyl.

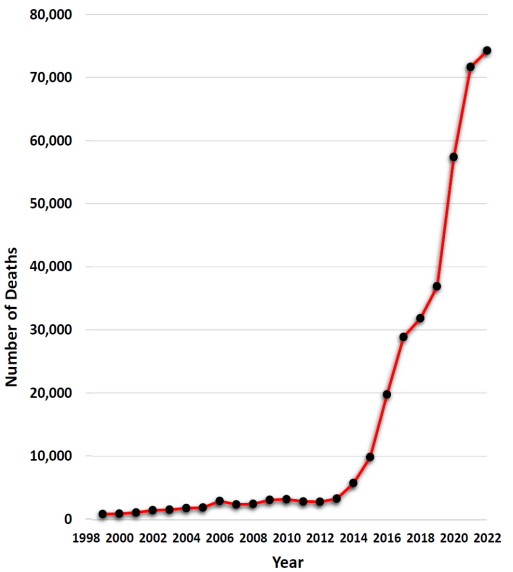

Figure 1. Number of deaths per year for years 1999 through 2022.

***Corresponding author: djnelson@ou.edu**

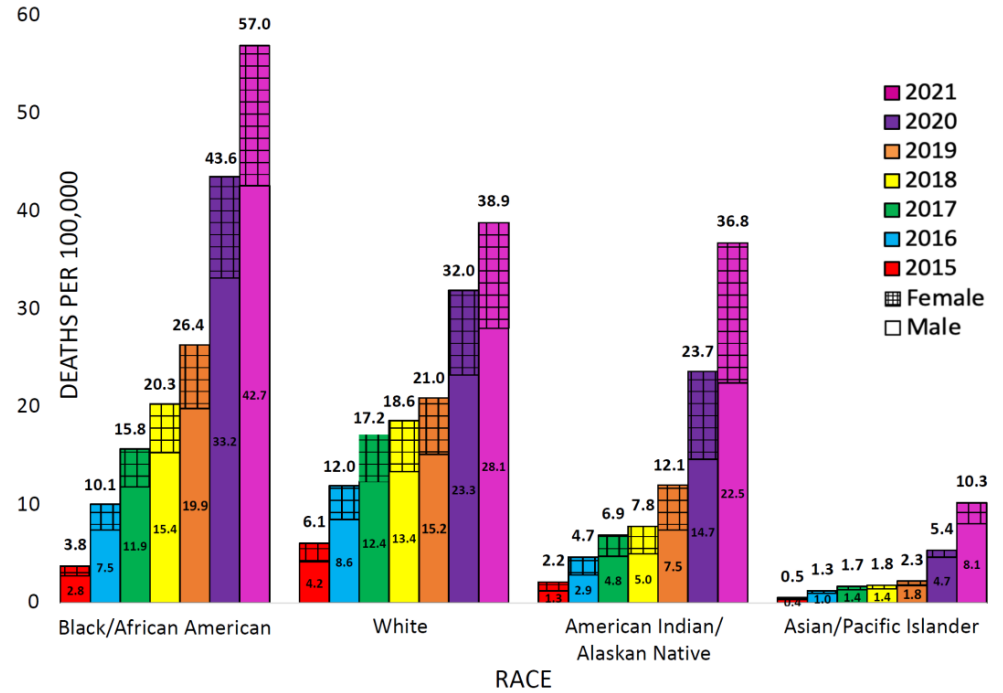

Figure 2. Fentanyl death rates for years 2015 through 2021, disaggregated by race and gender.

Accomplishing the work needed to reduce deaths will require talents from multiple scientific disciplines, and the corresponding scientists being inspired to make the effort. However, scientists appreciate order and are uncomfortable with confusion. Solid reliable research can't be built upon anomalies.

Fentanyl displays anomalous chemical behavior,[4] and some fentanyl data were handled in anomalous ways [4-8]. Anomalies in fentanyl data compilation and analysis were caused by researchers, so these can be clarified and resolved. Anomalies in fentanyl reactivity can't be eliminated, but we can recognize and understand them, so we must accommodate and work around the anomalies when possible. Some examples of anomalous chemical behaviors of fentanyl and poor data compilation and analysis are listed and categorized below. Both types of anomalies, in addition to social challenges faced by people taking illicit fentanyl, and involvement by forces from other countries have combined to create a wicked problem, multi-faceted, difficult to analyze, and unattractive due to anomalies and sheer size – a perfect storm in science. Currently, research on fentanyl has many anomalies; some examples are listed below.

Anomalies in fentanyl chemical behavior

Some specific anomalous chemical behaviors of fentanyl: (a) Research literature gives many different ratios of fentanyl versus morphine relative potencies, with ratios ranging at least as widely as 0.6 to 165.[4] The potency ratios of fentanyl and morphine versus other fentalogs, also vary considerably, with wide-ranging relative potency values. (b) Several unexpected properties of fentanyl were reported recently, [4] such as (i) increased ability to interact within the active site due to its conformational flexibility, (ii) access to the active site through the lipophilic pathway, and (iii) reduced sensitivity to reversal by naloxone compared to other opioids.

Anomalies in data compilation and analysis

Uncertainty in fentanyl data can also be caused by inappropriate data compilation and analysis.

In some cases, data selected for inclusion in reports or review articles weren't obtained under similar reaction or collection conditions and could not give accurate comparisons.[4,6] For example, a very important international publication,[5] intended to inform researchers globally, tabulated and compared many relative potencies for fentanyl, morphine, and other fentalogs obtained by assorted research groups using different reaction conditions.[6,8] This unnecessarily introduced discrepancies, because potency values were available for almost all the fentalogs listed, having been originally determined by Janssen under identical conditions.[7]

Furthermore, these illogical comparisons among fentalog potencies were made, without considering (i) the ease of retrieving the cited data, (ii) the methodology for its generation, nor (iii) the information details sufficient to compare the data without obtaining the source document. Obtaining the original manuscript reporting these data is especially difficult in the following case.[5,6] Tracking the fentanyl:morphine ratio back through references [6] to the source [8] leads to a decades-old article, in an obscure journal, difficult to obtain, and written in Chinese, with no translation available. The methodology and reaction conditions had to be obtained by purchasing the article [8] through the National Library of Medicine and translating the text from Chinese. This revealed that the data were not obtained under identical conditions and are therefore not confidently comparable to the other data in the table.[5]

Moreover, it was not necessary to use data from this obscure article because data obtained under consistent conditions were readily available in Janssen's manuscripts.[7] Greater care for consistent methodology is warranted. Furthermore, unnecessarily using obscure data seems counter to the current goals for open access. More scientists may be attracted and inspired to research fentanyl and illicit fentanyl in the future, if its data are more consistent and easily available.

It is desirable to have accurate and comparable potencies of fentalogs, with a common reference point, requiring that the potency determinations are carried out under the same conditions and methodology. This provides a knowledge base with a strong foundation.

Social influences and challenges to resolve; activities to build upon

Social aspects of illicit fentanyl must be considered also. Fentanyl is very high potency, so only a small amount laced into other street drugs is necessary to produce a dangerous high. If too much fentanyl is added to the street drug, or if the user takes too much, the user dies; each street drug user unwittingly plays Russian roulette. Thus, hundreds of people are poisoned in the U.S. each year. Solutions, clarifications, and consistency are urgently needed for illicit fentanyl, because stakes are high, and measured in terms of human lives. Time is also a factor, because the death rate is rising.[1,2]

One social challenge, which may be more symbolic than substantive is that fentanyl is frequently mispronounced as fentanol, especially by news people and those in government. [9] Some attempts to mitigate damages have been tried, but more are needed. For example, hanging fentanyl information posters for students in middle schools and high schools [10] didn't slow the increasing annual death rate. Recently another vaccine against effects of fentanyl was discovered, and more such research and development are necessary.[3] The SHIFT program [11] at The University of Texas at Austin draws on students to inform other students about the dangers of illicit fentanyl, in order to SHIFT the campus culture. All of these are helpful, but it seems that scientific research is not satisfying the public's thirst for progress on illicit fentanyl. Currently, the best approach to reach students seems to be peer-to-peer communication, such as is used in the SHIFT program.

Government influences and activities

Recent activities motivated the U.S. government to act regarding illicit fentanyl. For example, on Sep 14, 2022, eighteen U.S. State Attorneys General petitioned President Biden to declare it a Weapon of Mass Destruction.

[12] On Feb 15, 2023, there was a U.S. Senate hearing on illicit fentanyl coming into the U.S. from Mexico.[13] This confirmed that illegal fentanyl use in the U.S is encouraged and facilitated in part by some forces outside the U.S.; much illicit fentanyl comes from Mexico, where it is synthesized using precursors from China.[13] Recently, a congressional briefing made a case for declaring illicit fentanyl a weapon of mass destruction.[14]

Conclusions

This brief list of activities surrounding illicit fentanyl suggests a need for more research and more research support in this area. We must build a community, in order to work together widely on many fronts and track the status of fentanyl and its influences and consequences. Hopefully, the U.S. trend can be reversed from an annually increasing number of deaths caused by illegal fentanyl, to a declining number.

References

1. Families Against Fentanyl. *Fentanyl by the Numbers*. https://www.familiesagainstfentanyl.org/research/ (2022).
2. CDC - National Center for Health Statistics. *Drug Overdose Deaths 2021*. https://www. cdc.gov/nchs/pressroom/nchs_press_releases/2021/20211117.htm (2021).
3. A. Stone et al., Fentanyl conjugate vaccine by injected or mucosal delivery with dmLT or LTA1 adjuvants implicates IgA in protection from drug challenge. *npj Vaccines* **69**, 1-11 (2021).
4. E. Kelly et al., The anomalous pharmacology of fentanyl. *Br. Pharmacol.* **2021**, 1-16 (2021).
5. Recommended methods for the identification and analysis of fentanyl and its analogues in biological specimens. United Nations Office on Drugs and Crime. Page 19. United Nations, Vienna (2017).
6. I. Ujváry et al., Acryloylfentanyl, a recently emerged new psychoactive substance: a comprehensive review. *Forensic Toxicology*. **35**, 232–243 (2017).
7. W. Van Bever, C. Niemegeers, K. Schellekens, P. Janssen. *N*-4-substituted 1-(2-arylethyl)-4-piperidinyl-*N*-phenylpropanamides, a novel series of extremely potent analgesics with unusually high safety margin. *Arzneimittel-Forschung*, **26**, 1548–51 (1976), and references therein.
8. Y. Zhu et al., Studies on potent analgesics. I. Synthesis and analgesic activity of derivatives of fentanyl. Yaoxue Xuebao [Acta Pharmaceutica Sinica] **16**, 199-210 (1981).
9. President Joseph R. Biden, State of the Union Address, Washington, DC. (Feb 7, 2023). https://www.whitehouse.gov/state-of-the-union-2023/
10. Personal communication. Dr. Cato T. Laurencin, University of Connecticut. (Nov 4, 2022).
11. SHIFT the Campus Culture. The SHIFT Office, The University of Texas at Austin. Austin, TX. Accessed Feb 15, 2023. https://shift.utexas.edu/get-involved.html
12. A. Moody et al., 18 States Urge President Biden to Declare Fentanyl a Weapon of Mass Destruction. (Sep 14, 2022). https://www.scribd.com/document/594753242/9-15-Multistate-WMD-Letter-to-President-Biden#
13. Foreign Relations Committee, Full Committee Hearing. Countering Illicit Fentanyl Trafficking. (February 15, 2023). https://www.foreign.senate.gov/hearings/countering-illicit-fentanyl-trafficking
14. Congressional Briefing, The Case for Classifying Illicit Fentanyl as a Weapon of Mass Destruction. (Feb 27, 2022). https://drive.google.com/file/d/13TTe51EhhWBSfjGEtviJb--ISsxNDq9k/view

Submitted April 10, 2023 Accepted October 30, 2023

High-Symmetry Low-Coordinate Complexes of Cerium(III) and Uranium(III): Tris[bis(trimethylsilyl)amido] Phosphine Oxide Compounds for Empirical *f*-Element Electronic Structure Investigations

Stewart B. Younger-Mertz
Department of Chemistry, University of Oklahoma, Norman, OK 73019

Donna J. Nelson
Department of Chemistry, University of Oklahoma, Norman, OK 73019

Abstract: This work reports the synthesis and characterization of trivalent four-coordinate tris(silylamide) phosphine oxide complexes of Uranium and Cerium with approximate C_3 symmetry. The pseudo-C_3 symmetric four-coordinate tris[bis(trimethylsilyl)amido] triphenylphosphine oxide framework has only been reported for La, Sm, Eu, Er, Lu, Y, and U. Only the Lanthanum and Uranium derivatives have been characterized by X-ray crystallography, and ^{31}P NMR spectra have only been reported for the diamagnetic derivatives (La and Y). To our knowledge, f-element tris(silylamido) phosphine oxide complexes with substituted-aryl phosphine oxide ligands have not been characterized via XRD or NMR. Substituted aryl-derivatives exhibit different reactivities and spectroscopic properties than the simple triphenylphosphine oxide framework, because the relative electron densities on the phosphorus and oxygen atoms are highly influenced by the electronic character of the organic substituents bound to the phosphorus. The nature of the organic substituents on phosphorus therefore highly influences the nature of the metal-oxygen bond in phosphine oxide coordination complexes. These axially symmetric four-coordinate silylamide phosphine oxide complexes are suitable models for studying the relative differences in Ln/An metal-ligand covalency using ^{31}P-NMR spectroscopy and X-ray emission spectroscopy. Expanding this structural framework to other Lanthanide and Actinide metals, and fully characterizing a series of pseudoisostructural complexes featuring various organic substituents on the phosphine oxide (beyond triphenylphosphine oxide), would provide considerable insight concerning phosphine oxide bonding interactions with f-block metals. In addition to being convenient ligands for spectroscopic studies of f-element electronic structure, phosphine oxides (and the details of their interactions with f-block metals) are directly relevant to the nuclear fuel cycle. The fundamental nature of f-block metal phosphine oxide bonds is not well understood, and deeper empirical insight into the nature of these interactions is needed in order to facilitate large-scale computational screening of potential extractants for trivalent Ln/An separations. Herein we report the synthesis, X-ray crystallography, and paramagnetic NMR spectroscopy of a series of trivalent Cerium and Uranium tris(silylamido) phosphine oxide complexes, as well as the X-ray and gamma emission spectra for $Ce[N(SiMe_3)_2]_3[OPPh_3]$. It was observed in this work that phosphine oxide coordination to the metal center increases the length of the metal-amide bond, which could perhaps explain the enhanced protonolysis reactivity with $HPPh_2$ that was observed decades ago for lanthanide tris(silylamide) phosphine oxide complexes, compared to their corresponding three-coordinate $Ln[N(SiMe_3)_2]_3$ analogues.

***Corresponding author: djnelson@ou.edu**

Introduction

This work reports the synthesis and characterization of trivalent four-coordinate tris(silylamide) phosphine oxide complexes of uranium and cerium with approximate C_3 symmetry. Cerium and uranium, along with the rest of the lanthanide and actinide elements, are considered "hard" Lewis acids and have large ionic radii [1-9]. The coordination chemistry of these elements is dominated by high coordination numbers (typically CN=7 or greater) and they tend to form complexes with "hard" fluoride and oxygen-donor ligands. Coordination numbers less than 6 are extremely rare in *f*-block coordination chemistry, and they were not observed for lanthanides until the three-coordinate tris[bis(trimethylsilyl) amide] complexes were synthesized in the 1970's [10-13]. These volatile, low-coordinate complexes with bulky silyl-amide ligands have led to important advances in the field [14-18]. They have served as gateways to new uncharted areas of *f*-block coordination chemistry via the "silyl-amide protonolysis route" [15, 19-23]; for example, the tris[bis(trimethylsilyl)amides] of the lanthanides have been used to install anionic, "soft-donor" sulfido [20,21], selenido [21], tellurido [22], and phosphido [19] ligands via protonolysis. The volatility of lanthanide and actinide tris(silyl)amides makes them naturally attractive for metal-organic chemical vapor deposition (MOCVD) applications. The sulfido (thiolate) complexes have been used as precursors for the synthesis of high-purity lanthanide sulfide (Ln_2S_3) materials [2]. The tris-silylamides themselves can be used for the synthesis of lanthanide nitride (LnN) materials [15,24, 25], and uranium tris-amides can also be used to make uranium nitride (UN) [26], which has been attracting a lot of attention as a next generation nuclear fuel [26]. Nitride fuels have several advantages, such as high thermal conductivity, thermal stability, and fissile metal

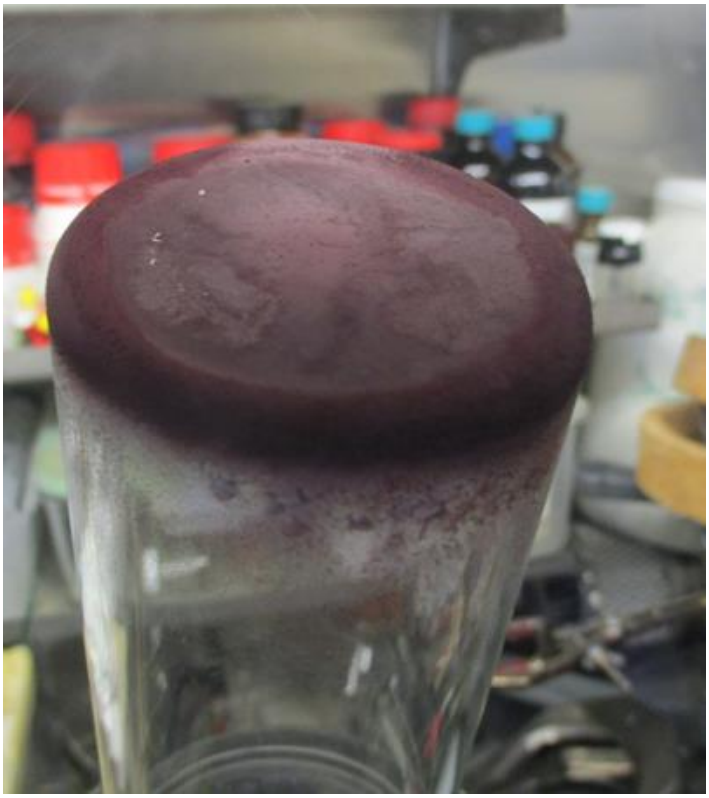

Figure 1: Sublimed $U[N(SiMe_3)_2]_3$

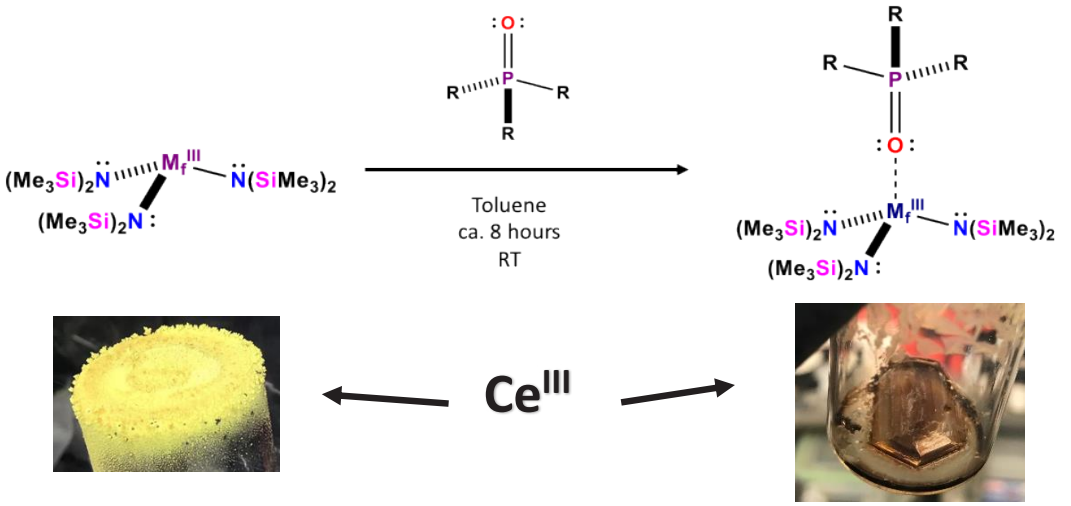

Scheme 1: General Synthesis of M_f^{III} $[OPR_3][N(SiMe_3)_2]_3$

density; however, the synthesis of high purity actinide nitrides has been proven very difficult using conventional carbothermic reduction methods from metal oxides [26]. Molecular actinide amide precursors provide a potential alternative for the synthesis of high purity actinide nitride fuels [26].

$Gd[N(SiMe_3)_2]_3$ and $Nd[N(SiMe_3)_2]_3$ have recently been used as single-source precursors for the synthesis of bimetallic MRI contrasts agents (Gd) [27] and efficient photoabsorbers (Nd) [28], respectively. $U[N(SiMe_3)_2]_3$ and $Er[N(SiMe_3)_2]_3$ exhibit slow magnetic relaxation and are single-ion magnets [29,30]. *f*-Element single-ion magnets, and their potential applications in quantum technologies, has been the subject of a few excellent review articles in recent years [30-33]. $Ce[N(SiMe_3)_2]_3$ (Figure 1a) has served as a gateway for the synthesis of four-coordinate Cerium(IV) halide complexes [34-38]. These new tetravalent Cerium halide compounds represent an important advance in Ce^{IV} chemistry [38] and provide a high-symmetry platform for investigating the uranium-like covalency that has recently been observed in Ce^{IV} metal-ligand bonding [8]. Tris(silyl)amides have also provided straightforward and reliable routes to low-coordinate tetravalent uranium [39,40] and plutonium [24,25] halide compounds, as well as tetravalent, pentavalent, and hexavalent uranium complexes with metal-ligand multiple bonds [33-38]. Indeed, it is an exciting time to be involved in *f*-element coordination chemistry.

Over the decades since $Ln[N(SiMe_3)_2]_3$ compounds were first synthesized, they have also been used to synthesize four-coordinate trivalent adducts with Lewis-bases, such as triphenylphosphine oxide [49-51]. The triphenylphosphine oxide adducts have exhibtied interesting reactivity. In a previous study, the four-coordinate triphenylphosphine oxide adducts showed enhanced protonolysis reactivity with diphenylphosphine ($HPPh_2$) compared to the base-free three-coordinate $Ln[N(SiMe_3)_2]_3$ compounds [19]. These protonolysis reactions resulted in the synthesis of lanthanum, europium, and yttrium phosphido complexes. Very few lanthanide complexes with anionic phosphorus-donor ligands have been reported in the literature [2,19,52,53]. This observed enhancement in reactivity has yet to be further explored since it was first reported decades ago, and it is worth revisiting and investigating further. The pseudo-C_3 symmetric four-coordinate tris[bis(trimethylsilyl)amido] triphenylphosphine oxide framework has only been reported for La [19], Sm [51], Eu [19], Er [50], Lu [19], Y [19], and U [39]. Only the lanthanum and uranium derivatives that have been characterized by X-ray crystallography

[19,39], and ^{31}P NMR spectra have only been reported for the diamagnetic derivatives (La and Y) [19]. To our knowledge, tris(silylamido) phosphine oxide complexes with *substituted-aryl* phosphine oxide ligands have not been characterized via XRD or NMR. Substituted aryl-derivatives exhibit different reactivities and spectroscopic properties than the simple triphenylphosphine oxide framework, because the relative electron density on the phosphorus and oxygen atoms is highly influenced by the electronic character of the organic substituents bound to the phosphorus. The nature of the organic substituents on phosphorus therefore highly influences the nature of the metal-oxygen bond in phosphine oxide coordination complexes.

These axially symmetric four-coordinate silyl-amide phosphine oxide complexes are suitable models for studying the relative differences in Ln/An metal-ligand covalency using ^{31}P-NMR spectroscopy and X-ray emission spectroscopy. Expanding this structural framework to other lanthanide and actinide metals, and fully characterizing a series of *pseudo*-isostructural complexes featuring various organic substituents on the phosphine

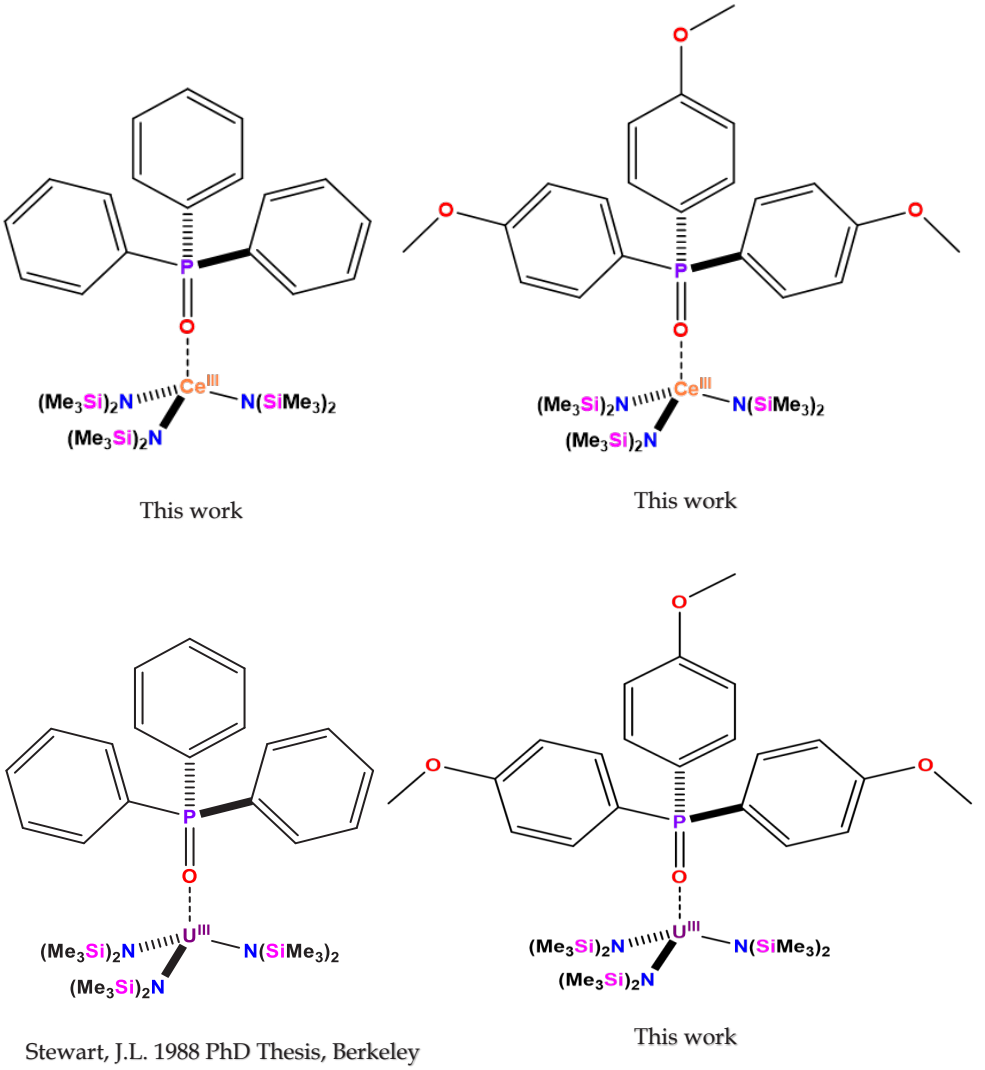

Figure 2: Structurally Characterized $M_f^{III}[OPAr_3][N(SiMe_3)_2]_3$ Compounds

oxide (beyond triphenylphosphine oxide), would provide considerable insight concerning phosphine oxide bonding interactions with *f*-block metals. In addition to being convenient ligands for spectroscopic studies of *f*-element electronic structure, phosphine oxides (and the details of their interactions with *f*-block metals) are directly relevant to the nuclear fuel cycle [54]. Phosphine oxides have been used effectively for advanced trivalent lanthanide/actinide separations [54-56]. The fundamental nature of *f*-block metal-phosphine oxide bonds is not well understood [7,57,58,59], and deeper empirical insight into the nature of these interactions is needed in order to facilitate large-scale computational screening of potential extractants for trivalent Ln/An separations.

Herein we report the synthesis, X-ray crystallography, and paramagnetic NMR spectroscopy of a series of trivalent cerium and uranium tris(silylamido) phosphine oxide complexes, as well as the X-ray and gamma emission spectra for $Ce[N(SiMe_3)_2]_3[OPPh_3]$.

Experimental

All experimental operations were conducted with rigorous exclusion of air and moisture using Schlenk techniques, standard glove-box methods using a Vacuum Atmospheres glovebox with a recirculating dinitrogen atmosphere, and standard glove-bag methods using a Captair Pyramid disposable glove-box under Argon. Solvents were bought anhydrous or HPLC grade (pentane, hexane, toluene, acetonitrile, THF, diethyl ether) and further purified using a Vacuum Atmospheres Solvent Purifier System. 1,4-dioxane, THF, and diethyl ether were dried over sodium benzophenone ketyl, and degassed by three freeze-pump-thaw cycles prior to use. All solvents were stored under dinitrogen in a glove-box, and stored over 4 Å molecular sieves for at least 24 hours prior to use. Glassware was dried at 150°C before use. ^{1}H and ^{31}P NMR spectra were recorded using a Bruker 400 MHz spectrometer at 298 K. Deuterated benzene (Cambridge Isotopes) was stored over 4 Å molecular sieves for at least 24 hours prior to use. Elemental analysis was conducted using particle-induced X-ray emission spectrometry (PIXE) and particle-induced gamma-ray emission spectrometry (PIGE) using a 3 MeV proton beam generated by a 3MV Tandem Accelerator (National Electrostatics Corporation). X-rays were detected using two high-energy Bruker SDD detectors, and one low-energy Bruker SDD detector. Gamma-rays were detected using a liquid nitrogen-cooled high-purity germanium (HPGe) detector. The sample for elemental analysis was secured between two pieces of 8 μm Kapton film under nitrogen and brought out into the atmosphere for external ion beam analysis. Single crystal X-ray diffraction was conducted using a Bruker XRD instrument with a Mo-Kα X-ray source.

Oxide encrustations were removed from the uranium metal using concentrated nitric acid [60]. Once the turnings achieved a brilliant lustre, the nitric acid was decanted, and the turnings were rinsed with acetone and stored in a dinitrogen atmosphere glovebox. Iodine (sublimed) was used as purchased (Aldrich). $KN(SiMe_3)_2$ and $CeCl_3$ (anhydrous) was used as purchased (Aldrich). Phosphine oxides were synthesized from commercially obtained tertiary-arylphosphines (Aldrich) using literature methods [61, 62]. $UI_3(1,4\text{-dioxane})_{1.5}$ was prepared using literature methods [60]. $Ce[N(SiMe_3)_2]_3$ [63] and $U[N(SiMe_3)_2]_3$ [60] were synthesized using literature methods and sublimed prior to use.

Caution! *Depleted uranium (primary isotope ^{238}U) is a weak* α*-emitter (4.197 MeV) with a half-life of 4.47 x 10^9 years; manipulations and reactions should be carried out in monitored fume hoods or in an inert atmosphere drybox in a radiation laboratory equipped with* α- and β-*counting equipment*.

Synthesis of $Ce[OPPh_3][N(SiMe_3)_2]_3$

0.739 grams (1.19 mmol) of freshly sublimed $Ce[N(SiMe_3)_2]_3$ was dissolved in 10 mL of toluene, and added to a flask with 0.331 grams (1.19 mmol) of triphenylphosphine oxide, and stirred overnight at room temperature. The vibrant yellow color of the $Ce[N(SiMe_3)_2]_3$ slowly fades to transparent as the triphenylphosphine oxide

coordinates to the Cerium ion. The solvent was removed *in-vacuo*, and the residue was extracted with 20 mL of pentane, and filtered through a Celite-padded, medium porosity fritted-filter. The pentane was removed from the product *in vacuo*, and a beige-tan solid was afforded in 87% yield (0.928 grams). Large crystals were grown from a concentrated pentane solution with a minimal amount of toluene. The crystals initially submitted were twinned, and the product was recrystallized from a pentane/toluene solution to yield a large (ca. 0.5 g) crystal with smaller single crystals surrounding it. The smaller crystals were submitted for single crystal X-ray diffraction, and the crystal structure obtained confirmed that the compound was indeed the four-coordinate complex tris(silyl) amide phosphine oxide complex. The proton NMR for the complex features a large, broad, paramagnetically shifted $SiMe_3$ peak at -0.78 ppm, which is relatively more deshielded than the three-coordinate precursor (-3.3 ppm). Very broad aromatic NMR signals also show up at 6.4 ppm and 4.6 ppm, relatively more shielded compared to the free ligand. The observation of only two aromatic signals is consistent with the isostructural Yttrium complex [49]. Only one ^{31}P NMR resonance was observed at 54 ppm, significantly deshielded compared to the free ligand at 29 ppm. The large crystal was submitted for ion beam analysis, and the X-ray spectrum obtained via PIXE nearly confirms the correct stoichiometry of the complex. The relative Ce and Si concentrations were almost correct; however, the P concentrations were somewhat high, presumably due to the phosphine oxide crust that formed on the crystal over time. *Crystal Data*: $C_{36}H_{69}CeN_3OPSi_6$ (1-Ce), M = 899.57, triclinic, space group , a = 12.3341(10) Å, b = 12.3809(10) Å, c = 19.7051(17) Å, α = 100.0905(13)°, β = 93.0661(14)°, γ = 118.9017(12)°, U = 2560.0(4) Å^3, Z = 2, D_c = 1.167 g cm^{-3}, Mo-Kα radiation [λ = 0.71073 Å, μ(Mo-Kα) = 1.087 mm^{-1}]. *NMR Data* (C_6D_6): ^1H δ -0.78 ppm ($SiMe_3$ 54H), δ 6.4 ppm (aromatic 9H), δ 4.6 ppm (aromatic 6H); ^{31}P δ 53.57 ppm. *Elemental Analysis* (PIXE): Calculated Ce 15.58 P 3.44 Si 18.73; Found: Ce 15.58 P 6.48 Si 19.67.

Synthesis of Ce[OP(*p*-anisyl)$_3$][N(SiMe$_3$)$_2$]$_3$

0.021 grams (0.034 mmol) of freshly sublimed Ce[N(SiMe$_3$)$_2$]$_3$ was dissolved in 3 mL of toluene, and added to a flask with 0.012 grams (0.034 mmol) of tris(*p*-anisyl) phosphine oxide, and stirred overnight at room

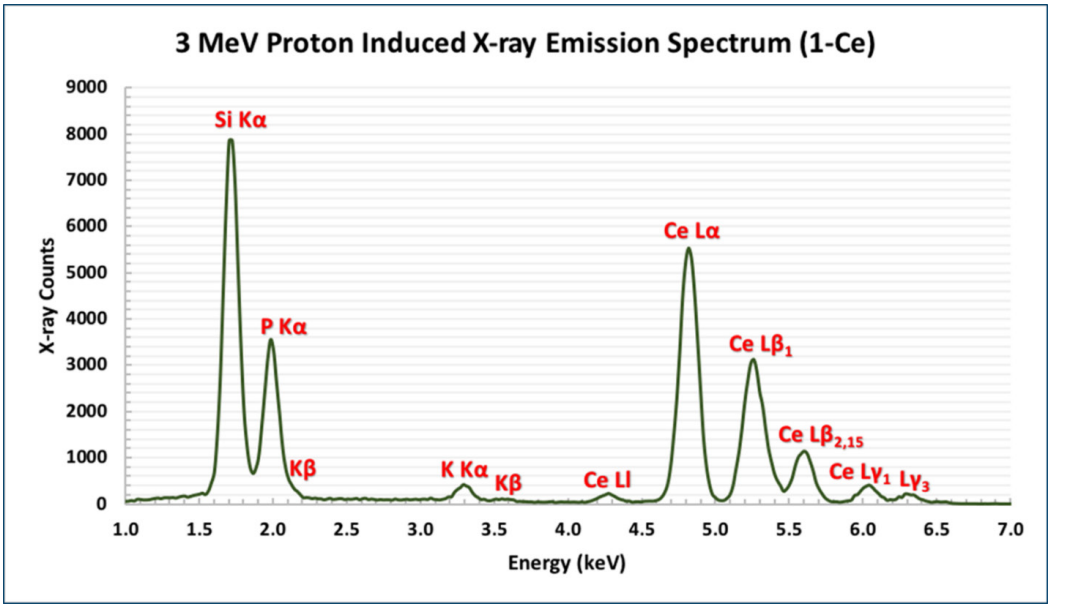

Figure 3: Energy-Dispersive X-ray Emission Spectrum for Ce[OPPh$_3$][N(SiMe$_3$)$_2$]$_3$

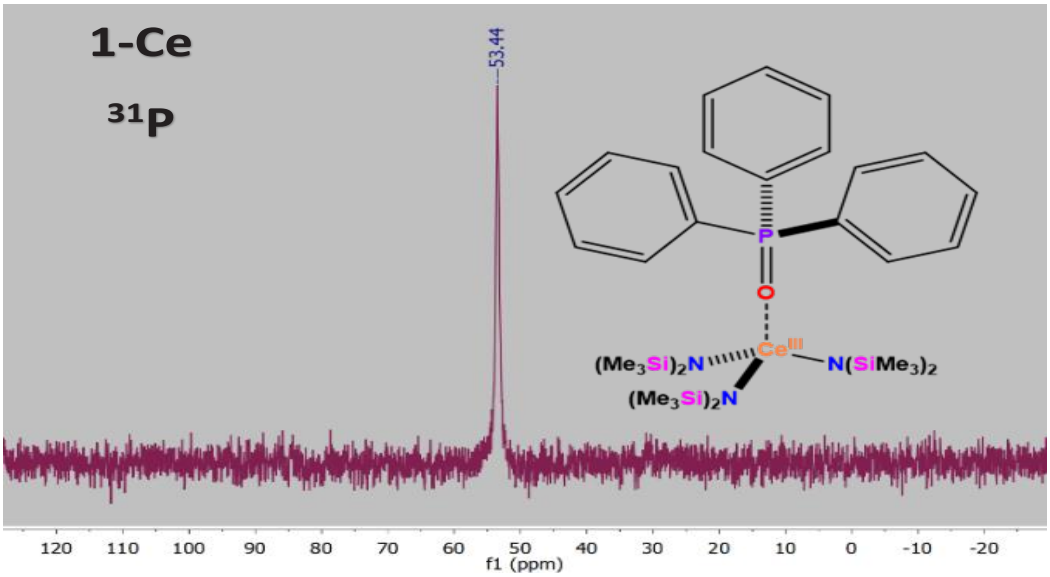

Figure 4: ^{31}P NMR Spectrum for Ce[OPPh$_3$][N(SiMe$_3$)$_2$]$_3$

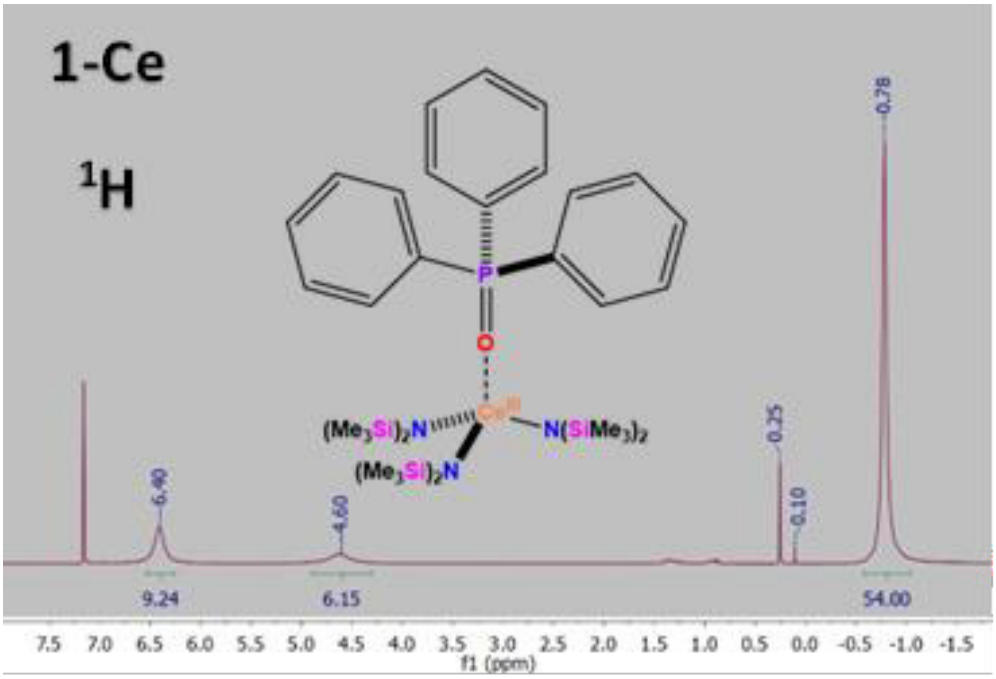

Figure 5: ^{1}H NMR Spectrum for Ce[OPPh$_3$][N(SiMe$_3$)$_2$]$_3$

temperature. The vibrant yellow color of the Ce[N(SiMe$_3$)$_2$]$_3$ slowly fades to transparent as the tris(*p*-anisyl)phosphine oxide coordinates to the cerium ion. The solvent was removed *in-vacuo*, and the residue was extracted with 10 mL of pentane, and filtered through a Celite-padded, medium porosity fritted-filter. The pentane was removed from the product *in vacuo*, and a colorless solid was afforded in ca. 100% yield (0.033 grams). Single crystals were grown from a concentrated pentane solution via slow evaporation at room temperature after a few

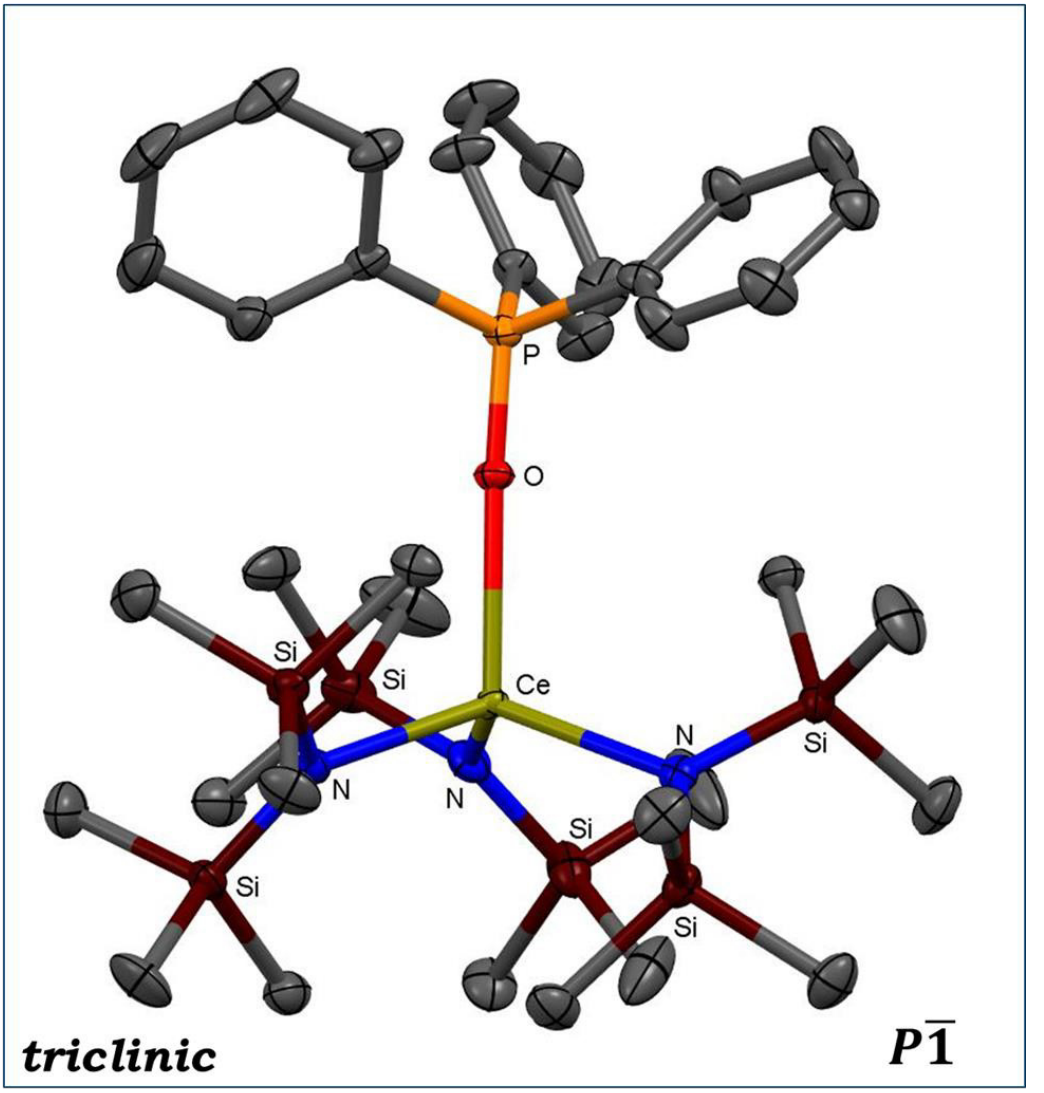

Figure 6: Single-Crystal XRD Structure for $Ce[OPPh_3][N(SiMe_3)_2]_3$

days and submitted for X-ray diffraction. *Crystal* Data: $C_{39}H_{75}CeN_3O_4PSi_6$ (2-Ce), M = 989.65, monoclinic, space group $P2_1/c$, a = 16.1035(9) Å, b = 13.8776(8) Å, c = 23.0565(13) Å, α = 90°, β = 91.9766(9)°, γ = 90°, U = 5149.6(5) Å^3, Z = 4, D_c = 1.276 g cm^{-3}, Mo-Kα radiation [λ = 0.71073 Å, μ(Mo-Kα) = 1.092 mm^{-1}]. *NMR Data* (C_6D_6): ^{1}H δ -0.77 ppm ($SiMe_3$ 54H), δ 6.14 ppm (aromatic 6H), δ 4.92 ppm (aromatic 6H), δ 2.98 ppm (OCH_3 9H); ^{31}P δ 54.39 ppm.

Synthesis of $U[OP(p\text{-anisyl})_3][N(SiMe_3)_2]_3$

0.719 grams (1.03 mmol) of freshly sublimed $U[N(SiMe_3)_2]_3$ was dissolved in 10 mL of toluene, and added to a flask with 0.379 grams (1.03 mmol) of tris(*p*-anisyl)phosphine oxide, and stirred overnight at room temperature. The reddish-purple color of the $U[N(SiMe_3)_2]_3$ appears to gradually change to a darker shade of purple very subtly as the tris(*p*-anisyl) phosphine oxide coordinates to the uranium ion. The solvent was removed *in-vacuo*, and the residue was extracted with 20 mL of pentane, and filtered through a Celite-padded, medium porosity fritted-filter. The pentane was removed from the product *in vacuo*, and a purple solid

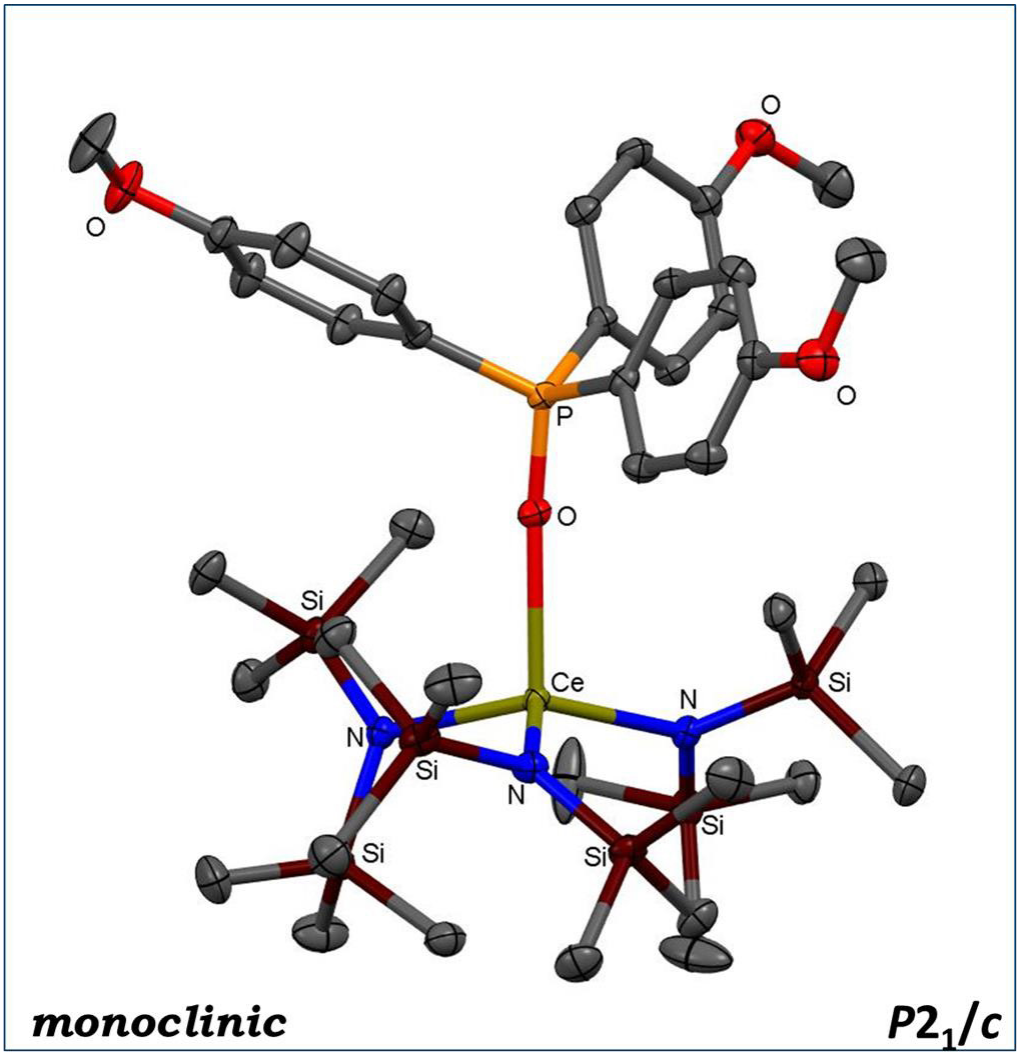

Figure 7: Single-Crystal XRD Structure for Ce[OP(*p*-anisyl)$_3$][N(SiMe$_3$)$_2$]$_3$

was afforded in 46% yield (0.519 grams).

Alternative procedure 0.051 grams (0.068 mmol) of $UI_3(1,4\text{-dioxane})_{1.5}$ was dissolved in 5 mL of THF. Three equivalents of $KN(SiMe_3)_2$ and a threefold excess of t tris(*p*-anisyl)phosphine oxide (with respect to uranium) was dissolved in 5 mL of THF, and added dropwise to the UI_3/THF solution while stirring at room temperature with slight evolution of fumes upon addition. The dark brown (almost black) solution was stirred overnight, and the solvent was removed *in vacuo*. The residue was extracted with toluene, and the potassium iodide salts were removed by filtering the extract through a Celite-padded medium porosity fritted filter. The solvent was removed *in vacuo* yielding a dark-brown/black solid, and the residue was extracted with *n*-pentane. The remaining salts and unidentified insoluble by-products were removed by filtering the purple *n*-pentane extract through a Celite-padded medium-porosity fritted filter. The solvent was removed *in vacuo*, affording a purple solid in ca 50% yield. Purple single-crystals of the complex were grown from a concentrated pentane solution via slow evaporation at -30°C after a few days and submitted for X-ray diffraction. *Crystal Data*: $C_{39}H_{75}N_3O_4PSi_6U$ (3-U), M = 1087.56, monoclinic, space group $P2_1/c$, a = 16.063(2) Å, b = 13.9300(19) Å, c

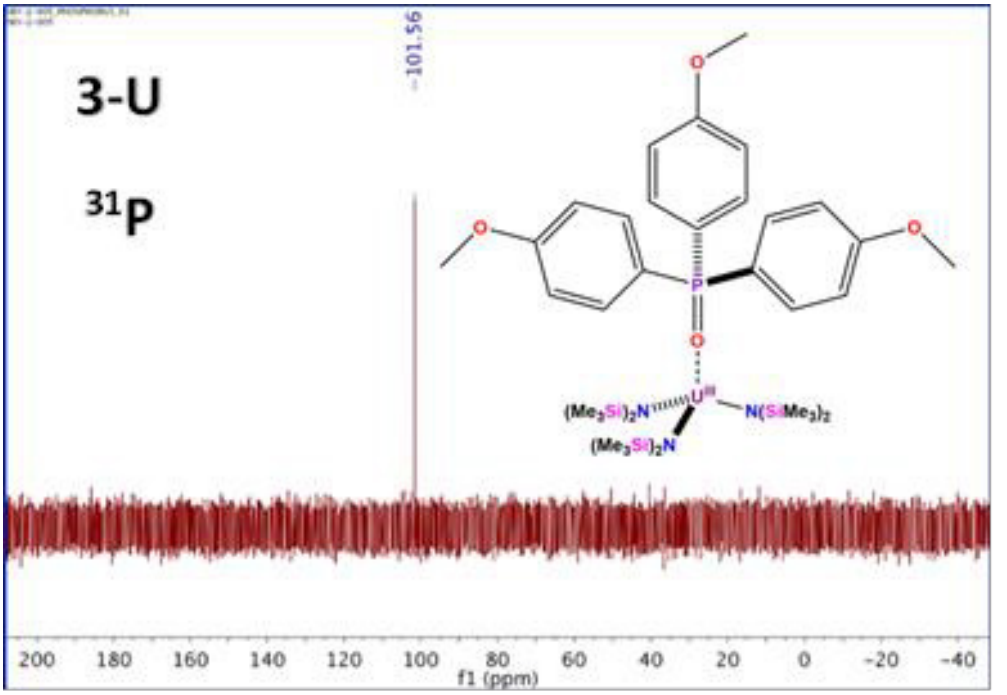

Figure 8: ^{31}P NMR Spectrum for U[OP(*p*-anisyl)$_3$][N(SiMe$_3$)$_2$]$_3$

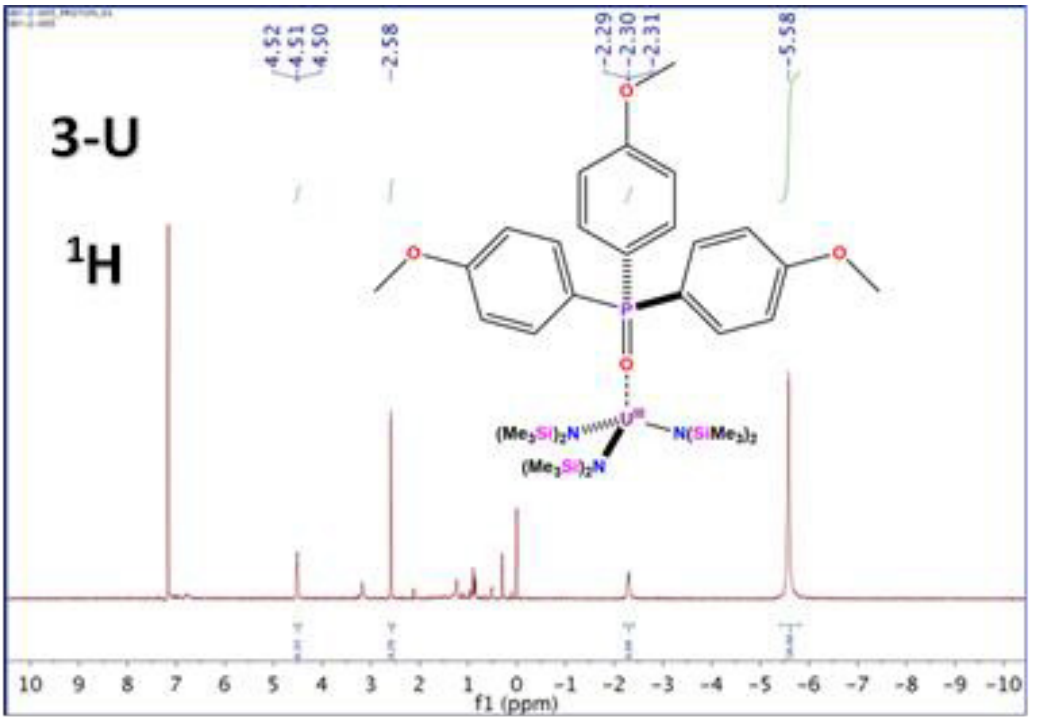

Figure 9: ^{1}H NMR Spectrum for U[OP(*p*-anisyl)$_3$][N(SiMe$_3$)$_2$]$_3$

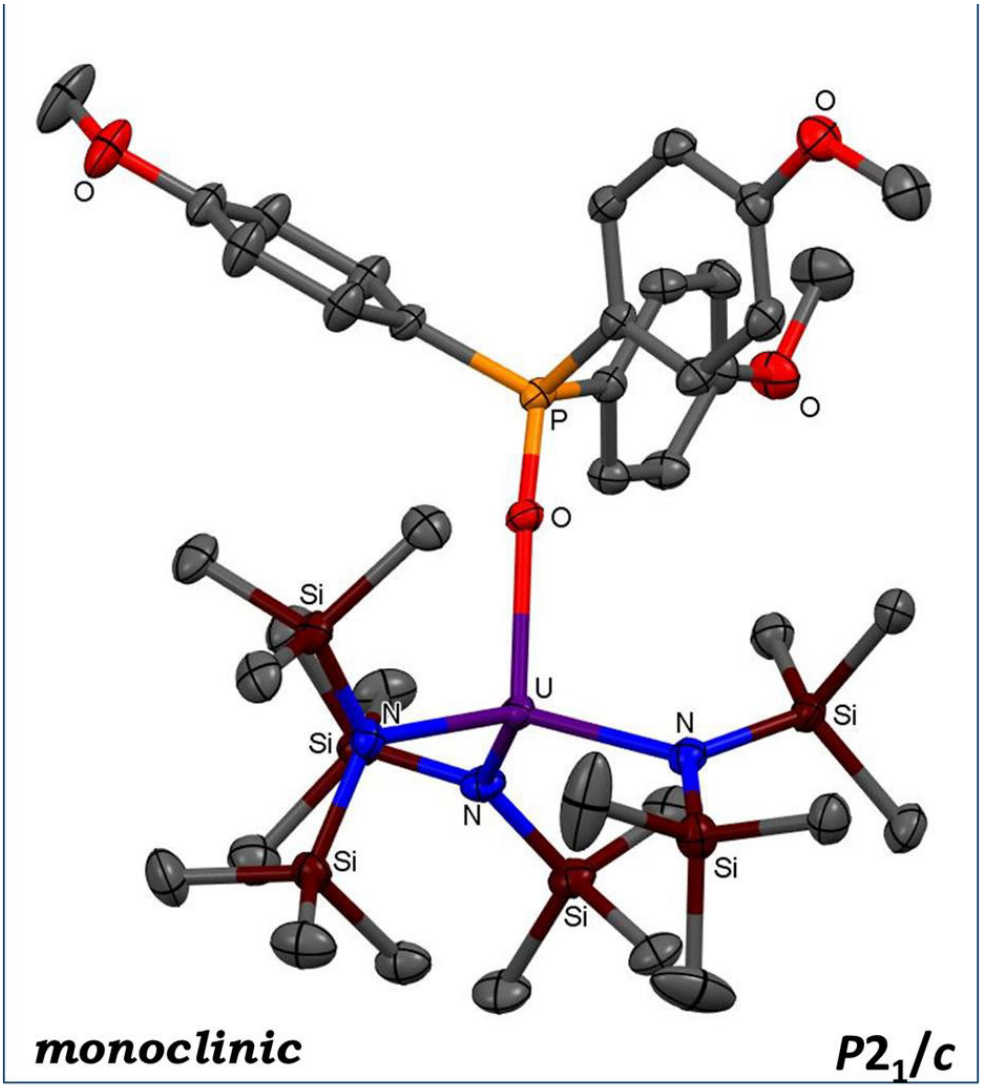

Figure 10: Single-Crystal XRD Structure for U[OP(*p*-anisyl)$_3$][N(SiMe$_3$)$_2$]$_3$

= 23.043(3) Å, α =90°, β = 91.895(2)°, γ = 90°, U = 5153.2(12) Å^3, Z = 4, D_c = 1.402 g cm^{-3}, Mo-Kα radiation [λ = 0.71073 Å, μ(Mo-Kα) = 3.357 mm^{-1}]. *NMR Data* (C_6D_6): ^{1}H δ -5.68 ppm (SiMe$_3$ 54H), δ 4.47 ppm (aromatic 6H), δ -2.51 ppm (aromatic 6H), δ 2.56 ppm (OCH$_3$ 9H); ^{31}P δ 102.6 ppm.

Synthesis of Ce[OP(*p*-tolyl$_3$][N(SiMe$_3$)$_2$]$_3$

0.009 grams (0.0148 mmol) of freshly sublimed Ce[N(SiMe$_3$)$_2$]$_3$ was dissolved in 3 mL of toluene, and added to a flask with 0.005 grams (0.0148 mmol) of tris(*p*-tolyl)phosphine oxide, and stirred overnight at room temperature. The vibrant yellow color of the Ce[N(SiMe$_3$)$_2$]$_3$ slowly fades to transparent as the tris(*p*-tolyl) phosphine oxide coordinates to the cerium ion. The solvent was removed *in-vacuo*, and the residue was extracted with 10 mL of pentane, and filtered through a Celite-padded, medium porosity fritted-filter. The pentane was removed from the product *in vacuo*, and a beige solid was afforded in 52 % yield (0.007 grams). *NMR Data* (C_6D_6): ^{1}H δ -0.74 ppm (SiMe$_3$ 54H), δ 5.45 ppm (aromatic 9H), δ 4.67 ppm (aromatic 6H); ^{31}P δ 54.55 ppm.

Table 1. Crystallographic Data for R_3P=O-Met-$[N(SiMe_3)_2]_3$

		bond length (Å)						bond angle (°)					
R	Met	Met-O	O-P	Met-N1	Met-N2	Met-N3	M-N_{avg}	Met-O=P	N1-Met-N2	N1-Met-N3	N2-Met-N3	N-Met-N_{avg}	ref
MeOPh	Ce	2.3952(12)	1.5161(12)	2.3612(14)	2.4000(14)	2.4065(14)	2.389	174.44(7)	107.37(5)	114.43(5)	121.53(5)	114.44	
Ph	Ce	2.403(2)	1.512(2)	2.357(2)	2.373(3)	2.388(2)	2.373	176.85(13)	108.83(9)	110.90(9)	116.96(9)	112.23	
MeOPh	U	2.376(3)	1.519(3)	2.344(4)	2.390(4)	2.398(4)	2.377	174.2(2)	108.55(14)	112.84(14)	120.88(14)	114.09	
Ph	U	2.382(2)	1.512(2)	2.343(4)	2.362(4)	2.367(3)	2.357	176.5(2)	109.8(1)	110.7(1)	115.6(1)	112.03	[26]
Ph	La	2.40(2)	1.52(2)	2.38(2)	2.40(3)	2.41(2)	2.397	174.6	109.2(9)	112.7(8)	116.4(6)	112.77	[49]

Table 2. Data for Ph_3P=O-Met-$[N(SiMe_3)_2]_3$ NMR data (ppm)

Met	^{31}P	^{1}H $SiMe_3$	^{1}H Aromatic	ref
U	105.19	-5.66	6.46-4.56	
Ce	53.57	-0.78	6.40, 4.63	
La	39	0.07	7.57	[49]
Y	38	0.3	6.8-7.9	[49]
Sm	N/A	N/A	N/A	[51]
Eu	N/A	-1.43	4.9	[49]
Er	N/A	N/A	N/A	[50]
Lu	N/A	0.1	7.5	[49]

Results and Discussion

Reactions of extremely air sensitive $Ce[N(SiMe_3)_2]_3$ (CeN^*_3) and $U[N(SiMe_3)_2]_3$ (UN^*_3) with one equivalent of aryl-phosphine oxide ligands in toluene at room temperature for several hours afforded $M[OPAr_3][N^*]_3$ compounds in moderate to excellent yields (46%-100%). Optimum yields were obtained for the *para*-methoxy substituted aryl-phosphine oxide derivative (quantitative), and in general, cerium derivatives were obtained in better yields than the uranium derivatives. $U[OP(p\text{-anisyl})_3][N(SiMe_3)_2]_3$ could also be obtained in one step from directly $UI_3(1,4\text{-dioxane})_{1.5}$, thereby circumventing the difficulties involved with obtaining impurity-free $U[N(SiMe_3)_2]_3$. The four-coordinate aryl-phosphine oxide adducts, unsurprisingly, are more air-stable and robust than their three-coordinate tris-amide precursors; however, the phosphine oxide adducts are still extremely air/moisture-sensitive, just less so than the extremely coordinatively unsaturated three-coordinate precursors. These aryl-phosphine oxide adducts are highly crystalline, and large single-crystals can be obtained via slow evaporation of *n*-pentane and/or toluene at room temperature or -30°C.

Single-crystal X-ray structures were obtained for $U[OP(p\text{-anisyl})_3][N(SiMe_3)_2]_3$, $Ce[OP(p\text{-anisyl})_3][N(SiMe_3)_2]_3$, and $Ce[OPPh_3][N(SiMe_3)_2]_3$, which facilitated useful comparisons with the two other structurally characterized tris(silyl)amido-triphenylphosphine oxide complexes reported in the literature, $La[OPPh_3][N(SiMe_3)_2]_3$ and $U[OPPh_3][N(SiMe_3)_2]_3$. These compounds also facilitated useful comparisons with the base-free tri-coordinate $M[N(SiMe_3)_2]_3$ complexes that have been structurally characterized [M = Ce [64], Pr [65], Nd [66], Sm [67], Eu [68], Tb [69], Dy [70], Er [70], Tm [71], Yb [72], Lu [73], Y [74], Sc [68], U [75], and Pu [76]). Additional comparisons can also be made with other *f*-element phosphine oxide complexes that have been structurally characterized [59]; however, to limit the scope of this discussion, attention will be focused on the extremely short list of monomeric four-coordinate tris[bis(trimethylsilyl)amido] Lewis-base adducts of the *f*-elements that have been structurally characterized. The three crystal structures obtained, along with the previously reported La and U derivatives, are *pseudo*-

isostructural, and feature nearly linear metal-oxygen-phosphorus bond angles (174-176°). Bond lengths and bond angles for this *pseudo*-isostructural series are given in Table 1. Table 4 gives the average metal-nitrogen bond lengths for the structurally characterized $M[N(SiMe_3)_2]_3$ derivatives for comparison.

The XRD data obtained in this work, in conjunction with previous XRD results, indicate that coordination of an aryl-phosphine oxide ligand to the tris(silyl)amido framework results in a subtle, but noticeable, lengthening of the metal-nitrogen bonds compared to the three-coordinate base-free analogues. The cerium-nitrogen bond in CeN^*_3 (2.320 Å) increases to 2.403 Å in $Ce[OPPh_3][N(SiMe_3)_2]_3$ and 2.395 Å in 2-Ce. The uranium-nitrogen bond in UN^*_3 (2.320 Å) increases to 2.382 Å in $U[OPPh_3][N(SiMe_3)_2]_3$ and 2.376 Å in 3-U. The metal-oxygen-phosphorus (M-O-P) bond angles are nearly linear in all the complexes. The M-O-P angles for the triphenylphosphine oxide complexes $Ce[OPPh_3][N(SiMe_3)_2]_3$ and $U[OPPh_3][N(SiMe_3)_2]_3$ are ca. 176°, and 174° for $Ce[OP(p\text{-anisyl})_3][N(SiMe_3)_2]_3$, $U[OP(p\text{-anisyl})_3][N(SiMe_3)_2]_3$, and $La[OPPh_3][N(SiMe_3)_2]_3$. The three triphenylphosphine oxide complexes have N-M-N angles of about 112° (average), and the angles for the substituted aryl derivatives are slightly larger, 114° (average). As a whole, the geometrical parameters are extremely similar for the five tris(silyl)amido-phosphine oxide complexes that have been structurally characterized by XRD in this work and previous work.

The data in Table 4 shows a gradual decrease in lanthanide-nitrogen bond distances across the 4*f* series from Ce-Yb as the relative ionic radius of the lanthanide ion decreases. The metal-nitrogen bond lengths in $Ce[N(SiMe_3)_2]_3$ and $U[N(SiMe_3)_2]_3$ are identical (2.320 Å), which is consistent with their nearly identical trivalent ionic radii. Since the ionic radii of La^{3+} (117.2 pm), Ce^{3+} (115 pm), and U^{3+} (116 pm) [2] are so similar, one might expect there to be little to no difference in the metal-oxygen bond lengths shown in Table 1. However, the uranium-oxygen bonds are measurably shorter than the cerium and lanthanum bonds. The differences in bond lengths are very subtle (only about 0.02 Å); however, this could be evidence of increased metal-ligand covalency in the uranium complexes compared to the cerium and lanthanum analogues, presumably due to slightly increased ligand 2*p* orbital mixing into 6*d* and 7*p* manifolds. However, very little can be said definitively about the orbital interactions involved based on this slight difference in bond length.

The bonding in these *f*-element amide complexes is largely ionic in character, and most

Table 3. Data for R_3P=O-Met-$[N(SiMe_3)_2]_3$ NMR data (ppm)

R	Met	^{31}P	^{1}H $SiMe_3$	^{1}H Aromatic	^{1}H Alkyl	ref
t-Bu	Ce	91.77	-1.17	-	-5.14	
MePh	Ce	54.55	-0.74	5.45, 4.67	1.56	
MeOPh	Ce	54.39	-0.77	6.14, 4.92	2.98	
Ph	Ce	53.57	-0.78	6.40, 4.63	-	
MePh	U	98.34	-5.53	6.25, 4.63	-7.22	
t-Bu	U	368.58	-3.16	-	-8.75	
MeOPh	U	102.6	-5.68	4.47, -2.51	2.56	
Ph_2(tolyl)	U	104.48	-5.52	6.85-4.51	-2.83	
Ph	U	105.19	-5.66	6.46-4.56	-	
Ph	La	39	0.07	7.57	-	[49]

Table 4. $M_f^{III}[N(SiMe_3)_2]_3$

$Ln^{III}[N(SiMe_3)_2]_3$	^1H NMR	ref	Ln-N Bond	ref
La	0.25	[10]		
Ce	-3.39	[63]	2.320(3)	[64]
Pr	-8.64	[10]	2.31(4)	[65]
Nd	-6.25	[63]	2.29(4)	[66]
Sm	-1.58	[10]	2.284(3)	[67]
Eu	6.43	[10]	2.259(9)	[68]
Gd	-11.07	[63]		
Tb			2.233(12)	[69]
Dy			2.212(2)	[70]
Ho				
Er	62.89	[63]	2.21(1)	[70]
Tm			2.198(9)	[71]
Yb			2.158(13)	[72]
Lu	0.1	[10]	2.168(12)	[73]
Y	0.28	[10]	2.224(6)	[74]
Sc			2.047(6)	[68]
$An^{III}[N(SiMe_3)_2]_3$				
U	-11	[14]	2.320(4)	[75]
Np	3.01	[14]		
Pu	0.74	[14]	2.315(10)	[76]

of the structural data can be rationalized in terms of the ionic radius of the central metal cation, and the steric properties of the ligand framework. However, the relative amount of metal-ligand covalency in lanthanide amide complexes appears to have been initially underestimated, with the assumption that the limited radial extent of the core-like 4*f* orbitals prevented nitrogen-metal π-interactions, leading to negligible metal-ligand covalency. Photoelectron studies seemed to confirm this assertion [77]. However, subsequent computational studies suggested that lanthanide amides have a considerable degree of covalent character. While affirming the conclusions of previous studies with respect to the non-involvement of the 4*f* electrons in chemical bonding, some computational results emphasize the importance of the 5*d* and 6*p* orbitals in lanthanide-nitrogen bonds [93]. Empirical structural and spectroscopic data for lanthanide amide and phosphine oxide complexes are scarce, and more isostructural complexes of the other members of the lanthanide series and actinide series need to be synthesized and characterized. Sophisticated computational and spectroscopic studies must also be conducted on these complexes before any real conclusions about the nature of the metal-ligand bonds in these complexes can be made. This work is a small step in that direction.

Paramagnetic ^1H and ^{31}P NMR spectra were obtained for $Ce[OP(p\text{-anisyl})_3][N(SiMe_3)_2]_3$, $Ce[OPPh_3][N(SiMe_3)_2]_3$, and $U[OP(p\text{-anisyl})_3][N(SiMe_3)_2]_3$, along with other substituted aryl- and alkyl-derivatives. Derivatives other than $Ce[OP(p\text{-anisyl})_3][N(SiMe_3)_2]_3$, $Ce[OPPh_3][N(SiMe_3)_2]_3$, and $U[OP(p\text{-anisyl})_3][N(SiMe_3)_2]_3$

have not yet been fully characterized or obtained in pure form; however, tentative assignments for additional aryl and alkyl derivatives could still be made for the paramagnetically shifted NMR resonances that were observed, so they are included here for comparison. Table 2 features the NMR data for $Ce[OPPh_3][N(SiMe_3)_2]_3$, as well as all the NMR data available in the literature for $M[OPPh_3][N(SiMe_3)_2]_3$complexes. Table 3 features the NMR data for $Ce[OP(p\text{-anisyl})_3][N(SiMe_3)_2]_3$, $Ce[OPPh_3][N(SiMe_3)_2]_3$, and $U[OP(p\text{-anisyl})_3][N(SiMe_3)_2]_3$, along with additional data for complexes that have not been fully characterized or obtained in pure form. Tables 2 and 3 also include NMR data for the previously reported $U[OPPh_3][N(SiMe_3)_2]_3$. No NMR data was previously reported for this complex, though its crystal structure was reported in Stewart's 1988 dissertation. Synthetic difficulties were encountered in this work while trying to reproduce the $U[OPPh_3][N(SiMe_3)_2]_3$ complex, similar to the difficulties Stewart reported in her 1988 dissertation. Presumably the instability of the complex is what prevented the NMR data from being acquired. Stewart reported that the purple solid complex decomposed to a brown microcrystalline solid after prolonged exposure to vacuum. In our hands, the characteristic purple color of the complex persisted for a short time while in an inert-atmosphere glove-box; however, by the time the compound was worked-up, isolated, and analyzed by NMR, the purple color had turned to brown, and complex NMR spectra were obtained that were difficult to assign. However, synthesis of $U[OPPh_3][N(SiMe_3)_2]_3$ directly from $UI_3(1,4\text{-dioxane})_{1.5}$ (described in the experimental section for the alternative synthesis $U[OP(p\text{-anisyl})_3][N(SiMe_3)_2]_3$), yielded NMR spectra that could be assigned with a relatively high degree of confidence. One of the more interesting results of this work is that the *para*-methoxy-substituted aryl-phosphine oxide complex, $U[OP(p\text{-anisyl})_3][N(SiMe_3)_2]_3$, seems to be more stable than $U[N(SiMe_3)_2]_3[OPPh_3]$. $U[OP(p\text{-anisyl})_3][N(SiMe_3)_2]_3$ repeatedly gave clear, easily assignable NMR spectra. The alternative route directly from $UI_3(1,4\text{-dioxane})_{1.5}$ gave cleaner, reproducible results for the synthesis of $U[OP(p\text{-anisyl})_3][N(SiMe_3)_2]_3$ and the other aryl- and alkyl-substituted phosphine oxide complexes shown in Table 3.

The NMR spectra obtained for $Ce[OP(p\text{-anisyl})_3][N(SiMe_3)_2]_3$, $Ce[OPPh_3][N(SiMe_3)_2]_3$, and $U[OP(p\text{-anisyl})_3][N(SiMe_3)_2]_3$, and other less characterized systems, exhibited large paramagnetic shifts in both the ^1H and ^{31}P NMR spectra. The paramagnetic shifts for the uranium complexes were much larger than the cerium complexes, which is consistent with the fact that uranium has more unpaired *f*-electrons with an f^3 configuration compared to cerium with an f^1 configuration. The pseudocontact contribution is the primary influence on the NMR spectra of *f*-elements [2,10,49,78,79], and the large shifts caused by the interactions between unpaired *f*-electrons and ligand nuclei in $Ce[OP(p\text{-anisyl})_3][N(SiMe_3)_2]_3$, $Ce[OPPh_3][N(SiMe_3)_2]_3$, and $U[OP(p\text{-anisyl})_3][N(SiMe_3)_2]_3$ are mainly dipolar in origin [2,80]. *f*-electrons are very localized and core-like, and do not tend to delocalize onto ligand atoms to a large extent. *f*-electron interactions with ligand nuclei are "through-space" interactions [2,80]. These "through-space" interactions require the *f*-metal ion to have an anisotropic distribution of *f*-electrons [81]. The following equation predicts the relative variation in dipolar shifts for the lanthanide series (assuming axial symmetry):

$$\delta^{pcs} = \frac{-\mu_0}{4\pi}\frac{g_J^2\mu_B^2 J(J+1)(2J-1)(2J+3)}{60(kT)^2}\frac{D_z(3cos^2\theta-1)}{r^3}$$

where

$$g_J = 1 + \frac{J(J+1) - L(L+1) + S(S+1)}{2J(J+1)}$$

Cerium(III) has a $^2F_{5/2}$ ground state [2,81]; therefore, the Landé factor (g_J) is equal to 6/7. Uranium(III) has a $^4I_{9/2}$ ground state [2,82], with a Landé factor (g_J) equal to 8/11. In some rare cases, when suitable delocalization mechanisms are involved, a small covalent contribution to metal-ligand bonding in *f*-element systems can occur. As a result, a "contact" shift can occur due to delocalization of unpaired *f*-electron density onto the ligand atoms [2,80,81]. The

mechanism of the spin density delocalization is due to weak covalent bonding involving the 6*s* orbital, which in turn can transfer unpaired spin density onto ligand nuclei via spin polarization from 4*f* orbitals [81].

NMR studies of $Ln[N(SiMe_3)_2]_3$ and $Ln[N(SiMe_3)_2]_3[OPPh_3]$ demonstrate the predominance of the pseudo-contact contribution to the paramagnetic shifts in this series [10,49]; however, some of the data suggest that a contact contribution is involved, and there is considerable evidence that lanthanide amides have significant contact contributions to their paramagnetic shifts [10,49]. Separating the pseudocontact and contact contributions for the shifts observed for $Ce[OP(p\text{-anisyl})_3][N(SiMe_3)_2]_3$, $Ce[OPPh_3][N(SiMe_3)_2]_3$, and $U[OP(p\text{-anisyl})_3][N(SiMe_3)_2]_3$ is beyond the scope of this discussion, and is the subject of future work using Density Functional Theory (DFT) and Quantum Theory of Atoms in Molecules (QTAIM). QTAIM has recently been used to analyze the paramagnetic NMR shifts of actinide complexes in order to estimate relative metal-ligand covalency via the QTAIM *delocalization index* [83].

The X-ray emission spectrum for $Ce[OPPh_3][N(SiMe_3)_2]_3$ (obtained using a low-energy SDD detector) is shown in Figure 4.3. The characteristic X-ray lines for cerium, phosphorus, and silicon are present, and concentrations obtained from the Ce Lα (4.84 keV), P Kα (2.015 keV), and Si Kα (1.739 keV) peaks are close to the predict values (Calculated: Ce 15.58 P 3.44 Si 18.73; Found: Ce 15.58 P 6.48 Si 19.67). The relative cerium/silicon ratio is almost correct, but the relative phosphorus concentration is a little high (presumably due to the formation of a phosphine oxide crust on the crystal and sample decomposition over time). Potassium is also present in trace amounts (6578 ppm, 0.65 wt. %) due to the presence of unremoved KCl or unreacted $K(SiMe_3)_2$. This result shows that multiple sublimations are indeed necessary to remove the potassium salts, as has been done by some researchers [77]. The cerium Kα peak was also observed at 34.717 keV in the high-energy X-ray emission spectrum with very low statistics.

In addition to the cerium $L\alpha_1$ X-ray emission, the $L\beta_1$, $L\beta_{2,15}$, $L\gamma_1$, Ll emissions were also observed (Figures 4.3 and 4.12). The 4.84 keV $L\alpha_1$ X-ray emission is a $M_5 \rightarrow L_3$, ($3d_{5/2} \rightarrow 2p_{3/2}$) electronic transition. The 4.3 keV Ll X-ray emission is a $M_1 \rightarrow L_3$ ($3s_{1/2} \rightarrow 2p_{3/2}$) electronic transition. The 5.262 keV $L\beta_1$ X-ray emission is a $M_4 \rightarrow L_2$ ($3d_{3/2} \rightarrow 2p_{1/2}$) electronic transition. The $L\beta_2$ and $L\beta_{15}$ X-ray emissions at ca. 5.7 keV are $N_5 \rightarrow L_3$ and $N_4 \rightarrow L_3$ ($4d_{5/2} \rightarrow 2p_{3/2}$ and $4d_{3/2} \rightarrow 2p_{3/2}$) electronic transitions, respectively. The

Table 5. ^{31}P NMR Chemical Shifts for $M[N(SiMe_3)_2]_3[OPR_3]$ NMR data (ppm)

f^n	M	R	$M[N(SiMe_3)_2]_3[OPR_3]$	$[OPR_3]$	Δδ	ref
f^1	Ce	*t*-Bu	91.77	41	50.77	
f^1	Ce	MePh	54.55	29.88	24.67	
f^1	Ce	MeOPh	54.39	29.3	25.09	
f^1	Ce	Ph	53.57	29.65	23.92	
f^3	U	*t*-Bu	368.58	41	327.6	
f^3	U	MePh	98.34	29.88	68.46	
f^3	U	MeOPh	102.6	29.3	73.3	
f^3	U	Ph_2(tolyl)	104.48	27.71	76.77	
f^3	U	Ph	105.19	29.65	75.54	
f^0	La	Ph	39	29.65	9.35	[49]

Table 6. ^{1}H NMR Chemical Shifts ($SiMe_3$-54H) NMR data (ppm)

f^n	M	R	$M[N(SiMe_3)_2]_3[OPR_3]$	Free $M[N(SiMe_3)_2]_3$	Δδ	ref
f^1	Ce	*t*-Bu	-1.17	-3.39	2.22	
f^1	Ce	MePh	-0.74	-3.39	2.65	
f^1	Ce	MeOPh	-0.77	-3.39	2.62	
f^1	Ce	Ph	-0.78	-3.39	2.61	
f^3	U	*t*-Bu	-3.16	-11	7.84	
f^3	U	MePh	-5.53	-11	5.47	
f^3	U	MeOPh	-5.68	-11	5.32	
f^3	U	Ph_2(tolyl)	-5.52	-11	5.48	
f^3	U	Ph	-5.66	-11	5.34	
f^0	La	Ph	0.7	0.25	-0.45	[10,49]
f^0	Y	Ph	0.3	0.28	-0.02	[10,49]
f^{14}	Lu	Ph	0.1	0.3	0.2	[10,49]
f^6	Eu	Ph	-1.43	6.43	-7.86	[10,49]

6.1 keV $L\gamma_1$ X-ray emission is a $N_4 \rightarrow L_2$ ($4d_{3/2} \rightarrow 2p_{1/2}$) electronic transition. The 6.33 keV $L\gamma_3$ X-ray emission is a $N_3 \rightarrow L_1$ ($4p_{3/2} \rightarrow 2s_{1/2}$) electronic transition. The 6.53 keV $L\gamma_4$ X-ray emission is a $O_3 \rightarrow L_1$ ($5p_{3/2} \rightarrow 2s_{1/2}$) electronic transition. A fair degree of fine structure can also be seen in the *L*γ emissions. TD-DFT calculations could potentially be used to analyze the fine structure observed. The *L* emission series of cerium is sensitive to the chemical state of the complex, especially the higher energy transitions. It has recently been shown that the *L* emission energies and intensity ratios in energy-dispersive X-ray emission spectra vary depending on the chemical environment of rare-earth cations [84,85]. Comparison of the *L* emissions for a variety of Ce^{III} and Ce^{IV} compounds should be the subject of future work.

In addition to the silicon and phosphorus Kα X-ray emissions peaks ($L_{2,3} \rightarrow K$ or $2p \rightarrow 1s$ transitions), the phosphorus Kβ emission was also observed (Figure 4.13), albeit with very low statistics. The phosphorus $K\beta_1$ X-ray emission is a $M_3 \rightarrow K$, or $3p_{3/2} \rightarrow 1s$, electronic transition. This transition is highly sensitive to the chemical environment of the phosphorus atom because it is a valence-to-core transition. However, high resolution wavelength-dispersive X-ray emission using a crystal monochromator is required in order to achieve high enough resolution to carry out phosphorus Kβ analysis. Recent studies have shown that small ion accelerators can be used to perform wavelength-dispersive phosphorus Kβ X-ray emission spectroscopy (WD-PIXE) [89]. These studies demonstrated that WD-PIXE yields results comparable to those obtained from advanced synchrotron light sources [89]. Phosphorus X-ray emission studies from other groups over the past several decades [86-89] have motivated us to use WD-PIXE for phosphorus Kβ analysis for a variety of lanthanide and actinide compounds with phosphorus-based ligands. The phosphorus Kβ X-ray emission from phosphine oxides and other phosphorus-based ligands has the potential to provide great insight into the nature *f*-metal-ligand bonding, especially when combined with results from phosphorus-31 NMR spectroscopy. This XES/NMR approach can facilitate the investigation of both *orbital-energy near-degeneracy driven covalency*, and *symmetry-restricted overlap driven covalency* in lanthanide and actinide coordination complexes. This should be the subject of future work. Such studies could potentially reveal periodic trends in metal-ligand orbital mixing for the *f*-block elements.

The proton-induced gamma emission spectrum for $Ce[OPPh_3][N(SiMe_3)_2]_3$ is shown is Figure 4.14. The gamma-emission at 1266 keV

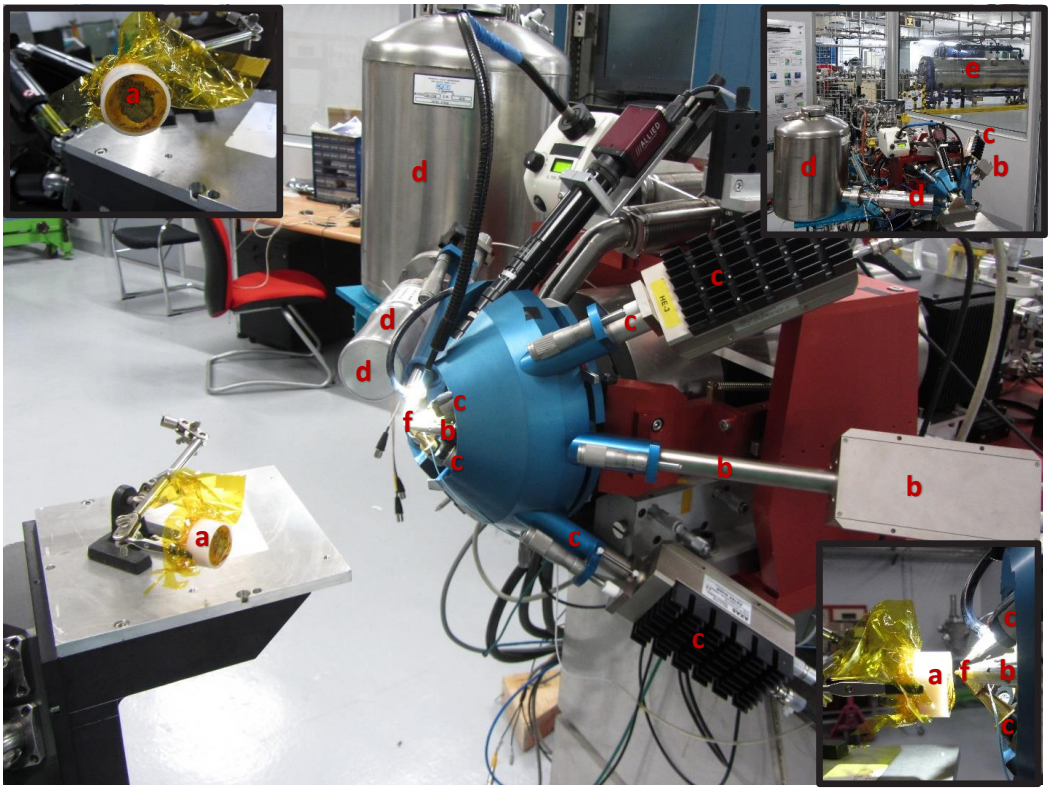

Figure 11: External Ion Beam Analysis setup at AGLAE, Louvre Museum, Paris, France. a) $Ce[OPPh_3][N(SiMe_3)_2]_3$ in sample holder, b) low-energy SDD X-ray detector, c) high-energy SDD X-ray detectors, d) HPGe Gamma detector, e) 3 MV Tandem Accelerator, f) 3 MeV proton beam exit window (Si_3N_4).

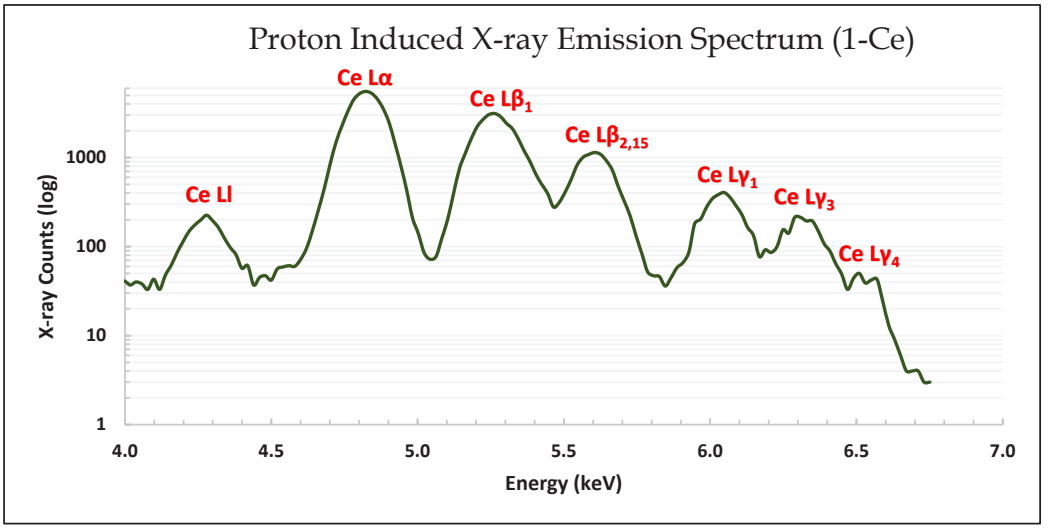

Figure 12: Cerium L X-ray Emission Series for $Ce[OPPh_3][N(SiMe_3)_2]_3$.

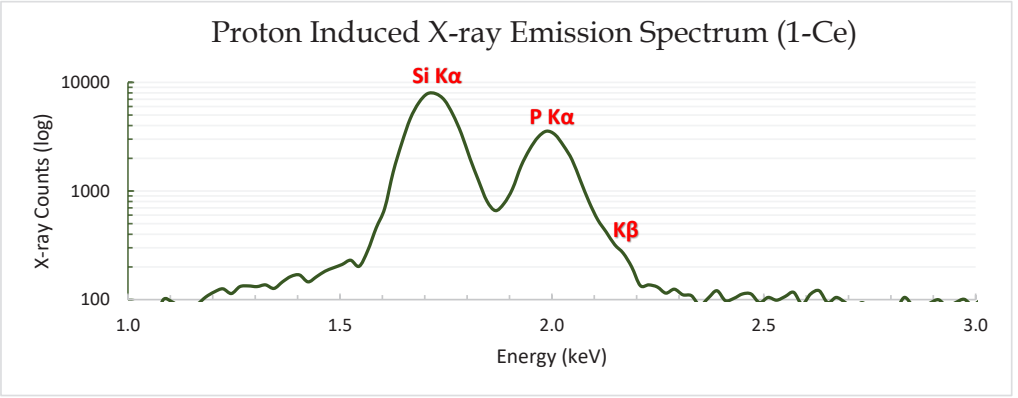

Figure 13: Silicon and Phosphorus K X-ray Emissions for $Ce[OPPh_3][N(SiMe_3)_2]_3$.

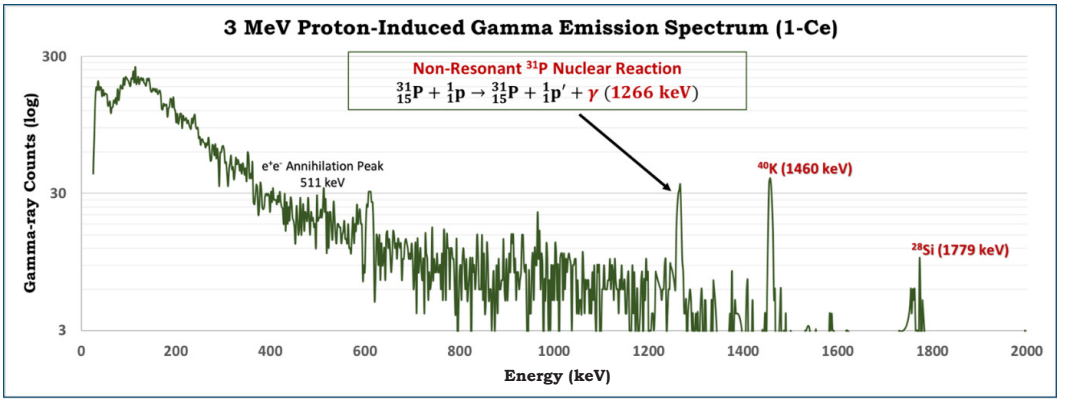

Figure 14: Proton-Induced Gamma Emission Spectrum for $Ce[OPPh_3][N(SiMe_3)_2]_3$.

corresponds to the non-resonant $^{31}P(p, p\gamma)^{31}P$ nuclear reaction. The e^+e^- annihilation peak was also observed at 511 keV. The observation of the emission resulting from the $^{31}P_{3/2} \rightarrow {}^{31}P_{1/2}$ nuclear transition has inspired us to use this signal for nuclear electric field gradient studies *f*-metal complexes, similar to NQR (nuclear quadrupole resonance) electric field gradient studies that have been conducted on metal fluorides using time-differential perturbed angular distribution analysis (TD-PAD), which involves using an MeV proton beam to induce fluorine gamma-emission [90-92]. This should be the subject of future work.

Conclusion

Four-coordinate complexes of the lanthanides and actinides are extremely rare, and $Ce[OP(p\text{-anisyl})_3][N(SiMe_3)_2]_3$, $Ce[OPPh_3][N(SiMe_3)_2]_3$, and $U[OP(p\text{-anisyl})_3][N(SiMe_3)_2]_3$ are valuable contributions to *f*-element coordination chemistry. The X-ray crystal structures and paramagnetic NMR spectra for $Ce[OP(p\text{-anisyl})_3][N(SiMe_3)_2]_3$, $Ce[OPPh_3][N(SiMe_3)_2]_3$, and $U[OP(p\text{-anisyl})_3][N(SiMe_3)_2]_3$ are reported in this work, along with X-ray and gamma emission spectra for $Ce[OPPh_3][N(SiMe_3)_2]_3$. The results were presented in the context of data available from the previous literature, which allowed further insight into the nature of monomeric cerium(III) and uranium(III)

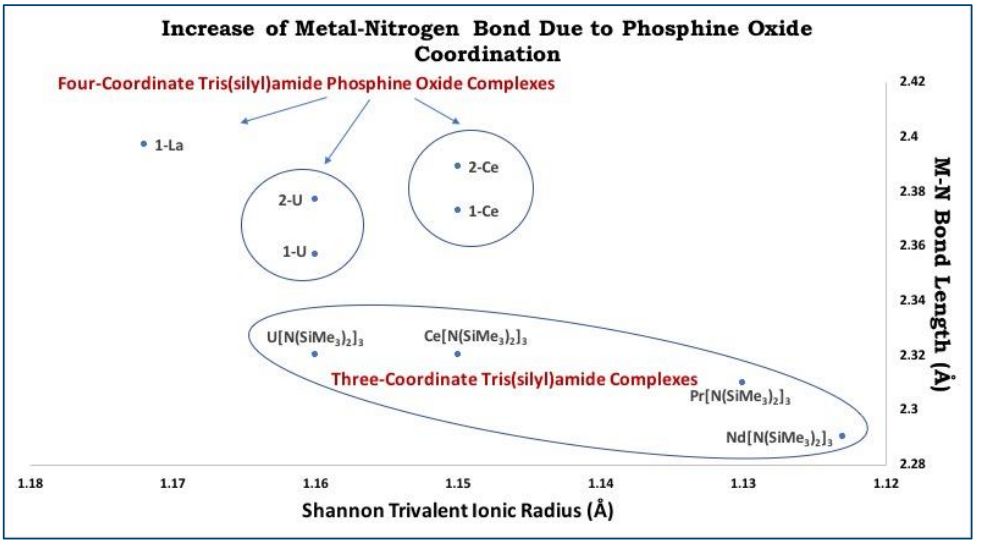

Figure 15: Increase in Metal-Nitrogen Bond Length with Phosphine Oxide Coordination

complexes with silylamide and phosphine oxide ligands. More insight will be achieved in future theoretical and experimental investigations of these model complexes. $Ce[OP(p\text{-anisyl})_3][N(SiMe_3)_2]_3$, $Ce[OPPh_3][N(SiMe_3)_2]_3$, and $U[OP(p\text{-anisyl})_3][N(SiMe_3)_2]_3$ can be used to investigate the previously observed enhancement in protonolysis reactivity of phosphine oxide adducts with diphenylphosphine ($HPPh_2$) compared to the base-free three-coordinate $Ln[N(SiMe_3)_2]_3$ compounds [19]. It was observed in this work that phosphine oxide coordination to the metal center increases the length of the metal-amide bond (see Figure 4.15), which could perhaps explain the enhanced protonolysis reactivity observed for similar rare-earth complexes decades ago [19].

Acknowledgements

The authors would like to thank the University of Oklahoma and the Department of Chemistry and Biochemistry for supporting this research. We would also like to thank Claire Pacheco, Thomas Calligaro, Quentin Lemasson, and Laurent Pichon for allowing the lead author to conduct external Ion Beam Analysis on 1-Ce at the AGLAE laboratory at C2RMF at the Louvre Museum in Paris, France. We would also like to thank Susan Nimmo at the University of Oklahoma NMR laboratory for her support and assistance.

References

[1] Kaltsoyannis, Nikolas and Peter Scott. 1999. *The f elements*. Oxford University Press, Oxford.

[2] Aspinall, Helen C. 2001. *Chemistry of the f-Block Elements*. Gordon and Breach Science Publishers, Amsterdam.

[3] Sastri, V.S., J.-C. Bünzli, V. Ramachandra Rao, G.V.S. Rayudu, and J.R. Perumareddi. 2003. *Modern Aspects of Rare Earths and their Complexes.* Elsevier, Amsterdam.

[4] Cotton, Simon. 2006. *Lanthanide and Actinide Chemistry*. John Wiley & Sons, Ltd, Cichester.

[5] Morss, Lester R., Norman M. Edelstein, Jean Fuger, Joseph J. Katz. *The Chemistry of the Actinide and Transactinide Elements*. Third edition. Springer, Dordrecht.

[6] Atwood, David A. 2012. *The Rare Earth Elements: Fundamentals and Applications*. John Wiley & Sons, Ltd, Chichester.

[7] Kaltsoyannis, Nikolas and Andrew Kerridge. 2014. "Chemical Bonding of Lanthanides and Actinides." In *The Chemical Bond: Chemical Bonding Across the Periodic Table*, pp.337-355, edited by Gernot Frenking and Sason Shaik. Wiley-VCH, Weinheim.

[8] Kerridge, Andrew. 2017. "Quantification of f-element covalency through analysis of the electron density: insights from simulation." *Chemical Communication* 53: 6685-6695.

[9] Dognon, Jean-Pierre. 2017. "Electronic structure theory to decipher the chemical bonding in actinide systems." *Coordination Chemistry Reviews* 344: 150-162.

[10] Bradley, Donald C., Joginder S. Ghotra, and F. Alan Hart. "Low Co-ordination Numbers in Lanthanide and Actinide Compounds. Part I. The Preparation and Characterization of Tris{bis(trimethylsilyl)-amido}lanthanides." *Journal of the Chemical Society Dalton Transactions* 1973: 1021.

[11] Ghotra, Joginder S., Michael B. Hursthouse, and Alan J. Welch. "Three-co-oridinate Scandium(III) and Europium(III); Crystal aand Molecular Structures of their Trishexamethyldisilylamides." 1973: 669.

[12] Bradley, D.C. and J.S. Ghotra. 1975. "Mass Spectroscopic Studies on Metal Organosilylamides. Part I. Mass Spectra of Tris{bis(trimethylsilyl)amido}lanthanides. *Inorganic Chimica Acta* 13: 11-16.

[13] Andersen, Richard A. 1979. "Tris((hexamethyldisilyl)amido)uranium(III): Preparation and Coordination Chemistry. *Inorganic Chemistry* 18(6): 1507.

[14] Avens, Larry R., Simon G. Bott, David L. Clark, Alfred Sattelberger, John G. Watkin, and Bill D. Zwick. 1994. "A Convenient Entry into Trivalent Actinide Chemistry: Synthesis and Characterization of $AnI_3(THF)_4$ and $An[N(SiMe_3)_2]_3$ (An = U, Np, Pu)." *Inorganic Chemistry* 33: 2248-2256.

[15] Anwander, Reiner. 1996. "Lanthanide Amides." *Topics in Current Chemistry* 179: 33-112.

[16] Drożdżyński, Janusz. 2005. "Tervalent uranium compounds." *Coordination Chemistry Reviews* 249: 2351-2373. University of Wroclaw, Poland.

[17]Baker, Robert J. 2012. "The coordination and organometallic chemistry of UI_3 and $U\{N(SiMe_3)_2\}_3$: Synthetic reagents par excellence." *Coordination Chemistry Reviews* 256: 2843-2871.

[18] Emslie, David J. H. 2018. "Actinides: Amido Complexes." *Encyclopedia of Inorganic and Bioinorganic Chemistry*, John Wiley & Sons, Ltd., pp. 1-18.

[19] Aspinall, Helen C., Donald C. Bradley, and Keith D. Sales. 1988. "Diphenylphosphido Complexes of the Lanthanides: Reactions of Compounds $[Ln\{N(SiMe_3)_2\}_3]$ (Ln = La or Eu) or $[Ln\{N(SiMe_3)_2\}_3(Ph_3PO)]$ (Ln = La, Eu, or Y) with Ph_2PH to give $[Ln\{N(SiMe_3)_2\}_2(PPh_2)]$ or $[Ln\{N(SiMe_3)_2\}_2(PPh_2)(Ph_3PO)]$." *Journal of the Chemical Society Dalton Transactions*: 2211-2213.

[20] Roger, Mathieu, Noémi Barros, Thérèse Arliguie, Pierre Thuéry, Laurent Maron, and Michel Ephritikhine. 2006. "$U(SMes^*)_n$ (n = 3, 4) and $Ln(SMes^*)_3$ (Ln = La, Ce, Pr, Nd): Lanthanide(III)/Actinide(III) Differentiation in Agostic Interactions and an Unprecedented η^3 Ligation Mode of the Arylthiolate Ligand, from X-ray Diffraction and DFT Analysis." *Journal of the American Chemical Society* 128: 8790-8802.

[21] Aspinall, Helen C., Sharron A. Cunningham, Patirck Maestro, and Pierre Macaudierre. 1998. "Lanthanide Tris(*tert*-butylthiolates) and the Crystal Structure of $[Yb(SBu^t)_2(\mu_2\text{-}SBu^t)(Bipy)]_2$." *Inorganic Chemistry* 37: 5396-5398.

[22] Cary, Douglas R. and John Arnold. 1993. "Preparation of Lanthanide Tellurolates and Evidence for the Formation of Cluster Intermediates in Their Thermal Decomposition to Bulk Metal Tellurides." *Journal of the American Chemical Society* 115: 2520-2521.

[23] Gaunt, Andrew J., Sean D. Reilly, Alejanddro E. Enriquez, Brian L. Scott, James A. Ibers, Permal Sekar, Kieran I.M. Ingram, Nikolas Kaltsoyannis, and Mary P. Neu. 2008. "Experimental and Theoretical Comparison of Actinide and Lanthanide Bonding in $M[N(EPR_2)_2]_3$ Complexes (M = U, Pu, La, Ce; E = S, Se, Te; R = Ph, *i*Pr, H)." *Inorganic Chemistry* 47: 29-41.

[24] LaDuca, Robert L. and Peter T. Wolczanski. 1992. "Preparation of Lanthanide Nitrides via Ammonolysis of Molten $\{(Me_3Si)_2N\}_3Ln$: Onset of Crystallization Catalyzed by $LiNH_2$ and LiCl." *Inorganic Chemistry* 31: 1311-1313.

[25] Baxter, David V., Malcom H. Chrisholm, Gennaro J. Gama, and Vincent F. Distasi. 1996. "Molecular Routes to Metal Carbides, Nitrides, and Oxides. 2. Studies of the Ammonolysis of Metal Dialkylamides and Hexamethyldisilylamides." *Chemistry of Materials* 8: 1222-1228.

[26] Czerwinski, K., and T. Hartmann. 2006. *Solution-Based Synthesis of Nitride Fuels*. UNLV, Fuels Campaign: Transmutation Research Program Projects.

[27] Siribbal, Shifaa M., Johannes Schläfer, Shaista Liyas, Zhangjun Hu, Kajsa Uvdal, Martin Valldor, and Sanjay Mathur. 2018. "Air-Stable Gadolinium Precursors for the Facile Microwave-Assisted Synthesis of Gd_2O_3 Nanocontrast Agents for Magnetic Resonances Imaging." *Crystal Growth and Design* 18: 633-641.

[28] Jamil, Aida, Johannes Schläfer, Yakup Gönüllü, Ashish Lepcha, and Sanjay Mathur. 2016. "Precursor-Derived Rare Earth Metal Pyrochlores: $Nd_2Sn_2O_7$ Nanofibers and Thin Films As Efficient Photoabsorbers." *Crystal Growth and Design* 16: 5260-5267.

[29] Zhang, Peng, Li Zhang, Chao Wang, Shufang Xue, Shuang-Yan Lin, and Jinkui Tang. 2014. "Equatorially Coordinated Lanthanide Single Ion Magnets." *Journal of the American Chemical Society* 136: 4484-4487.

[30] McAdams, Simon G., Ana-Maria Ariciu, Andreas K. Kostopoulos, James P.S. Walsh, and Floriana Tuna. 2017. "Molecular single-ion magnets based on lanthanides and actinides: Design considerations and new advances in the context of quantum technologies." *Coordination Chemistry Reviews* 346: 216-239.

[31] Liddle, Stephen T. and Joris van Slageren. 2015. "Improving f-element single molecule magnets." *Chemical Society Reviews* 44: 6655-6669.

[32] Meihaus, Katie R. and Jeffery R. Long. 2015. "Actinide-based single-molecule magnets." *Daltons Transactions* 44: 2517-2528.

[33] a) Tang, J. and P Zhang. 2015. *Lanthanide Single Molecule Magnets*. Springer-Verlag, Berlin. b) Layfield, Richard A. and Muralee Murugesu. 2015. *Lanthanides and Actinides in Molecular Magnetism*. Wiley-VCH, Verlag.

[34] Eisenstein, Odlie, Peter B. Hitchcock, Alexander G. Hulkes, Michael F. Lappert, and Laurent Maron. 2001. "Cerium masquerading as a Group 4 element: synthesis, structure and computational characterization of $[CeCl\{N(SiMe_3)_2\}_3]$." *Chemical Communications*: 1560-1561.

[35] Dröse, Peter, Alan R. Crozier, Samira Lashkari, Jochen Gottriedsen, Steffen Blaurock, Cristian G. Hrib, Cäcilla Maichle-Mössmer, Christoph Schädle, Reiner Anwander, and Frank T. Edelmann. 2010. "Facile Access to tetravalent Cerium Compounds: One-Electron Oxidation Using Iodine(III) Reagents." *Journal of the American Chemical Society Communication* 132: 14046-14047.

[36] Williams, Ursula J., Jerome R. Robinson, Andrew J. Lewis, Patirick J. Caroll, Patrick J. Walsh, and Eric J. Schelter. 2014. "Synthesis, Bonding, and Reactvity of a Cerium(IV) Fluoride Complex." *Inorganic Chemistry* 53: 27-29.

[37] Williams, Ursula J., Patrick J. Carroll, and Eric J. Schelter. 2014. "Synthesis and Analysis of a Family of Cerium(IV) Halide and Pseudohalide Compounds." *Inorganic Chemistry* 53: 6338-6345.

[38] So, Yat-Ming and Wa-Hung Leung. 2017. "Recent advances in the coordination chemistry of cerium(IV) complexes." *Coordination Chemistry Reviews* 340: 172-197.

[39] Stewart, Joanne Lee. 1988. *Tris[bis(trimethylsilyl)amido]uranium: Compounds with Tri-, Tetra-, and Penta-valent Uranium*. PhD Dissertation, University of California, Berkeley. Berkeley, California.

[40] Thomson, R.K., C.R. Graves, B.L. Scott, and J.L. Kiplinger. 2011. "Straightforward and efficient oxidation of tris(aryloxide) and tris(amide) uranium(III) complexes using copper(I) halide reagents." *Inorganic Chemistry Communications* 14: 1742-1744.

[41] Gaunt, Andrew J., Alejandro E. Enriquez, Sean D. Reilly, Brian L. Scott, and Mary P. Neu. 2008. "Structural Characterization of $Pu[N(SiMe_3)_2]_3$, a Synthetically Useful Nonaqueous Plutonium(III) Precursor." *Inorganic Chemistry* 47: 26-28.

[42] Gaunt, Andrew J., Sean D. Reillym Alejandro E. Enriquez, Trevor W. Hayton, James M. Boncella, Brian L. Scott, and Mary P. Neu. 2008. "Low Valent molecular Plutonium Halide Complexes." *Inorganic Chemistry* 47: 8412-8419.

[43] Fortier, Skye, Jessie L. Brown, Nikolas Kaltsoyannis, Guang Wu, and Trevor Hayton. 2012. "Synthesis, Molecular, and Electronic Structure of $U^V(O)[N(SiMe_3)_2]_3$." *Inorganic Chemstry* 51: 1625-1633.

[34] Lewis, Andrew J., Eiko Nakamaru-Ogiso, James M. Kikkawa, Patrick J. Carroll, and Eric J. Schelter. 2012. "Pentavalent uranium *trans*-dihalides and -pseudohalides." *Chemical Communications* 48: 4977-4979.

[35] Brown, Jessie L., Skye Fortier, Richard A. Lewis, Guang Wu, and Trevor W. Hayton. 2012. "A Complete Family of Terminal Uranium Chalcogenides, $[U(N\{SiMe_3\}_2)_3]^-$ (E = O, S, Se, Te)." *Journal of the American Chemical Society* 134: 15468-15475.

[36] Smiles, Danil E., Guang Wu, and Trevor Hayton. 2014. "Synthesis of Uranium-Ligand Multiple Bonds by Cleavage of a Trityl Protecting Group." *Journal of the American Chemical Society* 136: 96-99.

[37] Smiles, Danil E., Guang Wu, and Trevor Hayton. 2014. "Reversible Chalcogen-Atom Transfer to a Terminal Uranium Sulfide." *Inorganic Chemistry* 53: 12683-12685.

[48] Smiles, Danil E., Guang Wu, and Trevor Hayton. 2014. "Synthesis of Terminal Monochalcogenide and Dichalcogenide Complexes of Uranium Using Polychalcogenides, $[E_n\}^{2-}$ (E = Te, n = 2; E = Se, n = 4), as Chalcogen Atom Transfer Reagents." *Inorganic Chemistry* 53: 10240-10247.

[49] Bradley, Donald C., Joginder S. Ghotra, F. Alan Hart, Michael B. Hursthouse, and Paul R. Raithby. 1977. "Low Co-ordination Numbers in Lanthanoid and Actinoid Compounds. Part 2. Syntheses, Properties, and Crystal and Molecular Structures of Triphenylphosphine Oxide and Peroxo-derivatives of [Bis(trimethylsilyl)-amido] lanthanoids." *Journal of the Chemical Society Dalton Transactions*: 1166-1172.

[50] Jank, Stefan, Clemens Guteenberger, Hauke Reddmann, Jan Hanss, and Hanns-Dieter Amberger. 2006. "Zur Electronenstruktur hochsymmetrischer Verbindungen der f-Elemente. 41. Syntheses, Kristall-, Molekül- und Elektronenstruktur eines Bis(cyclohexylisonitrol)-Addukts des Grundkörpers Tris(bis(trimethylsilyl) amidoerbium(III) sowie Electronenstrukturen ausgewählter Monoaddukte." *Zeitschrift für Anorganische und Allgemeine Chemie* 632: 2429-2438.

[51] Jank, Stefan, Hauke reddmann, Lixin Zhang, and Hanns-Dieter Amberger. 2012. "Zur Electronenstruktur hochsymmetrischer Verbindungen der f-Elemente. 45. Ungewöhnliche spektrochemische Eigenschaften des Triphenylphosphanoxido-Liganden im Falle von Mono- und Bisaddukten homoleptischer Samaraium(III)silylamide." *Zeitschrift für Anorganische und Allgemeine Chemie* 638: 1159-1166.

[52] Schumann, H. and G.M. Frisch. 1982. *Zeitschrift für Naturforschung, Teil B* 36: 1244.

[53] Evans, W.J., I. Bloom, W.E. Hunter, and J.L. Atwood. 1983. *Organometallics* 2: 709.

[54] Law, J.D., K.N. Brewer, R.S. Herbst, T.A. Todd, and D.J. Wood. 1999. "Development and demonstration of solvent extraction processes for the separation of radionuclides from acidic radioactive waste." *Waste Management* 19: 27-37.

[55] Krahn, Elizabeth, Cécile Marie, and Kenneth Nash. 2016. Probing organic phase ligand exchange kinetics of 4f/5f solvent extraction systems with NMR spectroscopy. *Coordination Chemistry Reviews* 316: 21-35.

[56] Romanovsky, V.N. 1998. *R&D Activities on Partitioning in Russia*. V.G. Khlopin Radium Institute, pp. 1-9.

[57] Häller, L.J.L, N. Kaltsoyannis, M.J. Sarsfield, L. May, S.M. Cornet, M.P. Redmond, and M. Helliwell. 2007. *Inorganic Chemistry* 46: 4868.

[58] Platt, Andrew W.G. 2017. "Lanthanide phosphine oxide complexes." *Coordination Chemistry Reviews* 340: 62-78.

[59] Lobana, T.S. 1992. "Coordination chemistry of phosphine chalcogenides and their analytical and catalytic applications." In *The Chemistry of Organophosphorus Compounds, Volume 2, Phosphine Oxides, Sulphides, Selenides, and Tellurides*, edited by Frank Hartley, pp. 409-566. John Wiley & Sons, Ltd.

[60] Monreal, Marisa J., Robert K. Thomson, Thibault Cantat, Micholas E. Travia, Brian L. Scott, and Jaqueline L. Kiplinger. 2011. "UI_4(1,4-dioxane)$_2$, [UCl_4(1,4-dioxane)]$_2$, and UI_3(1,4-dioxane)$_{1.5}$: Stable and Versatile Starting Materials for Low- and High-Valent Uranium Chemistry." *Organometallics* 30: 2031-2038

[61] Woollins, J. Derek. 2010. *Inorganic Experiments. Third Edition*. Wiley-VCH, Weinheim.

[62] Denton, Ross M., Jie An, Beatrice Adeniran, Alexander J. Blake, William Lewis, and Andrew Poulton. 2011. "Catalytic Phosphorus(V)-Mediated Nucleophilic Substitution Reactions: Development of a Catalytic Appel Reaction." *Journal of Organic Chemistry* 76: 6749-6767.

[63] Edleman, Nikki L., Anchuan Wang, John A. Belot, Andrew W. Metz, Jason R. Babcock, Amber M. Kawaoka, Jun Ni, Matthew V. Metz, Christine J. Flashenriem, Charlotte L. Stern, Louise M. Liable-Sands, Arnold L. Rheingold, Paul R. Markworth, Robert P.H. Chang, Michael P. Chudzik, Carl R. Kannewurf, and Tobin J. Marks. 2002. "Synthesis and Characterization of Volatile, Fluorine-Free β-Ketoiminate Lanthanide MOCVD Precursors and Their Implementation in Low-Temperature Growth of Epitaxial CeO_2 Buffer Layers for Superconducting Electronics." *Inorganic Chemistry* 41: 5005-5023.

[64] Rees, Jr., William S., Oliver Just, and Donald S. van Derveer. 1999. "Molecular design of dopant precursors for atomic layer epitaxy of SrS:Ce." *Journal of Material Chemistry* 9: 249-252.

[65] Fjeldberg, T., Andersen, R.A. 1985. *Journal of Molecular Structure* 129: 93.

[66] Andersen, R.A., D.H. Templeton, and A. Zalkin. 1978. *Inorganic Chemistry* 8: 2317.

[67] Brady, Erik D., David L. Clark, John C. Gordon, P. Jeffery Hay, D. Webster Keogh, Rinaldo Poli, Brian L. Scott, and John G. Watkin. 2003. "Tris(bis(trimethylsilyl)amido) samarium: X-ray Structure and DFT Study." *Inorganic Chemistry* 42: 6682-6690.

[68] Ghotra, J.S., M.B. Hursthouse, and A.J. Welch. 1973. *Journal of the Chemical Society Chemical Communications*: 669.

[69] Hitchcock, Peter B., Alexander G. Hulkes, Michael F. Lappert, and Zhengning Li. 2004. "Cerium(III) dialkyl dithiocarbamates from [$Ce\{N(SiMe_3)_2\}_3$] and tetraalkylthiuram disulfides, and [$Ce(\kappa^2\text{-}S_2CNEt_2)_4$] from the Ce^{III} precursor; Tb^{III} and Nd^{III} analogues." *Dalton Transactions* 129-136.

[70] Hermann, W.A., R. Anwander, F.C. Munck, W. Scherer, V. Dufaud, N.W. Huber, and G.R.J. Artus. 1994. *Zeitschrift für Naturforschung* B49: 1789.

[71] Bienfait, André M., Benjamin M. Wolf, Karl W. Törnoos, and Reiner Anwander. 2018. "Trivalent Rare-earth-Metal Bis(trimethylsilyl)amide Halide Complexes by Targeted Oxidations." *Inorganic Chemistry* 57: 5204-5212.

[72] Niemeyer, Mark. 2002. "Synthese und strukturelle Charakteriserung verschiedener Ytterdiumbis(trimethylsilyl)amide darunter σ-donorfreies [$Yb\{N(SiMe_3)_2\}_2(\mu\text{-}Cl)]_2$ – Ein koordinativ ungesättiger Komplex mit zusätzlichen agostichen Yb···(H_3C-Si) Wechselwirkungen." *Zeitschrift für Anorganische und Allgemeine Chemie* 628: 647-657.

[73] Anwander, R. 1992. Thesis. Technical University, Munich.

[74] Westerhausen, M., M. Hartmann, A. Pfitzner, and W. Schwarz. 1995. *Zeitschrift für Anorganische und Allgemeine Chemie* 621:837.

[75] Stewart, Joanne L. and Richard A. Andersen. 1998. "Trivalent uranium chemistry: molecular structure of $[(Me_3Si)_2N]_3U$." *Polyhedron* 17(5-6): 953-958.

[76] Gaunt, Andrew J., Alejandro E. Enriquez, Sean D. Reilly, Brian L. Scott, and Mary P. Neu. 2008. "Structural Characterization of $Pu[N(SiMe_3)_2]_3$, a Synthetically Useful Nonaqueous Plutonium(III) Precursor." *Inorganic Chemistry* 47: 26-28.

[77] Lappert, M.F., J.B. Pedley, G.J. Sharp, D.C. Bradely. 1976. *Journal of the Chemical Society Dalton Transactions*: 1737. Green, J.C., M. Payne, E.A. Seddon, R.A. Andersen. 1982. *Journal of the Chemical Society Dalton Transactions*: 887.

[78] Bleaney, B., C.M. Dobson, B.A. Levine, R.B. Martin, R.J.P. Williams, and A.V. Xavier. 1972. *Journal of the Chemical Society Chemical Communications* 791.

[79] Bleaney, B. 1972. *Journal of Magnetic Resonance* 8: 91.

[80] Le Mar, G.N., W. DeW. Horrocks, Jr., R.H. Holm. 1973. *NMR of Paramagnetic Molecules*. Academic Press, Inc.

[81] Bertini, Ivano, Claudio Luchinat, Giacomo Parigi, and Enrico Ravera. 2017. *NMR of Paramagnetic Molecules*. Elsevier.

[82] Boudreaux, E.A. and L.N. Mulay. 1976. *Theory and Applications of Molecular Paramagnetism.* John Wiley & Sons, New York.

[83] Smiles, Danil E., Guang Wu, Peter Hrobárik, and Trevor W. Hayton. 2016. "Use of ^{77}Se and NMR Spectroscopy to Probe Covalency of the Actinide-Chalcogen Bonding in $[Th(E_n)\{N(SiMe_3)_2\}_3]^-$ (E = Se, Te; n = 1, 2) and Their Oxo-Uranium(VI) Congeners." *Journal of the American Chemical Society* 138: 814-825.

[84] Durdağı, Sevil. 2017. "Chemical environment change analysis on *L* X-ray emission spectra of some lanthanide compounds." *Microchemical Journal* 130: 27-32.

[85] Durdağı, Sevil. 2013. "Effect of applied external magnetic field on the *L* X-ray emission line structures of the lanthanide elements." *Radiation Physics and Chemistry* 92: 1-7.

[86] Takahashi, Yoshihitio. 1972. "The X-ray Emission Spectra of the Compounds of Third-Period Elements. II. The *K* Spectra of Phosphorus in Compounds." *Bulletin of the Chemical Society of Japan* 45(4): 4-7.

[87] Yumatov, V.D., L.N. Mazalov, and E.A. Il'inchik. 1980. "Electronic Structure of a Series of Organic Compounds of Phosphrous and the Nature of the Chemical Bond Between Phosphorus and Oxygen." *Zhurnal Strukturnoi Khimii* 21(5): 24-28.

[88] Sugiura, Chikara, Hiroharu Yorikawa, and Shinji Muramatsu. 1996. "*K*β X-Ray Emission Spectra and Chemical Environments of Phosphorus in Some Selected Compounds." *Journal of the Physical Society of Japan* 65(9): 2940-2945.

[89] Petric, Marko, Rok Bohinc, Klemen Bučar, Matjaž Žitnik, Jakub Szlachetko, and Matjaž Kavčič. 2015. "Chemical State Analysis of Phosphorus Performed by X-ray Emission Spectroscopy." *Analytical Chemical* 87: 5632-5639.

[90] Blank, H. -R., M. Frank, M. Geĺger, J. -M. Greneche, M. Ismaier, M. Kaltenhäuser, R. Kapp, W. Kreische, M. Leblanc, U. Lossen, and B. Zapf. 1994. "Systematic Investigation of MF_3 Crystalline Compounds (M = Al, Cr, Fe, Ga, In, Sc, Ti, and V) and $Fe_{1-x}M_xF_3$ Mixed Series (M = Ga, Cr, V)." *Zeitschrift für Naturforschung* 49a: 361-366.

[91] Smith, J.A.S. 1986. "Nuclear Quadrupole Resonance: The Present State and Further Development." *Zeitschrift für Naturforschung* 41a: 453-462.

[92] Frank, Michael. 1999. "On Systematics in the ^{19}F Electric Hyperfine Interactions." *Forschritte der Physik* 4: 335-388.

[93] Jingqing, Ren and Xu Guangxian. 1987. "Electronic Structure and Chemical Bonding of Bis(Trimethylsilyl) Amide Derivatives of Lanthanides ($Ln(N(SiMe_3)_2)_3$, Ln = Nd, Eu, Yb)." *Scientia Sinica B* 30(4): 337-346.

Submitted May 1, 2023 Accepted October 30, 2023

Relationship Between Cell Surface Hydrophobicity and Biofilm Adhesion in Opportunistic *Serratia* Species with Disparate Susceptivity to Triclosan Sensitization

Katherine Nehmzow
Department of Natural Sciences, Northeastern State University, Broken Arrow, OK 74014

Abby S. Rigsbee
Department of Biochemistry and Microbiology, Oklahoma State University Center for Health Sciences, Tulsa, OK 74107

Christopher F. Godman
College of Medicine, Oklahoma State University Center for Health Sciences, Tulsa, OK 74107

Samuel K. Hudgeons
College of Medicine, Oklahoma State University Center for Health Sciences, Tulsa, OK 74107

Sue Katz Amburn
Department of Biochemistry and Microbiology, Oklahoma State University Center for Health Sciences, Tulsa, OK 74107

Franklin R. Champlin*
Department of Biochemistry and Microbiology, Oklahoma State University Center for Health Sciences, Tulsa, OK 74107

Abstract: We have recently reported that ten opportunistically pathogenic *Serratia* species markedly differ regarding susceptivity to sensitization to the hydrophobic biocide triclosan by outer membrane permeabilization. Representative organisms exhibiting slight (*Serratia marcescens*), complete (*Serratia fonticola*), transitorily complete (*Serratia liquefaciens*), and intermediate (*Serratia rubidaea*) susceptivity were selected for further analysis. The purpose of the present study was to determine if such phenotypic susceptivity is related to cell surface hydrophobicity properties and the proclivity to implement biofilm adhesion. Hydrocarbon adherence and hydrophobic fluorescent probe assays were employed to quantitate cell surface hydrophobicity properties, while an *in vitro* biofilm assay was used to assess adhesion of planktonic cells to a nonpolar substrate. While *S. rubidaea* was seen to be extremely hydrophobic, *S. marcescens* and *S. liquefaciens* were slightly to moderately hydrophobic, and *S. fonticola* was relatively hydrophilic. *S. rubidaea* adhered to the polystyrene substrate more readily than *S. fonticola* or *S. liquefaciens*, while *S. marcescens* adhesion was intermediate. These data do not support the notion that the degree of susceptivity to triclosan sensitization by outer membrane permeabilization is directly related to cell surface hydrophobicity. However, the initial adhesion stage of biofilm formation appears to be influenced at least in part by cell surface hydrophobicity properties.

***Corresponding author: franklin.champlin1@gmail.com**

Proc. Okla. Acad. Sci. 103: pp 130 - 139 (2023)

Introduction

Triclosan (5-choro-2-(2,4-dichlorophenoxy) phenol) is a hydrophobic diphenyl ether biocide (Figure 1). It possesses broad spectrum antibacterial activity that is utilized as an antiseptic or preservative in many medical, personal care, industrial, and household settings. Municipal water treatment processes are relatively ineffective at triclosan removal due to the stability of the biocide combined with its widespread use, thereby resulting in its environmental accumulation as a pollutant (Thompson et al. 2005; Bester 2005; Welsch and Gillock 2011; Dhillon et al. 2015; McNamara and Levy 2016). The mechanism of action of triclosan involves inhibition of enoyl-acyl carrier protein reductase, an essential cytoplasmic enzyme involved in bacterial fatty acid biosynthesis (McMurry et al. 1998). In order to reach its mechanistic target in gram-negative bacteria, the biocide must transverse the outer membrane to enter the periplasmic space where it can then passively partition through the phospholipid bilayer of the cytoplasmic membrane into the cytoplasm due to its hydrophobic nature.

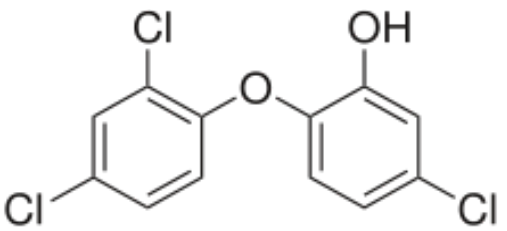

Figure 1. Molecular structure of triclosan.

As a broad-spectrum antibacterial agent (Dhillon et al. 2015), triclosan must passively traverse the outer membrane of gram-negative bacteria despite the fact most are typically impermeable to hydrophobic substances due to the asymmetric presence lipopolysaccharide in the outer leaflet (Nikaido 2003; Silhavy et al. 2010). However, the gram-negative nosocomial opportunists *Pseudomonas aeruginosa* and *Serratia marcescens* are markedly resistant (Jones et al. 2006; Schweizer 2001) and outer membrane impermeability has been shown to contribute significantly to the underlying resistance mechanism in both organisms (Boyina et al. 2023; Champlin et al. 2005; Ellison et al. 2007).

A plethora of published information exists regarding the basic biology and pathogenic properties of the *Serratia* type species *S. marcescens*. In contrast, a paucity of such research exists for other species in the genus which have also been shown to be etiologic agents in humans. Our laboratory has recently reported that 10 *Serratia* species capable of opportunistic pathogenicity differed dramatically regarding their relationship with triclosan by exhibiting phenotypes ranging from intrinsically resistant to extremely susceptible (Boyina et al. 2023). Moreover, resistant species exhibited disparate susceptivity levels to triclosan sensitization using compound 48/80, a cationic detergent that selectively permeabilizes the gram-negative outer membrane (Katsu et al. 1985). These data supported the overall notion that while outer membrane impermeability for hydrophobic substances was involved to different degrees in the resistance mechanisms of phenotypically disparate species, ancillary resistance mechanisms appeared to play supportive roles in some species and constitutive multi-drug efflux systems were suspected.

The disparate synergistic relationships between triclosan and compound 48/80 seen among the refractory species are suggestive of potential outer cell envelope characteristics which could influence the expression of virulence factors such as the proclivity to form biofilms. In order to more fully investigate this possibility, species representing the different susceptivity phenotypes were selected for further analysis of their cell surface hydrophobicity (CSH) and biofilm formation properties in the present study. CHS properties influence how bacteria interact with their environment and their ability to act as etiological agents of infection as they adhere to abiotic substances and biotic tissues (Krasowska and Sigler 2014). Evidence for this relationship has been published for *S. marcescens* (Rosenberg et al. 1986), but similar research is lacking for other known biofilm-forming *Serratia* species

to include *Serratia liquefacians* (Remuzgo-Martinez et al. 2015), *Serratia plymuthica* (Van Houdt et al. 2005), and *Serratia proteamaculans* (Alavi and Hansen 2013).

Additional research is necessary to determine if the physiological consequences of gram-negative CSH properties influence the ability of pathogenic *Serratia* species to adhere to substrates in the initial adhesion step of biofilm formation. We have previously shown CSH to be particularly important in this regard for the pulmonary gram-negative opportunist *Burkholderia multivorans* (Ruskoski and Champlin 2017; Ruskoski et al. 2024). While production of extracellular polysaccharide (EPS) was seen to be necessary for the maturation of stable *in vitro* biofilms, its production appeared to be down regulated in order not to interfere with the initial attachment stage.

We hypothesized that CSH properties underlie (a) the disparate susceptivity to triclosan sensitization by perturbation of outer membrane impermeability for hydrophobic substances and (b) the initial adhesion stage of biofilm formation in opportunistically pathogenic *Serratia* species. The purpose of the present investigation was to quantify the CHS properties of four triclosan sensitization variant *Serratia* species and examine their respective proclivities for initiating biofilm formation on a hydrophobic polystyrene substrate.

Materials and Methods

Bacterial isolates, maintenance, and cultivation conditions: *S. marcescens* ATCC 13880, *Serratia fonticola* ATCC 29844, *S. liquefaciens* ATCC 27592, and *Serratia rubidaea* ATCC 27593 (Table 1) were obtained from the American Type Culture Collection (Manassas, VA) and are the type strains of their respective species. *E. coli* ATCC 25922 and *Pasteurella multocida* P-1581 are maintained in our laboratory and were included for comparative control purposes. All cultures were stored under cryoprotective conditions as described elsewhere (Darnell et al. 1987).

Working cultures were obtained by streak inoculating Mueller Hinton Agar (MHA; Becton, Dickinson and Co., Sparks, MD) plates with cells from cryopreserved stock cultures and incubating for 18 h at 37°C prior to storing at 4°C until needed. Starter cultures were prepared by inoculating 20 mL of Mueller Hinton Broth (MHB: Becton Dickinson and Co.) contained in 125-mL screw-capped glass Erlenmeyer flasks with working culture cells and incubating for 12-15 h at 37°C and 180 rpm (Excella E24 incubator shaker; New Brunswick Scientific, Edison, NJ) to provide stationary-phase inocula for experimental test cultures.

Disk agar diffusion bioassay: Susceptibility of *S. marcescens* ATCC 13880 and *E. coli* ATCC 25922 to triclosan and four hydrophobic antibiotics was assessed using a standardized disk agar diffusion bioassay routinely employed in our laboratory (Clayborn et al. 2011). Starter culture cells were used to inoculate MHB test cultures which were incubated at 37°C and 180 rpm (Excella E24 shaker incubator) until an OD_{620} of 0.10 (Spectronic 20D+ optical spectrophotometer; Thermo Fisher Scientific Inc., Waltham, MA) was obtained.

Adhesive ring formation: Overnight starter cultures of the test *Serratia* spp. were examined visually for rings of biomass adhering to glass growth flasks after incubation at 37°C for 12-15 h with rotary aeration at 180 rpm in an Excella E24 shaker incubator.

Hydrocarbon adherence: CHS properties were quantitated by assessing the degree to which test culture cells adhered to the hydrocarbon n-hexadecane using the method of Rosenberg et al. (1980) as modified for use in our laboratory (Thies and Champlin 1989; Ruskoski and Champlin 2017). Test culture inocula were prepared by inoculating 210 mL of MHB with starter culture cells to an OD_{620} of 0.05 (Spectronic 20D+ optical spectrophotometer). Aliquots of 100 mL were dispensed into each of two 250-mL screw-capped culture flasks which were incubated at 37°C and 180 rpm (Excella E24 shaker incubator) until late exponential-phase growth was obtained (OD_{620} of approx.

0.40).

NPN uptake: Confirmation of CSH results was accomplished by assessing the degree to which test culture cells associated with the hydrophobic fluorescence probe 1-*N*-phenylnaphthylamine (NPN) using the method of Helander and Matilla-Sandholm (2000) as modified for use in our laboratory (Ellison and Champlin 2007; Ruskoski and Champlin 2017). Test culture inocula were prepared by inoculating 50 mL of MHB in 125-mL screw-capped culture flasks with starter culture cells to an OD_{620} of 0.05 (Spectronic 20D+ optical spectrophotometer). Flasks were incubated at 37°C and 180 rpm (Excella E24 shaker incubator) until mid-to-late exponential-phase growth was obtained (OD_{620} of approx. 0.30 to 0.40).

***In vitro* biofilm formation:** The proclivity of test culture cells to carry out the initial adhesion stage of *in vitro* biofilm formation was determined using a conventional μ-titer plate assay (O'Toole and Kolter 1998) as modified for use in our laboratory (Ruskoski et al. 2024). Test culture inocula were prepared by titrating 5.0-mL volumes of MHB contained in 18-mm diameter Kimax culture tube/sample holders with starter culture cells to an OD_{620} of 0.25 (Spectronic 20D+ optical spectrophotometer). Aliquots of 100 μL were dispensed into appropriate wells in hydrophobic (untreated) polystyrene 96-well microtiter plates (Cellstar; Greiner Bio-One Inc., Monroe, NC) which were placed in a closable plastic container with a beaker of deionized water and incubated at 37°C for 4 h.

Statistical analysis: All quantitative values represent the means of three-to-four independent determinations ± standard deviation. Differences between means were analyzed for statistical significance using SigmaPlot® version 15.0 (SigmaPlot Graphing Software, Palo Alto, CA) by determining *P* values using one-way ANOVA with Holm-Sidak comparisons. *P* values of less than 0.05 indicated statistical differences at the 5.0 % confidence level.

Results and Discussion

Previous work in our laboratory revealed outer membrane exclusionary properties of four different *S. marcescens* strains to be responsible to different degrees for their shared intrinsic resistance to the hydrophobic biocide triclosan (Boyina et al. 2023). Data in Figure 2 reveal the *S. marcescens* type strain to be resistant to five mechanistically disparate hydrophobic antibacterial agents in a manner like that seen for *E. coli* ATCC 25922 which differs only in being susceptible to triclosan. Such uniform resistance to antibacterial compounds having different mechanistic targets supports the notion that the *S. marcescens* outer membrane is generally impermeable to hydrophobic substances.

Boyina et al. (2023) reported that all but one of 10 *Serratia* species known to be capable of opportunistic pathogenicity are intrinsically

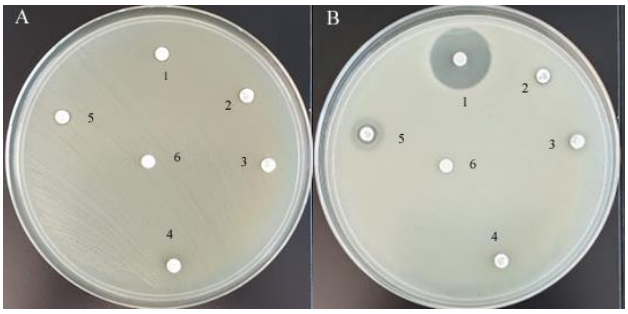

Figure 2. Disk agar diffusion bioassay for triclosan and representative hydrophobic antibiotics. Panel A, *S. marcescens* ATCC 13880; Panel B, *E. coli* ATCC 25922. Disk (potency): 1, triclosan (0.2 μg); 2, novobiocin (5.0 μg); 3, vancomycin (30 μg); 4, clindamycin (2.0 μg); 5, rifampin (5.0 μg), 6, ethanol control (95 %).

resistant to the hydrophobic biocide triclosan. However, they differed markedly regarding their susceptivity to triclosan sensitization by outer membrane permeabilization using the cationic detergent compound 48/80. These disparities formed the basis for the development of an intrinsic resistance model system consisting of species representing four phenotypically different groups to include (i) *S. marcescens* ATCC 13880, slight susceptivity; (ii) *S. fonticola* ATCC 29844, complete susceptivity; (iii) *S. liquefaciens* ATCC 27592, transitory complete susceptivity; and (iv) *S. rubidaea* ATCC 27593, moderate susceptivity (Table 1).

Initial evidence for the possibility that these species might differ regarding their proclivities to bind to nonpolar surfaces was provided by the observation that they bound borosilicate glass growth flasks to different degrees during batch cultural growth (Figure 3). When viewed with the data presented in Figure 5 below, it can be seen that the more hydrophobic organism *S. rubidaea* formed a heavy biomass ring around the growth flask, while the less hydrophobic species *S. marcescens* and *S. liquefaciens* formed slight to moderate rings. The hydrophilic organism *S. fonticola* failed to form a biomass ring. Because glass is more hydrophobic than the aqueous medium, these data support the conclusion that ring formation is dependent on the CSH properties of the organisms.

These observations allowed for the hypothesis that outer CSH properties underlie the disparate susceptivity levels to triclosan sensitization by perturbation of outer membrane impermeability for hydrophobic substances represented by the four species under examination. This hypothesis was tested by quantitatively determining their cell surface hydrophobicity properties by assessing the degree to which they were able to adhere to the hydrocarbon n-hexadecane using the hydrocarbon adherence method of Rosenberg et al. (1980) as modified for use in our laboratory (Thies and Champlin 1989; Ruskoski and Champlin 2017). This is a more direct measure of cell surface hydrophobicity than other methods because it is a simple assessment of the amount of biomass that is able to partition into a nonpolar hydrocarbon phase within the restrictions of the assay protocol. There are fewer if any opportunities for secondary effects which could result in anomalous falsely positive results. Validation was provided by conducting a control experiment that employed two organisms for which this method had previously been employed (Figure 4).

As can be seen in Figure 5, *S. fonticola* is hydrophilic relative to the other organisms as it exhibited very little partitioning into the hydrocarbon. *S. marcescens* and *S. liquefaciens* are moderately hydrophobic while *S. rubiaea* can be seen to be extremely hydrophobic with over 80 % of its biomass partitioned into the hydrocarbon. These data do not support the notion that the degree of susceptivity to triclosan sensitization by outer membrane permeabilization (Boyina et al. 2023) is directly related to cell surface hydrophobicity properties due to the absence of correlation.

The relationship between CSH properties and triclosan sensitization by perturbation of outer membrane impermeability for hydrophobic substances was further tested by assessing the degree to which the selected *Serratia* species were able to associate with the hydrophobic fluorescence probe NPN using the method

Figure 3. Representative starter cultures exhibiting disparate degrees of biomass ring formation on flask sides.

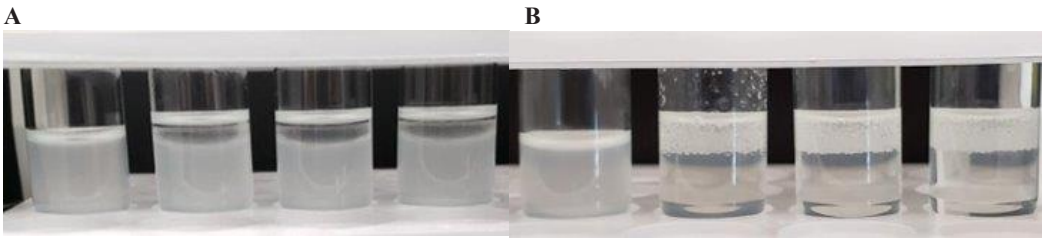

Figure 4. Control hydrocarbon adherence assays. Panel A, *E. coli* ATCC 25922 (hydrophilic; Rosenberg et al. 1980); Panel B, *P. multocida* P-1581 (hydrophobic, Darnell et al. 1987).

of Helander and Mattila-Sandholm (2000) as modified for use in our laboratory (Ellison and Champlin 2007; Ruskoski and Champlin 2017) (Figure 6). *S. marcescens*, *S. fonticola*, and *S. liquefaciens* exhibited similar CSH levels which were clearly less than that of *S. rubidaea*. These data support the conclusion reached with the hydrocarbon adherence method in that there is no direct correlation between association with the hydrophobic probe and susceptivity to triclosan sensitization by outer membrane permeabilization (Boyina et al. 2023).

Based on these findings, a hypothesis was formulated that posited outer cell surface hydrophobicity properties underlie the initial adhesion stage of biofilm formation in opportunistically pathogenic *Serratia* species. This hypothesis was tested by determining the degree to which the selected *Serratia* species were able carry out the initial adhesion stage of biofilm formation by assessing adherence to polystyrene at 4 h post-inoculation using a conventional μ-titer plate assay (O'Toole and Kolter 1998) as modified for use in our laboratory (Ruskoski et al. 2024) (Figure 7).

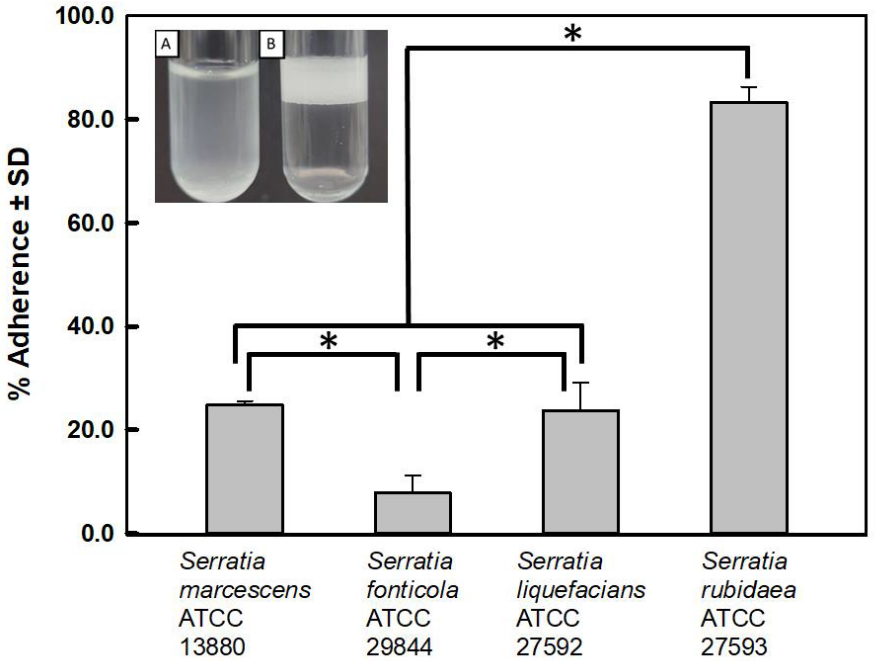

Figure 5. Cell surface hydrophobicity properties determined based on the degree to which cells associated with n-hexadecane as measured turbidimetrically using the method of Rosenberg et al. (1980) as modified by Ruskoski and Champlin (2017). Inset: Representative untreated control (A) and test (B) samples of *S. marcescens* ATCC 13880.

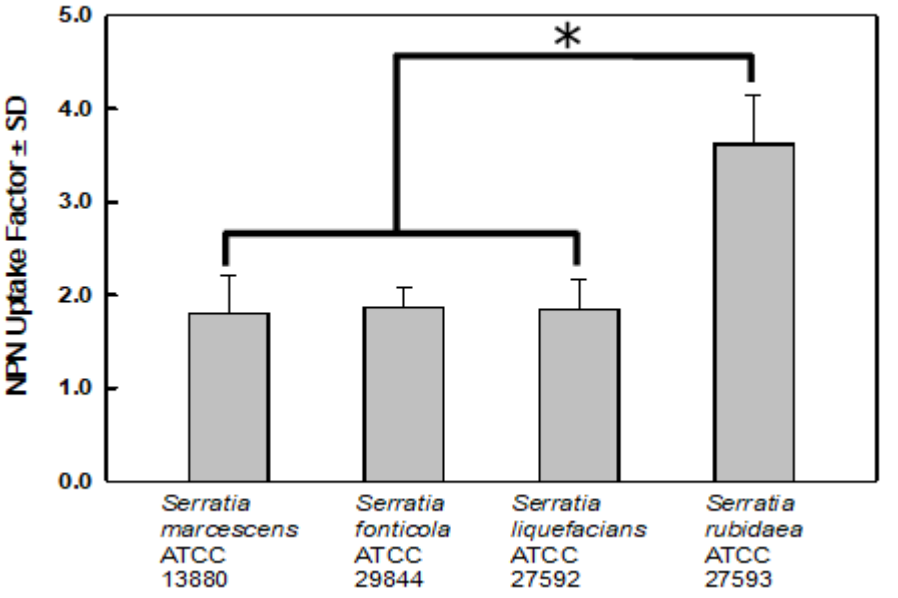

Figure 6. Cell surface hydrophobicity properties determined based on the degree to which NPN partitioned into outer membranes as measured fluorometrically using the method of Helander and Mattila-Sandholm (2000) as modified by Ruskoski and Champlin (2017).

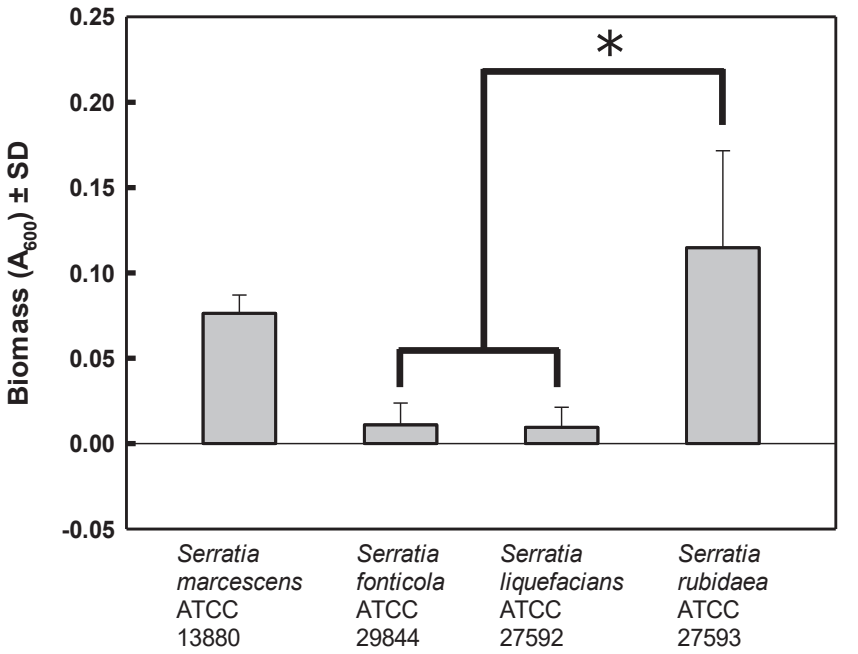

Figure 7. Initial biofilm adhesion (4.0 h) based on the amount of biomass adherence to hydrophobic (untreated) polystyrene microtiter plates as measured spectrophotometrically using the method of O'Toole and Kolter (1998) as modified by Ruskoski and Champlin (2024).

Table 1: Summarized results for *Serratia* model system species employed for this study.

Organisms[a]	Source	Phenotypic susceptivity to triclosan sensitization	Cell surface hydrophobicity	Biofilm adhesion
S. marcescens ATCC 13880	Environment	Slight susceptivity	Hydrophobic	Moderate
S. fonticola ATCC 29844	Environment	Complete susceptivity	Hydrophilic	Slight
S. liquefaciens ATCC 27592	Milk	Transitory complete susceptivity	Hydrophobic	Slight
S. rubidaea ATCC 27593	Unknown	Moderate susceptivity	Extremely hydrophobic	Heavy

[a]Representative *Serratia* species selected for the present study on the basis of the degree to which they exhibited susceptivity to triclosan sensitization with outer membrane permeabilizer compound 48/80 (Boyina et al. 2023).

S. rubidaea, the most hydrophobic organism in the model system (Figures 5 and 6), adhered most efficiently to the hydrophobic polystyrene substrate in the initial adhesion stage of biofilm formation. *S. marcescens* exhibited intermediate CSH properties and was the second most adherent. Both organisms formed heavy biomass rings in growth flasks (Figure 3). *S. liquefaciens* also exhibited intermediate CSH properties but was only slightly adherent to both glass growth flasks and the polystyrene biofilm substrate. *S. fonticola* was the most hydrophilic bacterium, produced no biomass rings, and was only slightly adherent to the polystyrene biofilm substrate. *Serratia odorifera*, an organism not included in the present model system, was determined to be the most hydrophilic bacterium tested, unable to form biomass rings on glass growth flasks, and nonadherent in the biofilm attachment assay (data not shown). These data suggest that factors exposed on the surfaces of these bacteria which influence CSH properties are involved in the cellular and molecular mechanisms underlying the first stage of biofilm formation on hydrophobic substrates (Table 1). However, they do not directly correlate with cell envelope factors which determine the susceptivity of the individual *Serratia* species to triclosan sensitization by chemical permeabilization of their outer membranes.

Conclusion

The degree of susceptivity to triclosan sensitization by outer membrane permeabilization in opportunistically pathogenic *Serratia* species as previously reported by our laboratory (Boyina et al. 2023) is not directly related to CSH properties. However, phenotypic differences in the initial adhesion stage of *in vitro* biofilm formation appear to be influenced to some degree by the propensity with which the bacterial cell surface is able to associate with hydrophobic substances.

Acknowledgements

We are grateful to the Oklahoma State University Center for Health Sciences Office of the Vice President for Research for an intramural pilot grant to F.R.C. and the Office of Medical Student Research for a summer research award to C.F.G. Gratis triclosan (Irgasan DP 300) was generously provided by Ciba Specialty Chemicals (High Point, NC).

References

Alavi H.E.D., and Hansen L.T. 2013. Kinetics of biofilm formation and desiccation survival of Listeria monocytogenes in single and dual species biofilms with Pseudomonas fluorescens, Serratia proteamaculans or Shewanella baltica on food-grade stainless steel surfaces. Biofouling. 29:1253-1268. doi: 10.1080/08927014.2013.835805.

Bester K. 2005. Fate of triclosan and triclosan-methyl in sewage treatment plants and surface waters. Arch Environ Contam Toxicol. 49:9-17. doi: 10.1007/s00244-004-0155-4.

Boyina K., King B., Rigsbee A.S., Yang J.G., Sprinkles W., Patel V.M., McDonald A.A., Katz Amburn S., and Champlin F.R. 2023. Influence of outer membrane permeabilisation on intrinsic resistance to the hydrophobic biocide triclosan in opportunistic Serratia species. Heliyon. 9:e15385. doi: 10.1016/j.heliyon.2023.e15385.

Champlin F.R., Ellison M.L., Bullard J.W., and Conrad R.S. 2005. Effect of outer membrane permeabilization on intrinsic resistance to low triclosan levels in Pseudomonas aeruginosa. Int J Antimicrob Agents. 26:159-164. doi: 10.1016/j.ijantimicag.2005.04.020.

Clayborn A.B., Toofan S.N., and Champlin F.R. 2011. Influence of methylation on the antibacterial properties of triclosan in Pasteurella multocida and Pseudomonas aeruginosa variant strains. J Hosp Infect. 77:129-133. doi: 10.1016/j.jhin.2010.09.021.

Darnell K.R., Hart M.E., and Champlin F.R. 1987. Variability of cell surface hydrophobicity among Pasteurella multocida somatic serotype and Actinobacillus lignieresii strains. J Clin Microbiol. 25:67-71. doi: 10.1128/jcm.25.1.67-71.1987.

Dhillon G.S., Kaur S., Pulicharla R., Brar S.K., Cledón M., Verma M., and Surampalli R.Y. 2015. Triclosan: current status, occurrence, environmental risks and bioaccumulation potential. Int J Environ Res Public Health. 12:5657-5684. doi: 10.3390/ijerph120505657.

Ellison M.L., and Champlin F.R. 2007. Outer membrane permeability for nonpolar antimicrobial agents underlies extreme susceptibility of Pasteurella multocida to the hydrophobic biocide triclosan. Vet Microbiol. 124:310-318. doi: org/10.1016/j.vetmic.2007.04.038.

Ellison M.L., Roberts A.L., and Champlin F.R. 2007. Susceptibility of compound 48/80-sensitized Pseudomonas aeruginosa to the hydrophobic biocide triclosan. 269:295-300. doi: 10.1111/j.1574-6968.2007.00640.x.

Helander I.M., and Mattila-Sandholm T. 2000. Fluorometric assessment of Gram-negative bacterial permeabilization. J Appl Microbiol. 88:213-21. doi: 10.1046/j.1365-2672.2000.00971.x.

Jones G.L., Muller C.T., O'Reilly M., and Stickler, D.J. 2006. Effect of triclosan on the development of bacterial biofilms by urinary tract pathogens on urinary catheters. J Antimicrob Chemother. 57:266-272. doi: org/10.1093/jac/dki447.

Katsu T., Shibata M., and Fujita Y. 1985. Increased permeability of the outer membrane of Escherichia coli induced by the dimer in compound 48/80. Chem Pharm Bull. 33:893-895. doi: org/10.1248/cpb.33.893.

Krasowska A., and Sigler K. 2014. How microorganisms use hydrophobicity and what does this mean for human needs? Front Cellular Infect Microbiol. 4:1-7. doi: org/10.3389/fcimb.2014.00112.

McMurry L.M., Oethinger M., and Levy S.B. 1998. Triclosan targets lipid synthesis. Nature. 394:531-532. doi: org/10.1038/28970.

McNamara P.J., and Levy S.B. 2016. Triclosan: an instructive tale. Antimicrob Agents Chemother. 60:7015-7016. doi: 10.1128/AAC.02105-16.

Nikaido H. 2003. Molecular basis of bacterial outer membrane permeability revisited. Microbiol Molec Biol Rev. 67:593-656. doi: 10.1128/MMBR.67.4.593-656.2003.

O'Toole G.A., and Kolter R. 1998. Initiation of biofilm formation in Pseudomonas fluorescens WCS365 proceeds via multiple, convergent signaling pathways: a genetic analysis. Molec Microbiol. 28:449-461. doi: 10.1046/j.1365-2958.1998.00797.x.

Remuzgo-Martínez S., Lazaro-Diez M., Mayer C., Aranzamendi-Zaldumbide M., Padilla D., Calvo J., Marco F., Martinez-Martinez L., Icardo J.M., Otero A., and Ramos-Vivas J. 2015. Biofilm formation and quorum-sensing-molecule production by clinical isolates of Serratia liquefaciens. Appl Environ Microbiol. 81:3306-3315. doi: 10.1128/AEM.00088-15.

Rosenberg M., Blumberger Y., Judes H., Bar-Ness R., Rubinstein E., and Mazor Y. 1986. Cell surface hydrophobicity of pigmented and nonpigmented clinical Serratia marcescens strains. Infect Immun. 51:932-935. doi: 10.1128/iai.51.3.932-935.1986.

Rosenberg M., Gutnick D., and Rosenberg E. 1980. Adherence of bacteria to hydrocarbons: a simple method for measuring cell-surface hydrophobicity. FEMS Microbiol Lett. 9:29-33. doi: org/10.1111/j.1574-6968.1980.tb05599.x.

Ruskoski S.A., and Champlin F.R. 2017. Cell surface physiology and outer cell envelope impermeability for hydrophobic substances in Burkholderia multivorans. J Med Microbiol. 66:965-971. doi: 10.1099/jmm.0.000532.

Ruskoski S.A., Köhler G.A., Assefa S., and Champlin F.R. 2024. Relationship between extracellular polysaccharide production and in vitro biofilm formation in Burkholderia multivorans. J Med Microbiol. In preparation.

Schweizer H.P. 2001. Triclosan: a widely used biocide and its link to antibiotics. FEMS Microbiol Lett. 202:1-7. doi: 10.1111/j.1574-6968.2001.tb10772.x.

Silhavy T.J., Kahne D., and Walker S. 2010. The bacterial cell envelope. Cold Spring Harb Perspect Biol. 2:a000414.

Thies K.L., and Champlin F.R. 1989. Compositional factors influencing cell surface hydrophobicity of Pasteurella multocida variants. Curr Microbiol. 18:385-390. https://link.springer.com/article/10.1007/BF01571133.

Thompson A., Griffin P., Stuetz R., and Cartmell E. 2005. The fate and removal of triclosan during wastewater treatment. Water Environ Res. 77:63-67. doi: 10.2175/106143005x41636.

Van Houdt R., Moons P., Jansen A., Vanoirbeek K., and Michiels C.W. 2005. Genotypic and phenotypic characterization of a biofilm-forming Serratia plymuthica isolate from a raw vegetable processing line. FEMS Microbiol Lett. 246:265-272. doi: org/10.1016/j.femsle.2005.04.016.

Welsch T.T., and Gillock E.T. 2011. Triclosan resistant bacteria isolated from feedlot and residential soils. J Environ Sci Health A Tox Hazard Subst Environ Eng. 46:436-440. doi: 10.1080/10934529.2011.549407.

Submitted July 13, 2023 Accepted December 28, 2023

In Vitro Anticancer Effects of *Taraxacum* Genus Extracts: A Review

Brooke N. Stoutjesdyk
Department of Biology, College of Mathematics and Science, University of Central Oklahoma, Edmond, OK 73034

Melville B. Vaughan
Department of Biology, College of Mathematics and Science, University of Central Oklahoma, Edmond, OK 73034

Christina G. Hendrickson*
Department of Biology, Petree College of Arts & Sciences, Oklahoma City University, Oklahoma City, OK 73106

Abstract: Cancer is one of the leading causes of death across the globe, affecting millions of lives. Natural products derived from traditional medicines have been used to treat many illnesses including cancer. *Taraxacum officinale*, commonly known as dandelion, and other similar species have been a growing topic of interest for their potential anticancer effects. A review of the current literature showed that researchers have experimented with crude extracts from different organs of the dandelion plant, notably root, leaf, flower, and whole plant extracts, to show their effect on cancer cell lines. A comparison of these extracts' anticancer potential was conducted. Based on published literature, research has "room to grow" studying extracts from dandelion leaves, seeds, and flowers, in addition to numerous untested species. Several studies have conducted phytochemical analysis and assessed the cytotoxicity of both the crude extract and its individual fractions. Most studies have found that none of the isolated fractions exhibited the same level of potency as the crude extract. To unravel how these distinct components combine to replicate the effects of traditional medicines, a synergistic research approach is required to identify the optimal combination of these fractions or bioactive molecules.

Introduction

Taraxacum officinale, more commonly known as the dandelion, can be traced back to glacial and interglacial times in Europe (Godwin 1956). It is believed that various species of the genus *Taraxacum* colonized the western hemisphere prior to the Gondwana supercontinent split about 180 million years ago (Richards 1973). It has been used in herbal Native American, Mexican (Sansores-España, Pech-Aguilar et al. 2022), Greek, Chinese medicine, and others (Sharifi-Rad, Roberts et al. 2018) for centuries due to its anti-inflammatory and anti-oxidative properties (Yarnell and Abascal 2009). In the United States, dandelions are considered invasive weeds that serve no purpose. Dandelions are found throughout Oklahoma (Palmer 2007, 2022), and are the second earliest blooming plant in central Oklahoma (Osborn 2015). What makes these weeds so special and gives them the potential to aid in treating one of the most prolific diseases seen across the globe?

According to the Integrated Taxonomic Information System (ITIS), as of March 2023, there are 15 species of *Taraxacum* in addition to *Taraxacum officinale* (Brouillet 2023). Medicinal aspects of the genus *Taraxacum* have been a popular topic of academic studies for

***Corresponding author: chendrickson1@okcu.edu**

decades. Almost half of the reported biomedical research are from studies on *Taraxacum officinale* alone (Martinez, Poirrier et al. 2015).

Due to the versatility of uses these plants have offered to holistic and herbal medicine cultures, scientists have been attempting to validate these uses for more clinical settings. In particular, the antimicrobial effects of the *Taraxacum* genus have been thoroughly investigated. Researchers found that the plants were effective in inducing growth arrest, or "halo zones" in agar plates of multiple bacteria. Notably, different species of *Taraxacum* plants were found to create halo zones against *Klebsiella pneumoniae* (Shahidi Bonjar, Aghighi et al. 2004), *Staphylococcus aureus* (Demin 2010), and *Bacillus subtilis* (Tahir, Nazir et al. 2017), all of which are incredibly common in the environment and are known to cause many different aliments.

In more recent years, multiple studies have examined the possible anticancer effects of *Taraxacum* plants to fight against more serious illnesses. There has been a spike in researchers running experiments to examine the possible anticancer effects of *Taraxacum officinale* and related *Taraxacum* species. Cancer is the second leading cause of death in the United States. In 2021, approximately 1.9 million new cancer cases were diagnosed, and 608,570 cancer-caused deaths occurred (Siegel, Miller et al. 2022). As the number of cancer diagnoses increases, the number of new forms of cancer therapy increases. However, there continues to be a high rate of death associated with these cancers. The need for new, innovative, less expensive cancer therapies having fewer harsh side effects is ever growing.

While many studies have identified compounds present in *Taraxacum*, there is surprisingly less research on crude extracts or compound mixtures to determine if such combinations will provide similar effects to those reported with traditional medicines (Martinez, Poirrier et al. 2015, Scaria, Sood et al. 2020). The purpose of this review is to focus on dandelion crude extract research reported in the literature, with specific emphasis on *in vitro* cancer cell culture studies. These studies include isolated plant parts or mixtures, or the whole plant. During active growth, dandelions continuously demonstrate leaves and roots; less often, other parts related to reproduction (e.g., flowers, seeds, petals, bracts, seed heads) are present (Vijverberg, Welten et al. 2021) (**Table 1**). Many of the studies reported here do not adequately describe which parts are included in the extracts that were tested, nor which species was extracted, leaving room for interpretation of results.

In this work, we review the current state of knowledge regarding the anticancer effects of *Taraxacum officinale* and related species. Because the dandelion is a complex plant with a diverse biochemical composition, coupled with variations in the parts utilized across different studies, we decided to structure the review into sections by the part of the plant used (whole plant extract, roots, roots, leaves, flowers, and seeds). We then discuss the overall knowledge based on analysis of the data and highlight potential areas for future research.

Methods

We searched databases available online and written in English through the University of Central Oklahoma, including Google Scholar, JSTOR, ProQuest, PubMed, Science Direct, and Web of Science using keywords such as "taraxacum" or "dandelion" with "crude extract", "in vitro" "phytochemistry", "pharmacology" "cancer cell". Each abstract was read to determine if crude extracts of *Taraxacum* were used, and what kind of *in vitro* cells/experiments were conducted. From this evaluation, the papers collected were read in their entirety for further preparation.

Dandelion Whole Plant Extracts

Multiple studies using extracts from the whole dandelion plant (dandelion whole extract, or DWE) have been reported. DWE had a negative effect on triple-negative breast cancer (TNBC) migration, proliferation, and its ability to invade tumor-associated macrophages (TAMs) (Deng, Jiao et al. 2021). When tested

Table 1. Summary of dandelion crude extracts tested in experimental models.

Extract type	Species extracted	Experimental model*	Cell lines	Refs
Whole Plant Extract	*T. officinale*	Breast cancer stem cells	Primary cell culture	(Trinh, Doan-Phuong Dang et al. 2016)
		Breast cancer cells	MCF-7	(Rawa'a, Dhia et al. 2018)
		Normal liver cells	WRL-68	(Rawa'a, Dhia et al. 2018)
		Pediatric cancer cells (18)	RAMOS, MV4-11, etc.	(Menke, Schwermer et al. 2018)
		Normal human fibroblasts	NHDF-C	(Menke, Schwermer et al. 2018)
	T. formosanum	Bronchial epithelial cells	BEAS-2B	(Chien, Chang et al. 2018)
		Lung adenocarcinoma cells (2)	CL1-0 CL1-5	(Chien, Chang et al. 2018)
		Breast cancer cell lines (3)	MDA-MB-231 ZR75-1 MCF-7	(Lin, Chen et al. 2022)
	T. mongolicum	Breast cancer cell lines (3)	MDA-MB-231 ZR75-1 MCF-7	(Lin, Chen et al. 2022)
		Monocytic leukemia cells	U937	(Deng, Jiao et al. 2021)
		Breast cancer cells (2)	MDA-MB-231 MDA-MB-468	(Deng, Jiao et al. 2021)
		Breast cancer cells (2)	MDA-MB-231 MCF-7	(Li, He et al. 2017)
		Embryonic kidney cells	HEK293	(Li, He et al. 2017)
		Breast cancer cells (2)	MDA-MB-231 MDA-MB-468	(Wang, Hao et al. 2022)
		Normal mammary epithelial cells	MCF-10A	(Wang, Hao et al. 2022)
Unknown source	*Taraxacum sp.*	Lung adenocarcinoma cells	A549	(Man, Wu et al. 2022)
Root Extract	*T. officinale*	Breast cancer cells	MCF-7/AZ	(Sigstedt, Hooten et al. 2008)
		Prostate cancer cells	LNCaP C4-2B	(Sigstedt, Hooten et al. 2008)
		Normal colon mucosal epithelial cells	NCM460	(Ding and Wen 2018)
		Prostate cancer cells (2)	DU-145 PC-3	(Nguyen, Mehaidli et al. 2019)
		Colonic epithelial cells	FHC	(Nguyen, Mehaidli et al. 2019)
		Colon cancer cells (2)	HT-29 HCT116	(Ovadje, Ammar et al. 2016)
		Colonic epithelial cells	NCM460	(Ovadje, Ammar et al. 2016)
	Taraxacum sp.	Esophageal SCC (4)	KYSE450 NEC Eca109 EC9706	(Duan, Pan et al. 2021)
		Normal esophageal cells	NE3	(Duan, Pan et al. 2021)

Table 1. Continued.

		Cancer cells (3)	HepG2 MCF7 GCT116	(Rehman, Hamayun et al. 2017)
		Normal cells	HS27	(Rehman, Hamayun et al. 2017)
		Gastric cancer cells (2)	SGC7901 BGC823	(Zhu, Zhao et al. 2017)
		Normal gastric epithelial cells	GES-1	(Zhu, Zhao et al. 2017)
		Melanoma cells (2)	A375, G361	(Chatterjee, Ovadje et al. 2011)
		Normal human fibroblasts	Primary	(Chatterjee, Ovadje et al. 2011)
		T-cell leukemia (2)	Jurkat E6-1 dnFADD Jurkat	(Ovadje, Chatterjee et al. 2011, Ovadje, Hamm et al. 2012)
		Peripheral blood mononuclear cells	Primary	(Ovadje, Chatterjee et al. 2011, Ovadje, Hamm et al. 2012)
		Chronic myelomonocytic leukemia cells (3)	MV-4-11 HL-60 U-937	(Ovadje, Hamm et al. 2012)
		Pancreatic cancer cells (2)	BxPC-3 PANC-1	(Ovadje, Chochkeh et al. 2012)
		Normal human fibroblasts	Primary	(Ovadje, Chochkeh et al. 2012)
Leaf Extract	*T. officinale*	Breast cancer cells	MCF-7/AZ	(Sigstedt, Hooten et al. 2008)
		Prostate cancer cells	LNCaP C4-2B	(Sigstedt, Hooten et al. 2008)
	Taraxacum sp.	Colon cancer cells	HT-29	(Xue, Zhang et al. 2017)
Flower Extract	*T. officinale*	Breast cancer cells	MCF-7/AZ	(Sigstedt, Hooten et al. 2008)
		Prostate cancer cells	LNCaP C4-2B	(Sigstedt, Hooten et al. 2008)
		Colorectal cancer cells	Caco-2	(Hu and Kitts 2003)
Seed Extract	*T. officinale*	Hypopharyngeal cancer cells	FaDu	(Milovanovic, Grzegorczyk et al. 2022)
		Cervical cancer cells	HeLa	(Milovanovic, Grzegorczyk et al. 2022)
		Kidney epithelial cells	Vero	(Milovanovic, Grzegorczyk et al. 2022)
		Normal fibroblasts	CCD-1059Sk	(Milovanovic, Grzegorczyk et al. 2022)
	Taraxacum sp.	Esophageal SCC cells (5)	KYSE450 Eca109 NEC EC9706 TE-13	(Li, Deng et al. 2022)

*Number in parentheses indicates number of cell lines tested.

on non-small-cell lung cancer (NSCLC), DWE exhibited antioxidant effects as well as anticancer effects. DWE was unable to decrease cancer cell proliferation in a significant manner, but it was able to decrease the number of colonies formed by the cancer. It was also found that DWE exhibited inhibitory effects on the migration of cancer cells. DWE treatment decreased phosphorylation of ERK1/2 but did not have effects on p38 and JNK1/2 (Chien, Chang et al. 2018). In another study using breast cancer stem cells (BCSC), DWE was shown to inhibit BCSC proliferation by inducing apoptosis. DWE also increased the ROS in cancer stem cells (Trinh, Doan-Phuong Dang et al. 2016). While these studies reported effects only on diseased cells, another study compared DWE effects on cancer vs. non-cancerous cells, using MCF-7 (human breast cancer) cells against WRL-68 (normal human hepatic) cells. The study demonstrated that DWE significantly reduced cell viability of the cancerous cells but not the non-cancerous cells (Rawa'a, Dhia et al. 2018). Another study tested a panel of 18 cancer cell lines against a normal human fibroblast line and found DWE was more potent against the cancer cells than normal cells (Menke, Schwermer et al. 2018).

One study using *T. mongolicum* and *T. formosanum* aqueous extracts tested against 3 breast cancer cell lines showed mixed results on the cell lines; both extracts reduced cell migration and colony formation, but *T. mongolicum* was more cytotoxic to the tested cell lines (Lin, Chen et al. 2022). A similar study found *T. mongolicum* DWE extract inhibited triple-negative breast cancer cell viability and induced apoptosis (Li, He et al. 2017). A follow-up study using a multi-omics approach showed the effects were exerted mainly by seven compounds including luteolin, and through interference with lipid metabolism (including phospholipid and fatty acid metabolism) (Wang, Hao et al. 2022).

A crude extract from an unknown dandelion species and plant part was tested against A549 lung adenocarcinoma cells, where it was shown to be cytotoxic in a dose-dependent manner (Man, Wu et al. 2022). Further investigation into the metabolomic profile showed deficiencies in purine metabolism, but also glycerophospholipid metabolism, which was also reported in (Wang, Hao et al. 2022). These and other noted metabolic changes suggested DWE affected malignant proliferation, membrane stability/structure, and cells' ability to adhere to their extracellular matrix, all providing the stimulus for apoptosis.

While these studies offer substantial evidence supporting the potential therapeutic benefits of DWE, the absence of detailed information regarding specific plant parts included in the DWE description introduces some ambiguity when interpreting or comparing results with other studies. Additionally, the extraction methods varied from cold aqueous, hot aqueous, or ethanol to ethyl acetate processes (Lin, Chen et al. 2022; Deng, Jiao et al. 2021; Chien, Chang et al. 2018). This variability suggests that the substances extracted for testing may differ, potentially yielding diverse results.

Dandelion Root Extracts

One part of the dandelion that is consistently present year-round is the root, and consequently much of the published *in vitro* cancer studies focused on dandelion root extracts (DRE). Root aqueous extracts reduced viability but not cell growth of LNCaP C4-2B prostate cancer cells and MCF-7/AZ breast cancer cells. ERK phosphorylation was unaffected in either of the cell lines. DRE treatment blocked *in vitro* collagen invasion of MCF-7/AZ but not LNCaP C4-2B (Sigstedt, Hooten et al. 2008). Another study showed aqueous DRE was effective against esophageal squamous cell carcinoma (ESCC) cell growth, proliferation, migration, and invasion, but was less effective against normal esophageal cells. DRE inhibited *in vivo* tumorigenesis and induced apoptosis (Duan, Pan et al. 2021).

Another DRE study combined *in vitro* testing with an *in vivo* mouse model. Aqueous DRE increased cell viability and prevented apoptosis of NCM460 colonocytes induced by dextran sodium sulfate (DSS), correlated with reduced ROS production. Using female C57BL/6 mice as a model for humans, DRE inhibited DSS-induced ulcerative colitis and reduced

inflammation and oxidative stress in the colon of the mice (Ding and Wen 2018).

A series of studies with DRE compared cancer cell effects against non-cancerous cells, to provide further support for future clinical studies. One study compared DRE effects on gastric cancer versus normal gastric epithelial cells (Zhu, Zhao et al. 2017). DRE inhibited cancerous but not normal gastric cells, in part by targeting a long-noncoding RNA, CCAT1. Another study showed DRE (aqueous extract)-treated A375 melanoma cells exhibited a decrease in cell viability, while having no viability reduction in normal human fibroblasts. DRE treatment induced caspase-8 dependent apoptosis in the melanoma cells, correlated with increased mitochondrial ROS production. Other apoptotic markers were observed, including dissipation of the mitochondria membrane potential. Higher DRE doses were necessary to decrease viability in another melanoma cell line (G361) compared to the A375 cell line (Chatterjee, Ovadje et al. 2011). Another study compared aqueous DRE with ethanolic extract of lemongrass, using both *in vitro* and xenograft *in vivo* testing. DRE induced caspase-dependent apoptosis in two prostate cancer cell lines, but not normal colonic epithelial cells. Using immunocompromised CD1 nu/nu mice as an *in vivo* model, DRE was able to reduce tumor weight and volume (Nguyen, Mehaidli et al. 2019). When aqueous DRE was tested against human leukemia (Jurkat) cells, the higher the concentration of DRE used to treat the cells, the higher the amount of apoptosis was exhibited by the cells. DRE was able to reduce the cell viability of the leukemia cells by 60%. This apoptosis was shown to be caused by the activation of caspase 8, which then activated caspase 3, resulting in apoptosis. To ensure that the DRE was not damaging non-cancerous cells, peripheral blood mononuclear cells were treated with DRE and there were no significant damage and changes reported after treatment (Ovadje, Chatterjee et al. 2011). Another human leukemia cell line derived from chronic myelomonocytic leukemia (CMML) demonstrated 60% viability decrease. The remaining viable 40% were treated with a second round of aqueous DRE, which induced apoptosis through the extrinsic pathway, damaged the mitochondrial membrane, and induced autophagy. Normal peripheral blood monocytes under the same treatment regimen were unaffected (Ovadje, Hamm et al. 2012). In a similar fashion, aqueous DRE was tested on pancreatic cancer cells (BxPC-3 and PANC-1) versus non-cancerous pancreatic cells. DRE was shown to induce apoptosis in the BxPC-3 cells at 48 hours and PANC-1 cells at 24 hours. Multiple low-concentration doses were more effective inducing apoptosis than one large concentration dose. As with the Jurkat and CMML results, apoptosis occurred through the extrinsic pathway and autophagy was induced. These treatments were nontoxic to normal human fibroblasts (Ovadje, Chochkeh et al. 2012). More recently, aqueous DRE was tested against colon cancer cells (HT-29 and HCT166) and decreased cell viability in both cell lines by 50% yet did not decrease the cell viability of non-cancerous colon epithelial cells (NCM460). When a migration scratch assay was performed, DRE was successful in inhibiting cell migration of HT-29 and HCT166 cell lines while failing to inhibit the NCM460 cell line. DRE increased ROS in the cancerous HT-29 cells but not the non-cancerous colorectal cells. Multiple pathways of apoptosis were induced in the colorectal cancer cells. (Ovadje, Ammar et al. 2016). Because many of the DRE studies compared cancerous to non-cancerous cells, this *in vitro* evidence suggests that future studies *in vivo* are warranted.

Collectively, DRE has been tested on more cell types than other plant parts. The results indicate that DRE selectively inhibits cancerous cells, compared to normal cells. Similar to DWE, various preparation methods were used, and unnamed species extracted, making it challenging for future studies to reproduce reported results. The intricate mechanisms behind cell-type selectivity and potential off-target effects remain to be determined. Nevertheless, these findings suggest a promising avenue for future *in vitro*, *in vivo*, and clinical studies to determine the therapeutic potential of DRE**.**

Dandelion Leaf Extracts

Numerous studies have investigated the antioxidant potential of dandelion leaf extract (DLE) to protect against ROS damage in various cell and animal models; however, the published data on DLE effects on cancer cells is limited. Aqueous DLE was able to decrease the viability of MCF-7/AZ breast cancer cells and LNCaP C4-2B prostate cancer cells by 50%; cell growth of the breast cancer cell line was reduced by 40%. The DLE treatment resulted in a decrease of ERK activity, but not a decrease in the levels of ERK in the breast cancer cell line. DLE treatment did not influence the prostate cancer's cell growth. Finally, it was discovered that DLE was unable to inhibit the *in vitro* collagen matrix invasion of MCF-7/AZ cells. DLE was able to block the invasion of LNCaP C4-2B cells (Sigstedt, Hooten et al. 2008).

Another study compared the amount of phenolics and flavonoids in extracts taken from the root, flower, stem, and leaves of the dandelion (Xue, Zhang et al. 2017). 50% ethanolic DLE contained a higher phenolic content than all the other extracts while extracts from the leaves and the flowers were found to have the highest flavonoid content than the other extracts. This study also compared the antioxidant activity between dandelion root, flower, stem, and leaf extracts. The high phenolic content of DLE was correlated with higher antioxidant activity over the other extracts. Further DLE experiments concluded that DLE had a suppressive effect on the ROS production of the HT-29 cells (human colonic epithelial cells). Finally, anti-inflammatory activity testing was performed using HT-29 cells. DLE inhibited activation of p65 (an NF-kappa B signaling molecule) and inhibited inflammatory signaling molecules (Xue, Zhang et al. 2017).

Dandelion Flower Extracts

Few studies have been conducted using *Taraxacum officinale* flowers. In one study, flower extracts were tested for anticancer effects on human colon colorectal adenocarcinoma (Caco-2) cells, using ethyl acetate (EAF) and a water fraction (WF). The DFEs were subjected to antioxidant testing and it was observed that DFE suppressed the formation of conjugated dienes and led to prolonged lag phase durations and lower rates of propagation. It was found that a high ROS concentration of EAF DFE prevented the formation of conjugated dienes and the negative charge of hLDL. The WF DFE showed no antioxidant activity. Both EAF and WF DFEs were cytotoxic to Caco-2 cells at a concentration of 0.1 mg/mL. HPLC profile showed the presence compounds including luteolin and luteolin-7 glucoside, which were shown to be more cytotoxic than EAF and WF (Hu and Kitts 2003).

Aqueous DFE, among other extracts, was tested against MCF-7/AZ breast cancer cells and LNCaP C4-2B prostate cancer cells to observe the anticancer effects against these cell lines. The viability of the breast cancer cells was unaffected by DFE treatment. However, prostate cell viability decreased significantly in the presence of DFE. Researchers ran assays to see if DFE could inhibit ERK, and therefore stop cell growth, in both cancer cell lines. It was concluded that DFE treatment did not affect ERK and cell growth in either of the cell lines. Both cancer lines were able to invade an *in vitro* collagen invasion assay. Through additional assays it was shown that DFE treatment could not block this invasion in MCF-7/AZ cells nor in the LNCaP C4-2B cells (Sigstedt, Hooten et al. 2008)

Dandelion Seed Extracts

Dandelion seeds and fruits are similar; the fruit functions akin to a seed coat and is difficult to separate from the seed (Dr. Jenna Messick, UCO, personal communication). While some dandelion fruit extract (DFE) antioxidant studies have been published, no published cancer reports using dandelion fruit extracts were identified. Two publications about the medicinal properties of dandelion seed extract (DSE) were recently published. DSE was able to reduce the survival and proliferation rates of esophageal squamous cell carcinoma (ESCC) cells. Additionally, DSE induced apoptosis and suppressed migration, invasion, and angiogenesis (Li, Deng et al. 2022). A second study tested DSE against hypopharyngeal cancer (FaDu), cervical

adenocarcinoma (HeLa), and colon cancer (RKO) cells versus normal kidney cells and skin fibroblasts. When all cell types were tested for cytotoxicity, the extract showed selectivity for the hypopharyngeal and colon cancer cells compared to the normal cells, while HeLa cells were resistant to the DSE (Milovanovic, Grzegorczyk et al. 2022).

Dandelion extract effects when combined with other plant extracts

An additional publication described research using extracts that contain a mixture of mushrooms and plants, including dandelion. Specifically, the mixture included *Coix* seed, *Lentinula edodes* (shiitake mushroom), *Asparagus officinalis L., Houttuynia cordata* (chameleon plant), Dandelion, and *Grifola frondosa* (hen of the wood mushroom) (Chen, Yue et al. 2021).

Discussion

Dandelion has a long history of use as a medical herb. It has been shown to have antioxidant and anti-inflammatory benefits. Many of the above publications are from recent years, especially those that work with dandelion seed extract. This research is still in its infancy and needs to be expanded upon in future experiments. Since there are so few publications on this topic pertaining to each part of the dandelion, more experiments will need to be conducted with each extract before the research can move towards clinical use.

Because research teams used different types of cancer cells for their experiments it is difficult to make direct comparisons between the different types of extracts. However, there are clear trends that these extracts do, in fact, exhibit anticancer effects. Many of the researchers ran similar assays, including proliferation, viability, and migration assays. There is evidence that membrane stability is compromised through lipid metabolism effects. In nearly every case, no matter which extract was used and no matter what cancer cell lines were used, the cancer cells were inhibited by the extract treatment. This indicates a trend that dandelion extracts are showing signs of having anticancer properties that should have limited cytotoxicity to the non-cancerous cell environment.

In more recent years, researchers have begun fractionating dandelion extracts to find their biocomponents, in hopes of isolating purified anticancer chemicals. These publications evaluated the total flavonoids of an extract (He, Han et al. 2011, Kang, Miao et al. 2021), dandelion polysaccharides (Ren, Yang et al. 2021), and specific components, such as inulin fructan (Zhang, Song et al. 2021), taraxasterol (Ovadje, Ammar et al. 2016), and luteolin (Tsai, Tsai et al. 2021). The phytochemical analysis of dandelion roots, leaves, and flowers has been published extensively. Common components found in all three include caffeic acid, chlorogenic acid (Hu and Kitts 2003, González-Castejón, Visioli et al. 2012, Xue, Zhang et al. 2017), syringic acid, ferulic acid, and chicoric acid (González-Castejón, Visioli et al. 2012, Xue, Zhang et al. 2017) **(Table 2)**. While there is one publication detailing the phytochemical components of dandelion fruit (Lis, Jedrejek et al. 2020) there are no recent publications showing the phytochemical components of dandelion seeds.

Cancer is not the only aliment that dandelion extracts have been shown to combat. A China-based research group from the South-Central University for Nationalities used an ethyl acetate extract of dandelion and observed its anti-asthma effects (Sarı and Keçeci 2019). The Chinese Academy of Sciences published work showing the anti-influenza potential of dandelion (Zhao, Liu et al. 2020). A Canadian team showed that dandelion extracts could be used to protect human cells from UV radiation (Yang and Li 2015). In 2022, researchers from King Saud University used DSE to treat mice with hypercholesterolemia and determine the effect (El-Nagar, Al-Dahmash et al. 2022).

Much work has been done to characterize dandelion extracts, their chemicals, and effects *in vitro* and *in vivo*. However, many of these studies do not identify the species tested. Reported methods of extraction differ, leaving

Table 2. Phytochemical components of extracted dandelion plant parts. Data are from references (Hu and Kitts 2003, González-Castejón, Visioli et al. 2012, Xue, Zhang et al. 2017).

Biocomponent	DWE	DRE	DLE	DFE
10,15-octadecadienoic acid	x			
11,13-dihydro-taraxinic acid β-glucopyranoside		x	x	
11β,13-dihydrolactucin		x		
4-caffeoylquinic acid	x	x		
4-coumaric acid			x	x
4-hydroxybenzoic acid	x			
9,10,11-trihydroxy-(12Z)-octadecanienoic acid	x			
9,10,11-trihydroxy-9,11-octadecadienoic acid	x			
Acylated γ-butyrolactone glycoside		x		
Aesculin			x	
Ainslioside		x		
Apigenin 7-*O*-glucoside			x	
Apigenin				x
Arnidiol		x	x	
Caffeic acid	x	x	x	x
Caffeoyl hexoside	x			
Caffeoyl-D-glucose	x			
Caftaric acid	x			
Chicoric acid	x	x	x	x
Chlorogenic acid	x	x	x	x
Chrysoeriol			x	
Cichoriin			x	
Cis-caftaric acid	x			
Esculetin	x	x		
Faradiol		x		
Ferulic acid	x	x	x	x
Gallic acid			x	
Hesperidin	x			
Hydroxy-10,12,15-Octadecatrienoic acid	x			
Hydroxycinnamic acid derivative	x			
Isorhamnetin	x			x
Ixerin D		x		
Lupeol		x		
Luteolin	x			x
Luteolin 7-diglucoside			x	
Luteolin 7-glucoside	x		x	x
Luteolin hexoside	x			
Luteolin-7-O-rutinoside	x		x	
Monocaffeoyltartaric acid		x	x	
Picrasinoside F.	x			
Protocatechuic acid		x		
Quercetin	x		x	x

Table 2. Continued.

Quercetin-7-O-glucoside			x	
Rutin			x	
Scopoletin		x		
Stigmasterol		x		
Syringic acid	x	x	x	x
Taraxacolide-O-β-glucopyranoside		x		
Taraxacoside		x		
Taraxasterol		x		
Taraxinic acid β-glucopyranoside		x	x	
Tetrahydroridentin B		x		
Trans-cinnamic acid			x	x
Umbelliferone		x		
Vanillic acid	x	x	x	
α-amyrin		x		
β-amyrin		x	x	
β-sitosterol		x	x	
β-sitosterol-β-D-glucopyranoside		x		
ρ-coumaric acid	x	x		
ρ-hydroxybenzoic acid		x	x	
ρ-hydroxyphenylacetic acid		x		

it difficult to compare one study to another. Studies often use different cell types for testing, making comparisons difficult. More clinical studies are needed (Li, Chen et al. 2022), but current knowledge should be fine-tuned before proceeding (Sharifi-Rad, Roberts et al. 2018), in order to compare results to traditional medicine (Martinez, Poirrier et al. 2015, Scaria, Sood et al. 2020). Only a few of the known dandelion species have been tested; untested species may have anticancer potential (Li, Chen et al. 2022). Future work with big data set analysis of phytochemical mixtures combined with observed health benefits and/or "symptomics" should begin to tease out specific benefits of dandelion constituents for future therapies.

Acknowledgements

The authors would like to thank Dr. Adam Ryburn (Botanist at Oklahoma City University, Oklahoma, USA) and Dr. Jenna Messick (Botanist at University of Central Oklahoma, Oklahoma, USA) for their helpful discussion and expert advice, Sara Alexander at ITIS for technical assistance, Dr. Mostafa Elshahed and anonymous reviewers for suggestions to improve the manuscript. This work was funded by a student RCSA grant from the Office of High Impact Practices and the CMS CURE-STEM program at the University of Central Oklahoma.

References

Brouillet, L. (2023). "Taraxacum F.H. Wigg." Retrieved 5/30, 2023, from https://www.itis.gov/servlet/SingleRpt/SingleRpt?search_topic=TSN&search_value=36199#null.

Chatterjee, S. J., P. Ovadje, M. Mousa, C. Hamm and S. Pandey (2011). "The efficacy of dandelion root extract in inducing apoptosis in drug-resistant human melanoma cells." Evid Based Complement Alternat Med **2011**: 129045.

Chen, X., W. Yue, L. Tian, N. Li, Y. Chen, L. Zhang and J. Chen (2021). "A plant-based medicinal food inhibits the growth of human gastric carcinoma by reversing epithelial–mesenchymal transition via the canonical Wnt/β-catenin signaling pathway." BMC Complementary Medicine and Therapies **21**(1): 137.

Chien, J. T., R.-H. Chang, C.-H. Hsieh, C.-Y. Hsu and C.-C. Wang (2018). "Antioxidant property of Taraxacum formosanum Kitam and its antitumor activity in non-small-cell lung cancer cells." Phytomedicine **49**: 1-10.

Demin, G. (2010). "Analysis of nutritional components of Taraxacum mongolicum and its antibacterial activity." Pharmacognosy Journal **2**(12): 502-505.

Deng, X.-X., Y.-N. Jiao, H.-F. Hao, D. Xue, C.-C. Bai and S.-Y. Han (2021). "Taraxacum mongolicum extract inhibited malignant phenotype of triple-negative breast cancer cells in tumor-associated macrophages microenvironment through suppressing IL-10 / STAT3 / PD-L1 signaling pathways." Journal of Ethnopharmacology **274**: 113978.

Ding, A. and X. Wen (2018). "Dandelion root extract protects NCM460 colonic cells and relieves experimental mouse colitis." J Nat Med **72**(4): 857-866.

Duan, X., L. Pan, Y. Deng, Y. Liu, X. Han, H. Fu, Y. Li, M. Li and T. Wang (2021). "Dandelion root extract affects ESCC progression via regulating multiple signal pathways." Food Funct **12**(19): 9486-9502.

El-Nagar, D. M., B. A. Al-Dahmash, S. Alkahtani, A. A. Kalu and A. Rady (2022). "Dandelion (Taraxacum officinale) seeds extract attenuates hypercholesterolemia in swiss albino mice." Journal of King Saud University - Science **34**(7): 102198.

Godwin, H (1956). The history of the British flora. Cambridge University, Cambridge, UK. 384 pp.

González-Castejón, M., F. Visioli and A. Rodriguez-Casado (2012). "Diverse biological activities of dandelion." Nutrition Reviews **70**(9): 534-547.

He, W., H. Han, W. Wang and B. Gao (2011). "Anti-influenza virus effect of aqueous extracts from dandelion." Virol J **8**: 538.

Hu, C. and D. D. Kitts (2003). "Antioxidant, Prooxidant, and Cytotoxic Activities of Solvent-Fractionated Dandelion (Taraxacum officinale) Flower Extracts in Vitro." Journal of Agricultural and Food Chemistry **51**(1): 301-310.

Kang, L., M.-s. Miao, Y.-g. Song, X.-y. Fang, J. Zhang, Y.-n. Zhang and J.-x. Miao (2021). "Total flavonoids of Taraxacum mongolicum inhibit non-small cell lung cancer by regulating immune function." Journal of Ethnopharmacology **281**: 114514.

Li, X. H., X. R. He, Y. Y. Zhou, H. Y. Zhao, W. X. Zheng, S. T. Jiang, Q. Zhou, P. P. P. Li and S. Y. Han (2017). "Taraxacum mongolicum extract induced endoplasmic reticulum stress associated-apoptosis in triple-negative breast cancer cells." J Ethnopharmacol **206**: 55-64.

Li, Y., Y. Chen and D. Sun-Waterhouse (2022). "The potential of dandelion in the fight against gastrointestinal diseases: A review." J Ethnopharmacol **293**: 115272.

Li, Y., Y. Deng, X. Zhang, H. Fu, X. Han, W. Guo, W. Zhao, X. Zhao, C. Yu, H. Li, K. Lei and T. Wang (2022). "Dandelion Seed Extract Affects Tumor Progression and Enhances the Sensitivity of Cisplatin in Esophageal Squamous Cell Carcinoma." Frontiers in Pharmacology **13**.

Lin, C. J., J. T. Chen, L. J. Yeh, R. C. Yang, S. M. Huang and T. W. Chen (2022). "Characteristics of the Cytotoxicity of Taraxacum mongolicum and Taraxacum formosanum in Human Breast Cancer Cells." Int J Mol Sci **23**(19).

Lis, B., D. Jedrejek, J. Rywaniak, A. Soluch, A. Stochmal and B. Olas (2020). "Flavonoid Preparations from Taraxacum officinale L. Fruits—A Phytochemical, Antioxidant and Hemostasis Studies." Molecules **25**(22): 5402.

Man, J., L. Wu, P. Han, Y. Hao, J. Li, Z. Gao, J. Wang, W. Yang and Y. Tian (2022). "Revealing the metabolic mechanism of dandelion extract against A549 cells using UPLC-QTOF MS." Biomed Chromatogr **36**(3): e5272.

Martinez, M., P. Poirrier, R. Chamy, D. Prüfer, C. Schulze-Gronover, L. Jorquera and G. Ruiz (2015). "Taraxacum officinale and related species—An ethnopharmacological review and its potential as a commercial medicinal plant." Journal of Ethnopharmacology **169**: 244-262.

Menke, K., M. Schwermer, J. Felenda, C. Beckmann, F. Stintzing, A. Schramm and T. J. Zuzak (2018). "Taraxacum officinale extract shows antitumor effects on pediatric cancer cells and enhance mistletoe therapy." Complement Ther Med **40**: 158-164.

Milovanovic, S., A. Grzegorczyk, Ł. Świątek, A. Dębczak, K. Tyskiewicz and M. Konkol (2022). "Dandelion seeds as a new and valuable source of bioactive extracts obtained using the supercritical fluid extraction technique." Sustainable Chemistry and Pharmacy **29**: 100796.

Nguyen, C., A. Mehaidli, K. Baskaran, S. Grewal, A. Pupulin, I. Ruvinov, B. Scaria, K. Parashar, C. Vegh and S. Pandey (2019). "Dandelion Root and Lemongrass Extracts Induce Apoptosis, Enhance Chemotherapeutic Efficacy, and Reduce Tumour Xenograft Growth In Vivo in Prostate Cancer." Evid Based Complement Alternat Med **2019**: 2951428.

Osborn, B. (2015). "First Flowering Dates for Central Oklahoma." Oklahoma Native Plant Record **15**(1).

Ovadje, P., S. Ammar, J. A. Guerrero, J. T. Arnason and S. Pandey (2016). "Dandelion root extract affects colorectal cancer proliferation and survival through the activation of multiple death signalling pathways." Oncotarget **7**(45): 73080-73100.

Ovadje, P., S. Chatterjee, C. Griffin, C. Tran, C. Hamm and S. Pandey (2011). "Selective induction of apoptosis through activation of caspase-8 in human leukemia cells (Jurkat) by dandelion root extract." Journal of Ethnopharmacology **133**(1): 86-91.

Ovadje, P., M. Chochkeh, P. Akbari-Asl, C. Hamm and S. Pandey (2012). "Selective induction of apoptosis and autophagy through treatment with dandelion root extract in human pancreatic cancer cells." Pancreas **41**(7): 1039-1047.

Ovadje, P., C. Hamm and S. Pandey (2012). "Efficient Induction of Extrinsic Cell Death by Dandelion Root Extract in Human Chronic Myelomonocytic Leukemia (CMML) Cells." PLOS ONE **7**(2): e30604.

Palmer, M. W. (2007). "The Vascular Flora of the Tallgrass Prairie Preserve, Osage County, Oklahoma." Castanea **72**(4): 235-246.

Rawa'a, A. M., S. H. Dhia and K. I. Nabeel (2018). "Cytotoxic Activity of Taraxacum officinale Ethanolic Plant Extract against Human Breast Cancer (MCF-7) Cells and Human Hepatic (WRL-68) Cells." Iraqi Journal of Cancer and Medical Genetics المجلة العراقية للسرطان والوراثة الطبية 11(1): 16-21.

Rehman, G., M. Hamayun, A. Iqbal, S. A. Khan, H. Khan, A. Shehzad, A. L. Khan, A. Hussain, H. Y. Kim, J. Ahmad, A. Ahmad, A. Ali and I. J. Lee (2017). "Effect of Methanolic Extract of Dandelion Roots on Cancer Cell Lines and AMP-Activated Protein Kinase Pathway." Front Pharmacol **8**: 875.

Ren, F., Y. Yang, K. Wu, T. Zhao, Y. Shi, M. Song and J. Li (2021). "The Effects of Dandelion Polysaccharides on Iron Metabolism by Regulating Hepcidin via JAK/STAT Signaling Pathway." Oxid Med Cell Longev **2021**: 7184760.

Richards, A. J (1973). "The origin of Taraxacum agamospecies". Bot J Linn Soc **66**: 189-211.

Sansores-España, D., A. G. Pech-Aguilar, K. G. Cua-Pech, I. Medina-Vera, M. Guevara-Cruz, A. L. Gutiérrez-Solis, J. G. Reyes-García and A. Avila-Nava (2022). "Plants Used in Mexican Traditional Medicine for the Management of Urolithiasis: A Review of Preclinical Evidence, Bioactive Compounds, and Molecular Mechanisms." Molecules **27**(6).

Sarı, A. and Z. Keçeci (2019). "Phytochemical Investigations on Chemical Constituents of Taraxacum bessarabicum (Hornem.) Hand. -Mazz. subsp. bessarabicum (Hornem.) Hand. -Mazz." Iran J Pharm Res **18**(1): 400-405.

Scaria, B., S. Sood, C. Raad, J. Khanafer, R. Jayachandiran, A. Pupulin, S. Grewal, M. Okoko, M. Arora, L. Miles and S. Pandey (2020). "Natural Health Products (NHP's) and Natural Compounds as Therapeutic Agents

for the Treatment of Cancer; Mechanisms of Anticancer Activity of Natural Compounds and Overall Trends." Int J Mol Sci **21**(22).

Shahidi Bonjar, G., S. Aghighi and A. Karimi Nik (2004). "Antibacterial and antifungal survey in plants used in indigenous herbal-medicine of south east regions of Iran." Journal of Biological Sciences **4**(3): 405-412.

Sharifi-Rad, M., T. H. Roberts, K. R. Matthews, C. F. Bezerra, M. F. B. Morais-Braga, H. D. M. Coutinho, F. Sharopov, B. Salehi, Z. Yousaf, M. Sharifi-Rad, M. Del Mar Contreras, E. M. Varoni, D. R. Verma, M. Iriti and J. Sharifi-Rad (2018). "Ethnobotany of the genus Taraxacum-Phytochemicals and antimicrobial activity." Phytother Res **32**(11): 2131-2145.

Siegel, R. L., K. D. Miller, H. E. Fuchs and A. Jemal (2022). "Cancer statistics, 2022." CA: A Cancer Journal for Clinicians **72**(1): 7-33.

Sigstedt, S. C., C. J. Hooten, M. C. Callewaert, A. R. Jenkins, A. E. Romero, M. J. Pullin, A. Kornienko, T. K. Lowrey, S. V. Slambrouck and W. F. Steelant (2008). "Evaluation of aqueous extracts of Taraxacum officinale on growth and invasion of breast and prostate cancer cells." Int J Oncol **32**(5): 1085-1090.

Stork, H. E. (1920). "Studies in the genus Taraxacum." Bulletin of the Torrey Botanical Club **47**(5): 199-210.

Tahir, K., S. Nazir, A. Ahmad, B. Li, A. U. Khan, Z. U. Khan, F. U. Khan, Q. U. Khan, A. Khan and A. U. Rahman (2017). "Facile and green synthesis of phytochemicals capped platinum nanoparticles and in vitro their superior antibacterial activity." J Photochem Photobiol B **166**: 246-251.

Trinh, N. V., N. Doan-Phuong Dang, D. Hong Tran and P. Van Pham (2016). "Taraxacum officinale dandelion extracts efficiently inhibited the breast cancer stem cell proliferation." Biomedical Research and Therapy **3**(7): 34.

Tsai, K. J., H. Y. Tsai, C. C. Tsai, T. Y. Chen, T. H. Hsieh, C. L. Chen, L. Mbuyisa, Y. B. Huang and M. W. Lin (2021). "Luteolin Inhibits Breast Cancer Stemness and Enhances Chemosensitivity through the Nrf2-Mediated Pathway." Molecules **26**(21).

Vijverberg, K., M. Welten, M. Kraaij, B. J. van Heuven, E. Smets and B. Gravendeel (2021). "Sepal Identity of the Pappus and Floral Organ Development in the Common Dandelion (Taraxacum officinale; Asteraceae)." Plants **10**(8): 1682.

Wang, S., H. F. Hao, Y. N. Jiao, J. L. Fu, Z. W. Guo, Y. Guo, Y. Yuan, P. P. Li and S. Y. Han (2022). "Dandelion extract inhibits triple-negative breast cancer cell proliferation by interfering with glycerophospholipids and unsaturated fatty acids metabolism." Front Pharmacol **13**: 942996.

Xue, Y., S. Zhang, M. Du and M.-J. Zhu (2017). "Dandelion extract suppresses reactive oxidative species and inflammasome in intestinal epithelial cells." Journal of Functional Foods **29**: 10-18.

Yang, Y. and S. Li (2015). "Dandelion Extracts Protect Human Skin Fibroblasts from UVB Damage and Cellular Senescence." Oxid Med Cell Longev **2015**: 619560.

Yarnell, E. and K. Abascal (2009). "Dandelion (Taraxacum officinale and T. mongolicum)." Integrative Medicine **8**(2): 35-38.

Zhang, S., Z. Song, L. Shi, L. Zhou, J. Zhang, J. Cui, Y. Li, D.-Q. Jin, Y. Ohizumi, J. Xu and Y. Guo (2021). "A dandelion polysaccharide and its selenium nanoparticles: Structure features and evaluation of anti-tumor activity in zebrafish models." Carbohydrate Polymers **270**: 118365.

Zhao, P., J. Liu, Q. Ming, D. Tian, J. He, Z. Yang, J. Shen, Q. H. Liu and X. Yang (2020). "Dandelion extract relaxes mouse airway smooth muscle by blocking VDLCC and NSCC channels." Cell Biosci **10**: 125.

Zhu, H., H. Zhao, L. Zhang, J. Xu, C. Zhu, H. Zhao and G. Lv (2017). "Dandelion root extract suppressed gastric cancer cells proliferation and migration through targeting lncRNA-CCAT1." Biomedicine & Pharmacotherapy **93**: 1010-1017.

Submitted October 18, 2023 Accepted November 25, 2023

ABSTRACTS OF THE 112TH OKLAHOMA ACADEMY OF SCIENCE TECHNICAL MEETING

NOVEMBER 10, 2023

UNIVERSITY OF SCIENCE AND ARTS OF OKLAHOMA, CHICKASHA

(sorted by presenter's last name)

THE ROLE OF PHOSPHATE AND CALCIUM-REGULATED PROTEIN, PCRP, IN RESISTANCE OF A HUMAN PATHOGEN, *PSEUDOMONAS AERUGINOSA*, TO POLYMYXIN B

Maha Achour, Tarosha B. Salpadoru, and Marianna A. Patrauchan, Oklahoma State University-Stillwater

Pseudomonas aeruginosa (Pa) is a Gram-negative human pathogen and a leading cause of acute and chronic infections. It is known to cause airway blockage in patients with Cystic Fibrosis (CF) – leading to high morbidity and mortality. This pathogen has been of particular interest due to its multi-drug resistance, including "last resort antibiotic", polymyxin-B (PMB). Studies have shown that elevated calcium (Ca2+) and lowered phosphate (Pi) alter bacterial susceptibility to antimicrobial treatment – implying their regulatory role in Pa resistance. Previously, we showed that elevated Ca2+ levels, detected in airways of CF patients, enhance PMB resistance through novel Ca2+-dependent mechanisms. We have also shown that the upregulation of putative phophonatase PA2803, is mediated by both Ca2+ and Pi -- designating it as PcrP (phosphate and calcium-regulated protein). Although studies of pcrP deletion mutant supported its role in Pa PMB resistance, PcrP function remains unclear. Via enzymatic studies, we found that PcrP has no phosphonatase activity, and therefore explored its potential protein-binding function. By using protein-pull down assays in the presence or absence of Ca2+ and Pi starvation conditions, we identified several putative binding partners of PcrP followed by bacterial two-hybrid system (B2HS) for validation. The Beta-Galactosidase activity of the co-transformed constructs was assayed both qualitatively and quantitatively to evaluate the strength of protein-protein interactions. B2HS supported the earlier observed dimerization of PcrP and validated the interaction of PcrP with hypothetical protein PA3518 and Acyl-carrier protein 3, Acp3. Based on sequence analysis, PA3518 may have a role in heavy metal (notably, Cu2+) sensitivity. Acp3's interaction with Catalase shows it may be involved with reactive oxygen species (ROS) regulation in cells. Collectively, we showed that PcrP reduces Ca2+-dependent ROS production in Pa. Thus, the interaction of PcrP with Acp3 may contribute to Pa resistance to ROS and therefore enhance its resistance to PMB.

154

UNLOCKING THE POWER OF BIOINFORMATICS: PRACTICAL APPLICATIONS FOR UNDERGRADUATE RESEARCHERS

Evonn Annor and Julianna Goelzer, Oral Roberts University

Outstanding Undergraduate Paper in Science Communication and Education

Bioinformatics has revolutionized biological research, providing a powerful toolkit for analyzing and interpreting vast amounts of biological data. This presentation introduces undergraduate researchers to the practical applications of bioinformatics tools through a series of mini case studies. The presentation demonstrates the use of Wash U Epigenome Browser to visualize the organization of the entire genome within a nucleus, providing insights into gene regulation and cellular processes. Next, it demonstrates how NCBI BLAST can be used to select a suitable model organism for a specific research question based on sequence conservation. Finally, it extracts the DNA sequence of an enhancer or promoter region using Wash U Epigenome Browser and NCBI BLAST, designing a guide RNA (gRNA) for CRISPR-Cas9 gene editing. These case studies highlight the versatility of bioinformatics tools in addressing diverse biological questions and designing experiments, empowering undergraduates to make significant contributions to biological research and innovation.

EFFECTS OF IN OVO EXPOSURE TO POLYCYCLIC AROMATIC HYDROCARBONS (PAHS) ON HEPATIC TRANSCRIPTIONAL SHIFTS IN THE CHICK EMBRYO

Damon Corvelo, Yulianis Pagan, Hallum Ewbank, and Christopher G. Goodchild, University of Central Oklahoma

Outstanding Graduate Poster

Marine oil spills are known to cause immense damage to ecosystems, and this is known to affect avian populations as well. Most avian crude oil toxicity research has examined the physiological and behavioral changes that afflict the adult birds. However, nesting birds can expose their eggs to crude oil attached to the nesting material and their feathers. Eggshell oiling can result in polycyclic aromatic hydrocarbons (PAHs), toxic chemicals that occur naturally in crude oil, being transferred to the internal eggs contents, leading to embryonic exposure. Previous research in our lab has documented liver hypertrophy in chick embryos exposed to PAHs in ovo. Liver hypertrophy and concomitant shifts in hepatic gene expression of detoxification enzymes have been observed in adult birds exposed to crude oil. However, currently there is a lack of understanding of hepatic transcriptional shifts in chicken embryos exposed to PAHs. To test whether avian embryos can upregulate detoxification enzymes to metabolize PAHs in ovo, we exposed white leghorn chicken embryos to one of six PAHs (Fluoranthene, Anthracene, Pyrene, Benzo[a]pyrene, Chrysene, and Phenanthrene) on embryonic day 3. On embryonic day 18, we collected embryonic livers and examined mRNA expression of a suite of detoxification enzymes (IL6, GPx, GR, GST, SOD, Actin, and GAPDH) using qPCR. Preliminary analysis suggests that in ovo exposure to some PAHs alters hepatic expression of some detoxification enzymes.

CYTOTOXICITY OF 6-GINGEROL ON COLORECTAL CANCER CELL VIABILITY

Katherine Dempsey and Joel Gaikwad, Oral Roberts University

Outstanding Undergraduate Paper in Biomedical Sciences

Colorectal cancer is the third most common type of cancer and the second leading cause of cancer-related deaths in America. Common treatment options include invasive surgeries and chemotherapy but are often accompanied by complications of sepsis, bowel stress, and reduced immunity. Therefore, the search continues for natural therapeutic alternatives that differentiate between healthy and cancerous tissues. *Zingiber officinale*, commonly known as the ginger root, has been used for centuries in ancient Chinese and Indian Ayurvedic medicine due to its well-known anti-inflammatory and antioxidant properties. It was hypothesized that the main bioactive compound in ginger, 6-gingerol, may possess anticancer properties that would reduce the cell viability of colorectal cancer in a dose-dependent manner. Microscopic observations of HT-29 cells treated with gingerol were consistent with apoptotic morphology. Cell viability and caspase activity assays further supported the theory that gingerol induces apoptosis in cancer cells. In comparison, HEK293T cells displayed increased cell viability when treated with gingerol. Analysis of both qualitative and quantitative data suggest that gingerol is able to selectively target tumorigenic cells while promoting viability in noncancerous cells.

ANALYZING DIETARY DIVERSITY AND THE ECOLOGICAL SIGNIFICANCE OF THE GREEN SUNFISH (*LEPOMIS CYANELLUS*) IN AQUATIC ECOSYSTEMS OF THE GREAT PLAINS REGION

Jamie Eastep, Lindsey Bruckerhoff, and Keith Gido, Oklahoma State University-Stillwater

Outstanding Undergraduate Paper in Environmental Sciences

Green Sunfish (*Lepomis cyanellus*) are opportunistic predators, that readily consume a variety of invertebrates, with insects comprising a significant part of their diet. The consumption of insects by Green Sunfish has ecological implications, as they play a role in influencing insect populations in their habitats. Additionally, their ability to consume a variety of prey items contributes to their success as a species in a wide range of aquatic environments. Diet variability in fish is thought to be influenced by consumer body size due to gape limitations and indeterminate growth. However, prey availability and energetic benefits should also play a role, as suggested by optimal-foraging theory. In this study, our objective was to investigate the effects of body size of Green Sunfish on the number of unique prey items, variation in prey selection, and mean body size of prey. We hypothesized that as Green Sunfish increased in body size, there would be an increase in the number of unique prey items, variation in prey selection, and mean body size of prey. To test this hypothesis, we analyzed stomach contents from over 300 Green Sunfish in streams across the Kansas River Basin in the Flint Hills ecoregion of Kansas. Additionally, we conducted a mesocosm experiment to examine changes in diet variability with fish body size. This research is significant as green sunfish populations are growing due to habitat alterations and they likely serve as important meso-predators in streams.

156

BRIDGING DISCIPLINES ON MARS: SOUTHWESTERN OKLAHOMA STATE UNIVERSITY'S FIRST INTERCOLLEGIATE STUDY INTEGRATING BIOLOGY, COMPUTER SCIENCE, AND ARTIFICIAL INTELLIGENCE FOR MICROBIAL ANALYSIS AND PLANT GROWTH ON MARS

Payden Farnsley, Stevie Langstraat, Rachel Uhlig, Kade Flores, Lisa Boggs, and Sherry Westmoreland, Southwestern Oklahoma State University

With the increasing public demand for space exploration, astrobiology research is a growing scientific field, as colonies on extraterrestrial planets come closer to reality. For these colonies to be a success, efficient nutrient cycling in different environments must be studied. The NASA-affiliated Plant the Moon competition challenges research teams across multiple educational divisions to grow food in simulated Mars soil (regolith) – produced by the Exolith Lab at the University of Central Florida – within a given growth period. Multiple students at Southwestern Oklahoma State University have participated in this challenge and have studied the interactions between microbes, Mars regolith, mammal fecal matter, and the growth of plants that provide food production. With Mars regolith behaving differently than Earth soil, parameters involving the growth of crops have been tested on top of soil additives. In addition to documenting total plant yield, soil pH, seedling germination rates, and chlorophyll content have been assessed. These characteristics of plant growth have been tested in many crops including, but not limited to, lettuce, spinach, basil, and radishes. With the ever-growing field of computer science and artificial intelligence, a joint research project between two departments will perform parameter testing on soil additive concentrations and specific growth conditions, among other things. Using multiple parameter tests, we anticipate finding the best combination of growth conditions and concentrations for crop yield in extraterrestrial soils used in space exploration. Beyond these implications for food and waste management, the results we find may be beneficial to organic farmers and home gardeners.

INVESTIGATION OF L-LYXONIC ACID EFFECT ON CYTOCHROME BD-1 OXIDASE EXPRESSION

Eli Grasso and April Nesbit, East Central University

Escherichia coli is a widely utilized model organism in a vast number of biological investigations, yet the functions of roughly 1,264 of its genes have yet to be demonstrated. One such gene whose purpose has not been entirely established encodes for putative DNA-binding transcriptional regulator YfaX. The gene yfaX has been identified as being part of an operon responsible for the metabolism of L-lyxonate. This investigation sought to determine whether there is a link between YfaX putative transcription factor and expression of cydA promoter, which controls expression of cytochrome bd-1 oxidase that is involved in electron transport chain. The YfaX protein was of interest because previous labs have shown that it binds cydA promoter in vitro, and cydA expression decreases in the presence of L-lyxonic acid. Lyxonate may be a product of vitamin C degradation in human intestines. It is possible that a higher concentration of vitamin C may result in an increased concentration of lyxonate; this may disrupt overgrowth of *E. coli* in the intestines, preventing potential unforeseen health risks. The potential link was tested using an yfaX deletion mutant in a strain with cydA promoter fused to the reporter gene lacZ that allows measurements with β-galactosidase assays with growth in different sugars. Although cydA expression decreases in the presence of L-lyxonic acid, the deletion of yfaX did not have an effect. Moving forward, future investigation will utilize a fusion of lacZ to the yfaX promoter region for the purpose of determining if the yfaX gene responds to L-lyxonic acid as predicted by the role of other genes in that operon.

SPATIAL PHYLOGENETICS OF VASCULAR PLANTS IN THE SOUTH-CENTRAL US

Sierra Hubbard and Mark Fishbein, Oklahoma State University-Stillwater

Outstanding Graduate Paper

While traditional measures of biodiversity are typically based on the species present in an area, phylogeny-based measures are able to capture information about the evolutionary history represented in an assemblage of taxa. Investigations of diversity using a phylogenetic framework can reveal the distributions of evolutionary lineages and the relative ages of plant assemblages. The South-Central United States (made up of Oklahoma and Texas) is a floristically diverse region that contains [3]8,000 vascular plant species. This region is also climatically diverse, with strong abiotic gradients in temperature, precipitation, and elevation. The current understanding of spatial phylogenetics in this region comes from a few continental-scale studies utilizing herbarium data. However, the South-Central US has not yet been included in any regional-scale studies, which could potentially reveal finer-scale patterns not apparent across broader study regions. Additionally, much fewer data have been available from Oklahoma and Texas compared to many other regions of North America; this may have led to incomplete conclusions about the spatial phylogenetics of plants in this region. Recent and ongoing digitization and georeferencing efforts have addressed this data gap by mobilizing a wealth of herbarium records from Oklahoma and Texas. In this study, we aim to use these newly available herbarium data to characterize the spatial patterns of phylogenetic diversity (PD) and relative phylogenetic diversity (RPD) seen in the vascular flora of the South-Central US. This approach highlighted regions that contain young plant assemblages in the High Plains and Southwestern Tablelands and identified concentrations of old lineages in the Eastern Temperate Forest and Edwards Plateau. In addition, we tested for associations between PD, RPD, and climatic gradients in precipitation, temperature, and elevation. We found that bioclimatic variables related to precipitation were the best predictors of PD and RPD.

COMPARISON OF CONSERVATION AND DIVERGENCE IN GENE RL COMPARED TO GENE GIG

Jenna Knox, Katie McCullock, and Lindsey Long, Oklahoma Christian University

Outstanding Undergraduate Poster

The goal of this experiment is to understand how pathways evolve using the insulin/TOR pathway. *Drosophila* was used as the model organism to identify gene conservation among various species that have increasing divergence from *D. melanogaster*. The specific gene of interest for this project was rl. In a paper published by Alvarez Ponce, it is hypothesized that more connections results in slower evolution of a gene. To show this we compared divergence scores in species closely, intermediately, and loosely related to *D. melanogaster*. We hypothesized that rl will be less evolutionarily conserved when compared to gig.

158

MATCHING-BASED COALITION FORMATION FOR MULTI-ROBOT TASK ASSIGNMENT UNDER PARTIAL UNCERTAINTY

Brenden Latham and Vladimir Ufimtsev, East Central University

Ayan Dutta, University of North Florida

Outstanding Undergraduate Paper in Mathematics, Computer Science, & Statistics

In this research, we examine the multi-agent coalition formation problem for instantaneous task allocation (IA) where a group of agents needs to be allocated to a set of tasks so that the tasks can be finished optimally. We will present new results in coalition formation for multi-agent systems in the presence of large partial uncertainty. We pair ideas from the Interval Hungarian Algorithm with a One-To-Many Bipartite Matching algorithm to achieve a scalable, parallel solution for allocation under partial cost uncertainty.

DESIGNING AN ORAL MUCOSAL VACCINE FOR ENHANCED PROTECTION AGAINST *CLOSTRIDIOIDES DIFFICILE*

Joseph H. McCreary and and I-Hsiu Huang, Oklahoma State University-Center for Health Sciences

Saeed Manouchehri and Josh Ramsey, Oklahoma State University-Stillwater

Yi-Wen Liu and Yu-Shan Lin, National Cheng Kung University-Taiwan

Clostridioides difficile is a gram +, spore forming, toxin producing anaerobe that is found throughout the environment. *C. difficile* is the leading agent of hospital acquired infections. Symptoms of *C. difficile* infection (CDI) can range from diarrhea to pseudomembranous colitis and if left untreated can lead to death. *C. difficile* is currently only treated with the antibiotics Metronidazole, Vancomycin, and Fidaxomicin. These antibiotics are non-specific to *C. difficile* and have the side effect of killing the normal microbiota of the gut. This microbiota helps to keep the gut resistant to CDI, and its destruction can lead to relapses of disease. Ongoing work in our lab is looking at preventing CDI using a nanoparticle based oral vaccine. In a mouse model of CDI, we previously demonstrated that using the receptor-binding domain of *C. difficile* toxin B (TcdB) as the antigen was effective in producing robust antigen specific IgA and IgG antibodies. These robust antibody responses to the *C. difficile* toxin were enough to prevent disease, however, it was not able to reduce bacterial burden leaving the potential for asymptomatic spread and relapses of disease. To fight this problem, we are working on two solutions. The first being a nanoparticle polymer that specifically is designed to be M cell targeting and pH activated. Second, we are also evaluating the immunogenicity using fusion proteins combining rTcdB with *C. difficile* surface proteins in a mouse model. We hypothesize that a two-target approach may decrease the bacterial load and lead to complete protection against *C. difficile* infections. Preliminary results looking at four formulations of this polymer all including rTcdB indicate a trend in IgG responses. More tests are needed to further validate these trends.

CO-EXPOSURE TO TWO POLYCYCLIC AROMATIC HYDROCARBONS (PAHS) ALTERS GROSS ORGAN MASS AND METABOLIC RATE OF CHICK EMBRYOS

Yulianis Pagan, Hallum Ewbank, and Christopher Goodchild, University of Central Oklahoma

Outstanding Undergraduate Paper in Applied Ecology & Conservation

Polycyclic aromatic hydrocarbons (PAHs) are naturally occurring toxic chemicals found in crude oil and are known to transfer from the external eggshell surface to egg contents. Previously, we conducted an egg-injection study with White Leghorn chicken (*Gallus gallus*) eggs and identified two PAHs, chrysene (Chr) and phenanthrene (Phe), that increased embryonic heart mass and decreased embryonic heart rate. In this study, we investigated whether co-exposure to Chr and Phe resulted in additive or synergistic effects on chick embryo development. On embryonic day (ED) 3, chicken embryos were exposed to Chr (800 ng / g of egg mass), Phe (800 ng / g egg mass), and Chr and Phe in combination (∑ PAH 1600 ng /g ng egg mass) via egg-injection. We then collected embryonic organ mass, heart rate, metabolic rate, and cardiac and hepatic mRNA expression of detoxification enzymes on ED 18. We observed a decrease in ED 18 heart rate across all treatments. We also saw an increase in ED 18 liver mass in eggs exposed to Chr and Phe simultaneously, and shifts in metabolic rate and mRNA expression of cardiac detoxification enzymes. Collectively, these data suggest in ovo exposure to PAHs may lead to congenital heart defects, which may have long-term implications for hatching success and hatchling survival.

OBJECTIVE COMPARATIVE GENOME SEQUENCE ALIGNMENT OF THE HOMININI SPECIES USING A HIGH-PERFORMANCE COMPUTING ALGORITHM TO REVEAL PHYLOGENETIC INSIGHTS

Christof Rosler, Derick DuFriend, Evonn Annor, Rita Njoroge, William P. Ranahan II, Matthew H. Goelzer, Stephen Wheat, and Julianna A. Goelzer, Oral Roberts University

Outstanding Undergraduate Paper in Biological Sciences - Zoology

The branching of the Hominidae family has long engrossed the minds of zoologists as the taxa includes *Homo sapiens*. Phylogenetic trees have been constructed using morphology, proteins, and genes yet often the genetic segments used neglect regulatory, non-coding genes. With a greater understanding of the importance of these genes due to advances in biochemical research, we reanalyzed the historical percent similarities, 96-98.4%, between the sister genus taxa *Pan* and *Homo* via direct base pair comparison across their whole genome. We used ORU's GeneCompare program on Titan, the high-performance computing system to examine whole genomes. The program can take two FASTA files and find exact matches of a minimum length between the two files, the experimental granularity. Each chromosome was individually tested in this manner, a base and against a target, until the whole genome was compared. The matches are recorded as genomic coordinates and can provide insightful data such as the total percent similarity between each specie's chromosomes. We found more enriched percent similarity relationships between *Pan paniscus*, *Pan troglodytes*, and *Homo sapiens* as specific chromosomes expressed a lower and upper range of 59.66-93.1%, and a total mean of 81.8% (excluding Y-chromosome). Using bioinformatics as a tool to expand the scope of zoology new insight into the phylogenetic relationships between the Hominini species was found.

160

THE DISTRIBUTION OF INVASIVE HONEYSUCKLE IN EASTERN OKLAHOMA

Sarah Short, Oklahoma State University-Stillwater

Outstanding Undergraduate Paper in Biological Sciences - Botany

The introduction and spread of invasive plant species has been an increasingly concerning environmental issue in recent decades due to the harmful impacts their presence has on the ecosystems they've been introduced to. Due to many factors, non-native species may have survival or reproductive advantages over native plant species in their introduced habitats, which can lead to direct and indirect negative impacts on these ecosystems and their biodiversity. These effects are often logistically difficult and expensive to manage, and they often lead to larger long-term issues down the line. *Lonicera maackii* and *L. japonica* are invasive honeysuckle species that have formed naturalized populations in Oklahoma, where they outcompete, inhibit, and reduce the growth of native species, thus posing a threat to local biodiversity. Both species reproduce quickly, grow aggressively, lack competitors and herbivores, and survive in a wider range of environmental conditions for longer periods than most native plant species. Using data collected from field surveys and herbarium records, my study aims to provide new information to the existing knowledge of the distribution of both honeysuckle species throughout eastern Oklahoma. Parks and public recreation areas of all 47 counties of eastern Oklahoma were surveyed. Between herbarium data and observation records from the field surveys, this research observed *L. maackii* in fewer counties than expected and *L. japonica* in nearly all counties surveyed. Data analysis shows a strong correlation between the presence of *L. maackii* and the population size of a town.

EVOLUTIONARY CONSERVATION OF GIG AND SLMB IN *DROSOPHILA*

Heather Sparks, Jackson Taubel, Lindsey J. Long, Oklahoma Christian University

Laura Reed, Genomics Education Program-University of Alabama

Outstanding Undergraduate Paper in Biochemistry & Molecular Biology

The insulin pathway functions to uptake glucose molecules into fat or muscle cells. This pathway is vital for several biological processes, such as cell metabolism, growth, proliferation, and differentiation. In this study, the insulin pathway was studied in *Drosophila*. Gig and slmb are two genes in the insulin pathway. The genetic interactions of these genes were analyzed, leading to a hypothesis. It was predicted that gig and slmb have similar evolutionary conservations in the insulin pathway of *Drosophila*. Using bioinformatic data, genes of *D. melanogaster* were compared to genes of other species. Genetic comparisons were performed using gene annotation data, nucleotide and protein sequences, as well as percent identities and similarities. This information was combined in order to calculate divergence scores. Results from data analysis showed that gig is less conserved and diverged faster than slmb.

EVALUATING CYTOKINE RESPONSES IN BLADDER CELLS INFECTED WITH UROPATHOGENIC *ESCHERICHIA COLI* AND *KLEBSIELLA PNEUMONIAE*

Tia Tafla and Janaki K Iyer, Northeastern State University

Outstanding Undergraduate Paper in Microbiology

Urinary tract infections (UTIs) are prevalent infections that are caused by different types of bacteria including *Escherichia coli* (*E. coli*) and *Klebsiella pneumoniae* (*K. pneumoniae*). When the bladder cells become infected, they respond by producing pro-inflammatory cytokines and chemokines. To gain a deeper understanding of the host's response to different uropathogens, we conducted an Enzyme-Linked ImmunoSpot (ELISpot) assay. This approach allowed us to assess the expression of multiple pro-inflammatory cytokines in a sample. We hypothesized that infections with various uropathogens would lead to varying levels of pro-inflammatory cytokine expression due to differences among uropathogens. To test this hypothesis, we infected human 5637 bladder cells with uropathogenic *E. coli* and *K. pneumoniae* strains for 24 hours and evaluated cytokine protein expression. The ELISpot results revealed that uropathogenic *E. coli* caused the secretion of IL-1ra, IL-6, IL-1a, and IL-1b compared to uninfected cells. However, the response of IL-6 and IL-1b was reduced in bladder cells infected with *K. pneumoniae* strains, thereby supporting our hypothesis. To differentiate between cytokine production and secretion, we decided to perform intracellular cytokine staining followed by flow cytometry. Brefeldin A (BFA) is commonly used in these experiments to prevent cytokine secretion. We conducted an MTT cell viability assay to evaluate any cytotoxic effects of BFA. Our results showed no statistically significant differences among the various BFA concentrations tested. Ongoing experiments will help us establish optimal conditions for detecting cytokine production by flow cytometry. These findings will enhance our insights into how uropathogens modulate innate immune responses in bladder cells during the infection process, contributing to the development of more effective UTI treatments.

PROBIOTIC EFFECTS OF *LACTOCOCCUS LACTIS* AND *LEUCONOSTOC MESENTEROIDES* ON MORPHOLOGY, FECUNDITY, AND LONGEVITY IN *CAENORHABDITIS ELEGANS*

Brenda Tinoco-Bravo, Mylissa A. Stover, Crystal A. Shults, Sydney Marouk, Ratnakar Deole and Jacob R. Manjarrez, Oklahoma State University-Center for Health Sciences

Probiotic supplementation has been widely studied showing that it can sustain significant therapeutic benefits to overall health, which depends on the overall composition of the microbiome. In this study, we investigated the supplementation of potential probiotic lactic acid bacteria *Lactococcus lactis* and *Leuconostoc mesenteroides* in the gut of *Caenorhabditis elegans* and observed their effects in survival, size and morphology, and fecundity. Survival assays were used to analyze median and total lifespan, where analysis was performed until death. Fecundity assays were performed with the number of progenies counted daily. Body morphometrics were analyzed where length, width, area, and speed were recorded. Intestinal permeability was also evaluated using a dye-leakage assay (Smurf). Survival analysis using CeMbio, a *C. elegans* natural microbiome, demonstrated a decrease in survival when supplemented with *L. lactis* and *L. mesenteroides*. When *L. lactis* and *L. mesenteroides* was used as a sole food source or were supplemented to the standard *E. coli*, OP50, diet it showed an increase in survival. In terms of morphometrics, OP50-fed *C. elegans* supplemented with *L. mesenteroides* were smaller and slower when compared to *L. lactis*-supplemented OP50, which were larger and faster. Fecundity showed that OP50 supplementation with *L. mesenteroides* or *L. lactis* produced higher amounts of progeny than the *L. mesenteroides* or *L. lactis* monocultures. Intestinal permeability was shown to be higher in both *L. lactis* and *L. mesenteroides*, which also show to have an increase in longevity when compared to OP50. These results highlight the potential and beneficial applications for these lactic acid bacteria as a therapeutic probiotic. Our study indicates that both *L. lactis* and *L. mesenteroides* when supplemented with OP50 has a positive influence on the overall health and longevity of *C. elegans*.

TERRESTRIAL MAMMALS OF THE OKC METRO AREA

Zachary Woods and Daniel Gomes da Rocha, Southern Nazarene University

Urbanization is growing world-wide, and particularly in North America. As urbanization grows, so does our dependence on remaining urban green areas (e.g., parks, reserves, green belts) to preserve biodiversity and ecosystem services. The objective of this study is to understand how effective these green areas are in preserving species diversity. Additionally, we aim to identify environmental and anthropogenic variables that are influential to species diversity. We focused on the medium and large terrestrial mammal community in the highly urbanized Oklahoma City Metro area. Here we report preliminary data on 12 camera trap sites (active for ^{3}75 days during Summer 2022), in combination with site covariates (NDVI, road intensity, elevation, and number of domestic records) collected at and around the camera locations. We used Poisson Generalized Linear models (GLM) to test the effect of site covariates on mammal species richness. We also plotted species cumulative curves to assess the survey completeness. In total we detected 11 wild and 3 domestic medium and large terrestrial mammal species. We detected the majority of mammals species expected to occur in this region (with the exception of larger predators). Sites varied greatly in species richness (4-10) and composition. All site variables had a statistically non-significant effect (p-values>0.05) on species richness. This result is not unexpected considering the small sample size, but revealed some promising covariates to be tested as new data is added to the database (data from the Summer 2023 survey is being processed). Our species inventory serves as a baseline for future wildlife monitoring programs in the OKC metro area.

OKLAHOMA ACADEMY OF SCIENCE

2023 OFFICERS

President
Dr. Karen Williams
East Central University

President-Elect
Dr. Jerry Bowen
Rogers State University

Editor, *Proceedings*
Dr. Mostafa S. Elshahed
Oklahoma State University

Immediate Past President
Dr. Robert Mather,
Mather Professional Services

Executive Director
Dr. Adam Ryburn
Oklahoma City University

Recording Secretary
Dr. Avi Mitra
Oklahoma State University

Section	Chair	Vice-Chair
A: *Biological Sciences*	Dr. Jason Shaw University of Science and Arts of Oklahoma	VACANT
B: *Geology*	Dr. Chris Shelton Rogers State University	VACANT
C: *Physical Sciences*	Dr. Benjamin Tayo, UCO University of Central Oklahoma	Dr. Amanda Nichols Oklahoma Christian University
D: *Social Sciences*	Dr. John Geiger Cameron University	Dr. Dustin Williams East Central University
E: *Science Communication & Education*	VACANT	VACANT
F: *Geography*	VACANT	VACANT
G: Applied Ecology & Conservation	Dr. Rickey Contran Southwestern Oklahoma State University	Dr. Renan Bosque Southwestern Oklahoma State University
H: *Microbiology*	Dr. Erika Lutter Oklahoma State University	Dr. Yanaki Iyer Northeastern State University
I: *Engineering Sciences*	Dr. Gang Xu University of Central Oklahoma	Dr. Nesreen Alsbou University of Central Oklahoma
J: *Biochemistry & Molecular Biology*	Dr. Feng Feng Oklahoma State University	Dr. Subhas Das Oklahoma State University
K: *Microscopy*	VACANT	VACANT
L: *Mathematics, Computer Science & Statistics*	Dr. Pierre Tiako IEEE Oklahoma City Section	Dr. Hyacinthe Aboudja Oklahoma City University
M: *Environmental Sciences*	Cheyanne Olson Rogers State University	Dr. Dan McInnes East Central University y
N: *Biomedical Sciences*	Dr. Hannah King Rogers State University	VACANT

Collegiate Academy of Science	*Director*	**Dr. Mark Peaden,** Rogers State University
Junior Academy	*Director*	**Dr. David Bass,** University of Central Oklahoma
OAS Technical Meeting, 2023	*Coordinator*	**Dr. Rachel Jones and Dr. Jason Shaw**, University of Science and Arts of Oklahoma, Chickasha
OAS Website	*Webmaster*	**Dr. Adam Ryburn,** Oklahoma City University

OKLAHOMA ACADEMY OF SCIENCE
STATEMENT OF REVENUES COLLECTED AND EXPENSES PAID
FOR THE YEAR ENDED DECEMBER 31, 2022

REVENUES COLLECTED:		
Membership Dues:		$1,735.00
Investment Income:		$18.01
Meetings:		$12,049.73
Registration – Fall Field Meeting	$5,465.17	
Registration – Technical Meeting	$6,584.56	
Donations		$231.24
POAS:		$5,372.08
Woody Plants:		$174.18
Other Income:		$63.94
Total Revenue Collected		**$19,644.18**
EXPENSES PAID		
Stipends and Other Compensation:		$7,149.68
Stipends	$6,141.24	
Social Security & Medicare	$1,008.44	
Meeting Expenses:		$9,498.95
Fall Field Meeting	$6,833.75	
Technical Meeting	$2,665.20	
Dues/Meetings of NAAS/AJAS/AAAS:		$1,446.90
POAS:		$4,492.39
POAS Editor	$3,000.00	
POAS Printing	$1,216.00	
POAS Mailing	$276.39	
Woody Plants:		$204.82
Other Expenditures:		$235.41
Total Expenses Paid:		**$23,048.23**
Revenues Collected Over Expenses Paid		**$-3,404.05**

OKLAHOMA ACADEMY OF SCIENCE
STATEMENT OF ASSETS, LIABILITIES, AND FUND BALANCE
ARISING FROM CASH TRANSACTIONS
FOR THE YEAR ENDED DECEMBER 31, 2022

ASSETS		
Cash:		$22,765.93
Checking Account	$16,686.46	
Savings Account	$3,278.67	
Endowment Savings Account	$2,800.80	
Investments:		$60,000
Certificate of Deposit	$60,000	
Total Assets:		**$82,765.93**
LIABILITIES AND FUND BALANCE		
Liabilities:	$0.00	
Fund balance:		
Beginning operation fund balance	$86,168.47	
Excess revenues collected over expenses	$-3402.54	
Total Funds:		**$82,765.93**

Name_____Affiliation _____
Last First Middle

Professional Address (if applicable) _____
Dept., Bldg., Office, etc. (if necessary for campus mail delivery)

_____
City State Zip

OR (not both)

Mailing Address (for home delivery) _____
Street, P.O. Box, Route, etc. City State Zip

Telephone_____E Mail _____

Please indicate whether this is a Renewal or New Membership. What year? _____

Note all annual memberships expire December 31 if you do not prepay for the following year.

Membership Type (check one):
_ Life $600 Professional $30 Family $35 Undergraduate/Graduate Student $20
$40 Library/Institute

Section Affiliations: Number up to three areas of interest. 1=first choice; 2=second choice; 3=third choice.

_____A Biological Sciences_____E Science Education_____I Engineering Sciences _____M Environ. Sci.
_____ B Geology _____F Geography_____J Biochemistry/Biophysics_____N Biomedical Sci.
_____ C Physical Sciences_____G Fish and Wildlife_____K Microscopy_____Y Collegiate Acad.
_____ D Social Sciences_____H Microbiology_____L Mathematics/Computer Sci_____Z Junior Academy

Make checks payable to the **Oklahoma Academy of Science**.

Mail completed form and payment to: Dr. Adam Ryburn, Executive Director, Oklahoma Academy of Science, Oklahoma City University, Biology Department, 2501 N. Blackwelder Ave., Oklahoma City, OK 73106. Or apply online

https://www.oklahomaacademyofscience.org/membership.html

Members, please photocopy this form and give that to a non member colleague or student. Help strengthen OAS by recruitment!

DONATION FORM

Make tax deductible donations in memory or honor of a family member, friend, or colleague. All donated fund are placed as principle into the OAS Endowment Account and the interest generated funds the Academy's programs.

_____

Donor _____
Mailing Address (Street or PO Box) City State Zip

Honoree _____
Amount

Editorial Policies and Practices

The *Proceedings of the Oklahoma Academy of Science* is published by the Oklahoma Academy of Science. Its editorial policies are established by the Editor and Associate Editors, under the general authority of the Publications Committee. The Editor is appointed by the Executive Committee of the Academy; Associate Editors are appointed by the Publications Committee in consultation with the Editor. The suitability for publication in the *Proceedings* of submitted manuscripts is judged by the Editor and the Associate Editors.

All manuscripts must be refereed critically. The *POAS* Editors have an obligation to the membership of the Academy and to the scientific community to insure, as far as possible, that the *Proceedings* is scientifically accurate. Expert refereeing is a tested, effective method by which the scientific community maintains a standard of excellence. In addition, expert refereeing frequently helps the author(s) to present the results in a clear, concise form that exceeds minimal standards.

The corresponding author is notified of the receipt of a manuscript, and the Editor sends the manuscript to at least two reviewers, anonymous to the author(s). After the initial review, the Editor either accepts the manuscript for publication, returns it to the author for clarification or revision, sends it to another referee for further review, or declines the manuscript.

A declined manuscript will have had at least two reviews, usually more. The Editors examine such manuscripts very carefully and take full responsibility. There are several grounds for declining a manuscript: the substance of the paper may not fall within the scope of the *Proceedings*; the work may not meet the standards that the *Proceedings* strives to maintain; the work may not be complete; the experimental evidence may not support the conclusion(s) that the author(s) would like to draw; the experimental approach may be equivocal; faulty design or technique may vitiate the results; or the manuscript may not make a sufficient contribution to the overall understanding of the system being studied, even though the quality of the experimental work is not in question.

A combination of these reasons is also possible grounds for declining to publish the MS. In most cases, the Editors rely on the judgment of the reviewers.

Reviewer's Responsibilities

We thank the reviewers who contribute so much to the quality of these *Proceedings*. They must remain anonymous to assure their freedom in making recommendations. The responsibilities or obligations of these reviewers are

- Because science depends on peer-reviewed publications, every scientist has an obligation to do a fair share of reviewing.
- A reviewer who has a conflict of interest or a schedule that will not allow rapid completion of the review will quickly return the manuscript; otherwise, the review will be completed and returned promptly.
- A reviewer shall respect the intellectual independence of the author(s). The review shall be objective, based on scientific merit alone, without regard to race, religion, nationality, sex, seniority, or institutional affiliation of the author(s). However, the reviewer may take into account the relationship of a manuscript under consideration to others previously or concurrently offered by the same author(s).
- A reviewer should not evaluate a manuscript by a person with whom the reviewer has a personal or professional connection if the relationship could reasonably be perceived as influencing judgment of the manuscript.
- The manuscript is a confidential document. If the reviewer seeks an opinion or discusses the manuscript with another, those consultations shall be revealed to the Editor.
- Reviewers must not use or disclose unpublished information, arguments, or interpretations contained in a manuscript under consideration, or in press, without the written consent of the author.
- Reviewers should explain and support their judgments and statements, so both the Editor and the author(s) may understand the basis of their comments.

Brief Instructions to Authors

The instructions to authors wishing to publish their research in the Proceedings of the Oklahoma Academy of Science are listed below. We ask the authors to recognize that the intent is not to establish a set of restrictive, arbitrary rules, but to provide a useful set of guidelines for authors, guidelines that, in most cases, are also binding on the Editors in their task of producing a sound and respected scientific journal.

A. Submission Process.

Manuscripts for the *Proceedings* should be submitted electronically via electronic mail (email) to:

poas@okstate.edu

Prospective authors should note carefully the policy statement "Policies of the *Proceedings*" on page ii. Complete instructions for manuscript formatting requirements, as well as a template for use may be found at:

https://ojs.library.okstate.edu/osu/index.php/OAS/submit

The Editors review the MS and carefully select other reviewers as described in "Editorial Policies and Practices" (see p. 167); all referee and editorial opinions are anonymous. Send a resubmitted and/ or revised manuscript and a point-by-point response to the reviewers'/Editor's comments.

All authors should approve all revisions (the corresponding author is responsible for insuring that all authors agree to the changes). A revised paper will retain its original date of receipt only if the revision is received by the Editor within two months after the date of the letter to the author(s).

B. Types of Manuscripts.

A manuscript may be a paper (report), review, note (communication), a technical comment, or a letter to the editor. All manuscripts should be submitted as a Microsoft Word document, 10-point Times New Roman font, single spaced, and include line numbers. Authors should carefully consider page size when producing manuscripts. The journal's page size is roughly 7 by 10 inches, portrait orientation, and does include margins.

Paper (a report; traditional research paper). A Paper may be of any length that is required to describe and to explain adequately the experimental observations.

Review. The Editor will usually solicit review articles, but will consider unsolicited ones. The prospective writer(s) of reviews should consult the Editor; in general, the Editor needs a synopsis of the area proposed for review and an outline of the paper before deciding. Reviews are typically peer- reviewed.

Note (Communication). The objective of a *Note* is to provide an effective form for communicating new results and ideas and/ or describing small but complete pieces of research. Thus, a *Note* is either a preliminary report or a complete account of a small investigation. *Notes* must not exceed four printed pages including text, figures, tables, and references. One journal page of standard text contains about 600 words; hence, there is space for presentation of considerable experimental detail. *Notes* are peer-reviewed.

Technical Comment. Technical comments (one journal page) may criticize material published in an earlier volume of *POAS* or may offer additional useful information. The author(s) of the original paper are asked for an opinion on the comment and, if the comment is published, are invited to reply in the same volume.

Letter to the Editor. Letters are selected for their pertinence to materials published in *POAS* or because they discuss problems of general interest to scientists and/or to Oklahomans. Letters pertaining to material published in *POAS* may correct errors, provide support or agreements, or offer different points of view, clarifications, or additional information.

Abstract. You may submit an abstract of your presentation at the OAS Technical Meeting. For specific instructions, contact the Editor. Even though abstracts are not peer-reviewed, they must align with the policies and scope of the *Proceedings*. The quality or relevance of work may not be in question, but the printed material is still subject to scientific accuracy.

The same guidelines that apply to manuscripts and notes submitted for peer-review, also apply to abstracts submitted for print. Just as manuscripts and notes are subject to thorough testing, so are comments written in abstracts (supported by data). The *Proceedings* understands that all disciplines are in a search for a deeper understanding of the world some of which are through creative expression and personal interpretation. Science is a system by which one discovers and records physical phenomena, dealing with hypotheses that are testable. The domain of "science" while working within nature is restricted to the observable world. There are many valid and important questions to be answered but lie outside the realm of science.

C. Manuscript Organization.

1. General organization.

For papers (reports), the subsections should typically include the following: Abstract, Introduction, Experimental Procedures (or Methods), Results, Discussion, Acknowledgments (if any), and References. In the case of notes or short papers, you may combine some headings, for example, "Results and Discussion":

I. The title should be short, clear, and informative; it should not exceed 150 characters and spaces (three lines in the journal), and include the name of the organism, compound, process, system, enzyme, etc., that is the major object of the study.

II. Provide a running title of fewer than 60 characters and spaces.

III. Spell out either the first or second given name of each author. For example, Otis C. Dermer, instead of O.C. Dermer, or H. Olin Spivey, instead of H.O. Spivey.

IV. Every manuscript (including Notes) must begin with a brief Abstract (up to 200 words) that presents clearly the plan, procedure, and significant results of the investigation. The Abstract should be understandable alone and should provide a comprehensive overview of the entire research effort.

V. The Introduction should state the purpose of the investigation and the relationship with other work in the same field. It should not be an extensive review of literature, but provide appropriate literature to demonstrate the context of the research.

VI. The Experimental Procedures (or Methods) section should be brief, but adequate for repetition of the work by a qualified experimenter. References to previously published procedures can reduce the length of this section. Refer to the original description of a procedure and describe any modifications.

VII. You may present the Results in tables or figures or both, but note that it is sometimes simpler and clearer to state the observations and the appropriate experimental values directly in the text. Present a given set of results *in only one form:* in a table, or figure, or the text.

VIII. The Discussion section should interpret the Results and how these observations fit with the results of others. Sometimes thecombination of Results and Discussion can give a clearer, more compact presentation.

IX. Acknowledgments of financial support and other aid are to be included.

X. References are discussed below.

2. References

POAS uses the name-year system for citing references. Citations in the text, tables and figure legends include the surname of the author or authors of the cited document and the year of publication. The references are listed alphabetically by authors' surnames in the reference list found at the end of the text of the article. Below are given several examples of correct formats for citing journal articles, books, theses and web resources. For Additional information regarding the name- year system, consult the CBE Manual [Scientific *Style and Format: The CBE Manual for Authors, Editors, and Publishers,* 6th edition]. Abbreviate journal names according to the *International List of Periodical Title Word Abbreviations.*

If it is necessary to refer to a manuscript that has been accepted for publication elsewhere but is not yet published, use the format shown below, with the volume and page numbers absent, the (estimated) publication year included and followed by the words *in press* for papers publications and *forthcoming* for all other forms (CBE 30.68). If the materials are published before the manuscript with that reference is published in *POAS,* notify the Editor of the appropriate volume and page numbers and make the changes as you revise.

Responsibility for the accuracy of bibliographic references rests entirely with the author(s); confirm all references through comparison of the final draft of the manuscript with the original publications. *We expect that the only changes in galley proof will be for typographical errors.* Any mention of *manuscript in preparation, unpublished experiments,* and *personal communication* should be in parenthesis. Use of *personal communication* should be with written permission of the communicator and should be entered only in the text, not in the Reference list.

Examples of References in CBE Style and Format

Journal Articles

Miller LF, Chance CJ. 1954. Fishing in the tail waters of TVS dams. Prog Fish-Cult 16:3-9.

Ortenburger AI, Hubbs CL. 1927. A report on the fishes of Oklahoma, with descriptions of new genera and species. Proc Okla Acad Sci 6:123-141.

Books

Book with Authors:

Miller RJ, Robison HW. 1980. The fishes of Oklahoma. Stillwater (OK): Oklahoma State University Press. 246 p.

Book with Editors:

Gilman AG, Rall TW, Nies AS, Taylor P, editors. 1990. The pharmacological basis of theraputics. 8th ed. New York: Pergamon. 1811 p.

Book with Organization as Author: International Union of Pure and Applied Chemistry, Physical Chemistry Division. 1993. Quantities, units, and symbols in physical chemistry. 3rd. Oxford (UK): Blackwell Science. 166 p.

Chapter in Book with Editors:

Hamilton K, Combs DL, Randolph JC. 1985. Sportfishing changes related to hydro- power generation and non-generation in the tailwater of Keystone Reservoir, Oklahoma. In: Olsen FW, White RG, Hamre RH, editors. Proceedings of the symposium on small

hydropower and fisheries. Bethesda (MD): American Fisheries Society. p 145-152.

Theses: Knapp MM. 1985. Effects of exploitation on crappie in a new reservoir [MSc thesis]. Stillwater (OK): Oklahoma State University. 84 p. Available from: OSU Library.

Internet: Oklahoma Climatological Survey. 2003. Climate of Oklahoma [online]. Available from: http://climate.ocs.ou.edu. (Accessed August 15, 2005).

D. Review Process.

The Editors review the MS and carefully select reviewers for all submitted manuscripts. All referee and editorial opinions are anonymous. A decision to accept, revise, or reject the manuscript is made by the editor after careful consideration of reviewers' comments and recommendations. If a "revise" decision is reached, the authors will be allowed to resubmit a revised version of the manuscript within a given time window. The authors are considered to address all reviewers' comments and concerns, or provide compelling reasons to explain why they chose not to do so. A point- by-point rebuttal letter is required with each revised manuscripts, which clearly indicates the nature and locations of corrections within the revised manuscript. All authors should approve all revisions, with the corresponding author being responsible for insuring that all authors agree to the changes.

E. Page Charges

The OAS will publish accepted MSs with the implicit understanding that the author(s) will pay a charge per published page. Page charges are billed at the cost per page for the given issue: current rates of $90 per page for nonmembers of the Academy and $45 for members. All authors are expected to honor these page charges. Billing for page charges and receipt of payment are handled by the Business Manager, who is also the Executive Secretary and Treasurer for the Academy.

Under exceptional circumstances, when no source of grant funds or other support exists, the author(s) may apply, at the time of submission, for a waiver of page charges.

F. Copyright Transfer

Before publication, authors must transfer copyright to the Oklahoma Academy of Science. All authors must sign, or the signing author must hold permission to sign for any coauthors. Copyright for papers reporting research by U.S. Government employees as part of their official duties will be transferred to the extent permitted by law.